VOLUME 9 (1958/59) No. 1

NUCLEAR PHYSICS

MONTHLY JOURNAL DEVOTED TO THE EXPERIMENTAL AND THEORETICAL STUDY OF ATOMIC NUCLEI, NUCLEAR FIELDS AND THE FUNDAMENTAL ASPECTS OF COSMIC RADIATION

EDITOR: L. ROSENFELD · COPENHAGEN

N. et C. MARTY, Frédéric Joliot (1900—1958) 1

A. A. KOMAR, Bremsstrahlung and pair production of particles of spin $\frac{1}{2}$ . . 6

M. EL-NADI and M. WAFIK, The characteristic level and the nuclear level density 22

F. FERRERO, R. MALVANO, S. MENARDI and O. TERRACINI, The nuclear photo-effect in Al^{27} 32

C. M. JOHANSSON and I. P. K. LINDGREN, Spins of bismuth isotopes of masses 203, 204, 205 and 206. 44

H. S. KÖHLER, On the inelastic scattering of nucleons by nuclei at high energies 49

R. J. EDEN, Series expansions and variational methods for the energy of a system of fermions 65

V. S. BARASHENKOV, V. A. BELYAKOV, E. G. BUBELEV, WANG SHOU FENG, V. M. MALTSEV, TEN GYN and K. D. TOLSTOV, Multiple production of particles in collisions between 9 GeV protons and nucleons 74

INGVAR MARKLUND, Decay of Eu^{152m} 83

INGVAR MARKLUND and LORNE A. PAGE, On the helicity of neutrinos 88

R. HUBY, M. Y. REFAI and G. R. SATCHLER, Predictions of the distorted wave theory of deuteron stripping reactions. 94

C. YTHIER, R. K. GIRGIS, R. A. RICCI and R. VAN LIESHOUT, The decay of ^{73}Ga . 108

P. MITTELSTAEDT, On the rearrangement energy of nuclear matter 116

T. PRADHAN, On the one-dimensional spinor model of Thirring 124

F. BECK, Einteilchen-Strahlungsübergänge im optischen Modell des Atomkerns 140

KERSTIN KJÄLLQUIST, On the calculation of the Y_{40} deformation in strongly deformed heavy nuclei. 163

Book Reviews 178

News Item 179

NORTH-HOLLAND PUBLISHING COMPANY - AMSTERDAM

November (3) 1958

EDITORIAL BOARD

AUSTRALIA & NEW ZEALAND:	H. Messel (Sydney), M. L. Oliphant (Canberra)
AUSTRIA:	B. Karlik, (Vienna), H. Thirring (Vienna)
BELGIUM:	M. de Hemptinne (Louvain), J. Verhaeghe (Ghent)
CANADA:	G. Volkoff (Vancouver)
DENMARK:	C. Møller (Copenhagen), S. Rozental (Copenhagen)
FINLAND:	L. Simons (Helsinki)
FRANCE:	A. Berthelot (Saclay), S. Gorodetzky (Strasbourg)
GERMANY (DEM. REP.):	G. Hertz (Leipzig)
GERMANY (FED. REP.):	W. Gentner (Freiburg i. B.), J. H. D. Jensen (Heidelberg)
GREAT BRITAIN:	S. Devons (Manchester), T. H. R. Skyrme (Harwell)
HUNGARY:	L. Janossy (Budapest)
INDIA:	H. Bhabha (Bombay), B. Peters (Bombay), R. Ramanna (Trombay)
IRISH REPUBLIC:	J. McConnell (Maynooth)
ISRAEL:	G. Racah (Jerusalem)
ITALY:	E. Amaldi (Rome)
JAPAN:	S. Kikuchi (Tokyo), S. Tomonaga (Tokyo)
MEXICO:	M. Moshinsky (Mexico)
NETHERLANDS:	H. Brinkman (Groningen), S. R. de Groot (Leiden)
NORWAY:	E. Hylleraas (Oslo), A. Lundby (Oslo), H. Wergeland (Trondheim)
POLAND:	L. Infeld (Warsaw)
PORTUGAL:	J. M. Araújo (Porto), J. R. de Almeida Santos (Coimbra)
SOUTH AMERICA:	G. Beck (Saõ Paulo), J. Leite Lopes (Rio de Janeiro)
SPAIN:	J. M. Otero (Madrid), C. Sanchez del Rio (Madrid)
SWEDEN:	O. Klein (Stockholm), K. Siegbahn (Uppsala), I. Waller (Uppsala)
SWITZERLAND:	P. Huber (Basel), P. Scherrer (Zürich)
U.A.R. & ARAB COUNTRIES:	F. El Bedewi (Alexandria), M. G. Nooh (Cairo)
U.S.A.:	V. Weisskopf (Cambridge, Mass.)
U.S.S.R.:	M. A. Markov (Moscow), I. S. Shapiro (Moscow), D. V. Skobeltzyn (Moscow)
YUGOSLAVIA:	I. Supek (Zagreb)

CONTRIBUTIONS may be sent to the Editor, Professor L. Rosenfeld, NORDITA, Blegdamsvej 17, Copenhagen Ø, either directly, or preferably through the intermediary of one of the members of the Editorial Board of the country or region in which the author is working. They may be written in English, French or German.

NUCLEAR PHYSICS is published in monthly issues. The subscription price a volume of 700 pages is fl 57.00; 114s; $ 15.00. Postfree.

SUBSCRIPTIONS should be sent to the publishers, NORTH-HOLLAND PUBLISHING COMPANY, P.O.Box 103, Amsterdam or to any subscription-agent.

BOOKS FOR REVIEW should be sent to Professor Rosenfeld.

No part of this issue may be reproduced in any form, by print, photoprint, microfilm or any other means without written permission from the publisher. Reprints, photoprints or microfilms are obtainable at cost from the publisher.

Printed in the Netherlands

THIS ISSUE OF NUCLEAR PHYSICS IS
DEDICATED TO THE MEMORY OF

FRÉDÉRIC JOLIOT

FRÉDÉRIC JOLIOT

(1900—1958)

10.C

Nuclear Physics 9 (1958/59) 1—5; © *North-Holland Publishing Co., Amsterdam*

Not to be reproduced by photoprint or microfilm without written permission from the publisher

FRÉDÉRIC JOLIOT
(1900—1958)

N. et C. MARTY

Laboratoire de Physique nucléaire, Faculté des Sciences, Orsay (S. & O.)

Reçu le 13 octobre 1958

Le 14 août dernier Frédéric JOLIOT mourait à Paris d'une maladie contre laquelle il luttait depuis longtemps. Sa disparition, deux ans après celle d'Irène Joliot-Curie, a été ressentie en France et aussi à l'étranger comme une perte irréparable. Tous ceux qui l'ont connu ou approché se souviendront de son extraordinaire vivacité d'esprit, de sa capacité d'enthousiasme, de son sens de l'humain.

Né à Paris en 1900, il y effectua ses études et entra en 1919 à l'Ecole de Physique et Chimie où il reçut un enseignement à la fois scientifique et technique. Cette période prend pour lui une importance exceptionnelle car elle marque ses premiers contacts avec Paul Langevin, alors professeur à l'Ecole. Le professeur devait avoir sur l'élève une grande influence que Joliot s'est plu à reconnaître toute sa vie.

Après un court stage dans l'industrie, sur la recommandation de Langevin, F. Joliot devient préparateur particulier de Marie Curie en 1925. C'est sous sa direction, à l'Institut du Radium, qu'il va s'initier aux méthodes de la radioactivité, puis peu à peu prendre part aux recherches du laboratoire. Il s'attaque à des problèmes variés: électrochimie des radioéléments, ionisation dûe aux rayons α. De cette époque date sa collaboration avec Irène Curie qui devint sa femme en 1926, collaboration qui, nous le verrons, devait être jalonnée de tant de travaux importants.

Vers 1930, malgré les nombreuses difficultés que cette hypothèse soulève, le noyau est considéré comme formé de protons et d'électrons. C'est alors qu'en Allemagne, Bothe et Becker montrent que l'irradiation par les rayons α du polonium d'éléments légers, tels le bore et le béryllium, donne naissance à des rayons plus pénétrants que les rayonnements connus à cette époque et qu'ils supposèrent cependant de nature électromagnétique. Deux ans après, ces expériences sont reprises et approfondies à Cambridge sous la direction de Chadwick et à l'Institut du Radium par Frédéric et Irène Joliot-Curie. Ceux-ci, utilisant une chambre d'ionisation à fenêtre très mince, puis une chambre de Wilson, montrent que le rayonnement pénétrant a la propriété de

projeter avec une grande vitesse les noyaux des atomes composant la substance traversée. Chadwick établissait peu de temps après que, pour expliquer ces projections, le rayonnement pénétrant devait être constitué de particules de masse voisine de celle du proton qu'il appela „neutrons". Par la suite, l'étude des différentes transmutations dues aux rayons α du polonium conduisait I. et F. Joliot à établir que la masse du neutron est supérieure à celle du proton.

Utilisant toujours les sources très intenses (Po+Be) qu'ils avaient préparées, I. et F. Joliot démontrent que les électrons positifs, signalés par plusieurs auteurs, sont dûs à l'absorption de rayons γ énergiques dans la matière, absorption d'autant plus grande que le numéro atomique de l'absorbant est plus élevé. Un cliché de chambre de Wilson où un électron négatif et un électron positif sont émis au même point les conduit à l'interprétation, désormais classique, du phénomène qu'ils dénomment „matérialisation" (1933): un photon de grande énergie rencontrant un noyau lourd se transforme en deux électrons de charges égales et opposées. Ainsi se trouvait expliqué ce qu'on appelait jusqu'alors l'absorption anormale de photons d'énergie plus grande que 1.1 MeV. C'est aussi la même année que F. Joliot donne la preuve expérimentale du phénomène, prévu par la théorie de Dirac, de l'annihilation de l'électron positif avec émission de deux photons d'environ 500 keV.

I. et F. Joliot avaient remarqué dans leurs recherches sur les neutrons que les transmutations par rayons α du bore, aluminium et magnésium s'accompagnaient d'émission d'électrons positifs. Cette émission, notaient-ils, „ne se produit qu'après quelques minutes d'irradiation et se poursuit quelque temps après la cessation de l'irradiation". C'était la découverte de la radioactivité artificielle qu'ils confirment par l'identification et la séparation chimique des éléments formés. L'importance de ce travail fut immédiatement comprise et en 1935 le prix Nobel de chimie venait récompenser les deux auteurs. Dès cette date F. Joliot pressent les développements que devait permettre la radioactivité artificielle: l'utilisation des indicateurs en biologie par exemple, mais surtout la possibilité de libération d'énergie nucléaire: „Nous sommes en droit de penser, dit-il dans sa conférence Nobel, que les chercheurs construisant ou brisant les éléments à volonté, sauront réaliser des transmutations à caractère explosif, véritables réactions chimiques à chaîne. Si de telles transformations arrivent à se propager dans la matière, on peut concevoir l'énorme libération d'énergie utilisable qui aura lieu".

A partir de cette époque Irène et Frédéric Joliot vont travailler chacun de leur côté. Comprenant la nécessité, si l'on veut développer en France la physique nucléaire, de construire des accélérateurs, F. Joliot s'y emploie tout d'abord au laboratoire de Synthèse Atomique du Centre National

de la Recherce Scientifique dont il a la charge en 1937, tandis que sa femme poursuit ses recherches à l'Institut du Radium. Nommé cette même année professeur au Collège de France, il met en construction avec l'aide de E. Lawrence et de Paxton un cyclotron de 7 MeV.

L'installation de ces nouveaux laboratoires progresse et des chercheurs de nationalités variées viennent y travailler. Lorsqu' en 1939 Hahn et Strassmann mettent en évidence par une méthode chimique le phénomène de la fission de l'uranium sous l'action des neutrons, F. Joliot imagine et réalise en quelques jours une expérience très simple qui, parallèlement aux recherches faites par Frisch, donnera la preuve physique de la rupture des noyaux: il recueille les fragments de fission arrachés par recul sur un support où il suivra leur évolution radioactive. Il met aussi en évidence ce phénomène à la chambre de Wilson. De nouveau une série de résultats importants sont établis en collaboration avec Halban et Kowarski: émission de neutrons lors de la fission, nombre et spectre énergétique des neutrons émis, possibilité de réactions en chaînes divergentes en utilisant des ralentisseurs tels que la paraffine, l'eau lourde, le graphite.

Mais c'est déjà la guerre. F. Joliot fait acheter par le gouvernement français le stock mondial d'eau lourde existant en Norvège. Les recherches sur la fission sont interrompues et après la défaite de juin 1940, Joliot, ses principaux collaborateurs partis en Angleterre, reste en France pour maintenir l'existence de ses laboratoires. C'est à ce moment qu'il entreprend au Collège de France, en collaboration avec des biologistes, des recherches sur le métabolisme de l'iode en utilisant des atomes marqués. Il n'était pas dans la nature de F. Joliot de rester insensible aux événements extérieurs: dès 1941 il prend une part active à la Résistance et en 1944 est obligé de passer dans la clandestinité.

A la libération de Paris, Joliot est nommé Directeur du Centre National de la Recherche Scientifique et donne une impulsion nouvelle à cet organisme en essayant de fournir aux travailleurs de toute discipline les moyens de développer les recherches fondamentales. Lorsque la France décide en 1946 de poursuivre les études sur la libération de l'énergie nucléaire et crée à cet effet le Commissariat à l'Energie Atomique, il en est nommé Haut-Commissaire. Sous sa direction et dans l'enthousiasme d'une équipe où se retrouvent nombre de ses anciens collaborateurs, les premiers services commencent à fonctionner au Fort de Châtillon. C'est là qu'en décembre 1948, diverge la première pile atomique française, Zoé. Le Commissariat s'agrandit très rapidement, un centre important d'études nucléaires est mis en construction à Saclay. Mais les idées politiques de F. Joliot, qu'il n'a jamais cachées et qui l'ont conduit, aux moments les plus dangereux de l'occupation, à devenir membre du parti communiste, ainsi que son action contre la bombe atomique, sont jugées par le gouvernement comme incompatibles avec sa fonction de

Haut-Commissaire. Il est révoqué en 1950. Très inquiet par les perspectives d'une guerre atomique, Joliot donne alors toute son activité au Conseil Mondial de la Paix qu'il anime comme il a animé tout ce à quoi il a participé.

Il continue pendant toutes ces années à s'occuper de ses laboratoires, en liaison avec l'Institut du Radium que dirige Irène Joliot-Curie. Devant l'expansion de la physique nucléaire, une autre tâche devient nécessaire: celle de donner à la recherche fondamentale française les moyens de progresser dans ce domaine. F. Joliot assiste sa femme dans l'élaboration des projets qui doivent conduire au regroupement des différents laboratoires dans le cadre de l'Université et lorsque Irène Joliot-Curie disparaît en mars 1956, c'est pour mener à bien cette œuvre qu'il accepte, quoique déjà gravement atteint par la maladie, de reprendre à la Faculté des Sciences de Paris la chaire de Physique Nucléaire et Radioactivité. Cachant parfois difficilement sa fatigue, il se dépense sans compter pour l'installation et le développement des nouveaux laboratoires à Orsay. Il aura la joie de voir réalisé enfin ce regroupement qu'il avait toujours souhaité.

S'il était absolument convaincu de la nécessité de doter la recherche en physique nucléaire des énormes moyens dont elle a besoin et s'employait à les lui faire accorder, F. Joliot avait néanmoins gardé le regret de ces expériences où avec peu de matériel, pourvu que l'on eût une profonde connaissance de la physique et ce sens expérimental qui lui était propre, on pouvait en quelques jours, quelques heures, faire une grande découverte. „Dans n'importe quelle expérience, avait-il coutume de dire, laissez toujours une fenêtre ouverte qui vous permettra de voir le phénomène nouveau, celui que vous n'avez pas prévu". Il craignait que la personnalité du chercheur ne soit écrasée par le déploiement d'appareils énormes, maintenant indispensables, et c'est cette préoccupation qu'il exprimait, peu de temps avant sa mort, lors du discours inaugural du Congrès de Physique Nucléaire de Paris.

Le vide immense qu'il laisse derrière lui fait sentir la place que son esprit généreux et enthousiaste lui avait acquis.

Principales Publications

Preuves expérimentales de l'existence du neutron (en coll. avec I. Curie), J. de Phys. **4** (1933) 21

Mass of the neutron (en coll. avec I. Curie), Nature **133** (1934) 721

Electrons de matérialisation et de transmutation (en coll. avec I. Curie), J. de Phys. **4** (1933) 494

Preuve expérimentale de l'annihilation des électrons positifs, J. de Phys. **5** (1934) 299

Production artificielle d'éléments radioactifs. Preuve chimique de la transmutation des éléments (en coll. avec I. Curie), J. de Phys. **5** (1934) 153

Sur la rupture explosive des noyaux U et Th sous l'action des neutrons, J. de Phys. **10** (1939) 159

Number of neutrons liberated in the nuclear fission of uranium induced by thermal neutrons (en coll. avec H. Halban et L. Kowarski) Nature **143** (1939) 939

Mise en évidence d'une réaction nucléaire en chaîne au sein d'une masse uranifère (en coll. avec H. Halban, L. Kowarski et F. Perrin) J. de Phys. **10** (1939) 428

Sur la possibilité de produire dans un milieu uranifère des réactions nucléaires en chaîne illimitée (en coll. avec H. Halban et L. Kowarski), pli cacheté du 30 octobre 1939, ouvert le 18 août 1948, C. R. Acad. des Sciences **229** (1949) 909

3.C:8.B *Nuclear Physics* **9** (1958/59) 6—21; © *North-Holland Publishing Co., Amsterdam*
Not to be reproduced by photoprint or microfilm without written permission from the publisher

BREMSSTRAHLUNG AND PAIR PRODUCTION OF PARTICLES OF SPIN $\frac{3}{2}$

A. A. KOMAR
P. N. Lebedev Physical Institute, USSR Academy of Sciences, Moscow

Received 21 May 1958

Abstract: Bremsstrahlung and pair production for spin $\frac{3}{2}$ particles are computed in the lowest perturbation theory approximation. The ultrarelativistic case is considered in detail. The importance of small impact parameters is demonstrated. For a pure Coulomb nuclear field the cross sections are proportional to E^6, where E is the incident particle or photon energy. The effect of deviation of the nuclear electric field from that of a point Coulomb source is discussed.

1. Introduction

Of the various phenomena which can be employed to determine the spins of new charged particles phenomena including electromagnetic interactions are the simplest and best studied and may be rather accurately calculated. This is true if one neglects some difficulties of principle connected with non-renormalizability of the higher approximations and with the restricted region of applicability of the lower approximation in the theories involving spin 1 or higher [1]). As a rule electromagnetic phenomena critically depend on the spin as is manifested in the angular distributions and energy dependence of the cross sections and this circumstance can be exploited in distinguishing between the various types of theories. It may be recalled that for the determination of the spin of the μ meson use was previously made of the peculiarities in the behaviour of the so-called "large bursts" produced by μ meson bremsstrahlung. Already at that time a comparison of the theoretical calculations for spins of 0, $\frac{1}{2}$, 1 with experiment indicated that the correct value should be $\frac{1}{2}$ (see e.g. ref.[2])) although this value could not be accepted conclusively because of the absence of calculations for a spin $\frac{3}{2}$. At present this question has been settled by the experiments of Lederman *et al.*[3]) which yielded for the μ meson a g factor equal to 2 and a spin equal to $\frac{1}{2}$ (for a $\frac{3}{2}$ spin one would have $g = \frac{2}{3}$ [5])).

In the present paper calculations of bremsstrahlung and pair production of spin $\frac{3}{2}$ particles have been performed with the aim of elucidating those peculiarities of these effects which can be exploited to study the spins of new particles and in particular of particles of the hyperon group. Though the latest experimental data point to a spin of $\frac{1}{2}$ for Σ^- particles [4]) the spin of the

cascade hyperon Ξ^- still remains unknown. Moreover, the method used in the spin determination is based on the assumption of conservation of angular momentum in the particle decays. This may be a very plausible hypothesis but as yet it is in need of a direct proof. Electromagnetic phenomena on the other hand permit one to determine the initial spin without making recourse to this assumption.

The technical aspects of the calculations for the specific case of bremsstrahlung are described in some detail in sections 2, 3, 4. In particular the deduction of the formula for summation over the polarization states of a spin $\frac{3}{2}$ particle is presented in sec. 3. The bremsstrahlung cross section and the pair production cross section which can easily be derived from it are discussed in section 5 for the ultrarelativistic case. In distinction to spin $\frac{1}{2}$ particles large angles and large momentum transfers to the nucleus predominate. In the case of a pure Coulomb field integration over the angles is carried out and the total cross sections are derived. The effect of finite nuclear dimensions is demonstrated. During the writing of this paper we became acquainted with the paper of Mathews [6]) in which an estimate of the bremsstrahlung cross section of spin $\frac{3}{2}$ particles is made for high energies by the Weizsäcker-Williams method under some auxiliary assumptions. An analysis of this work and a comparison with our results are given in § 5.1.

2. Bremsstrahlung Matrix Element

The first non-vanishing approximations of perturbation theory corresponding to the diagrams are taken into account in the present calculations.

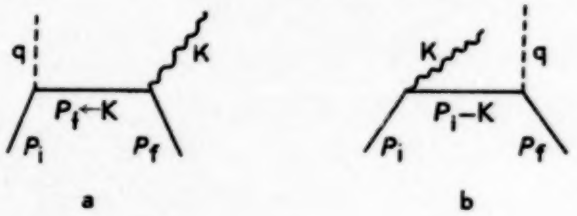

Fig. 1

The calculations are based on the inverse operator method discussed in Fainberg's paper [7]). Correct results can formally be obtained by applying the usual S-matrix procedure, providing that the expressions which appear for the propagation function $\langle \mathrm{T}(\psi(x)\bar{\psi}(x')) \rangle_0$ are replaced by an expression for the inverse operator as in the case of spin $\frac{3}{2}$ particles these expressions are not identical [7]). All calculations are carried out in spin-tensor notations [8]) which are technically very convenient since the calculations then reduce to work with the well-known Dirac matrices γ_m. The electromagnetic field is introduced in the Pauli-Fierz equation set by making the substitution

$$\frac{\partial}{\partial x_k} \to \frac{\partial}{\partial x_k} - ieA_k \quad (\hbar = c = 1),$$

the compatibility condition being fulfilled in this case.

In spin-tensor notations the corresponding equation set has the following form:

$$\begin{pmatrix} \left(\gamma_k \frac{\partial}{\partial x_k} + M\right)\delta_{mn} - \frac{1}{2}\gamma_m \frac{\partial}{\partial x_n} & -i\frac{\partial}{\partial x_m} + i\gamma_m\gamma_k \frac{\partial}{\partial x_k} \\ -i\frac{\partial}{\partial x_n} & -\frac{3}{2}\gamma_k \frac{\partial}{\partial x_k} + 3M \end{pmatrix} \begin{pmatrix} B^n \\ D \end{pmatrix} \tag{1}$$

$$= ie \begin{pmatrix} A_k\gamma_k\delta_{mn} - \frac{1}{2}\gamma_m A_n & -iA_m + \frac{i}{4}\gamma_m\gamma_k A_k \\ -iA_n & -\frac{3}{2}A_k\gamma_k \end{pmatrix} \begin{pmatrix} B^n \\ D \end{pmatrix}.$$

The symmetry condition is $\gamma_m B^m = 0$.

For convenience the spin-vector B^n and auxiliary spinor D are combined in a single column function and the equations are represented in matrix form. The symbols are the usual ones. We denote

$$\begin{pmatrix} B^n \\ D \end{pmatrix} = \Phi = \begin{pmatrix} \Phi_1 \\ \Phi_2 \\ \Phi_3 \\ \Phi_4 \\ \Phi_5 \end{pmatrix}.$$

Eq. (1) can then be written in the form

$$L_{\mu\rho}\Phi_\rho = A_{\mu\nu}\Phi_\nu \tag{1'}$$

(in all cases the Greek subscripts assume five values and the Latin four values). Here $L_{\mu\rho}$ is the left hand part, $A_{\mu\nu}$ corresponds to the interaction term. In the p representation the second order matrix element is

$$M^{(2)} = -i\bar{\Phi}_\alpha A_{\alpha\beta} K_{\beta\gamma} A_{\gamma\delta} \Phi_\delta \tag{2}$$

($\bar{\Phi}_\alpha = (\Phi^* \gamma_4)_\alpha$). Here $K_{\beta\gamma}$ is the inverse operator defined by the equation

$$L_{\alpha\beta} K_{\beta\gamma} = \delta_{\alpha\gamma}. \tag{3}$$

In the p-representation (p is the momentum of the internal line) its elements are [7])

$$K_{mn} = \frac{1}{i\gamma p + M}\left\{\delta_{mn} + \frac{p_n}{6M^2}\left[\gamma_m(\gamma p + 3iM) + 2p_m\right]\right\},$$

$$K_{m5} = -\frac{1}{3M^2}\left(p_m - \tfrac{1}{4}\gamma_m(\gamma p)\right), \quad K_{5n} = -\frac{1}{3M^2}p_n, \quad K_{55} = \frac{1}{6M^2}(i\gamma p + 2M). \tag{4}$$

The matrix element corresponding to diagrams a and b has the following form (account is taken of the fact that in the free state $D = 0$, and also $\gamma_m B^m = 0$, $\bar{B}^m \gamma_m = 0$).

$$M_{fi} = ie^2 a_4(q) \sqrt{\frac{2\pi}{k}} \bar{B}^m(p_f) \Big\{ \gamma e \frac{1}{i\gamma(p_f+k)+M}$$
$$\cdot \left[\delta_{mn} + \frac{(p_f+k)_k}{6M^2} \left(\gamma_m(\gamma(p_f+k)+3iM) + 2(p_f+k)_m \right) \right] (\gamma_4 \delta_{kn} - \tfrac{1}{2}\gamma_k \delta_{4n})$$
$$+ \frac{i}{3M^2} \gamma e [(p_f+k)_m - \tfrac{1}{4}\gamma_m \gamma(p_f+k)] \delta_{4n} + \frac{i}{3M^2} e_m (p_f+k)_k (\gamma_4 \delta_{kn} - \tfrac{1}{2}\gamma_k \delta_{4n})$$
$$- \frac{1}{6M^2} e_m (i\gamma(p_f+k)+2M) \delta_{n4} + \gamma_4 \frac{1}{i\gamma(p_i-k)+M}$$
$$\cdot \left[\delta_{mk} + \frac{(p_i-k)_k}{6M^2} \left(\gamma_m(\gamma(p_i-k)+3iM) + 2(p_i-k)_m \right) \right] (\gamma e \delta_{kn} - \tfrac{1}{2}\gamma_k e_n)$$
$$+ \frac{i}{3M^2} \gamma_4 [(p_i-k)_m - \tfrac{1}{4}\gamma_m \gamma(p_i-k)] e_n + \frac{i}{3M^2} \delta_{m4} (p_i-k)_k (\gamma e \delta_{kn} - \tfrac{1}{2}\gamma_k e_n)$$
$$- \frac{1}{6M^2} \delta_{m4} (i\gamma(p_i-k)+2M) e_n \Big\} B^n(p_i).$$

Here p_i and p_f are the initial and final 4 momenta of the decelerated particle, $k = (\mathbf{k}, ik)$ is the 4-momentum of the γ-quantum and $\mathbf{e}$ is its polarization vector. The quantity

$$a_4(q) = \int A_4^{\text{ext}}(x) e^{-iqx} \, d^4x$$

is the Fourier image of the external field, only the scalar component being assumed to differ from zero;

$$q = p_f + k - p_i.$$

If the external field is independent of the time x_0, then

$$a_4(q) = \int e^{iq_0 x_0} dx_0 \int A_4^{\text{ext}}(\mathbf{x}) e^{-i\mathbf{q}\cdot\mathbf{x}} d^3x = 2\pi\delta(q_0) a_4(\mathbf{q})$$

and therefore $M_{fi} = \tilde{M}_{fi} \delta(E_f + k - E_i)$. In the following only $\tilde{M}_{fi}$ will be involved and we shall therefore drop the ~ sign. After various simplifications the matrix element can finally be represented in the form

$$M_{fi} = -2\pi e^2 a_4(\mathbf{q}) \sqrt{\frac{2\pi}{k}} \bar{B}^m(p_f) \{ A\delta_{mn} + Bk_m \delta_{n4} + C\delta_{m4} k_n$$
$$+ De_m \delta_{n4} + E\delta_{m4} e_n + Fk_m (p_f+k)_n + G(k-p_i)_m k_n$$
$$+ He_m (p_f+k)_n + I(k-p_i)_m e_n \} B^n(p_i) = -2\pi e^2 a_4(\mathbf{q}) \bar{B}^m(p_f) T_{mn} B^n(p_i) \tag{5}$$

where

$$
\begin{aligned}
A &= \frac{1}{2(p_1k)}\gamma k\gamma e\gamma_4 + \frac{1}{2(p_1k)}\gamma_4\gamma e\gamma k + \gamma_4\left(\frac{(p_1e)}{(p_1k)} - \frac{(p_te)}{(p_tk)}\right)\\
B &= \frac{i\gamma e\gamma k}{3M(p_tk)} + \tfrac{2}{3}\gamma e\left(\frac{1}{M^2} + \frac{1}{(p_tk)}\right) + \frac{2i}{3M}\frac{(p_te)}{(p_tk)}\\
C &= -\frac{i\gamma k\gamma e}{3M(p_1k)} - \tfrac{2}{3}\gamma e\left(\frac{1}{M^2} - \frac{1}{(p_1k)}\right) + \frac{2i}{3M}\frac{(p_1e)}{(p_1k)}\\
D &= -\tfrac{2}{3}\gamma k\left(\frac{1}{M^2} + \frac{1}{(p_tk)}\right) - \frac{2i}{3M}\\
E &= \tfrac{2}{3}\gamma k\left(\frac{1}{M^2} - \frac{1}{(p_1k)}\right) - \frac{2i}{3M}\\
F &= \frac{\gamma k\gamma e\gamma_4}{3M^2(p_tk)} - \frac{i\gamma e\gamma_4}{3M(p_tk)} - \gamma_4\frac{2(p_te)}{3M^2(p_tk)}\\
G &= \frac{\gamma_4\gamma e\gamma k}{3M^2(p_1k)} + \frac{i\gamma_4\gamma e}{3M(p_1k)} + \gamma_4\frac{2(p_1e)}{3M^2(p_1k)}\\
H &= \frac{2}{3M^2}\gamma_4 + \frac{i}{3M(p_tk)}\gamma k\gamma_4\\
I &= -\tfrac{2}{3}M^2\gamma_4 - \frac{i}{3M(p_1k)}\gamma_4\gamma k.
\end{aligned}
\tag{6}
$$

This grouping of the terms seems to be the most rational one.

3. Summation over the Particle Spin States and Photon Polarizations

In order to derive the cross section the following expressions must be evaluated:

$$
\sum_{m_t,\,m_1,\,m_k}|M_{t1}|^2 = \frac{(2\pi)^3e^4}{k}|a_4(\mathbf{q})|^2\sum_{m_t,\,m_1,\,m_k}\bar{B}^i_{m_t}(p_t)_{ik}T\,B^k_{m_1}(p_1)\times\bar{B}^s_{m_1}(p_1)\bar{T}_{rs}\,B^r_{m_t}(p_t)
$$

where †

$$
\bar{T}_{rs} = \gamma_4T^+_{rs}\gamma_4.
$$

$B^k_{m_1}(p)$ is the solution of the free equation corresponding to the spin

† In terms of $T_{rs}{}^+$ containing δ_{r4} or δ_{s4} the sign should be changed in comparison with that of T_{rs}.

projection on the z-axis, $\sigma_z = m_1$. This in turn leads to the evaluation of expressions of the type

$$\sum_m [B_m{}^i(p)]_\nu [\bar{B}_m{}^k(p)]_{\nu'}$$

for a prescribed value of p (ν, ν' are spinor indices).

From the transformation properties of the indicated sum under a Lorentz transformation and from the fact that only two independent vectors γ_k, p_k exist for a free particle it follows that the expression under consideration can be represented in the form

$$\sum_m [B_m{}^i(p)]_\nu [\bar{B}_m{}^k(p)]_{\nu'} = [X(p^2, \gamma p)p_i p_k + Y(p^2, \gamma p)\delta_{ik} + Z(p^2, \gamma p)\gamma_k p_i + U(p^2, \gamma p)\gamma_i p_k + V(p^2, \gamma p)\gamma_i\gamma_k]_{\nu\nu'}$$

that is, as a $\nu\nu'$ element of the matrix defined in the square brackets. X, Y, Z, U, V are scalar functions of the invariants p^2 and γp. Obviously these functions are linear in γp as $(\gamma p)^2 = p^2$. Thus $X = \alpha(p^2) + \beta(p^2)\gamma p$, etc. The 10 unknown coefficients can be determined from the conditions $\gamma_i B^i = 0$, $\bar{B}^i \gamma_i = 0$, $p_i B^i = 0$, $\bar{B}^i p_i = 0$. This yields 8 relations between the coefficients, as the coefficients for an even and odd number of matrices should be considered independently (the separation can be easily performed by taking the trace of the initial expression). The two lacking relations can be derived from the normalization condition $B_m{}^{i*}(p)B^i_{m'}(p) = \delta_{mm'}$ or $\sum_m \bar{B}_m{}^i(p)B_m{}^i(p) = 4M/E_p$, and from the condition $(i\gamma p + M)B^i(p) = 0$ for a free particle, which yield two identical relations.

After determining the coefficients we obtain †

$$\sum_m [B_m{}^i(p)]_\nu [\bar{B}_m{}^k(p)]_{\nu'} = \frac{1}{6E_p M}\left[(M - i\gamma p)\left(\frac{2p_i p_k}{M} + 3M\delta_{ik} + i\gamma_i p_k - i\gamma_k p_i - M\gamma_i\gamma_k\right)\right]_{\nu\nu'}. \tag{7}$$

Thus,

$$\sum_{m_f, m_1, m_k} |M_{fi}|^2 \approx \sum_{m_f, m_1, m_k} [T_{ik}]_{\nu_1\nu_2}[B^k_{m_1}(p_i)]_{\nu_2}[\bar{B}^s_{m_1}(p_1)]_{\nu_3}[\bar{T}_{rs}]_{\nu_3\nu_4}[B^r_{m_f}(p_f)]_{\nu_4}[\bar{B}^i_{m_f}(p_f)]_{\nu_1}$$

$$= \sum_{m_k} [T_{ik}]_{\nu_1\nu_2}\left[\frac{M - i\gamma p_1}{6E_1 M}\left(\frac{2p_k{}^1 p_s{}^1}{M} + 3M\delta_{ks} + i\gamma_k p_s{}^1 - i\gamma_s p_k{}^1 - M\gamma_k\gamma_s\right)\right]_{\nu_2\nu_3}[\bar{T}_{rs}]_{\nu_3\nu_4}$$

$$\times \left[\frac{M - i\gamma p_f}{6E_f M}\left(\frac{2p_r{}^f p_i{}^f}{M} + 3M\delta_{ri} + i\gamma_r p_i{}^f - i\gamma_i p_r{}^f - M\gamma_r\gamma_i\right)\right]_{\nu_4\nu_1}$$

$$= \frac{1}{36E_1 E_f M^2}\sum_{m_k} \mathrm{tr}\left\{T_{ik}(M - i\gamma p_1)\left(\frac{2p_k{}^1 p_s{}^1}{M} + 3M\delta_{ks} + i\gamma_k p_s{}^1 - i\gamma_s p_k{}^1 - M\gamma_k\gamma_s\right)\right.$$

$$\left.\times \bar{T}_{rs}(M - i\gamma p_f)\left(\frac{2p_r{}^f p_i{}^f}{M} + 3M\delta_{ri} + i\gamma_r p_i{}^f - i\gamma_i p_r{}^f - M\gamma_r\gamma_i\right)\right\}.$$

† After completion of this work we became acquainted with the paper of Milford [19]) in which a similar method was employed to obtain an expression for the projection operator Λ^{ik} which removes the spin $\frac{1}{2}$ states from B^k. When multiplied from the right by the usual Casimir operator $(m - i\gamma p)/2E_p$ this operator coincides with our expression (7).

The dependence of the expression T_{ik} on the polarization vector can be represented as follows (see (5) and (6)):

$$T_{ik} = e_l T_l^{ik} + e_i T'_k + e_k T''_i = e_l (T_l^{ik} + \delta_{li} T'_k + \delta_{lk} T''_i) = e_l \hat{T}_l^{ik}.$$

In virtue of gauge-invariance the substitution $e_l \to k_l$ yields $k_l \hat{T}_l^{ik} = 0$. As in the case of spin $\frac{1}{2}$ this permits one to extend summation over l from 1 to 4 without affecting the result.

We finally obtain

$$\sum_{m_1, m_f, m_k} |M_{fi}|^2 = \frac{(2\pi)^3 e^4}{k} \frac{|a_4(\mathbf{q})|^2}{36 E_1 E_f M^2} \operatorname{tr} \left\{ \hat{T}_l^{ik} (M - i\gamma p_1) \left(\frac{2 p_k^1 p_s^1}{M} + 3M\delta_{ks} \right.\right.$$
$$+ i\gamma_k p_s^1 - i\gamma_s p_k^1 - M\gamma_k \gamma_s \Big) \hat{T}_l^{rs} (M - i\gamma p_f) \left(\frac{2 p_r^f p_i^f}{M} + 3M\delta_{ri} \right. \quad (8)$$
$$\left.\left. + i\gamma_r p_i^f - i\gamma_i p_r^f - M\gamma_r \gamma_i \Big) \right\}.$$

It should be mentioned that extension of the summation to all 4 photon polarizations does not give such an appreciable simplification for a spin $\frac{3}{2}$ as for a spin $\frac{1}{2}$ as regards the decrease of the number of matrices in the trace, as e_l is related not only to the matrices γ_l, but also to other vectors.

4. Method of Calculation

For the subsequent calculations it is important to note that simple term-by-term multiplication of the expressions under the tr sign involves an immense amount of work and it is therefore very important to group the terms rationally at each intermediate stage of the calculations. For this reason we shall consider this aspect of the calculations in some detail.

We introduce the notations

$$\begin{aligned} U_l &= p_m^f \hat{T}_l^{mn} p_n^f, & X_l^s &= p_m^f \hat{T}_l^{ms} \\ V_l &= \gamma_m \hat{T}_l^{mn} p_n^1, & X_l^{s'} &= \hat{T}_l^{sn} p_n^1 \\ V'_l &= p_m^f \hat{T}_l^{mn} \gamma_n, & Y_l^s &= \gamma_m \hat{T}_l^{ms} \\ W_l &= \gamma_m \hat{T}_l^{mn} \gamma_n, & Y_l^{s'} &= \hat{T}_l^{sn} \gamma_n. \end{aligned} \quad (9)$$

It should be noted that the matrices in $\hat{\tilde{T}}_l^{rs}$ are arranged in an inverse order with respect to $\hat{T}_l^{rs}$ †.

Taking into account moreover that tr $(\gamma_i \gamma_k \gamma_l \gamma_m)$ = tr $(\gamma_m \gamma_l \gamma_k \gamma_i)$ we can regroup the expression under the tr sign in formulae (8) as follows:

† In the following $\tilde{T}$ will designate the inverse order of the matrices in expression T and not the expression $\gamma_4 T^+ \gamma_4$, which can differ in sign.

$$\mathrm{tr}\Big\{8(2U_l+iM(V_l+V'_l))\bar{U}_l+4i\left(-\frac{2U_l}{M}+2iV'_l-iV_l\right)\gamma p_1\bar{U}_l$$
$$+4i\left(-\frac{2U_l}{M}+2iV_l-iV'_l\right)\bar{U}_l\gamma p_t+\frac{4}{M}\left(-\frac{U_l}{M}+i(V_l+V'_l)\right)\gamma p_1\bar{U}_l\gamma p_t$$
$$+2V_l(i\gamma p_1-2M)\bar{V}_l(M+i\gamma p_t)+2(i\gamma p_t-2M)V'_l(M+i\gamma p_1)\bar{V}'_l$$
$$-2V'_l(M+i\gamma p_1)\bar{V}_l(M+i\gamma p_t)$$
$$+(-2U_l-2iM(V_l+V'_l)+M^2W_l)(M+i\gamma p_1)\bar{W}_l(M+i\gamma p_t) \qquad (10)$$
$$+3M\left[2\left(2-\frac{i\gamma p_t}{M}\right)X_l^s(M-i\gamma p_1)\bar{X}_l^s+2X_l^{s'}\left(2-\frac{i\gamma p_1}{M}\right)\bar{X}_l^{s'}(M-i\gamma p_t)\right.$$
$$+2iX_l^s(M-i\gamma p_1)\bar{Y}_l^s(M+i\gamma p_t)+2iX_l^{s'}(M+i\gamma p_1)\bar{Y}_l^{s'}(M-i\gamma p_t)$$
$$\left.-MY_l^s(M-i\gamma p_1)\bar{Y}_l^s(M+i\gamma p_t)-MY_l^{s'}(M+i\gamma p_1)\bar{Y}_l^{s'}(M-i\gamma p_t)\right]$$
$$+9M^2\hat{T}_l^{rs}(M-i\gamma p_1)\hat{\bar{T}}_l^{rs}(M-i\gamma p_t)\Big\}.$$

Furthermore, the expression $\hat{T}_l^{ik}$ possesses the following type of symmetry. If we perform the substitution $i \rightleftarrows k$, $p_t \rightleftarrows -p_1$, change the sign if the number of matrices is odd, and read all matrix combinations in the inverse order, we find that $\hat{T}_l^{ik}$ will change into itself (see (5) and (6)). It can therefore be represented as follows:

$$\hat{T}_l^{ik} = (\tau_l^{ik})_{\text{even}}+(\tau_l^{ik})_{\text{odd}}+(\tau_l^{ki})'_{\text{even}}+(\tau_l^{ki})'_{\text{odd}} = \tau_l^{ik}+\tau_l^{ki'}.$$

The substitution $i \rightleftarrows k$, $p_t \rightleftarrows -p_1$, and change of the sign for odd number of matrices yield

$$(\tau_l^{ik})_{\text{even}} \rightleftarrows (\bar{\tau}_l^{ki})'_{\text{even}}$$
$$(\tau_l^{ik})_{\text{odd}} \rightleftarrows (\bar{\tau}_l^{ki})'_{\text{odd}}$$

or

$$\tau_l^{ik} \rightleftarrows \bar{\tau}_l^{ki'}.$$

The expressions $U_l = u_l+u'_l$, $W_l = w_l+w'_l$ derived from $\hat{T}_l^{ik}$ possess analogous properties and V_l and $\bar{V}'_l$ under the corresponding substitution change into each other. The X_l^s, Y_l^s go over to $\bar{X}_l^{s'}$, $\bar{Y}_l^{s'}$ if under the indicated transformation the sign of an even number of matrices is changed. This circumstance can be used to reduce the amount of the calculations substantially.

Indeed the expressions under the tr sign in formula (10) can be identified as one of the following types:

First type:

$$(\tau_l+\tau'_l)(a+i\gamma p_1 b)(\bar{\pi}_l+\bar{\pi}'_l)(a+i\gamma p_t b).$$

This expression breaks up into two parts:

$$\begin{aligned}\mathrm{tr}\,[&a^2(\tau_l\bar{\pi}_l+\tau'_l\bar{\pi}_l)-b^2(\tau_l\gamma p_l\bar{\pi}_l\gamma p_l+\tau'_l\gamma p_1\bar{\pi}_l\gamma p_l)\\&+iab(\tau_l\gamma p_1\bar{\pi}_l+\tau'_l\gamma p_1\bar{\pi}_l+\tau_l\bar{\pi}_l\gamma p_l+\tau'_l\bar{\pi}_l\gamma p_l)]\\&+\mathrm{tr}\,[a^2(\tau'_l\bar{\pi}'_l+\tau_l\bar{\pi}'_l)-b^2(\tau'_l\gamma p_1\bar{\pi}'_l\gamma p_l+\tau_l\gamma p_1\bar{\pi}'_l\gamma p_l)\\&+iab(\tau'_l\gamma p_1\bar{\pi}'_l+\tau_l\gamma p_1\bar{\pi}'_l+\tau'_l\bar{\pi}'_l\gamma p_l+\tau_l\bar{\pi}'_l\gamma p_l)],\end{aligned}$$

the latter being obtained from the former by the simple substitution $p_l \rightleftarrows -p_1$, as can readily be verified after simple transformations of the traces and taking into account that all combinations involving an odd number of matrices fall out.

Second type:

$$\sigma_l(\gamma p_1)(\bar{\pi}_l+\bar{\pi}'_l)+\sigma'_l(\bar{\pi}_l+\bar{\pi}'_l)(\gamma p_l).$$

Third type:

$$\rho_l(a+i\gamma p_1 b)\bar{\sigma}_l(c+i\gamma p_l d)+\rho'_l(c+i\gamma p_1 \mathrm{d})\bar{\sigma}'_l(a+i\gamma p_l b).$$

Similar considerations show that in these cases also the result obtained by taking the trace of the second term can be derived from that of the first by substituting in it $p_l \rightleftarrows -p_1$.

Fourth type:

$$\rho_l(a+i\gamma p_1 b)\bar{\rho}'_l(a+i\gamma p_1 b)=a^2\rho_l\bar{\rho}'_l-b^2\rho_l\gamma p_1\bar{\rho}'_l\gamma p_l+iab\rho_l\gamma p_1\bar{\rho}'_l+iab\rho_l\bar{\rho}'_l\gamma p_l.$$

In this case the trace of the third term can be obtained from that of the fourth term by substituting $p_l \rightleftarrows -p_1$.

On the basis of the preceding the fundamental expression (10) can be rewritten as follows:

$$\begin{aligned}\mathrm{tr}\Big\{&8(2U_l+iM(V_l+V'_l))\bar{u}_l+4i\left(-\frac{2U_l}{M}+2iV'_l-iV_l\right)\gamma p_1\bar{U}_l\\&+\frac{4}{M}\left(-\frac{U_l}{M}+i(V_l+V'_l)\right)\gamma p_1\bar{u}_l\gamma p_l+2V_l(i\gamma p_1-2M)\bar{V}_l(M+i\gamma p_l)\\&-2(M^2V'_l\bar{V}_l-V'_l\gamma p_1\bar{V}_l\gamma p_l+iMV'_l\gamma p_1\bar{V}_l)\\&+(-2U_l-2iM(V_l+V'_l)+M^2W_l)(M+i\gamma p_1)\bar{\omega}_l(M+i\gamma p_l)\qquad(11)\\&+3M\left[2\left(2-\frac{i\gamma p_l}{M}\right)X_l^s(M-i\gamma p_1)\bar{X}_l^s+2iX_l^s(M-i\gamma p_1)\bar{Y}_l^s(M+i\gamma p_l)\right.\\&\left.-MY_l^s(M-i\gamma p_1)\bar{Y}_l^s(M+i\gamma p_l)\right]+9M^2\hat{T}_l^{rs}(M-i\gamma p_1)\hat{\bar{\tau}}_l^{rs}(M-i\gamma p_l)\Big\}\\&+\text{ the expression obtained by substituting } p_l \rightleftarrows -p_1.\end{aligned}$$

Only the first part need be evaluated.

5. Results

5.1. BREMSSTRAHLUNG

The differential cross section for this process is related to $\sum_{m_f, m_1, m_k} |\tilde{M}_{fi}|^2$ as follows:

$$d\sigma = \tfrac{1}{4}\Big(\sum_{m_f, m_1, m_k} |\tilde{M}_{fi}|^2\Big) \frac{d^3k d^3p_f}{(2\pi)^6} \frac{E_1}{p_1} \frac{\delta(E_f+k-E_1)}{2\pi}$$

$$= \tfrac{1}{4} \cdot \frac{1}{(2\pi)^7} E_1 E_f \frac{p_f}{p_1} \Big(\sum_{m_f, m_1, m_k} |\tilde{M}_{fi}|^2\Big) d^3k \, d\Omega_f .$$

After tedious calculations we obtain an expression for $\sum_{m_f, m_1, m_k} |\tilde{M}_{fi}|^2$ which is very complicated and will not be presented here. We restrict ourselves in the future to the extreme relativistic case $E_1 \gg M$. In this case the differential cross section has the form

$$\frac{d\sigma}{d\Omega_k d\Omega_f dk} \approx \frac{e^4}{(2\pi)^4} \frac{4}{81M^8} \frac{p_f}{p_1} k |a_4(\mathbf{q})|^2 (p_1k)(p_fk)\{2[(p_1k)(p_4{}^fp_4{}^f)^2 - (p_fk)(p_4{}^1p_4{}^1)^2]$$
$$+2p_4{}^1p_4{}^f(2(p_fp_1)+(p_1k)-(p_fk))+2p_4{}^fk_4((p_fk)-(p_fp_1))$$
$$+2p_4{}^1k_4((p_fp_1)+(p_1k))-2(p_fp_1)^2-(p_1k)^2-(p_fk)^2-2(p_fp_1)((p_1k)-(p_fk))\}. \tag{12}$$

Denoting the angle between $\mathbf{p}_1$ and $\mathbf{k}$ by θ_k, between $\mathbf{p}_f$ and $\mathbf{p}_1$ by θ_f and between $\mathbf{p}_f$ and $\mathbf{k}$ by ψ where

$$\cos\psi = \cos\theta_k \cos\theta_f + \sin\theta_k \sin\theta_f \cos\varphi$$

and φ is the angle between the planes p_1, k and p_1, p_f we obtain after some transformations

$$\frac{d\sigma}{d\Omega_k d\Omega_f dk} = \frac{e^4}{(2\pi)^4} \frac{4}{81M^8} p_f{}^2k^3 |a_4(\mathbf{q})|^2 \Big(\cos\theta_k - \frac{E_1}{p_1}\Big)\Big(\cos\psi - \frac{E_f}{p_f}\Big)$$
$$\times[2E_1{}^2E_f{}^2 - 2p_f{}^2p_1{}^2\cos^2\theta_f + E_1{}^2k^2 - p_1{}^2k^2\cos^2\theta_k + E_f{}^2k^2 - p_f{}^2k^2\cos^2\psi$$
$$+2p_fp_1\cos\theta_f(p_fk\cos\psi - p_1k\cos\theta_k) - 2E_f{}^2p_1k\cos\theta_k + 2E_i{}^2p_fk\cos\psi]. \tag{13}$$

For not to very large † values of k, $E_f \approx p_f$ and since $E_1 \approx p_1$ one finds that for angles θ_k and θ_f close to zero (and hence ψ close to zero) the cross section is small compared with those values which it assumes for angles in the vicinity of 90°. Now small angles correspond to small values of $|\mathbf{q}| \approx |p_f+k-p_1| \approx M^2k/2p_fp_1$ and hence large impact parameters $r = 2p_fp_1/M^2k \gg 1/M$. For angles $\approx 90°$, $|q| \approx p_1$ and the impact parameter $r = 1/p_1 \ll 1/M$. For angles close to 180° and somewhat smaller r the cross section is again small but this circumstance does not change the qualitative picture. It is important that in our case small angles yield an insignificant

† It turns out (see (16) below) that the bremsstrahlung spectrum vanishes near the upper limit and the high energy photons do not contribute appreciably to the total cross section.

contribution to the total cross section and large impact parameters (and therefore screening of the nuclear field) can be neglected. In contrast, it should be taken into account that in the important region of small impact parameters the field of the nucleus may considerably differ from a point Coulomb field. Thus for a spin $\frac{3}{2}$ the entire situation is exactly opposite to that for a spin $\frac{1}{2}$.

From methodical consideration and for the sake of simplicity we shall first consider the case of a pure Coulomb field. In this case

$$a_4(\mathbf{q}) = -i\frac{4\pi Ze}{q^2}$$

and the cross section assumes the following form:

$$\frac{d\sigma}{d\Omega_k d\Omega_f dk} = \frac{Z^2e^6}{(2\pi)^2}\frac{16}{81M^8}p_f^2k^3\frac{1}{q^4}(\cos\theta_k-1)\left(\cos\psi-\frac{E_f}{p_f}\right) \tag{14}$$
$$\times[p_f^2(\mathbf{p}_1-\mathbf{k})^2-(\mathbf{p}_f\cdot(\mathbf{p}_1-\mathbf{k}))^2+p_1^2(\mathbf{k}+\mathbf{p}_f)^2-(\mathbf{p}_1\cdot(\mathbf{p}_f+\mathbf{k}))^2].$$

Small terms of the order of $(M/E_1)^2$ with respect to the remaining terms have been neglected here.

For subsequent integration over the angles it will be convenient to change the variables. Denote $\mathbf{k}-\mathbf{p}_1=\boldsymbol{\kappa}$. We shall measure the angle of $\mathbf{p}_f$ with respect to the direction of $\boldsymbol{\kappa}$ and denote it by θ'_f. The corresponding azimuthal angle measured with respect to the p_1, k plane will be denoted by φ'_f. In the new variables θ'_f, φ'_f, θ_k, φ_k

$$\cos\psi = \frac{k-p_1\cos\theta_k}{\kappa}\cos\theta'_f+\frac{p_1}{\kappa}\sin\theta'_f\sin\theta_k\cos\varphi'_f \tag{15a}$$

$$\cos\theta_f = \frac{k\cos\theta_k-p_1}{\kappa}\cos\theta'_f+\frac{k}{\kappa}\sin\theta'_f\sin\theta_k\cos\varphi'_f \tag{15b}$$

$$q^2 = \kappa^2+p_f^2+2p_f\kappa\cos\theta'_f. \tag{15c}$$

Integrating over φ'_f and φ_k, substituting $d(\cos\theta'_f)=dq^2/2p_f\kappa$ where $\cos\theta_f$ is defined in (15c) and grouping the terms we obtain

$$d\sigma = Z^2e^6\frac{16}{81M^8}p_f^2k^3dk\int_0^\pi\frac{(\cos\theta_k-1)\sin\theta_k d\theta_k}{2p_f\kappa}\int_{(\kappa-p_f)^2}^{(\kappa+p_f)^2}\frac{dq^2}{q^4}$$
$$\times[Aq^6+Bq^4+Cq^2+D] = Z^2e^6\frac{16}{81M^8}p_f^2k^3dk\int_0^\pi(\cos\theta_k-1)\sin\theta_k d\theta_k$$
$$\times\left[2A(\kappa^2+p_f^2)+2B+\frac{C}{\kappa p_f}\ln\frac{\kappa+p_f}{\kappa-p_f}+\frac{2D}{(\kappa^2-p_f^2)^2}\right].$$

Here A, B, C, D are fractional-rational functions of $\cos\theta_k$. Integration with

respect to the angle θ_k is elementary but cumbersome. The final result of the integration is

$$\begin{aligned}
d\sigma = \frac{Z^2e^6}{81M^8}p_f\frac{dk}{p_i^2}\Big\{&\frac{p_i}{p_f}\ln\frac{E_f-p_f}{E_f+p_f}\left[-p_f^6+p_f^4(3k^2-\tfrac{7}{3}p_i^2)\right.\\
&-p_f^2(\tfrac{61}{15}p_i^4+\tfrac{14}{3}p_i^2k^2+3k^4)+\tfrac{73}{105}p_i^6+\tfrac{137}{15}p_i^4k^2+7p_i^2k^4+k^6]\\
&+8\frac{k}{p_f}\ln\frac{p_i(E_f+p_f)}{Mk}\left[p_f^6+p_f^4(\tfrac{8}{3}k^2-p_i^2)+p_f^2(\tfrac{11}{15}k^4-\tfrac{8}{3}p_i^2k^2-p_i^4)\right.\\
&+p_i^6+\tfrac{8}{3}p_i^4k^2+\tfrac{11}{15}p_i^2k^4+\tfrac{2}{35}k^6]+\ln\frac{E_i+p_i}{E_i-p_i}[\tfrac{73}{105}p_f^6+p_f^4(\tfrac{137}{15}k^2-\tfrac{61}{15}p_i^2)\\
&+p_f^2(k^2-p_i^2)(\tfrac{7}{3}p_i^2+7k^2)+(k^2-p_i^2)^3]\\
&-\tfrac{8}{105}p_ik[121p_f^4+p_f^2(254k^2-418p_i^2)+121p_i^4+254p_i^2k^2+93k^4]\Big\}.
\end{aligned} \tag{16}$$

In contrast to particles of spin $\frac{1}{2}$ the bremsstrahlung spectrum defined by the major energy terms considered by us, does not diverge at the lower limit boundary. The infrared divergence appears only in the minor terms and is of the usual dk/k type. Near the upper boundary of the spectrum the cross section tends to zero. Integration over the bremsstrahlung spectrum yields (retaining the main terms in p_i/M)

$$\sigma = Z^2e^6\frac{17}{3645}\frac{p_i^6}{M^8}. \tag{17}$$

Thus in the ultra-relativistic case the cross section increases proportionally to the sixth power of the energy of the incident particle in distinction to the logarithmic growth for spin $\frac{1}{2}$ particles. The formula presented here cannot, of course, be used for very high energies because owing to the rapid increase of the cross section the lower approximation of perturbation theory becomes invalid [1]). For an energy of 10 M, where M is of the order of the hyperon mass,

$$\sigma \approx Z^2\, 8\times 10^{-31}\,\mathrm{cm}^2.$$

The infinite growth of the cross section with energy is a consequence of use of a pure Coulomb field. As was mentioned above, this type of approximation is, strictly speaking, incorrect and the finite dimensions of the nuclear charge must be taken into account. This effectively means the introduction of a form factor which reflects the distribution of the charge density:

$$a_4(\mathbf{q}) = -i\frac{4\pi Ze}{q^2}F(q^2)$$

where

$$F(q^2) = \int \rho(\mathbf{r})e^{i\mathbf{q}\cdot\mathbf{r}}d\mathbf{r}, \quad \int \rho(\mathbf{r})d\mathbf{r} = 1.$$

Thus the cross section is multiplied by the extra factor $[F(q^2)]^2$. The appearance of this factor substantially changes the behaviour of the cross section at high energies.

As an example we consider the following expressions for $F(q^2)$:

$$\text{a)} \quad F(q^2) = \frac{1}{1+q^2R^2} \qquad \rho(r) = \frac{1}{4\pi R^2}\frac{e^{-r/R}}{r}$$

$$\text{b)} \quad F(q^2) = \frac{1}{(1+q^2R^2)^2} \quad \text{relating to} \quad \rho(r) = \frac{1}{8\pi R^3}e^{-r/R} \tag{18}$$

$$\text{c)} \quad F(q^2) = e^{-\frac{1}{4}q^2R^2} \qquad \rho(r) = \frac{1}{\pi^{\frac{1}{2}}R^3}e^{-r^2/R^2}.$$

That part of the cross section which is represented by the factor before $[F(q^2)]^2$ increases with the energy as $\approx p_1^6$. (This can easily be seen from (14) without performing the integration over the angles if the dimensionless quantity $\varepsilon = k/p_1$ is introduced and it is taken into account that with a good accuracy $p_f = (1-\varepsilon)p_1$. Then p_1^6 can be factored out and integrals of dimensionless quantities remain). If it be taken into account that the main contribution to the cross section is due to large angles for which $q \approx p_1$, one finds that the energy dependence of the cross section in the ultra relativistic limit for cases (18a, b, c) will be the following:

$$\text{a)} \quad \sigma \approx p_1^2,$$

$$\text{b)} \quad \sigma \approx \frac{1}{p_1^2}, \tag{19}$$

$$\text{c)} \quad \sigma \approx p_1^6 e^{-\frac{1}{4}p_1^2R^2};$$

that is, it varies over a broad range depending on the choice of $F(q^2)$. This indicates that an exact knowledge of the nuclear charge distribution is very important for the process under consideration. At any rate, correct account of charge distribution ensures a reasonable behaviour of the cross section at infinitely large energies.

In conclusion we shall compare our results with the calculations of Mathews [6]) carried out by the Weizsäcker-Williams method. There a logarithmic energy dependence of the cross section was derived. This discrepancy with respect to our results obtained for a pure Coulomb field is not surprising inasmuch as the Weizsäcker-Williams method is not valid for small impact parameters and is essentially restricted by parameters $\approx 1/M$, whereas it is just the $r \ll 1/M$ which are significant in the cross section. Another difference is due to the fact that in Mathew's calculations the integral over the virtual quantum frequencies was cut off at the upper limit. However, $\omega_{max} \approx E_1/r_{min}M$ significantly depends not only on the

energy of the incident particle but on the minimum impact parameter as well. Mathew's expression for the cross section is $\approx \omega_{\max}^3 \ln E_1$, where $\omega_{\max}$ is assumed to be a constant. If we take into account that the essential impact parameters $v_{\min} \approx 1/E_1$ and substitute in Mathew's expression $\omega_{\max} = E_1/r_{\min} M = E_1^2/M$ (which, it is true, does not correspond to the conditions of applicability of the method employed by him) we immediately obtain $\sigma \approx E_1^6 \ln E_1$, which agrees with the result obtained by us.

5.2. PAIR PRODUCTION

The differential cross section for pair production of particles of spin $\frac{3}{2}$ and mass M can be obtained in the usual manner by multiplying the bremsstrahlung cross section by the ratio of the number of final states in the two cases and replacing in the square of the matrix element p_1 by p_- and p_f by $-p_+$. For $k \gg M$ the expression for the cross section has the form

$$\begin{aligned}
&\frac{d\sigma}{d\Omega_+ d\Omega_- dE_+} \\
&\quad \approx \frac{e^4}{(2\pi)^4} \frac{8}{81M^8} |a_4(\mathbf{q})|^2 \frac{p_- p_+}{k} (p_- k)(p_+ k)\{-2[E_+^2 (p_- k) + E_-^2 (p_+ k)] \\
&\quad +2E_- E_+ ((p_- k) + (p_+ k) - 2(p_+ p_-)) + 2E_+ k((p_+ p_-) - (p_+ k)) \qquad (20) \\
&\quad -2E_- k((p_- k) - (p_+ p_-)) - 2(p_+ p_-)^2 - (p_- k)^2 - (p_+ k)^2 \\
&\quad +2(p_+ p_-)((p_- k) + (p_+ k))\},
\end{aligned}$$

$$\mathbf{q} = \mathbf{k} - \mathbf{p}_- - \mathbf{p}_+.$$

The extra factor 2 (as compared to (12)) is due to the fact that the averaging in the present case is performed over the two polarizations of the incident γ-quantum, in distinction to the 4 polarization states of particles possessing a spin $\frac{3}{2}$. It is not difficult to see that all considerations regarding the magnitude of the transferred momentum q and the significant impact parameters can easily be applied to this case also. Indeed, due to the presence of terms containing $(p_- k)$, $(p_+ k)$ or $(p_+ p_-)$ the cross section is small for small angles as practically always $E_- \approx p_-$, $E_+ \approx p_+$. For small angles

$$|\mathbf{q}| \approx \frac{M^2 k}{2 p_- p_+}, \quad r \gg \frac{1}{M},$$

and for large angles

$$|\mathbf{q}| \approx k, \quad r \ll \frac{1}{M},$$

and small impact parameters play the main role. Integration over the angles in the case of a pure Coulomb field can be performed by applying a substitu-

tion similar to (15); this yields

$$\frac{d\sigma}{dE_+} = Z^2e^6 \frac{2}{81M^8} \frac{p_+}{k^2} \Big\{ \frac{p_-}{p_+} \ln \frac{E_+ + p_+}{E_+ - p_+} [p_+^6 - p_+^4(3k^2 - \tfrac{7}{3}p_-^2)$$
$$+ p_+^2(\tfrac{61}{15}p_-^4 + \tfrac{14}{3}p_-^2k^2 + 3k^4) - \tfrac{73}{105}p_-^6 - \tfrac{137}{15}p_-^4k^2 - 7p_-^2k^4 - k^6]$$
$$+ 8\frac{k}{p_+} \ln \frac{E_+E_- + p_+p_- + M^2}{Mk} [p_+^6 + p_+^4(\tfrac{8}{3}k^2 - p_-^2)$$
$$+ p_+^2(\tfrac{11}{15}k^4 - \tfrac{8}{3}p_-^2k^2 - p_-^4) + p_-^6 + \tfrac{8}{3}p_-^4k^2 + \tfrac{11}{15}p_-^2k^4 + \tfrac{2}{35}k^6] \qquad (21)$$
$$+ \ln \frac{E_- + p_-}{E_- - p_-} [-\tfrac{73}{105}p_+^6 + p_+^4(\tfrac{61}{15}p_-^2 - \tfrac{137}{15}k^2)$$
$$- p_+^2(k^2 - p_-^2)(\tfrac{7}{3}p_-^2 + 7k^2) - (k^2 - p_-^2)^3]$$
$$+ \tfrac{8}{105}p_-k[121p_+^4 + p_+^2(254k^2 - 418p_-^2) + 121p_-^4 + 254p_-^2k^2 + 93k^4] \Big\}.$$

The total cross section for pair production is

$$\sigma \approx Z^2e^6 \tfrac{184}{25515} \frac{k^6}{M^8}. \qquad (22)$$

For $k = 10M$ and an M of the order of the hyperon mass this yields

$$\sigma \approx Z^2 \times 10^{-30} \text{ cm}^2.$$

However, the approximate nature of this value should be kept in mind as the behaviour of the cross section at high energies may significantly change if the finite size of the nucleus is taken into account, and in reality it may be smaller.

6. Conclusion

The analysis carried out in the present paper shows that spin $\frac{3}{2}$ particles possess some peculiarities which spin $\frac{1}{2}$ particles do not possess. Thus, small impact parameters play an important role in bremsstrahlung and pair production and care should be exercised in taking into account the finite size of the nucleus. As far as the angular distributions are concerned this signifies large emission angles of the bremsstrahlung quantum relative to the direction of motion of the particle and large angles between the pair components and the direction of the γ-quantum.

In the case of a pure Coulomb field the cross sections increase rapidly with energy, in distinction to the logarithmic growth for spin $\frac{1}{2}$ particles. The infrared divergence does not occur in the bremsstrahlung spectrum at very high energies. It is interesting to note that a very similar situation is encountered in the case of spin one [9]). It is possible that some of the afore-

mentioned peculiarities are related to the approximations made in the calculations but the others should be of a more general significance. In particular, if a region of applicability of formula (17) exists the rapid increase of the bremsstrahlung cross section with energy should influence the energy losses of the particle in matter. This may be of some significance in investigations of the spins of new particles.

In conclusion I express my deep appreciation to Professor M. A. Markov for suggesting the subject of this paper and for helpful advice and continued interest in the work.

References

1) L. D. Landau, JETP **10** (1940) 718
2) R. E. Marshak, Meson Physics (McGraw-Hill Book Company, 1952) pp. 219–226
3) L. Lederman *et al.*, Phys. Rev. **105** (1957) 1415
4) F. Eisler, R. Plano, A. Prodell, N. Samios, M. Schwartz, I. Steinberger *et al.*, Nuovo Cimento **7** (1958) 222
5) F. I. Belinfante, Phys. Rev. **92** (1953) 997
6) I. Mathews, Phys. Rev. **102** (1956) 270
7) V. Ya. Fainberg, JETP **25** (1953) 644; Dissertation FIAN (1953)
8) V. L. Ginzburg, JETP **12** (1942) 425
9) R. F. Christy and S. Kusaka, Phys. Rev. **59** (1941) 405
10) Milford, Phys. Rev. **98** (1955) 1488

1.E.1:
2.D

Nuclear Physics 9 (1958/59) 22—31; © *North-Holland Publishing Co., Amsterdam*
Not to be reproduced by photoprint or microfilm without written permission from the publisher

THE CHARACTERISTIC LEVEL AND THE NUCLEAR LEVEL DENSITY

M. EL-NADI and M. WAFIK
Egyptian Atomic Energy Commission, Cairo

Received 11 August 1958

Abstract: The suggestions put forward by Bethe and Hurwitz that level densities ought to be measured from a standard energy, such as is given by the semi-empirical formula, and not from nuclear ground states is considered. The semi-empirical formula is corrected, following P. Fong, and this "characteristic level" is determined for nuclei from $A = 10$ to $A = 250$. The experimental data of D. Hughes *et al.* for the fast neutron cross sections are used to determine the level densities for the corresponding nuclei. These were found to be in agreement with the Fermi-gas model.

1. Introduction

The first attempt to calculate the density of nuclear energy levels was made by Bethe [1]). Subsequent studies have been made by other workers [2–5]) to refine Bethe's theory. By methods of statistical mechanics Bethe explained the dependence of the energy level density on the mass number A and on the excitation energy. It can be generally stated that these theories show an over-all agreement with experiment [6]), but are incapable of reproducing the observed irregularities, associated with odd-even [7]) and magic number [8]) nucleides. Moreover, some recent measurements of nuclear level densities lead to conflicting conclusions as to the validity of the Fermi gas model on which the above theories are based. In these experiments [10]) the excitation energy was measured, as usual, from the ground state. It may seem reasonable to study the possibility of attributing these deviations to fluctuations in the ground state of the nucleus due to even-odd and magic number effects. Eliminating these fluctuations in the ground state energies we may then study the applicability of the Fermi gas model to the nucleus. The introduction of a corrected ground level for nuclei, called the "characteristic level", was suggested by Hurwitz and Bethe [11]).

Fong [12]) in his study of the problem of asymmetric fission applied the Hurwitz-Bethe hypothesis to nuclei in the fission product region. This technique has succeeded in showing the applicability of the Fermi gas model to nuclei in this region. We have extended the work of Fong by carrying out the calculations for nearly all mass numbers between 10 and 250, including the fission-product region. The liquid drop model mass formula is corrected

for each nucleide. The position of the characteristic level is then determined. Analyzing the experimental data of fast neutron capture cross sections and using the above device, the Fermi gas model formula is tested, and the values of its parameters are determined. The results and their possible implications are finally discussed.

2. Theoretical Considerations

We assume a simple model of the nucleus, consisting of A identical non-interacting Fermi-Dirac particles with strong degeneracy. Let ε_i be the individual energy levels and E the energy of excitation of the nucleus. We are interested in calculating the number of distinct ways in which the A particles can be distributed among the allowed individual levels ε_i so as to give a total energy E'. We shall denote this number by $\rho(A, E')$. The exact solution of this problem is given by the well known Darwin-Fowler integral[13])

$$\rho(A, E') = (2\pi i)^{-2} \oint\oint \exp[\alpha A + \beta E' + \sum_i \ln(1+e^{-\alpha-\beta\varepsilon_i})] d\alpha d\beta, \qquad (1)$$

where α and β are two constants which have to be determined from the total number of particles and total energy E' of the nucleus. We can replace the last term in the exponent of eq. (1) by an integral and according to Sommerfeld [14]) we get

$$\sum_i \ln(1+e^{-\alpha-\beta\varepsilon_i}) = \int_0^\infty \rho(\varepsilon) \ln(1+e^{-\alpha-\beta\varepsilon}) d\varepsilon \simeq -\alpha A - \beta E_0 + (\pi^2/\sigma\beta^2)\rho(\varepsilon_0) \qquad (2)$$

where $\rho(\varepsilon_0)$ is the individual level density at the Fermi level ε_0 and E_0 is the energy of ground state of the entire system.

Evaluating the integral (1) by the saddle point method we get

$$\rho(A, E') = e^S/(2\pi D^{\frac{1}{2}}), \qquad (3)$$

where the "entropy" S is the value at the saddle point of the exponent of eq. (1), and D is the determinant formed from the second derivatives of S with respect to α and β.

A simple calculation finally gives for the level density the following expression:

$$\rho(A, E') = (48)^{-\frac{1}{2}} E'^{-1} \exp\left[\pi\left(\frac{2E'}{3\delta}\right)^{\frac{1}{2}}\right] \qquad (4)$$

where $\delta^{-1} = \rho(\varepsilon_0)$ is the individual-nucleon level density, which is linearly related to the mass number A:

$$\delta^{-1} = \text{Const.} \times A. \qquad (5)$$

Refining the above procedure for a case more directly applicable to the nucleus, we shall assume that the system consists of a mixture of protons

and neutrons. This combinatorial problem can be solved by the Darwin-Fowler method in a similar way and the result is

$$\rho(A, E) = \tfrac{1}{2}\left[\frac{\delta}{21\sigma E^5}\right]^{\frac{1}{4}} \exp\left[\pi\left(\frac{E2}{3\delta}\right)^{\frac{1}{2}}\right]. \tag{6}$$

Eq. (6) may take the form

$$\rho(A, E) = c \exp\left[\pi\left(\frac{2E}{3\delta}\right)^{\frac{1}{2}}\right] \tag{7}$$

where c is a slowly varying function of E and A.

To deduce δ from experiment, we write eq. (7) as follows:

$$\delta = \tfrac{2}{3}E\,[\pi/(\ln\rho - \ln c)]^2. \tag{7}$$

Eq. (6) can also be written in the familiar form

$$\rho(A, E) = c \exp\,[2(aE)^{\frac{1}{2}}] \tag{8}$$

where the parameters a and c are given by

$$c = \tfrac{1}{2}[\delta/(216E^5)]^{\frac{1}{4}}, \quad a = \pi^2/6\delta. \tag{8'}$$

3. Analysis and Results

By using the continuum theory of nuclear reactions [15]) it has been shown by Bethe [16]) that the average radiative neutron capture cross section $\langle\sigma(\mathrm{n},\gamma)\rangle$ is related to the radiation width Γ_γ and to the level density $\rho(E)$ by the following expression:

$$\rho(E) = \langle\sigma(\mathrm{n}, \gamma)\rangle/(2\pi^2\lambda^2\Gamma_\gamma). \tag{9}$$

Hughes *et al.*[17]) measured the cross section for radiative capture of fast fission neutrons of an effective energy of 1 MeV. Heidmann and Bethe [18]) studied the radiation widths, and showed that they exhibit a smooth A dependence. These data enable us to estimate the level densities from eq. (9) at an excitation energy $E = E_\mathrm{n}+1$ MeV, where E_n is the separation energy of the last neutron in the compound nucleus.

We shall make the assumption [12]) that two neighbouring nucleides A and A' have essentially the same parameters δ, c, and Γ_γ. This assumption is valid only when the excitation energies E and E' do not differ appreciably.

Correspondingly the individual-nucleon level spacing can be determined from eqs. (8') and (9) as follows:

$$\delta = \tfrac{2}{3}\,[\pi(\sqrt{E}-\sqrt{E'})/\{\ln\sigma(A)/\sigma(A')\}]^2. \tag{10}$$

The position of the ground state varies discontinuously with the mass number A, as a result of even-odd and magic number effects. Hurwitz and Bethe [11]) have found it necessary to suggest that the excitation energy should not be measured from that ground state, but from a "characteristic

level" which varies smoothly from one isotope to another. They pointed out that this characteristic level could be represented by a level calculated from the liquid drop mass formula excluding the even-odd energy term.

Consequently for the purpose of calculation of the excitation energy values one should determine the position of the characteristic level, using the well known Fermi-Weizsäcker semi-theoretical mass formula.

This formula takes the form

$$M(A, Z) = M_A + B_A(Z - Z_A)^2 + \delta_A \tag{11}$$

where

$$\begin{aligned} M_A &= 1.01464A + 0.014A^{\frac{2}{3}} - 0.041905Z_A \\ B_A &= 0.041905/Z_A \\ Z_A &= A/(1.980670 + 0.014962A^{\frac{2}{3}}) \end{aligned} \tag{12}$$

$$\delta_A = \frac{0.036}{A^{\frac{1}{2}}} \begin{cases} 1 & \text{odd} \\ 0 & \text{odd-mass} \\ -1 & \text{even.} \end{cases}$$

Mass values obtained from this formula, compared to mass-spectrometric ones, have shown errors of the order of 10 MeV. The Fermi-Weizsäcker formula is only an approximation and it does not take into account the existence of nuclear shell structure.

To account for the local deviations, the general procedure is to introduce some empirical corrections to M_A and Z_A (B_A and δ_A are assumed to be correct). Moreover, a discontinuous term μ analogous to the δ_A term may be introduced to account for the abrupt variations at the shell edges. The corrected mass formula may be expressed as follows:

$$M(A, Z) = M_A + \Delta M_A + B_A(Z - Z_A - \Delta Z_A)^2 + \delta_A + \mu. \tag{13}$$

To determine ΔZ_A we compare the Z_A values given by eq. (12) with the positions of the bottoms of the isobaric curves of the experimental beta-decay energies [19]). This comparison has been applied to isobaric nucleides of nearly all odd mass numbers between 11 and 243.

The deviations ΔZ_A may be positive or negative as seen in fig. 1. The charge corrections ΔZ_A are plotted, and a smooth curve may be drawn as shown in fig. 2.

To determine ΔM_A we compare the M_A values given by eq. (12) with the mass-spectroscopically determined masses of stable isotopes. The data used are those of Wapstra [20]). The mass corrections ΔM_A with their estimated errors are plotted against the mass number A, and a smooth curve may be passed through most of the points except the magic number nucleides. The ΔM_A term shows deviations at closed nuclear shells. Thus the introduction of μ may serve to account for the irregularities associated with magic

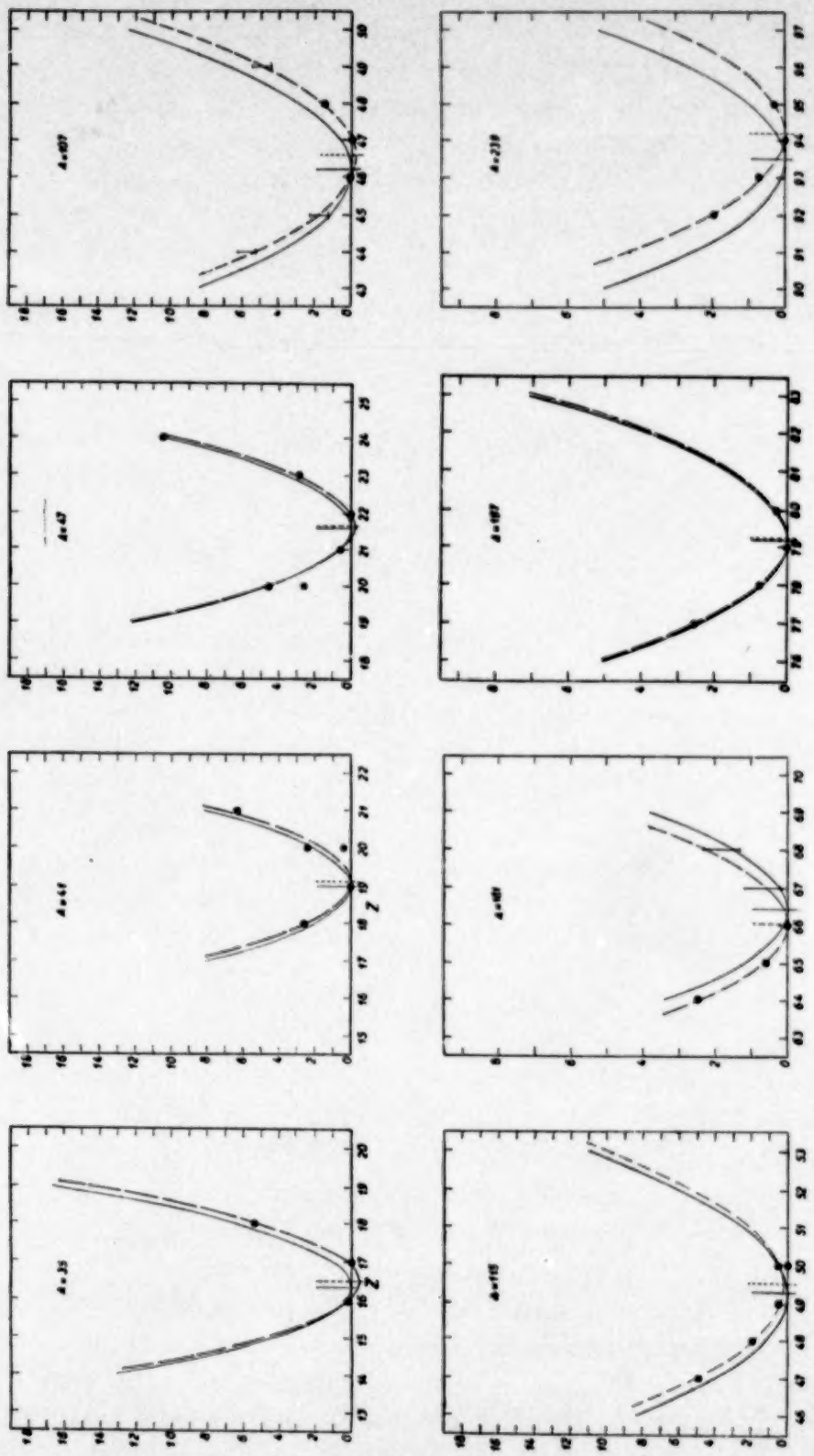

Fig. 1

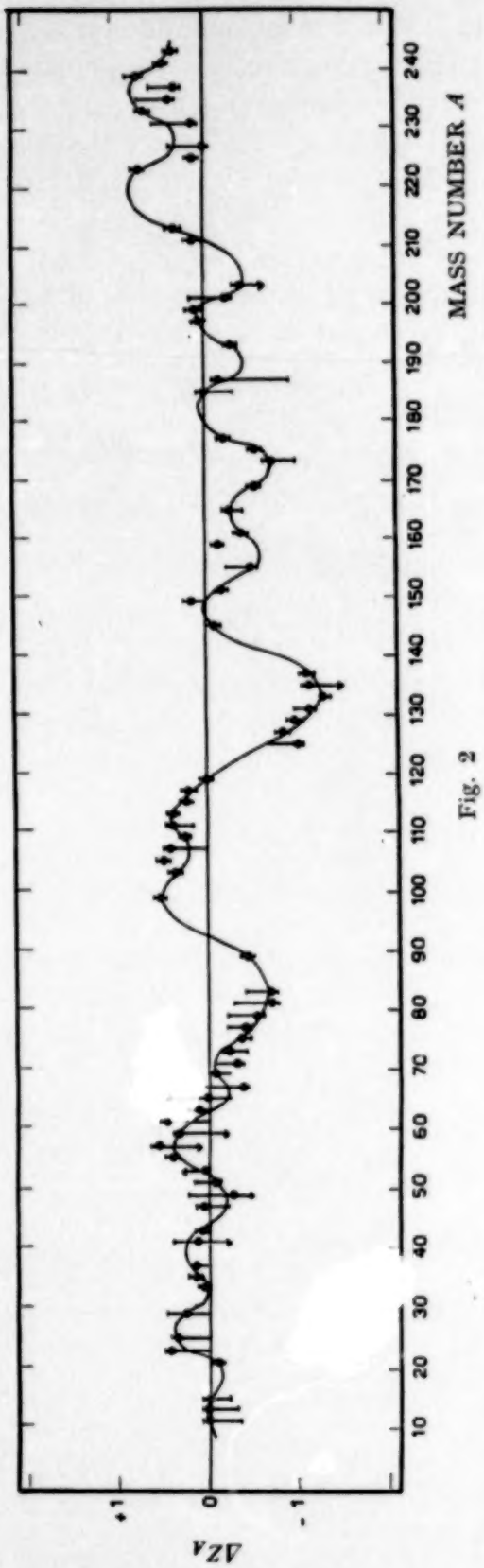
+1
0
-1
ΔZ_A
10 20 30 40 50 60 70 80 90 100 110 120 130 140 150 160 170 180 190 200 210 220 230 240
MASS NUMBER A

Fig. 2

numbers. The values of μ were found to be between -0.25 and -2.0 MeV. The isobaric curves involving a magic number nucleide cannot generally be represented by smooth parabolas, as can be seen in fig. 1. Better fitting may be obtained if the mass of the magic nucleide is corrected for the μ term.

Excluding the δ_A and μ terms eq. (13) varies smoothly with A and Z. It becomes free from odd-even effects and irregularities associated with the magic number nucleides, and so may be used as the definition of the characteristic energy level of any nucleus.

The characteristic levels of all nuclei may be assumed to coincide with the ground state of odd nuclei and is thus given by

$$M_c(A, Z) = M_A + \Delta M_A + B_A(Z - Z_A - \Delta Z_A)^2 + 0.036/A^{\frac{1}{2}}. \qquad (14)$$

The E-values may then be calculated as follows:

$$E = 931.162[M(A, Z) + M_n + 1 - M_c(A+1, Z)] \text{ MeV} \qquad (15)$$

where the masses are expressed in amu and the energies in MeV.

The individual-nucleon level spacing δ may now be determined (for the particularly selected nucleide pairs, referred to above) by substituting the values of the excitation energies into eq. (10) and using the experimental data of Hughes *et al.* for the fast neutron capture cross sections.

The quantity a [$\equiv \pi^2/68$] is then plotted for these nucleides against the mass number A, and a straight line may be drawn passing through most of the points. This straight line was found to be †

$$a = 0.03A \text{ MeV}^{-1}. \qquad (16)$$

To determine the actual values of a for other nucleides, we shall assume the validity of the linear relation (16) as a first approximation. Using eqs. (15), (8) and the measured values of the level densities, we can determine the values of the other parameter c. It is clear from the dependence of c and a on the mass number A, according to the Fermi gas model, that the values of the parameter c are not very sensitive to variations in A. Consequently, the calculated values of c may be smoothed out by a simple curve without producing much error in the values of a.

This curve was taken as a straight line in the work of Fong [12]). In the present work better representation (both for the a and c values) as obtained when the c values are represented by a slightly curved line represented by

$$c = 0.082 \times \exp\,[0.071A - 0.00026A^2]. \qquad (17)$$

With these values of c, which we assume to be correct, together with the predetermined level densities and eq. (8) we can calculate the values of the

† This is to be compared with the value $a = 0.05A$ MeV^{-1} obtained by Fong [12]) for the mass region 71 – 165.

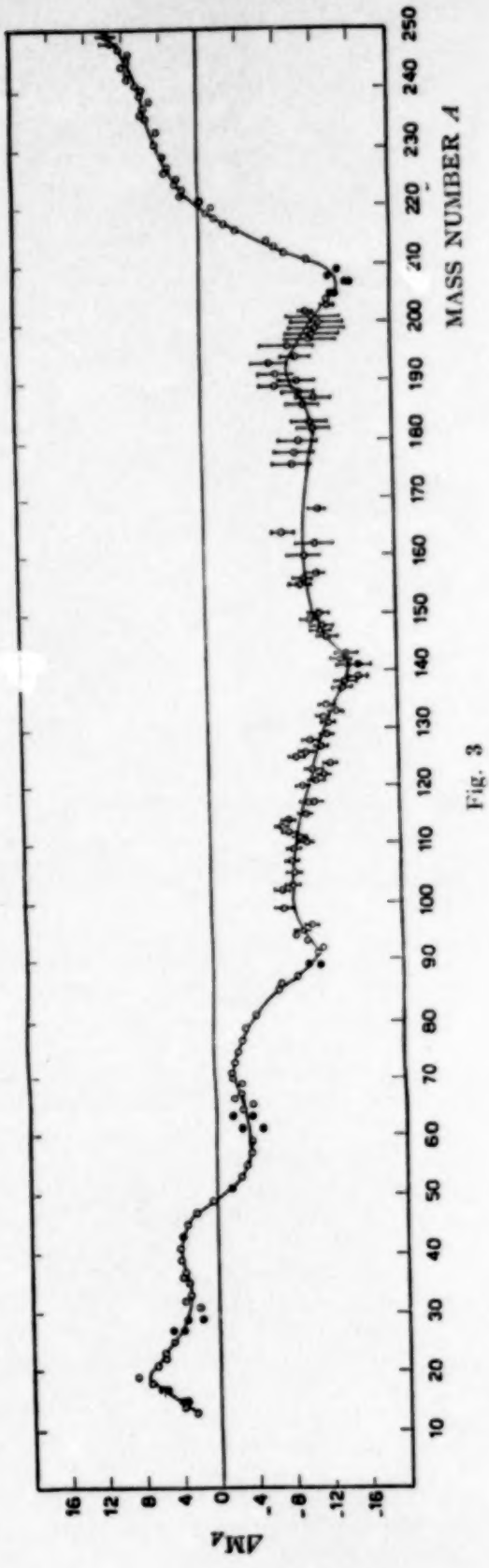
MASS NUMBER A
ΔM_A
10 20 30 40 50 60 70 80 90 100 110 120 130 140 150 160 170 180 190 200 210 220 230 240 250
16 12 8 4 0 -4 -8 -12 -16

Fig. 3

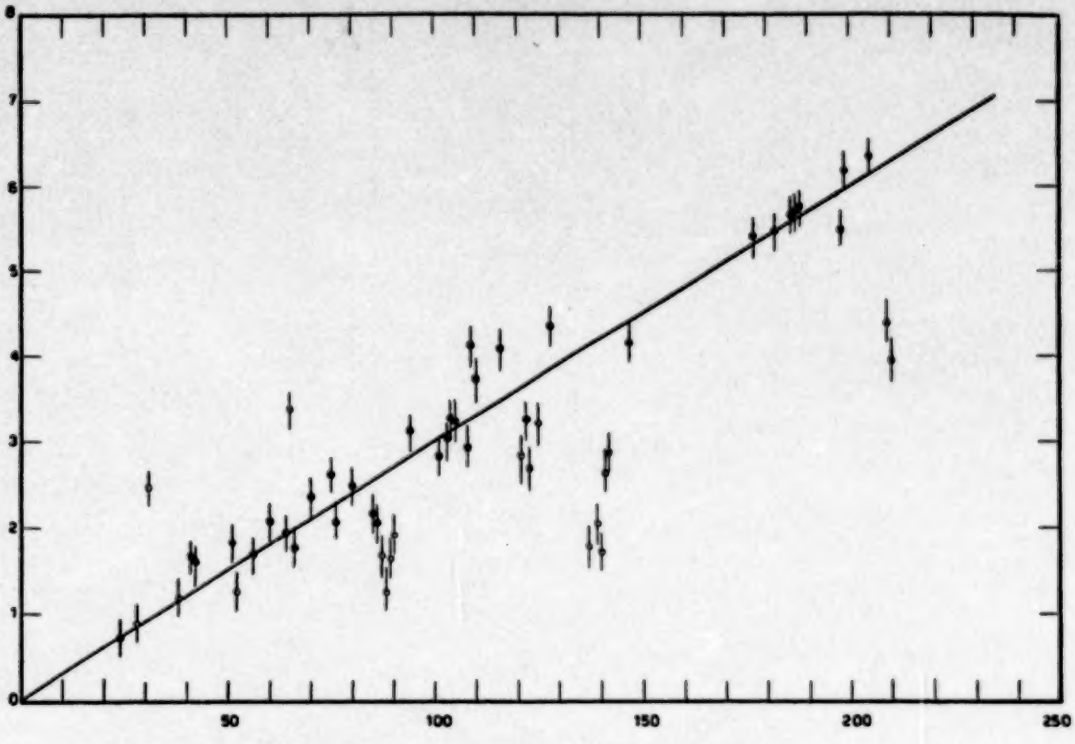

Fig. 4

parameter a for all nucleides. These are represented in fig. (4). This figure shows clearly the linear dependence of a on the mass number A which is in conformity with the predictions of the Fermi gas model.

References

1) H. A. Bethe, Phys. Rev. **50** (1936) 332; Revs. Mod. Phys. **9** (1957) 69
2) G. Van Lier and G. E. Uhlenbeck, Physica **4** (1937) 531
3) J. M. B. Lang and K. J. Le Couteur, Proc. Phys. Soc. A **67** (1954) 585
4) C. Bloch, Phys. Rev. **93** (1954) 1094
5) N. Rosenzweig, Phys. Rev. **105** (1957) 950
6) P. C. Gugelot, Phys. Rev. **81** (1951) 51; **93** (1954) 425
7) Feld, Fesbach, Goldberger, Goldstein and Weisskopf, U.S. Atomic Energy Commission, NYO–636 (unpublished) pp. 176, 185
8) H. W. Newson and R. H. Rohrer, Phys. Rev. **87** (1952) 177; Asaro and I. Perlman, Phys. Rev. **87** (1952) 393; P. Staehelin and P. Preiswerk, Helv. Phys. Acta **24** (1952)623; P. J. Grant, Proc. Phys. Soc. A **65** (1952) 150; B. B. Kinsey, Report to the Brookhaven Conference on Neutron Physics, November 1950 (unpublished)
9) G. Igo and H. E. Wegner, Phys. Rev. **100** (1955) 1364
10) K. G. Porges, Phys. Rev. **101** (1956) 225; Eisberg, Igo and Wegner, Phys. Rev. **100** (1955) 1309; G. Igo, Phys. Rev. **106** (1957) 256
11) H. Hurwitz and H. A. Bethe, Phys. Rev. **81** (1951) 898
12) P. Fong, Phys. Rev. **102** (1956) 434
13) R. H. Fowler, Statistical Mechanics (MacMillan, New York, 1936)
14) A. Sommerfeld, Z. Physik **67** (1958) 1

15) J. M. Blatt and V. F. Weisskopf, Theoretical Nuclear Physics (John Wiley and Sons, New York, 1952)
16) H. A. Bethe, Phys. Rev. **57** (1940) 1125
17) Hughes, Garth and Levin, Phys. Rev. **91** (1953) 1423
18) J. Heidmann and H. A. Bethe, Phys. Rev. **84** (1951) 274
19) Way, Fano, Scott and Thew, Nuclear Data, National Bureau of Standards Circular no. 499 (U.S. Government Printing Office, Washington, D. C., 1950) and Supplements; Way, King, McGinnis and Van Lieshout, Nuclear Level Schemes ($A = 40 - A = 92$), U.S. Atomic Energy Commission
20) A. H. Wapstra, Physica **21** (1955) 367

2.I *Nuclear Physics* 9 (1958/59) 32—43; © *North-Holland Publishing Co., Amsterdam*
Not to be reproduced by photoprint or microfilm without written permission from the publisher

THE NUCLEAR PHOTOEFFECT IN Al^{27}

F. FERRERO, R. MALVANO, S. MENARDI and O. TERRACINI †
Istituto di Fisica dell'Università di Torino,
Istituto Nazionale di Fisica Nucleare, Sezione di Torino

Received 29 July 1958

Abstract: In this paper are reported experimental results concerning the photoneutron cross sections obtained in different ways.

These results are discussed and compared with the predictions of the independent particle model. Some discrepancies that appeared in previous measurements have been clarified, whereas some others still remain unexplained.

1. Introduction

Al^{27} has been the object of many extensive studies; it gives rise to short lived β^+ residual activities, both in (γ, n) and (γ, 2n) reactions, of very similar half life (6.5, 7 sec). The first activity has been carefully examined, up to 22 MeV, by L. Katz and A. G. W. Cameron [1]) many years ago. These measurements have been repeated a few years later by R. N. H. Haslam *et al.*[2]) showing a very good agreement with earlier results. The (γ, n) cross section obtained in this way is about three times lower than the one obtained from the total neutron counting technique [3]). This discrepancy remained unexplained for a long time, until it was discovered that the fast β^+ activity comes from the first excited level (0^+) of Al^{26}, not from its ground state, placed 0.243 MeV below, which is an extremely slow β^+ emitter ($5+$; $T_{\frac{1}{2}} = 10^6$ y) [4]). This discrepancy being clarified, many other problems still remained open in the photoeffect of Al^{27}.

One of the most important parameters in photonuclear reactions is the absorption cross section σ_γ, that can be deduced, essentially, in three different ways, measuring

(a) the yields of all reaction products (n, p, d, np, . . . γ') that are energetically possible,

(b) the elastic scattering cross section σ_s, which is related to the absorption cross section through the functional relationship given in ref.[5]),

(c) the nuclear electromagnetic absorption by a thick sample.

In the case of Al^{27} there is one measurement concerning the evaluation of the absorption cross section through method (b), while there are a few

† Now at the C.N.R.N. of Ispra (Milano).

measurements of the reaction product yields. Unfortunately the major part of the above measurements end at 22 MeV where the absorption cross section does not yet seem to be negligible. Now there is, in the energy region above 22 MeV, a complete disagreement between the value of the absorption cross section as deduced from scattering and the data we have from the reaction product yields [6]).

Our aim is therefore to clarify, as far as possible, the various problems in the energy region above 22 MeV:

a) extending the measurements on $(\gamma, n)+(\gamma, 2n)$ reaction by the method of residual activity up to 31 MeV;

b) repeating with a moderated neutron detector the measurements on the total neutron yield up to the same energy;

c) studying, by means of a threshold detector, the fast neutron component up to the maximum energy available.

2. Experimental Apparatus

The experimental apparatus used to measure the short lived β^+ activity following (γ, n), $(\gamma, 2n)$ reactions, consists of a NaI crystal that detects the annihilation radiation arising from the β^+ captured in the sample; in this way the background of all β^- activities is avoided.

The block diagram of the electronic apparatus is sketched in fig. 1. A five channel time analyzer allows one very easily to follow the decaying activity, discriminating from the background and other eventually present activities of different half lives.

The X-ray dose is measured by means of an ionization chamber and electrometer: we had not to correct for the variable intensity of the beam during each irradiation, because this intensity is very constant, the fluctuations not exceeding 10 %. However, each point represents a minimum of 30 successive irradiations; this reduces by a factor of 5, at least, the error in the "effective dose" due [7]) to non-constancy of the beam intensity: actually the scattering of the experimental points did not exceed appreciably the pure statistical randomness and the instability of the betatron energy ($\approx \pm 30$ MeV). More details about this apparatus can be found elsewhere [8]).

The set up employed in the measurement of the total neutron yield is described in a paper by F. Ferrero *et al.*[9]). The Rh detector is placed in a large tank ($1 \times 1 \times 1$ m) full of water; the tank has a cylindrical hole in the middle, supporting the Al sample, and through which the X-ray beam passes. The distance between the centre of the sample and the axis of the Rh counter is 12 cm.

The measurements are done irradiating the sample for about 2 min; during this time the thin wall Geiger counter that detects the Rh β^- activity

is disconnected from the H.V.: after the irradiation the Rh activity is followed for 5 half-lives.

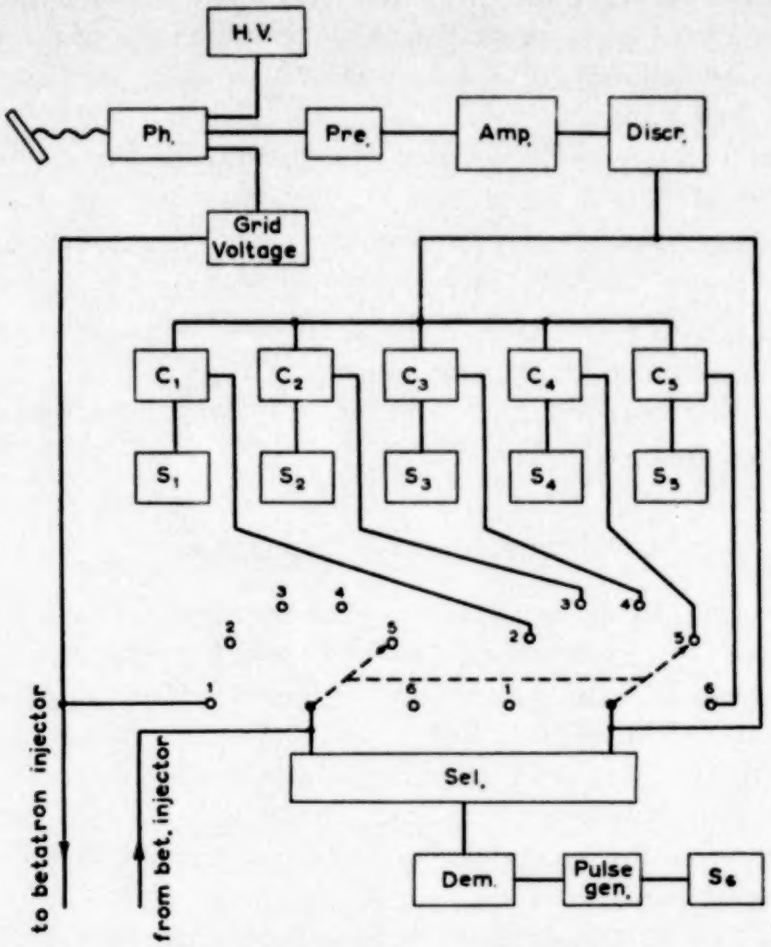

Fig. 1. Block diagram of the experimental apparatus.

The detector employed to measure the "fast neutron yield" is fully described in the same ref. [9]): it consists of $Si^{28}(n, p)$ threshold detector, that has an effective threshold of $\approx$ 5.5 MeV.

3. Experimental Results

The experimental results are collected in fig. 2, where yields for total neutron, residual activity and fast neutrons are given in the same scale; to avoid confusion the yield of the residual activity is multiplied by two. The total neutron (t.n.) yield is normalized to the values given by Montalbetti *et al.* up to 22 MeV [3]). On the other hand, the residual activity (r.a.) yield is calculated assuming for the maximum of the cross section the figure of 8.4 mb, as given by Haslam *et al.*[2]).

The absolute calibration of the fast neutron (f.n.) yield is obtained in two

different ways, which give results not differing from each other by more than 10 %.

The first method makes use of a calculated value of the irradiation and counting geometry, of the experimental value of the (n, p) cross section in Si^{28} [10]), and of the calculated efficiency of the counting apparatus. The well

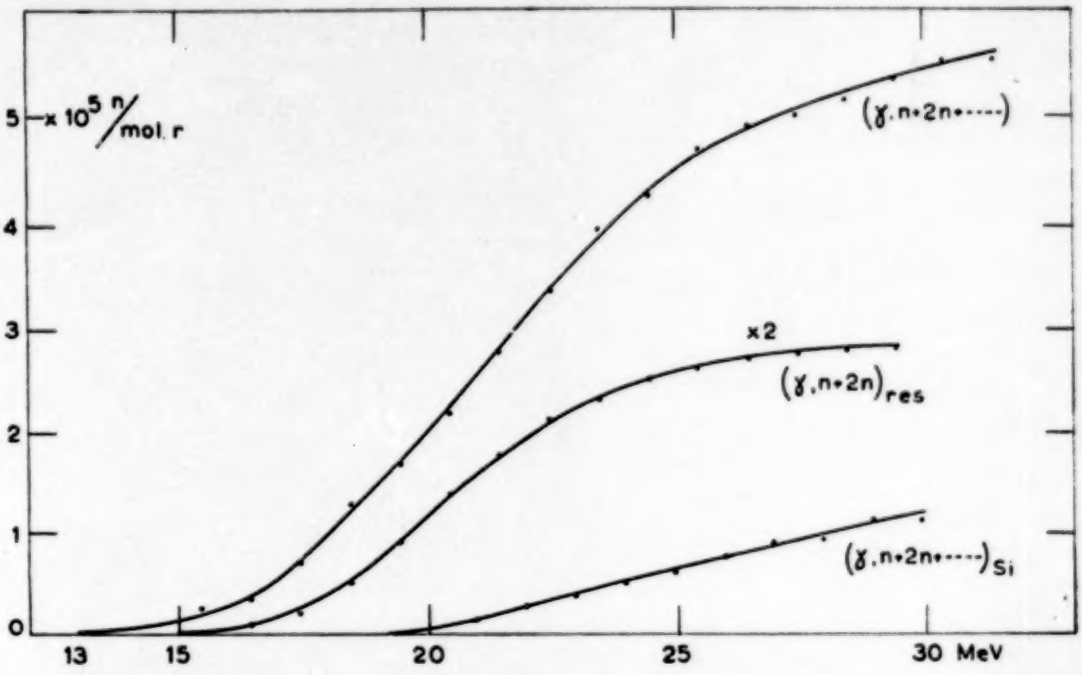

Fig. 2. Photoneutron yields in n/mol.r versus betatron energy.

known yield of $Si^{29}(\gamma, p)\ Al^{28}$ [11]) that gives rise to the same residual activity as the (n, p) reaction in Si^{28} allows an independent calibration of the counting efficiency.

The second method is completely independent from geometry and counting efficiency, making use of a carefully measured photoneutron spectrum from Ta at 30 MeV [12]). Taking into account these data we could evaluate the overall efficiency of the Si fast neutron counter (including all geometric factors). One has only to know the ratio between the f.n. yields of Ta and Al at 30 MeV and the t.n. yield of Ta at the same energy.

In fig. 3 are plotted the cross sections in mb deduced from the analysis of the yield curves. The lower part of the cross sections, up to 22 MeV, are consistent, with the accuracy obtainable in analyzing the yields, with the values given by Montalbetti [3]) (t.n.) and Katz (r.a.) [4]). The cross section above 22 MeV may be compared favourably with the values measured in ref. [6]). A certain doubt about the accuracy of Johnes and Terwilliger's data arose from the fact that they used a moderated neutron detector of the long counter type in a "large angle geometry". This doubt is now completely removed, because the measurements we have done with a completely

different type of moderated neutron detector match very well the preceding results.

We note that the peak positions of the r.a. and t.n. yields do not coincide

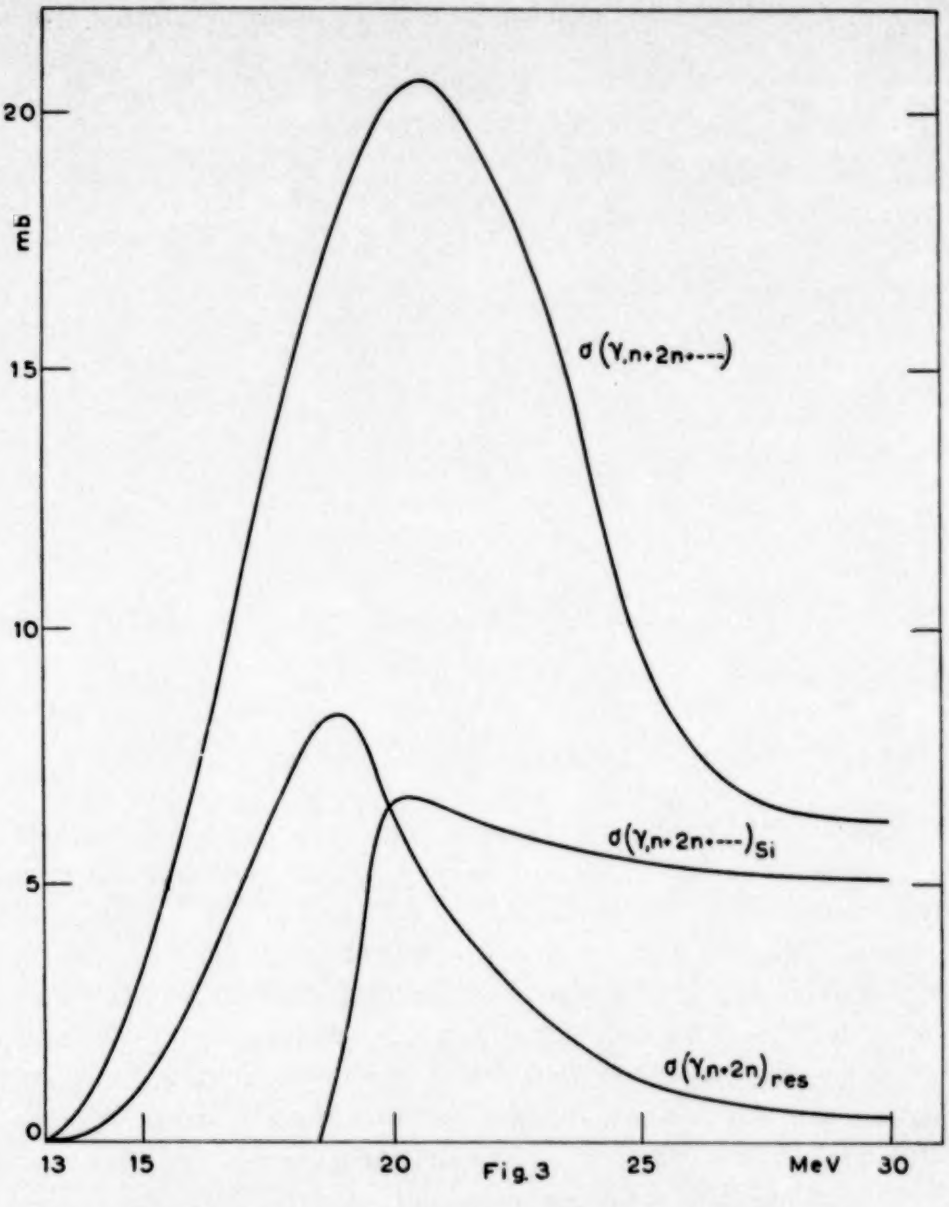

Fig. 3. Cross sections deduced by analyzing the yields of fig. 2.

in our measurements while they were considered nearly coincident in the previous measurements. We point out that our measurements were done with the same betatron and with the same energy calibration: therefore the difference of 1.5 MeV in the peak positions may be taken as real. Besides, the maximum of the t.n. cross section happens now to be nearly at the same energy as the maximum of the (γ, p) cross section [13]).

4. Discussion of the Experimental Results

The above experimental results may be summarized as follows:

1) the t.n. cross section decreases steadily from its $\approx$ 20 mb maximum value to $\approx$ 6 mb at 30 MeV;

2) the f.n. cross section is nearly constant above threshold, decreasing slowly from $\approx$ 6.5 mb at 20 MeV to $\approx$ 5 mb at 30 MeV;

3) the r.a. cross section, which describes the two different processes (photoexcitation of the 0^+ isomeric state of Al^{26} and of the ground state of Al^{25}) becomes negligible ($\approx$ 0.5 mb) above 25 MeV.

The most interesting feature of the results seems to be the fact that above 25 MeV the major contribution to t.n. cross section arises mainly from the f.n. component.

Before we try to explain these results, it will be useful to see what are the possible photoreactions that can contribute to the total and fast neutron yields; we have, therefore, listed in table 1 these reactions together with their thresholds.

TABLE 1

reaction	threshold (MeV)
(γ, n)	13
(γ, 2n)	24.4
(γ, np)	19.5
(γ, nα)	21.3

The contribution of the (γ, 2n) reaction to the t.n. yield is certainly very small, as can be inferred from the value of the r.a.: besides, being an evaporative process with a rather high threshold, it can only give a negligible contribution to the f.n. yield.

From the (γ, np) and (γ, nα) reactions, the former is certainly stronger than the latter, because threshold and Coulomb barrier are lower. To explain the high value of the f.n. yield, we ought therefore to take essentially into account the (γ, n) and (γ, np) reactions.

If we try to calculate the fraction of fast neutrons assuming a pure statistical process (this is certainly wrong, because of the rather strong anisotropy of the f.n. angular distribution: see below), we must assume a nuclear temperature (supposedly constant) lower than 2 MeV, according to the data of Dawson [14]) on the photoproton spectrum from Al and of Sargent [13]) on the photoneutron spectrum: this last measurement directly suggested a constant temperature of 1.8 MeV. With this figure the fraction $F_{\text{f.e.n.}}$ of fast (evaporative) neutrons,

$$F_{\text{f.e.n.}} = \frac{1}{\Theta^2}\int_{5.5\ \text{MeV}}^{\infty} E_n \exp\left(-\frac{E_n}{\Theta}\right) \mathrm{d}E_n \qquad (1)$$

comes out to be $\approx 20\ \%$, certainly too small in comparison with the experimental value.

We may try to add to the f.e.n. component a "direct" fraction, in the way indicated by Courant [16]). The cross section per nucleon suggested for this type of process is

$$\sigma = \tfrac{16}{3}\pi \frac{e^2}{\hbar c}\left(1-\frac{Z}{A}\right)^2 \left(\frac{DTR^2}{\hbar^3\omega^3[(\hbar\omega+T)^{\frac{1}{2}}+(\hbar\omega+T-D)^{\frac{1}{2}}]}\right)\left(\frac{\hbar^2}{2MR^2}\right)^{\frac{1}{2}} \qquad (2)$$

where T is the kinetic energy when the nucleon is in the nucleus and D is the depth of the nuclear well. At 30 MeV this term is of the order of a tenth of a mb, negligible therefore in comparison with our results.

On the other hand we cannot attribute entirely the non-evaporative part of the f.n. cross section (≈ 4 mb at 30 MeV) to the (γ, np) process, because in this case the t.n. cross section should have at least the double value, to take into account the elementary processes in which the fast particle is a proton instead of a neutron: it ought to be greater than 9 mb, while the experimental value is 6.

We now try, consequently, to see if the photoneutron process in Al^{27} could be entirely described in terms of the independent particle model worked out by Wilkinson [17]). According to this model, a nucleon (proton or neutron) can be raised from a closed shell (or subshell) to a higher "single-particle" state, differing from the former by one unit of orbital angular momentum.

The shell model configuration of Al^{27} has a closed subshell of neutrons ($6\ 1d_{\frac{3}{2}}$) and a hole in the same subshell of protons ($5\ 1d_{\frac{3}{2}}$). In the inset of fig. 4 are indicated the Al^{27} levels, whose relative distances have been calculated in ref. [18]). The energy scale has been found by identifying the $1d_{\frac{3}{2}} \rightarrow 1f_{\frac{7}{2}}$ transition with the energy of the giant resonance maximum, while the origin of the energy scale has been deduced from the correct value of the neutron binding energy. The possible transitions are indicated in the same figure and are listed in table 2, together with their relative intensity ε_i in per cent, calculated as in ref. [17]).

With the aid of the data of table 2 we have calculated the t.n. cross section, adding at each energy the contributions from the different transitions, which have been affected by a gaussian shape of 6 MeV half width †. The calculated

† The half width $\frac{1}{2}\Gamma$ used in the above calculation is greater than the imaginary part W of the potential in the optical model, in order to account for the spread of the transitions caused by the nuclear deformation that is present in Al [21]).

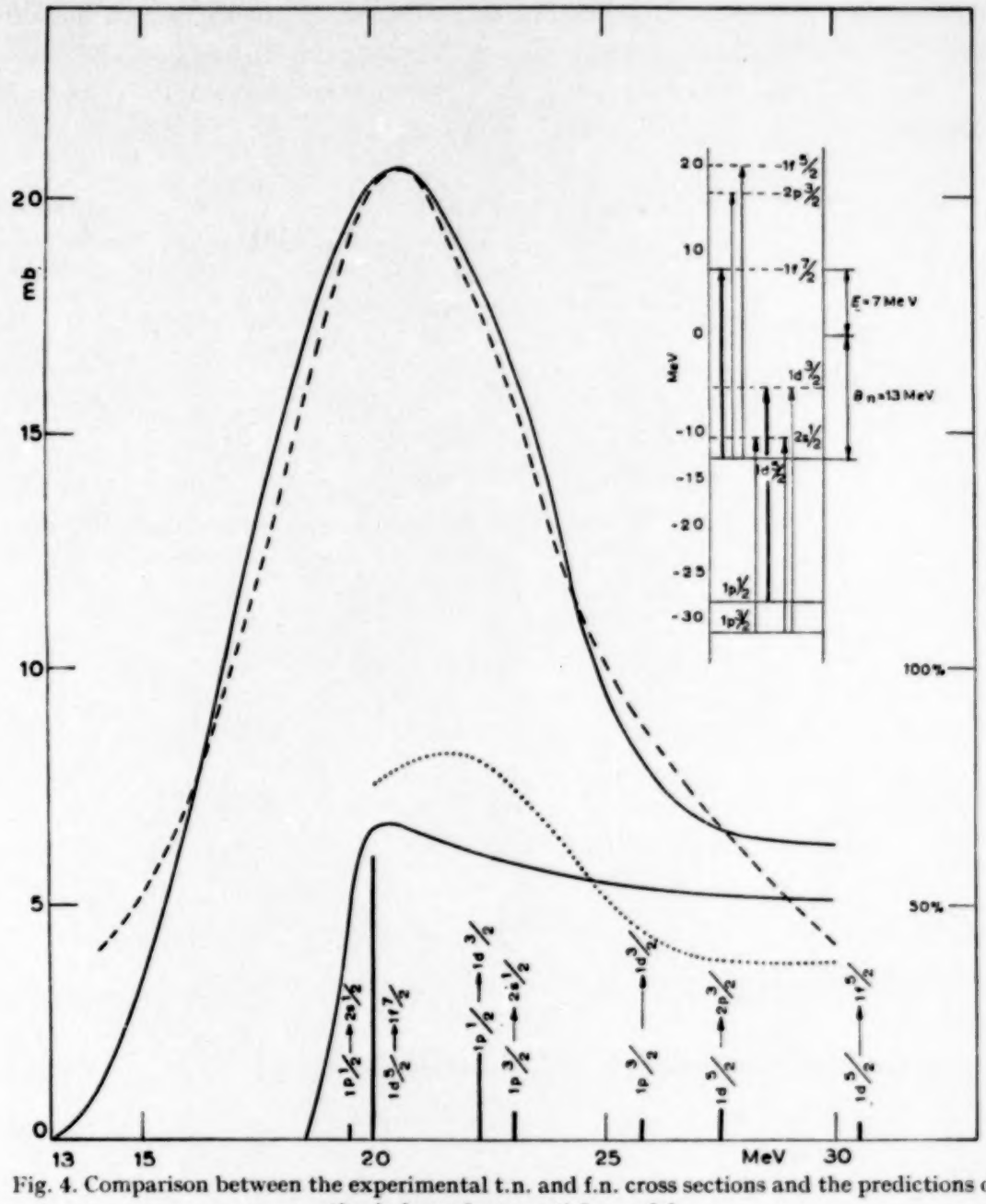

Fig. 4. Comparison between the experimental t.n. and f.n. cross sections and the predictions of the independent particle model.

TABLE 2

transition	intensity (%)
$1d_{\frac{3}{2}} - 1f_{\frac{7}{2}}$	59.6
$1d_{\frac{3}{2}} - 2p_{\frac{3}{2}}$	6.2
$1d_{\frac{3}{2}} - 1f_{\frac{5}{2}}$	3.0
$1p_{\frac{1}{2}} - 2s_{\frac{1}{2}}$	2.0
$1p_{\frac{1}{2}} - 1d_{\frac{3}{2}}$	20.0
$1p_{\frac{3}{2}} - 2s_{\frac{1}{2}}$	4.8
$1p_{\frac{3}{2}} - 1d_{\frac{3}{2}}$	4.0

cross section, normalized at its maximum value, is given (broken line) in fig. 4: the agreement with experiment seems to be rather good.

The fast neutron fraction $F_{\text{f.n.}}$ has been deduced from the following relation:

$$F_{\text{f.n.}} = \frac{\sum_l \dfrac{\Gamma_0 T_l(E_n)}{\Gamma_0 T_l(E_0)+2W}\,\varepsilon_l}{\sum_l \varepsilon_l}\left(1-\frac{1}{\Theta^2}\int_{5.5\text{ MeV}}^{\infty} E_n \exp\left(-\frac{E_n}{\Theta}\right)\mathrm{d}E_n\right) + \frac{1}{\Theta^2}\int_{5.5\text{ MeV}}^{\infty} E_n \exp\left(-\frac{E_n}{\Theta}\right)\mathrm{d}E_n, \tag{3}$$

with

$$2W \approx 3\text{ MeV}, \quad \Gamma_0 = (2k\hbar^2\times 10^{13})/(1.2A^{\frac{1}{3}}M);$$

T_l is the centrifugal barrier transmission for a particle of kinetic energy E_n leaving a state of orbital angular momentum l. In fig. 5 the calculated fraction $F_{\text{f.n.}}$ has been plotted (solid line) while the points are deduced from the

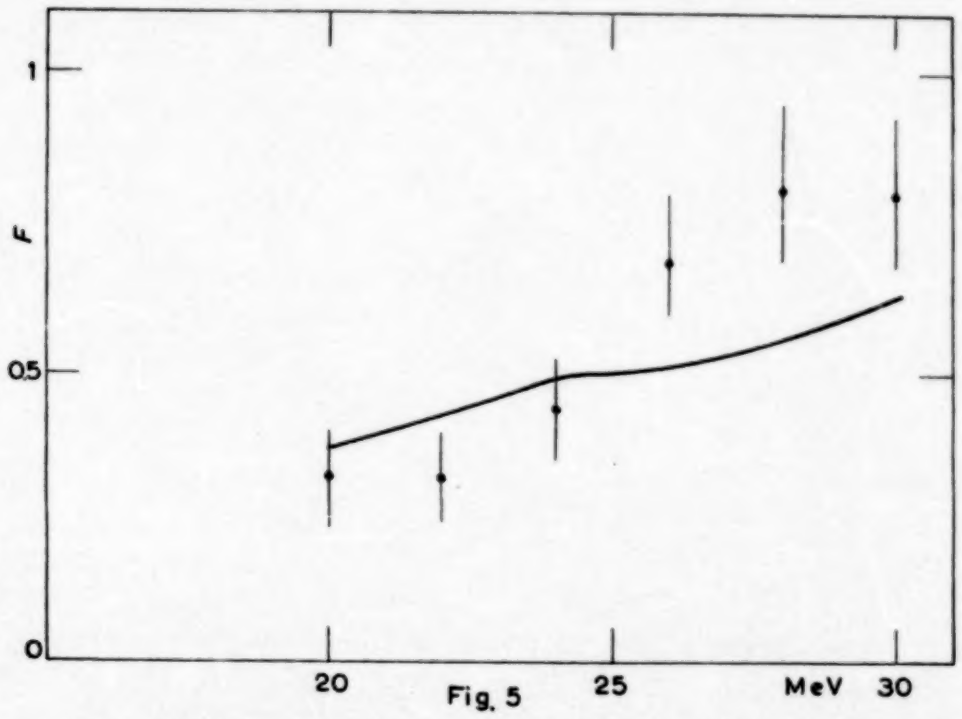

Fig. 5

Fig. 5. Fast neutron fraction. The points represent experimental values.

experimental cross section of fig. 3. The agreement up to 25 MeV is good, while above this energy the experimental values lie somewhat higher, indicating a greater fraction of direct processes than we could deduce on the basis of the independent particle model. Perhaps the higher energy transitions should be enhanced: besides, the (γ, np) contribution in this model has not been taken completely into account. The dotted line in fig. 4 represents the calculated f.n. cross section.

With the above interpretation we no longer have any qualitative difference between heavy nuclei, where we found [9]) that the f.n. component is contained inside the giant resonance, and light nuclei that apparently show a different behaviour: actually the various photon transitions are in this case more "diluted" in energy than for heavy nuclei.

Considering the above transitions and the expected angular distribution of neutrons ejected from a l-orbit [16])

$$W(\vartheta) = \begin{cases} 1+\dfrac{l+2}{2l}\sin^2\vartheta & \text{for} \quad l \to l+1 \\ \dfrac{l-1}{2(l+1)}\sin^2\vartheta & \text{for} \quad l \to l-1, \end{cases}$$

we can predict the f.n. angular distribution averaged on bremsstrahlung spectrum at 30 MeV. The calculated figure is 0.57 to be compared with our experimental value (0.52 ± 0.1).

The measurements made by Johanson [19]) cannot be directly compared with the above theoretical prediction, because the threshold detector he used has no very well defined threshold, and the energy of the bremsstrahlung spectrum used in his experiment was 70 MeV and we know from ref.[6]) that the t.n. cross section between 30 and 70 MeV is not negligible in the Al^{27} case.

The cross section for the activation of the 0^+ isomeric state decreases with photon energy much faster than the t.n. cross section. The arguments of the above discussion give us confidence that the major contribution to the t.n. cross section arises mainly from the (γ, n) reaction. We must conclude, therefore, that the branching ratio $\sigma(\gamma, n)_{0^+}/\sigma(\gamma, n)_{5^+}$ decreases rapidly for photon energies above 22 MeV. Besides, we know experimentally that the fraction of direct neutrons increases with energy: we may therefore relate the above two pieces of evidence. The ejection of a fast neutron from the d-subshell leaves a hole of $\frac{5}{2}$ units of orbital angular momentum. This neutron state couples itself with the other hole state in the d-proton subshell, giving preferentially a state of high angular momentum because of the greater value of the statistical weight; the decrease of the above branching ratio is therefore a further support to the assumption of "direct neutron emission".

Adding the t.n. cross section to the (γ, p) cross section [14]) we obtain the curve given in fig. 6. Above 24 MeV we have considered, according to A. H. Benade [20]), that the n/p ratio at high photon energy is about one. In the same figure is plotted the calculated photoabsorption cross section deduced inverting the integral relation [5])

$$\sigma_s(E_\gamma) = \frac{1}{6\pi\lambda^2}\left[\sigma_\gamma{}^2(E_\gamma) + \left(\frac{2E_\gamma}{\pi}\int_0^\infty \frac{\sigma_\gamma(E)\mathrm{d}E}{E^2 - E_\gamma{}^2}\right)^2\right] + \ldots \qquad (5)$$

and taking into account the data on the elastic nuclear scattering [5]). The

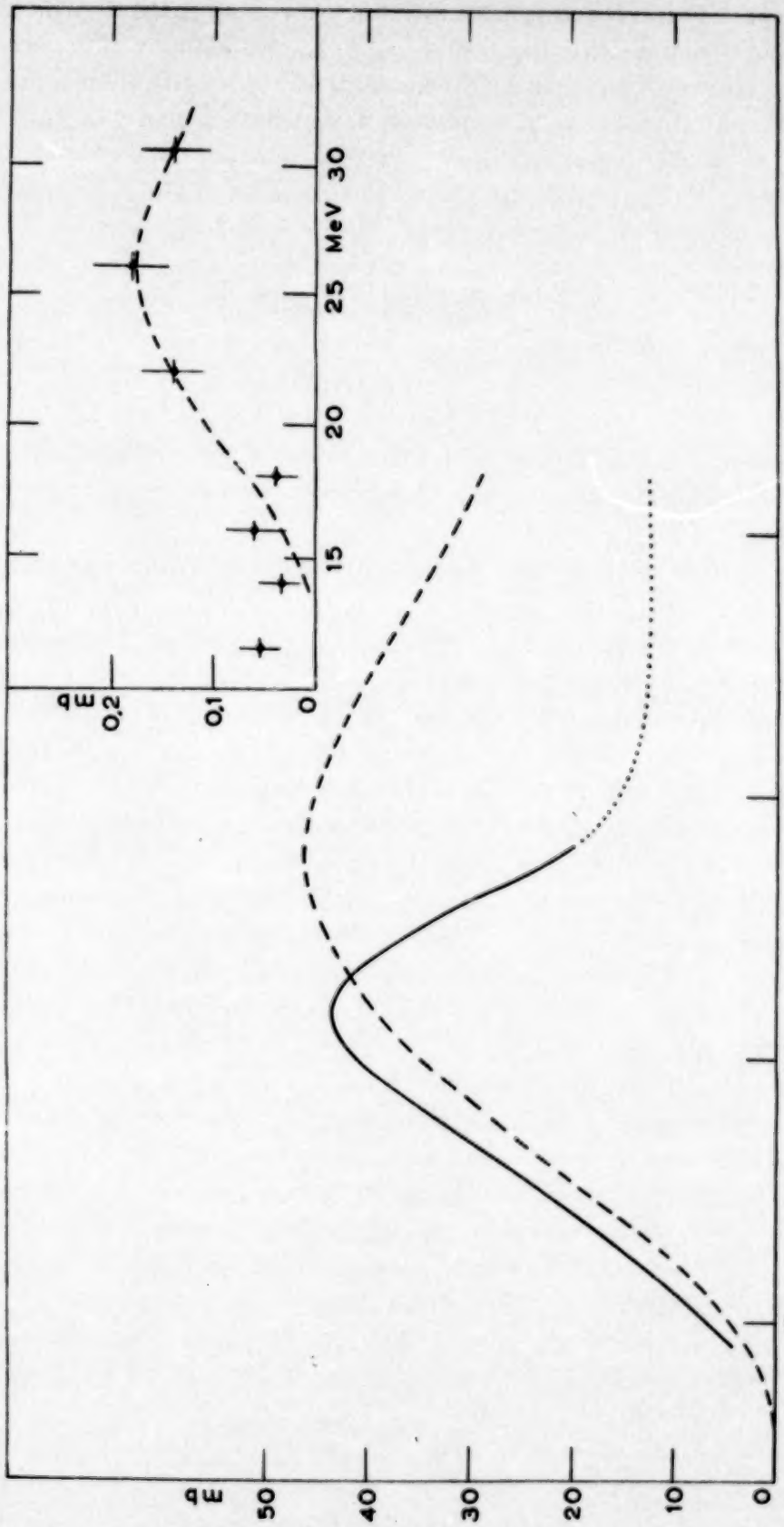

Fig. 6. Absorption cross section as deduced from elastic scattering (broken line) and from the yield of the reaction products (n and p).

disagreement above 22 MeV, as was pointed out in the same ref.[5]), is striking. This can be attributed to the fact that the above relation between elastic scattering and absorption is strictly valid at 0°, where the measurements, obviously, cannot be made, or in the backward direction only if we are dealing with pure dipole transitions. We know, however, from refs.[14]) and [19]) that the angular distribution of high energy protons, being peaked forward, contains a contribution from quadrupole transitions. The interference between dipole and quadrupole transitions in the energy region above 22 MeV gives rise to an enhancement of the elastic scattering at 120°, whose value cannot be transferred directly in eq. (5) to deduce the corresponding absorption cross section †.

We wish to thank dr. A. G. Fuller for very useful discussions.

† Another kind of interference effect may arise from the high value of the Al quadrupole moment (Fuller, private communication).

References

1) L. Katz and A. G. W. Cameron, Phys. Rev. **84** (1951) 111
2) R. N. H. Haslam, W. N. Roberts and O. S. Robb, Can. Journ. of Phys. **32** (1954) 361
3) R. Montalbetti, L. Katz and J. Goldemberg, Phys. Rev. **91** (1953) 659
4) J. R. Simanton *et al.*, Phys. Rev. **96** (1954) 1711
5) E. G. Fuller and E. Hayward, Phys. Rev. **101** (1956) 692;
Gell Mann, N. L. Goldberg, and W. E. Thirring, Phys. Rev. **95** (1954) 1612
6) L. W. Johnes and K. M. Terwillinger, Phys. Rev. **91** (1953) 699
7) R. N. H. Haslam, R. G. Summers Gill and E. H. Crosby, Can. Journ. Phys. **30** (1952) 257
8) U. Farinelli *et al.*, Photoexcitation of Pb^{207} (to be published)
9) F. Ferrero *et al.*, Nuovo Cimento **4** (1956) 418
10) I. B. Marion, R. M. Brugger and R. A. Chapman, Phys. Rev. **101** (1956) 247
11) L. Katz *et al.*, Can. Journ. Phys. **32** (1954) 580
12) G. Cortini *et al.*, Nuovo Cimento **9** (1958) 85
13) J. Halpern and A. K. Mann, Phys. Rev. **83** (1951) 370
14) W. K. Dawson, Can. Journ. Phys. **34** (1956) 1480
15) B. W. Sargent, Conference on Photonuclear Reactions, Washington (1958)
16) D. Courant, Phys. Rev. **82** (1951) 703
17) D. H. Wilkinson, Physica **22** (1956) 1039
18) A. E. S. Green, Nuclear Physics (1955) 373;
B. Čujec, J. Stefan Institute Reports **4** (1957) 95
19) S. A. E. Johanson, Phys. Rev. **97** (1955) 434
20) A. H. Benade, Conference on Photonuclear Reactions, Washington (1958)
21) D. H. Wilkinson, The giant photonuclear resonance in the rare earth region (to be published in the Proc. Roy. Soc.)

1.E.1 *Nuclear Physics* **9** (1958/59) 44—48; © *North-Holland Publishing Co., Amsterdam*
Not to be reproduced by photoprint or microfilm without written permission from the publisher

SPINS OF BISMUTH ISOTOPES OF MASSES 203, 204, 205 AND 206

C. M. JOHANSSON and I. P. K. LINDGREN
Institute of Physics, University of Uppsala

Received 8 June 1958

Abstract: The six-pole focusing atomic beam apparatus in Uppsala [1]) has been used for the measurement of the ground state spins of four neutron deficient bismuth isotopes. The experimental results are: for 12h Bi^{203}, $I = \frac{9}{2}$; for 13h Bi^{204}, $I = 6$; for 14.5d Bi^{205}, $I = \frac{9}{2}$; for 6.3d Bi^{206}, $I = 6$.

1. Introduction

Bismuth is an element in the nuclear lead region near the magic numbers 82 and 126 and therefore it is very interesting from the point of view of nuclear theory to know the spins, magnetic dipole and electric quadrupole moments of the different bismuth isotopes. The atomic beam magnetic resonance method has been used to measure the spins of four cyclotron produced bismuth isotopes, the measurements now being continued to get the magnetic dipole and electric quadrupole moments. The atomic ground state of bismuth is $^4S_{\frac{3}{2}}$ and therefore using the flop in technique [1–3]) two different transitions can be observed ($F = I+\frac{3}{2}$, $|m_F| = I+\frac{1}{2} \longleftrightarrow I-\frac{1}{2}$ and $F = I+\frac{1}{2}$, $|m_F| = I-\frac{1}{2} \longleftrightarrow I-\frac{3}{2}$). The g_J-value ($g_J = 1.6433 \pm 0.0002$), which is not in agreement with the Landé formula, has been measured for Bi^{209} with the atomic beam method [4]). The isotopes examined are easily identified by their half-lives [5–7]) (Bi^{203} 12 h, Bi^{204} 13 h, Bi^{205} 14.5 d, Bi^{206} 6.3 d) and by the fact that the even A isotopes have integral and the odd A isotopes half-integral spin values †.

2. Experimental Method

The two short lived isotopes Bi^{203} and Bi^{204} were produced by the reaction Pb(p, kn) Bi, in the synchrocyclotron at the Gustaf Werner Institute for Nuclear Chemistry in Uppsala using 35 MeV protons, and the

† These measurements were reported at the Third Molecular Beam Conference at Brookhaven (November 1957). The spin of Bi^{206} was reported at the same conference by W. B. Eubank *et al.* [13])

14.5 d and 6.3 d isotopes Bi^{205} and Bi^{206} in the cyclotron at the Nobel Institute of Physics in Stockholm by the reaction Pb(d, *k*n)Bi using 25 MeV deuterons. The target was soluted in HNO_3 and the radioactive bismuth together with some milligrams of natural bismuth was deposited on nickel powder by internal electrolysis [8]).

The oven was made of molybdenum and had a long channel 0.4 mm wide to conserve the radioactive material. It was heated by electron bombardment directed to the channel walls so that the channel got a much higher temperature than the rest of the oven. Ordinary bismuth vapour consists of molecules which, however, were partially dissociated when they collided with the channel walls. Heating the oven to between 600° and 700° C, measured at the back of the oven, we got an intense beam. The atoms were collected on sooted metal foils, which turned out to have a high sticking coefficient for these atoms and gave a reproducible detection.

As the isotopes decay by K-capture with an X-ray of about 80 keV, a 2 mm scintillation chrystal, 1″ in diameter, was used to measure the activity [9]). This gave a background counting for the whole line of about 2 c.p.m. As the foils were rather large, about 2 inches in diameter, they were folded together before counting.

C-field measurements were made with a potassium beam coming from a calibration oven and being detected with a conventional surface ionization detector. The spin measurements were first made at a C-field corresponding to a potassium frequency of the order of 2 Mc/s and then the two resonance lines were observed at higher C-fields to confirm the results.

3. Results

Figs. 1 and 2 show two typical resonance curves, the first for a $F = I+\frac{3}{2}$ and the second for a $F = I+\frac{1}{2}$ state transition.

The spin searches only gave signals for $I = \frac{9}{2}$ and $I = 6$. Measuring on Bi^{205} and Bi^{206} we allowed the short lived isotopes to decay away for some days before we made the chemical separation. The signals then received had the half-lives (6 ± 1) d for $I = 6$ and (13.5 ± 2) d for $I = \frac{9}{2}$ and we could therefore assign the spin value 6 to Bi^{206} and $\frac{9}{2}$ to Bi^{205}.

Bi^{203} has a radioactive daughter, the 52 h isotope Pb^{203}, decaying by K-capture with an X-ray of the same order of energy as that of Bi. This means that the activity from Bi^{203} should decrease much more slowly than that from Bi^{204}. Fig. 3 shows the decay of the spin setting $\frac{9}{2}$ signal analyzed into a (12+52) h activity superimposed on a 14.5 d activity. According to these curves the spin value $\frac{9}{2}$ can be assigned to Bi^{203}. Fig. 4 shows the decay of the $I = 6$ spin setting signal. This curve makes it possible to assign the spin value $I = 6$ to Bi^{204}.

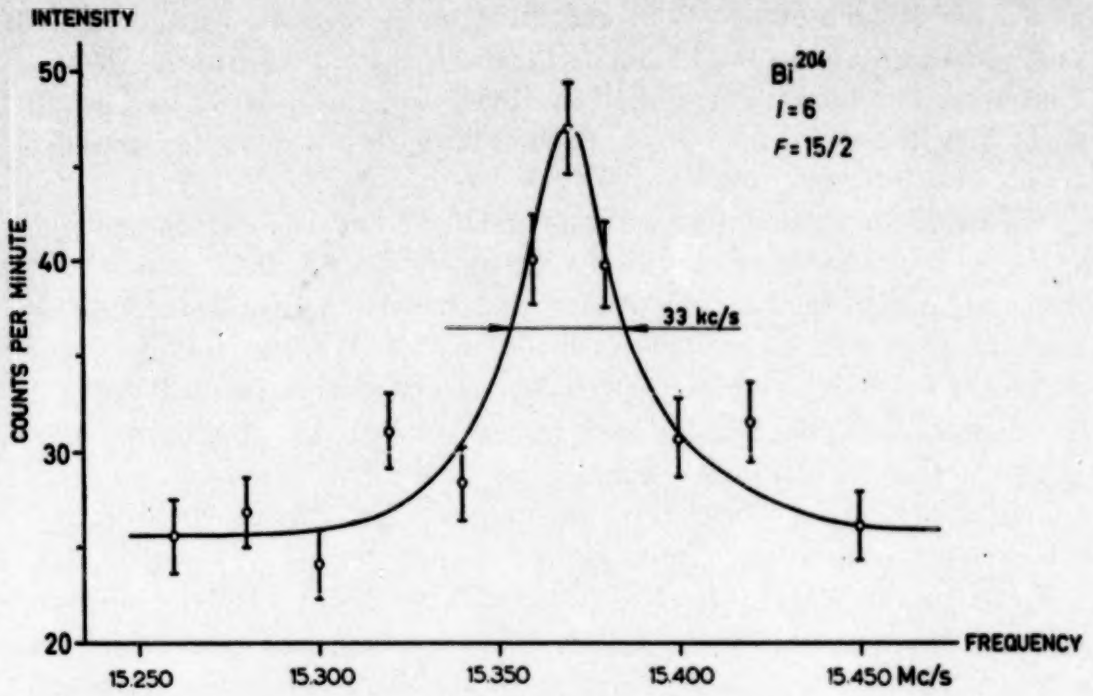

Fig. 1. Typical resonance curve of Bi^{204} in the state $F = \frac{15}{2}$.

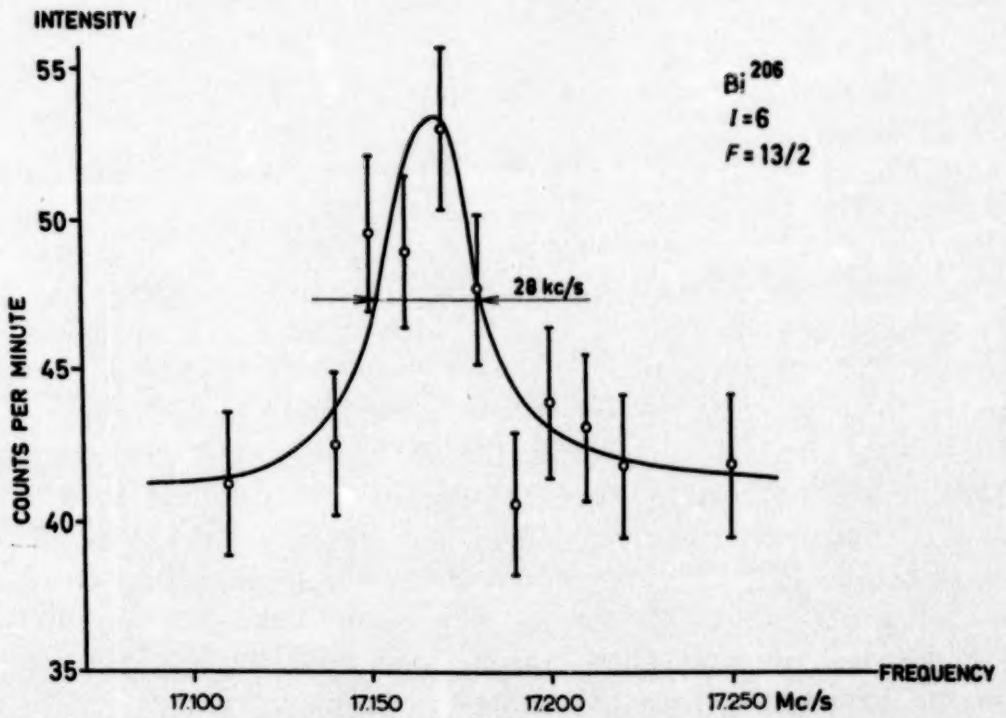

Fig. 2. Typical resonance curve of Bi^{206} in the state $F = \frac{13}{2}$.

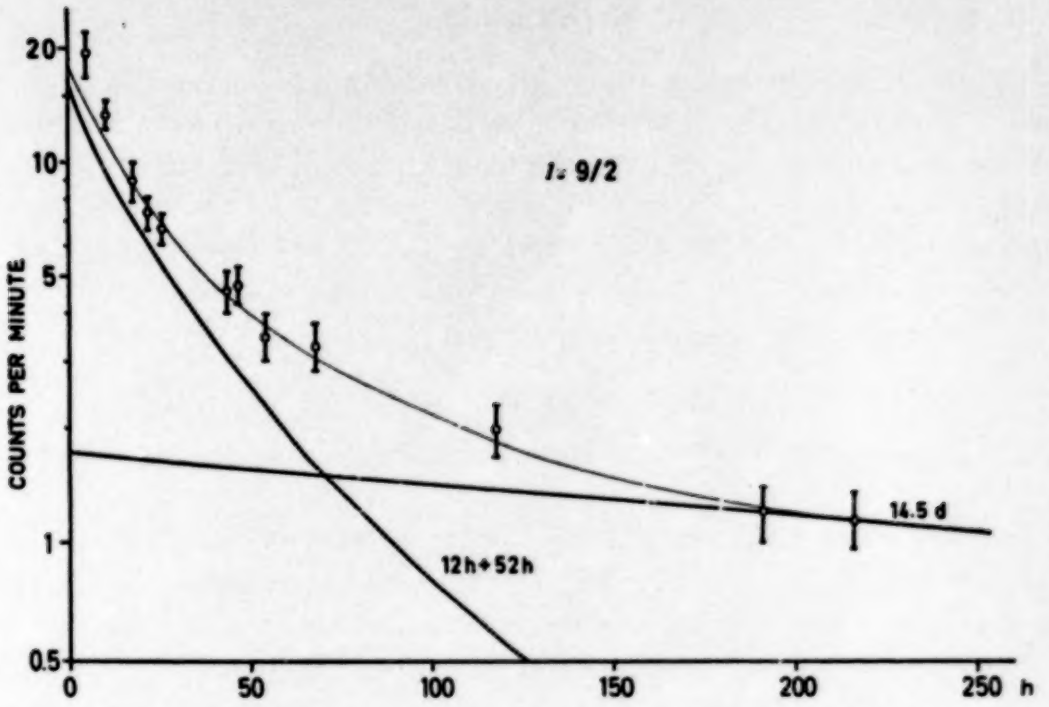

Fig. 3. Decay curve of a signal for $I = \frac{9}{2}$ analyzed into a (12+52) h and a 14.5 d activity.

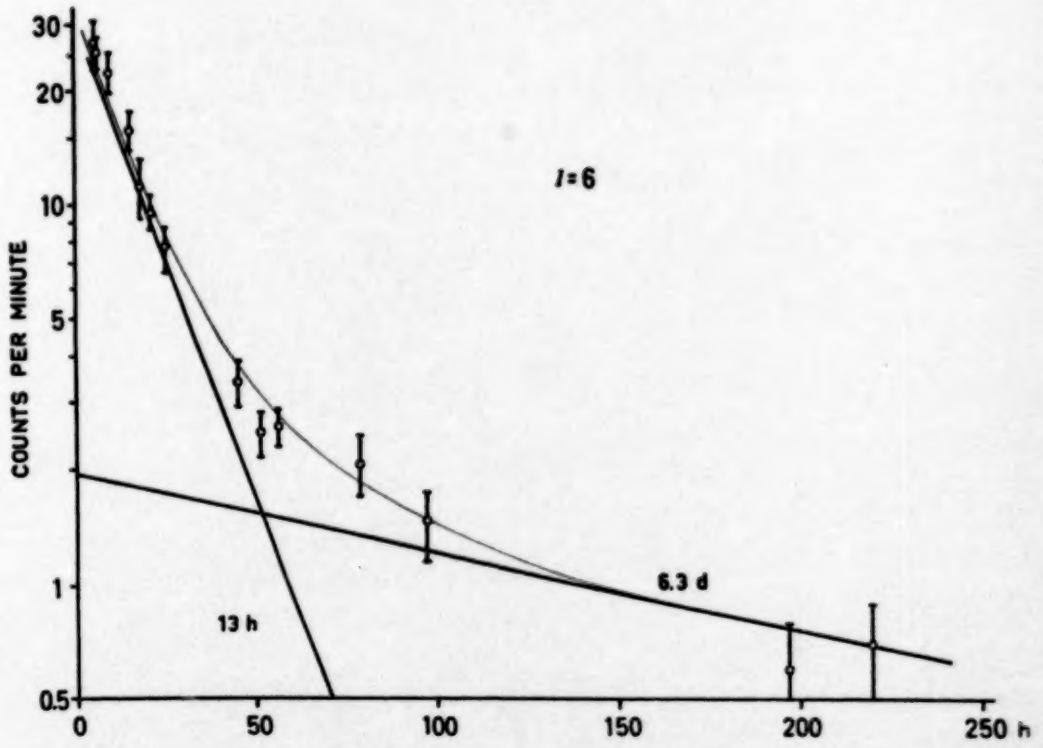

Fig. 4. Decay curve of a signal for $I = 6$ analyzed into a 13 h and a 6.5 d activity.

4. Discussion

The measured spin values are in agreement with those obtained from the nuclear shell model. The bismuth nucleus has 83 protons, which means that one proton is outside a closed shell in the level $h_{\frac{9}{2}}$. Consequently the odd A isotopes should have the spin $\frac{9}{2}$ [10]), which is the case for the two isotopes reported here as well as for the natural one Bi^{209}. The two even A isotopes have been calculated to have the following ground state configurations:

$$Bi^{204} \quad (\pi h_{\frac{9}{2}})(\nu f_{\frac{5}{2}})^{-3}(\nu p_{\frac{1}{2}})^{-2}$$

$$Bi^{206} \quad (\pi h_{\frac{9}{2}})(\nu f_{\frac{5}{2}})^{-1}(\nu p_{\frac{1}{2}})^{-2}$$

and the spin value 6 [11,12]), also in agreement with the measured value.

The authors wish to express their thanks to Professor Kai Siegbahn for his great interest in this work and to the cyclotron crews at the Gustaf Werner Institute and at the Nobel Institute for making the irradiations.

This work has been supported by the Swedish Atomic Committee.

References

1) I. Lindgren, Nuclear Instruments **3** (1958) 1
2) J. R. Zacharias, Phys. Rev. **61** (1942) 270
3) J. P. Hobson *et al.*, Phys. Rev. **104** (1956) 101
4) K. Smith, Report at the Second Molecular Beam Conference at Brookhaven (October 1956)
5) R. Stockendal *et al.*, Ark. f. Fys. **11** (1956) 165
6) D. G. Karraker and D. H. Templeton, Phys. Rev. **81** (1951) 510
7) E. Arbman, Nuclear Physics **3** (1951) 625
8) D. E. Alburger and G. Friedlander, Phys. Rev. **81** (1951) 523
9) J. C. Hubbs and W. A. Nierenberg, University of Calif., Radiation Lab. Report, UCRL 3434, June 1956 (unpublished)
10) M. H. L. Pryce, Nuclear Physics **2** (1956/57) 226
11) D. E. Alburger and M. H. L. Pryce, Phys. Rev. **95** (1954) 1482
12) S. Walborn, Nuclear Physics **3** (1957) 644
13) W. B. Eubank *et al.*, Bull. Am. Phys. Soc. **2** (1957) 383

2.L *Nuclear Physics* 9 (1958/59) 49—64; © *North-Holland Publishing Co., Amsterdam*
Not to be reproduced by photoprint or microfilm without written permission from the publisher

ON THE INELASTIC SCATTERING OF NUCLEONS BY NUCLEI AT HIGH ENERGIES

H. S. KÖHLER
CERN, *Geneva*

Received 9 August 1958

Abstract: The inelastic scattering of high energy nucleons by nuclei has been treated taking account of the nuclear distortion of the scattered wave in the high energy approximation. Using the collective model and including a Thomas-type spin-orbit interaction, treated as a perturbation, the explicit expression for the polarization previously obtained for elastic scattering is generalized to inelastic scattering as well.

The many-body problem of inelastic scattering is considered following the methods of Watson *et al.* This treatment is limited to transitions for which the two-nucleon scattering matrix is reduced as it is in elastic scattering on spin-zero nuclei. Then an explicit expression for the polarization is again derived similar to that for the elastic scattering but reflecting the angular dependence of nucleon-nucleon scattering.

1. Introduction

In recent years several measurements have been made of differential cross-sections and polarizations † of protons inelastically scattered by nuclei. Such experiments have been made at 220 MeV in Rochester [1]), at 155 and 173 MeV in Uppsala [2]) and at 135 and 95 MeV in Harwell [3]). A striking feature of these results is the similarity between the angular dependence of the polarization of particles scattered inelastically by exciting a low-lying level and the elastic polarization [2]). Even more striking is the agreement between polarizations of protons scattered inelastically by nuclei of different masses (fig. 1). In this paper we wish especially to understand these facts.

An explicit formula has previously been presented for the polarization of neutrons scattered elastically [4]). Then a spin-orbit coupling of the Thomas type was assumed. The correctness of this assumption is shown in the derivation of the optical model from nucleon-nucleon interaction [5, 6]). The essential approximation necessary for the derivation of the formula was the treatment of the spin-dependent part as a perturbation. The same formula is obtained if the whole interaction is treated in Born approximation.

Maris [7]) and Ruderman [8]) have shown that a treatment of the inelastic excitation in terms of the collective model in Born approximation does give the same explicit expression for elastic and inelastic polarization.

† In the approximations we make in this paper there will be no asymmetry-polarization difference.

Squires [9]) calculated the inelastic scattering off C^{12} using the shell-model and took care of the absorptive part of the distorting optical model potential. Notably he obtained in *L-S* coupling a polarization in good agreement with experiments.

Although there is so far no contradiction between experiments and calculations there is no a priori justification for neglecting either the real or the

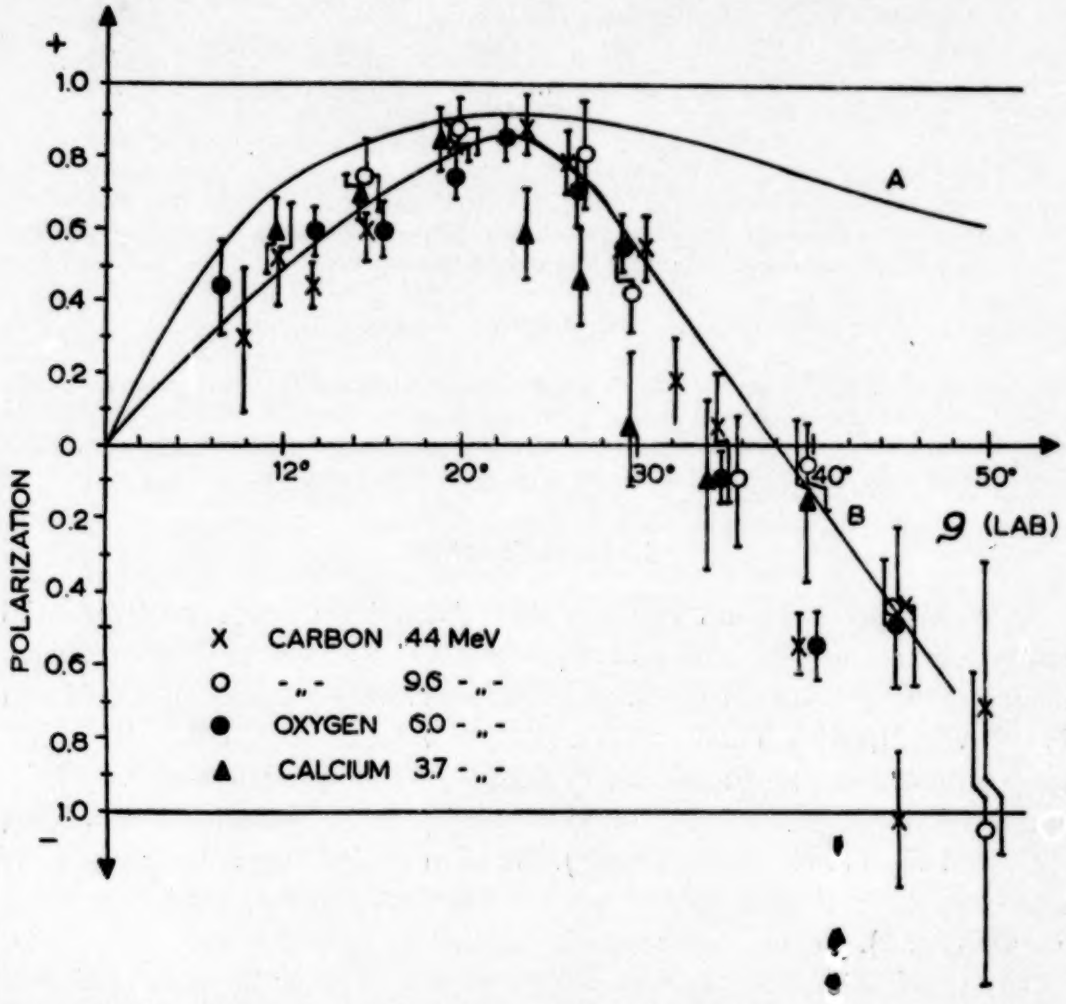

Fig. 1. Experimental results from Uppsala of polarization of low-lying levels of carbon, calcium and oxygen [2])††. Curve A shows a best fit curve with α constant (case A in the text). In curve B, α is a function of angle (case B in the text). Curve B is the same as in ref.[9]) and thus calculated from the Gammel-Thaler phase shifts for nucleon-nucleon scattering.

imaginary part of the central potential when calculating the distorted wave function. In this paper we treat the nuclear distortion † in a high energy approximation and treat the spin dependent part as a perturbation. Using

† We shall use the word "distortion" to denote the distortion of the wave function of the scattered particle due to the nuclear field. "Deformation" will mean the deformation of a nuclear surface.

†† Recent measurements [2a]) on other nuclei show the same behaviour. The author wishes to thank Drs. A. Johansson, G. Tibell and P. Hillman for the communication of these results.

the collective model and including a Thomas type spin-orbit coupling, we then find again the elastic polarization formula for the inelastic scattering. Following the methods of Watson *et al.*[10]) we also treat the many body problem and a similar expression for the polarization is obtained for transitions for which the nucleon-nucleon amplitude is reduced so as not to contain the spins of the nucleons in the nucleus, as is the case for elastic scattering on spin-zero nuclei.

We shall also be able to understand that the inelastic polarization is more independent of the mass of the scattering nucleus than is the elastic, as being due to the relative unimportance of the Coulomb field in the inelastic case in comparison with the elastic.

2. The High Energy Approximation

Molière [11]) has shown how to solve approximately the problem of scattering by a potential at high energies. The problem has also been treated by Glauber [12]). Most recently Schiff [13]) and Saxon and Schiff [14]) have derived approximate formulae for scattering amplitudes and wave functions in the high energy limit. In particular they have been able to deduce expressions for the scattering amplitudes, suitable for our treatment and valid for $\theta < (kR)^{-\frac{1}{2}}$ and for $\theta > (kR)^{-\frac{1}{2}}$, where θ is the scattering angle, k the wave number and R the nuclear radius. The small-angle result agrees essentially with that obtained by Molière and by Glauber. We note that essentially the same result is obtained if the phase shifts in a partial-wave analysis are calculated in the high energy W.K.B. approximation as has been conventionally done in many previous calculations on the optical model.

In this paper we shall use mainly the small-angle approximation of Schiff, although we shall also see that our main result is slightly more general but is still, for different reasons, expected to be valid for small angles only.

We now collect some formulae concerning the scattering amplitudes.

1. The scattering amplitude due to a potential $U(\mathbf{r})+v(\mathbf{r})$ is in the small-angle approximation

$$f(\mathbf{k}_f, \mathbf{k}_0) = -\frac{m}{2\pi\hbar^2}\int e^{i\mathbf{q}\cdot\mathbf{r}}(U+v)e^{-(ik/2E)\int_{-\infty}^{z}(U+v)dz}\,d\tau \tag{1}$$

with $\mathbf{q} = \mathbf{k}_0 - \mathbf{k}_f$ and E the energy; $\mathbf{q}\cdot\mathbf{r}$ stands for $q_x x + q_y y$ as $q_z z$ is small and is neglected. Through some partial integrations in the z-coordinate we can rewrite (1) and get

$$\begin{aligned} f(\mathbf{k}_f, \mathbf{k}_0) = &-\frac{m}{2\pi\hbar^2}\int e^{i\mathbf{q}\cdot\mathbf{r}}Ue^{-(ik/2E)\int_{-\infty}^{z}Udz}\,d\tau \\ &-\frac{m}{2\pi\hbar^2}\int e^{i\mathbf{q}\cdot\mathbf{r}}ve^{-(ik/2E)\int_{-\infty}^{+\infty}Udz-(ik/2E)\int_{-\infty}^{z}vdz}\,d\tau \end{aligned} \tag{2}$$

and to first order in v

$$f^1(\mathbf{k}_f,\mathbf{k}_0) = -\frac{m}{2\pi\hbar^2}\int e^{i\mathbf{q}\cdot\mathbf{r}}Ue^{-(ik/2E)\int_{-\infty}^{z}Udz}\,d\tau - \frac{m}{2\pi\hbar^2}\int e^{i\mathbf{q}\cdot\mathbf{r}}ve^{-(ik/2E)\int_{-\infty}^{+\infty}Udz}\,d\tau. \tag{3}$$

We shall also make use of the first order expansion in the form

$$f^1(\mathbf{k}_f,\mathbf{k}_0) = -\frac{m}{2\pi\hbar^2}\int e^{i\mathbf{q}\cdot\mathbf{r}}Ue^{-(ik/2E)\int_{-\infty}^{z}Udz}\,d\tau - \frac{m}{2\pi\hbar^2}\int e^{i\mathbf{q}\cdot\mathbf{r}}ve^{-(ik/2E)\int_{-\infty}^{z}Udz}\,d\tau - \frac{m}{2\pi\hbar^2}\int e^{i\mathbf{q}\cdot\mathbf{r}}U\left(-\frac{ik}{2E}\int_{-\infty}^{z}vdz\right)e^{-(ik/2E)\int_{-\infty}^{z}Udz}\,d\tau. \tag{4}$$

We compare (2) and (3) with the exact expressions for the two-potential problem derived by Gell-Mann and Goldberger [15]) and by Watson [16]):

$$f(\mathbf{k}_f,\mathbf{k}_0) = -\frac{m}{2\pi\hbar^2}[\langle\phi_b|U|\chi_a^+\rangle+\langle\chi_b^-|v|\psi_a^+\rangle], \tag{5}$$

$$f^1(\mathbf{k}_f,\mathbf{k}_0) = -\frac{m}{2\pi\hbar^2}[\langle\phi_b|U|\chi_a^+\rangle+\langle\chi_b^-|v|\chi_a^+\rangle], \tag{6}$$

where ϕ denotes the plane wave, $\chi^{\pm}$ the out- and in-going scattered wave solutions to the potential U, while $\psi^{\pm}$ are the corresponding solutions to the potential $U+v$.

We thus see that (2) and (3) agree with (5) and (6) respectively with

$$\chi_a^+ = e^{i\mathbf{k}_0\cdot\mathbf{r}-(ik/2E)\int_{-\infty}^{z}Udz} \qquad \chi_b^- = e^{i\mathbf{k}_f\cdot\mathbf{r}+(ik/2E)\int_{z}^{\infty}Udz}$$
$$\psi_a^+ = e^{i\mathbf{k}_0\cdot\mathbf{r}-(ik/2E)\int_{-\infty}^{z}(U+v)dz}. \tag{7}$$

2. We also treat two parts of the interaction as perturbations. We consider an interaction

$$\mathscr{V} = U+DU+Q(U+DU) \tag{8}$$

where D and Q are some operators to be treated in perturbation. In our application D will denote a direct interaction and Q the spin-orbit part of the interaction. From (2) we have

$$f(\mathbf{k}_f,\mathbf{k}_0) = -\frac{m}{2\pi\hbar^2}\int e^{i\mathbf{q}\cdot\mathbf{r}}Ue^{-(ik/2E)\int_{-\infty}^{z}Udz}\,d\tau - \frac{m}{2\pi\hbar^2}\int e^{i\mathbf{q}\cdot\mathbf{r}}(DU+QU+QDU) \times e^{-(ik/2E)\int_{-\infty}^{+\infty}Udz-(ik/2E)\int_{-\infty}^{z}(DU+QU+QDU)dz}\,d\tau. \tag{9}$$

We expand the last exponent in (9) and collect terms of order D, and QD. Noting that

$$\int_{-\infty}^{+\infty}\left[DU\int_{-\infty}^{z}QU\mathrm{d}z+QU\int_{-\infty}^{z}DU\mathrm{d}z\right]\mathrm{d}z=\int_{-\infty}^{+\infty}QU\mathrm{d}z\int_{-\infty}^{+\infty}DU\mathrm{d}z$$

we then obtain

$$\begin{aligned}f_D(\mathbf{k}_f,\mathbf{k}_0)=&-\frac{m}{2\pi\hbar^2}\int \mathrm{e}^{i\mathbf{q}\cdot\mathbf{r}}(DU+QDU)\mathrm{e}^{-(ik/2E)\int_{-\infty}^{+\infty}U\mathrm{d}z}\,\mathrm{d}\tau\\&-\frac{m}{2\pi\hbar^2}\int \mathrm{e}^{i\mathbf{q}\cdot\mathbf{r}}DU\int_{-\infty}^{+\infty}QU\mathrm{d}z\mathrm{e}^{-(ik/2E)\int_{-\infty}^{+\infty}U\mathrm{d}z}\,\mathrm{d}\tau.\end{aligned}\tag{10}$$

3. We consider scattering amplitudes of the type

$$\begin{aligned}f=&\int \mathrm{e}^{i\mathbf{q}\cdot\mathbf{r}}U_1\,\mathrm{e}^{-i\int_{-\infty}^{\nu z}U\mathrm{d}z}\,\mathrm{d}\tau+a\int \mathrm{e}^{i\mathbf{q}\cdot\mathbf{r}}\boldsymbol{\nabla}U_1\times\mathbf{K}\mathrm{e}^{-i\int_{-\infty}^{\nu z}U\mathrm{d}z}\,\mathrm{d}\tau\\&+a_1\int \mathrm{e}^{i\mathbf{q}\cdot\mathbf{r}}U_1\boldsymbol{\nabla}\times\mathbf{K}\mathrm{e}^{-i\int_{-\infty}^{\nu z}U\mathrm{d}z}\,\mathrm{d}\tau.\end{aligned}\tag{11}$$

Here ν is an arbitrary number and $\mathbf{K}$ is the unit vector in the z direction which thus suppresses the z derivative in the gradient operator. As before $q_z=0$, U_1 and U are functions of $\mathbf{r}$. By partial integration of the second term we rewrite this

$$\begin{aligned}a\int \mathrm{e}^{i\mathbf{q}\cdot\mathbf{r}}\boldsymbol{\nabla}U_1\times\mathbf{K}\,\mathrm{e}^{-i\int_{-\infty}^{\nu z}U\mathrm{d}z}\,\mathrm{d}\tau=&-ia\mathbf{q}\times\mathbf{K}\int \mathrm{e}^{i\mathbf{q}\cdot\mathbf{r}}U_1\mathrm{e}^{-i\int_{-\infty}^{\nu z}U\mathrm{d}z}\,\mathrm{d}\tau\\&-a\int \mathrm{e}^{i\mathbf{q}\cdot\mathbf{r}}U_1\boldsymbol{\nabla}\times\mathbf{K}\,\mathrm{e}^{-i\int_{-\infty}^{\nu z}U\mathrm{d}z}\,\mathrm{d}\tau.\end{aligned}\tag{12}$$

Putting this into (11) we get

$$f=(1-ia\mathbf{q}\times\mathbf{K})\int \mathrm{e}^{i\mathbf{q}\cdot\mathbf{r}}U_1\mathrm{e}^{-i\int_{-\infty}^{\nu z}U\mathrm{d}z}\,\mathrm{d}\tau+(a_1-a)\int \mathrm{e}^{i\mathbf{q}\cdot\mathbf{r}}\boldsymbol{\nabla}\times\mathbf{K}\,\mathrm{e}^{-i\int_{-\infty}^{\nu z}U\mathrm{d}z}\,\mathrm{d}\tau.\tag{13}$$

We note that (13) is obtained under the general condition $U_1\neq U$ and ν arbitrary, and that the last term vanishes for $a_1=a$ or $\nu\to-\infty$.

It will later be seen that the possibility of rewriting (11) as (13) considerably simplifies our final expressions especially for the polarization.

3. Collective Excitation

We will first consider the scattering in terms of the collective model. If we include the Thomas type spin-orbit term and neglect the electromagnetic interaction (this latter part will be discussed later) then the interaction with the nucleon will be

$$\mathscr{V}=\mathscr{V}(\mathbf{r}\alpha_\mu)(1+i\beta)+\frac{\alpha}{2\hbar}(1-i\gamma)\boldsymbol{\nabla}\mathscr{V}(\mathbf{r}\alpha_\mu)\times\mathbf{p}\cdot\boldsymbol{\sigma},\tag{14}$$

or to simplify notations,

$$\mathscr{V} = V(\mathbf{r}\alpha_\mu)+\frac{\alpha'}{2\hbar}\nabla V(\mathbf{r}\alpha_\mu)\times\mathbf{p}\cdot\boldsymbol{\sigma} \tag{14a}$$

where α_μ are the collective coordinates, $\alpha' = [(1-i\gamma)/(1+i\beta)]\alpha$ and $\alpha = \alpha_1\hbar^2/2M^2c^2$. Earlier estimates from elastic polarization have given $\alpha_1 \approx 30$.

If the nuclear boundary is described by a deformation of order two,

$$R(\theta\varphi) = R_0[1+\sum_m \alpha_m Y_{2m}(\theta\varphi)],$$

and the shape of the potential coincides with the shape of the nucleus we get in first order of α_μ(e.g. ref.[17]))

$$V(r\theta\varphi\alpha_\mu) = U_0(r)-r\frac{\mathrm{d}U_0(r)}{\mathrm{d}r}\sum_m \alpha_m Y_{2m}(\theta\varphi) \equiv U_0(r)+v(\mathbf{r}), \tag{15}$$

thus separating $V(\mathbf{r}\alpha_\mu)$ into a spherical and a deformed part. The nuclear wave function will be denoted ψ_n. We wish to use the adiabatic approximation, whose application to our problem has been discussed by Chase [18]). (See also a paper by Schiff [19]).) We thus emphasize that the nuclear deformation motions are slow compared to the velocity of the scattered nucleon.

If the scattering for each orientation of the nucleus is treated in the small-angle approximation, one obtains for the spin-dependent scattering amplitude

$$f(\mathbf{k}_f,\mathbf{k}_0) = -\frac{m}{2\pi\hbar^2}\langle\psi_f|\int \mathrm{e}^{i\mathbf{q}\cdot\mathbf{r}}\mathscr{V}\mathrm{e}^{-(ik/2E)\int_{-\infty}^{z}\mathscr{V}\mathrm{d}z}\,\mathrm{d}\tau|\psi_0\rangle. \tag{16}$$

Now the spin-orbit term in (14) is treated as a perturbing term. This is done by using (4) and we get, with the notation (14a),

$$\begin{aligned} f(\mathbf{k}_f,\mathbf{k}_0) = -\frac{m}{2\pi\hbar^2}\langle\psi_f|\,\mathrm{e}^{i\mathbf{q}\cdot\mathbf{r}-(ik/2E)\int_{-\infty}^{z}V(\mathbf{r}\alpha_\mu)\mathrm{d}z}\Big[V(\mathbf{r}\alpha_\mu)+\tfrac{1}{2}\alpha'\nabla V(\mathbf{r}\alpha_\mu)\times\mathbf{p}\cdot\boldsymbol{\sigma} \\ +V(\mathbf{r}\alpha_\mu)\left(-\frac{ik}{2E}\int_{-\infty}^{z}\tfrac{1}{2}\alpha'\nabla V(\mathbf{r}\alpha_\mu)\times\mathbf{p}\cdot\boldsymbol{\sigma}\mathrm{d}z\right)\Big]\,\mathrm{d}\tau|\psi_0\rangle. \end{aligned} \tag{17}$$

This expression we rewrite by using (11) to (13) with $U_1 = U = V(\mathbf{r}\alpha_\mu)$, $a_1 = a = \frac{1}{2}\alpha'$ and $\nu = 1$ (we observe that in our scattering approximation $\mathbf{p} = p\mathbf{K}$):

$$\begin{aligned} f(\mathbf{k}_f,\mathbf{k}_0) = -\frac{m}{2\pi\hbar^2}(1-\tfrac{1}{2}i\alpha'\,\mathbf{q}\times\mathbf{k}\cdot\boldsymbol{\sigma}) \\ \cdot\langle\psi_f|\int \mathrm{e}^{i\mathbf{q}\cdot\mathbf{r}}V(\mathbf{r}\alpha_\mu)\mathrm{e}^{-(ik/2E)\int_{-\infty}^{z}V(\mathbf{r}\alpha_\mu)\mathrm{d}z}\,\mathrm{d}\tau|\psi_0\rangle. \end{aligned} \tag{18}$$

Returning to the notation in (14) we thus get for the polarization as usually defined

$$P(\theta) = \frac{\alpha(\gamma+\beta)k^2 \sin\theta}{1+\beta^2+\frac{1}{4}\alpha^2 k^4(1+\gamma^2)\sin^2\theta}, \tag{19}$$

which we recognize as a result previously obtained for the elastic polarization of neutrons [4]). Here we obtain of course the elastic amplitude as a special case by putting $\psi_f = \psi_0$. The result (19) was obtained earlier by Maris [7]) and by Ruderman [8]) for the inelastic polarization using Born approximation. We obtain the Born approximation by neglecting V in the exponential in (18). Our improvement is thus to include the distortion of the scattered wave due to the central potential, and due to the spin-orbit interaction in first order. Nishimura and Ruderman [20]) calculated the polarization including the distortion due to the central potential but neglected the spin-orbit interaction in the distorted wave function †; they also used the large-angle approximation. These points may explain the difference of their result from ours.

For further discussion of our result (18) we separate the nuclear deformed part from the undeformed, which is accomplished by the use of (2), and we get

$$f(\mathbf{k}_f, \mathbf{k}_0) = -\frac{m}{2\pi\hbar^2}(1-\tfrac{1}{2}i\alpha'\,\mathbf{q}\times\mathbf{k}\cdot\boldsymbol{\sigma})\Big[\int e^{i\mathbf{q}\cdot\mathbf{r}} U_0(r) e^{-(ik/2E)\int_{-\infty}^{z} U_0(r)dz} d\tau \delta_{0f} + \langle\psi_f| \int e^{i\mathbf{q}\cdot\mathbf{r}} v(\mathbf{r}) e^{-(ik/2E)\int_{-\infty}^{+\infty} U_0(r)dz - (ik/2E)\int_{-\infty}^{z} v(\mathbf{r})dz} d\tau |\psi_0\rangle\Big]. \tag{20}$$

For the elastic scattering the first term within the brackets is the predominant one but for inelastic scattering it becomes zero due to the δ function. Thus

$$f_{\text{inel}}(\mathbf{k}_f, \mathbf{k}_0) = -\frac{m}{2\pi\hbar^2}(1-\tfrac{1}{2}i\alpha'\,\mathbf{q}\times\mathbf{k}\cdot\boldsymbol{\sigma}) \cdot \langle\psi_f| \int e^{i\mathbf{q}\cdot\mathbf{r}} v(\mathbf{r}) e^{-(ik/2E)\int_{-\infty}^{+\infty} U_0(r)dz - (ik/2E)\int_{-\infty}^{z} v(\mathbf{r})dz} d\tau |\psi_0\rangle. \tag{21}$$

In a perturbation treatment of $v(\mathbf{r})$, it is dropped in the exponential, a result which can be obtained directly from (10) with D the deformation and Q the spin-orbit operator. From (21) we deduce that the inelastic cross-section is not very sensitive to changes in the depth of the real part of the potential U_0 (as long as $v(\mathbf{r})$ is kept constant) as these mainly just change

† From the general treatment of the scattering by two potentials, of which one is treated as small we know that it is not correct only to neglect the distortion due to the small potential. The correct perturbation term is (6) $\langle\chi_b^-|v|\chi_a^+\rangle$ while the incorrect procedure would give $\langle\phi_b|v|\chi_a^+\rangle$. In the high energy (small-angle) approximation, we get in the first case

$$\int e^{i\mathbf{q}\cdot\mathbf{r}} v e^{i\int_{-\infty}^{+\infty} U dz}$$

and in the second

$$\int e^{i\mathbf{q}\cdot\mathbf{r}} v e^{i\int_{-\infty}^{z} U dz}.$$

the phase of the scattering amplitude. The imaginary (absorptive) part however affects the cross-section as a damping effect. We compare this discussion with the approximation in ref.[21]) where all phases $\int_{-\infty}^{+\infty} U_0(r)\mathrm{d}z$ were put constant, that is independent of impact parameter. Applying the same approximation to (21) would result in complete independence of the real part while the imaginary part would just give a damping factor, which, in case v (**r**) is treated as a perturbation, is applied to the Born approximation. That would probably not in general be as good an approximation in the inelastic case as it is in the elastic, just because the inelastic events occur mostly at larger angles.

It is known that in the case of elastic scattering the electromagnetic interaction is important by giving interference effects showing up not only in the differential cross-section but also in the polarization (e.g. ref.[21])). We include the electromagnetic field by adding to (14)

$$V_c + \frac{C}{2\hbar}\nabla V_c \times \mathbf{p}\cdot\boldsymbol{\sigma}, \qquad C = g_s\frac{\hbar^2}{2M^2c^2}.$$

We can now no longer arrive directly at (18). For a discussion we separate the deformed part of the nuclear interaction and get an inelastic amplitude

$$f_{\mathrm{inel}}(\mathbf{k}_f,\mathbf{k}_0) = -\frac{m}{2\pi\hbar^2}\langle\psi_f|\int \mathrm{e}^{i\mathbf{q}\cdot\mathbf{r}}\left(v(\mathbf{r}) + \frac{\alpha'}{2\hbar}\nabla v(\mathbf{r})\times\mathbf{p}\cdot\boldsymbol{\sigma}\right)$$
$$\cdot\,\mathrm{e}^{-(ik/2E)\int_{-\infty}^{+\infty}(U_0+(\alpha'/2\hbar)\nabla U_0\times\mathbf{p}\cdot\boldsymbol{\sigma}+V_c+(C/2\hbar)\nabla V_c\times\mathbf{p}\cdot\boldsymbol{\sigma})\mathrm{d}z} \qquad (22)$$
$$\cdot\,\mathrm{e}^{-(ik/2E)\int_{-\infty}^{z} v+(\alpha'/2\hbar)\nabla v\times\mathbf{p}\cdot\boldsymbol{\sigma}\mathrm{d}z}\,\mathrm{d}\tau|\psi_0\rangle.$$

We note that the integration $\mathrm{d}\tau$ goes over the nuclear volume only (in contrast to the elastic amplitude with Coulomb interaction). However, over this region of integration the (real) Coulomb phases $\int_{-\infty}^{+\infty} V_c\mathrm{d}z$ vary very little with the impact parameter † and a mean phase can be taken out. Also, the Coulomb spin-orbit phases are negligible in comparison with the nuclear spin-orbit phases not only because the Coulomb spin-orbit coupling is smaller but also due to the above mentioned constancy of the Coulomb phases. This is because the Coulomb spin-orbit phases are proportional to the derivative of the central Coulomb phases with respect to the impact parameter [4]). As a constant Coulomb phase is irrelevant in computing the cross-section we thus conclude that the switching on of the Coulomb interaction will affect our results (18) and (19) very little, and these are thus good also for proton scattering. As stated above, the Coulomb field is on the contrary important when one treats the elastic scattering. To clarify the difference between elastic and inelastic scattering we state it in words. The inelastic wavelets are produced within the nucleus but wavelets passing through the Coulomb

† This point is discussed in ref.[21]) in connection with elastic scattering.

field and outside the nucleus give no contribution to the inelastic scattering. On the other hand in the case of elastic scattering it is these waves passing through the Coulomb field outside the nucleus that give the characteristic Coulomb effects †.

If we interpret the mass-dependence of the elastic polarization to be a diffraction and Coulomb effect, we thus expect the inelastic polarization to be less dependent on the mass (or charge) of the scattering nucleus than the elastic. This is in agreement with experiment (fig. 1).

We finally wish to make a remark on the validity of our formula (19) for the polarization. We derived this using the small-angle approximation of Schiff. We note however that our derivation is not restricted to this approximation only. An essential difference between the small- and large-angle approximations is that the latter involves (in the nuclear distortion) an integration from $-\infty$ to $+\infty$ along the path of the scattered particle, while the former only involves integration from $-\infty$ to z, the "point of interaction". We have however noted that our derivation of (13) is independent of ν and thus also valid for $\nu \to +\infty$. If we thus approximate our integration along the path, composed of two straight lines, by that along one straight line ††, we again arrive at our formula (19) for the polarization, which we thus state is not necessarily restricted to small angles $\theta < (kR)^{-\frac{1}{2}}$.

We do expect (19) to break down in the angular region where the amplitude goes through a minimum, as has been discussed by various authors with reference to elastic scattering. As observed by Nishimura and Ruderman [20]) in the inelastic case this region will be at a larger angle than in the elastic, as the elastic amplitude varies approximately as $J_1(qR)$ and the inelastic as $J_2(qR)$ where J_ν is the Bessel function of order ν.

However, from the fundamental derivation of the optical model in terms of two-nucleon interactions, we expect that it is good for small-angle scattering only. So one should anyway be careful in applying the explicit polarization formula to angles beyond the forward elastic peak.

4. Many-Body Problem

In the preceding section we discussed the scattering in the collective model aspect of the nucleus. We now wish to study the many-body problem of a nucleon scattered by the nucleons in the nucleus. Watson *et al.*[10]) have shown how to solve such a problem and have especially applied the formalism to the elastic scattering [6]) and have shown how the optical model parameters can be derived from nucleon-nucleon scattering data. Bethe [22]) used the same

† As was pointed out earlier in this paper, a similar discussion leads to the conclusion that the value of the real part of $U_0(r)$ is not critical for the result.

†† It can be shown that this is not the necessary condition which is rather the equality $\mathbf{k}_f \approx \mathbf{k}_0$ in the spin orbit coupling term.

method and tried especially to discriminate between the different solutions of phaseshifts for nucleon-nucleon scattering at 300 MeV. Several authors have since made similar calculations [23]).

We start with the multiple scattering equations derived by Watson *et al.*:

$$\begin{aligned} \Omega &= 1+G\sum_{\alpha=1}^{A} t_\alpha \Omega(\alpha), \\ \Omega(\alpha) &= 1+G\sum_{\rho\neq\alpha}^{A} t_\beta \Omega(\beta); \end{aligned} \tag{23}$$

Ω is the wave matrix operator. Thus $\Omega\phi = \psi$ with ϕ the incident plane wave and ψ the total wave function of the many-body problem. t_α is the nucleon-nucleon scattering matrix in the nucleus as described by Watson. It will be approximated by $t_\alpha{}^0$, that is the t-matrix in free space, which is the impulse approximation. G is the Greens function $(E_a - H_0 + i\eta)^{-1}$ where E_a and H_0 are respectively the sums of nuclear and scattered nucleon energies and Hamiltonians. The positive parameter η gives as usual outgoing scattered waves.

We first review briefly Watson's treatment of elastic scattering. We get with $|\psi_0\rangle$ the ground state of the nucleus †

$$\langle\psi_0|\Omega|\psi_0\rangle = 1+G_0\sum_\alpha\sum_n \langle\psi_0|t_\alpha|\psi_n\rangle\langle\psi_n|\Omega(\alpha)|\psi_0\rangle \tag{24}$$

with

$$G_n = \langle\psi_n|G|\psi_n\rangle.$$

An approximation now introduced is to neglect transitions to excited intermediate states. Further we put $\langle\psi_0|\Omega(\alpha)|\psi_0\rangle = \langle\psi_0|\Omega|\psi_0\rangle$. Thus we have replaced the wave incident on the nucleon α by the total wave. We now get

$$\langle\psi_0|\Omega|\psi_0\rangle = 1+G_0U_{00}\langle\psi_0|\Omega|\psi_0\rangle \tag{25}$$

where

$$U_{00} = A\langle\psi_0|t^0|\psi_0\rangle \tag{25a}$$

is the optical model potential thus derived.

Now we wish to study the transition to a first excited state ψ_1 and get

$$\langle\psi_1|\Omega|\psi_0\rangle = G_1\sum_\alpha\sum_n \langle\psi_1|t_\alpha{}^0|\psi_n\rangle\langle\psi_n|\Omega(\alpha)|\psi_0\rangle. \tag{26}$$

We now neglect all intermediate states $|\psi_n\rangle$ except ψ_0 and ψ_1. This means that we allow the final state $|\psi_1\rangle$ to be fed from the initial state only but neglect those contributions to the final state that come from excitations to higher states and final deexcitation to the state we are interested in. We also put $\langle\psi_1|\Omega(\alpha)|\psi_0\rangle = \langle\psi_1|\Omega|\psi_0\rangle$ meaning that the inelastic wave hitting

† We let the angular brackets denote integration over the nuclear coordinates $r_1 \to r_A$ Round parentheses will mean integration over all coordinates $r_0 \to r_A$.

particle α will not differ much from the total inelastic wave as this is elastically scattered by α. Again we also put $\langle\psi_0|\Omega(\alpha)|\psi_0\rangle = \langle\psi_0|\Omega|\psi_0\rangle$ as in (25). Another approximation will be $A\langle\psi_1|t^0|\psi_1\rangle = A\langle\psi_0|t^0|\psi_0\rangle = U_{00}$ i.e. the optical potentials for the ground and a low excited state are put equal. We then obtain

$$\langle\psi_1|\Omega|\psi_0\rangle = G_1 U_{00}\langle\psi_1|\Omega|\psi_0\rangle + G_1 \sum_\alpha \langle\psi_1|t_\alpha{}^0|\psi_0\rangle\langle\psi_0|\Omega|\psi_0\rangle \tag{27}$$

$$\langle\psi_1|\Omega|\psi_0\rangle = \frac{G_1 \sum_\alpha \langle\psi_1|t_\alpha{}^0|\psi_0\rangle\langle\psi_0|\Omega|\psi_0\rangle}{1-G_1 U_{00}} \tag{27a}$$

which is our solution to the inelastic wave. The physical interpretation is that the inelastic wave is fed by the elastic wave within the potential U_{00}.

We also want to calculate the transition matrix

$$T = V\Omega = \sum_\alpha t_\alpha \Omega(\alpha) \tag{28}$$

where $\Omega(\alpha)$ is defined by (23). Thus

$$T_{10} = (\phi_1\psi_1|\sum_\alpha t_\alpha \Omega(\alpha)|\phi_0\psi_0) \tag{28a}$$

where ϕ_0 and ϕ_1 are the initial and final plane wave states of the scattered nucleon. We now separate t_α into diagonal and non-diagonal elements:

$$t_\alpha = \tau_\alpha + I_\alpha,$$

and get

$$T_{10} = (\phi_1\psi_1|\sum_\alpha \tau_\alpha \Omega|\phi_0\psi_0) + (\phi_1\psi_1|\sum_\alpha I_\alpha \Omega(\alpha)|\phi_0\psi_0) \tag{29}$$

where the approximation $\Omega(\alpha) \to \Omega$ is introduced in the first term as this only contains diagonal (elastic) scatterings. We rewrite

$$T_{10} = (\phi_1\psi_1|U_{00}\Omega + \sum_\alpha I_\alpha \Omega|\phi_0\psi_0) - (\phi_1\psi_1|\sum_\alpha I_\alpha(\Omega-\Omega(\alpha))|\phi_0\psi_0) \tag{30}$$

where we have again put

$$\langle\psi_1|\tau_\alpha|\psi_1\rangle = U_{00}.$$

The first term is rewritten according to (5) and

$$T_{10} = (\psi_1\chi_1^-|\sum I_\alpha \Omega|\psi_0\phi_0) - (\psi_1\phi_1|\sum I_\alpha(\Omega-\Omega(\alpha))|\psi_0\phi_0) \tag{31}$$

where χ_1 is the elastic wave solution for the potential U_{00}. We now note that we wish to study the transition from the ground state $|\psi_0\rangle$ to a first excited state $|\psi_1\rangle$. As I_α has only non-diagonal matrix-elements the last term is rewritten

$$\sum_{n\neq 1} (\psi_1\phi_1|\sum I_\alpha|\psi_n\rangle\langle\psi_n|(\Omega-\Omega(\alpha))|\psi_0\phi_0). \tag{32}$$

As in the derivation of (27), we now neglect all intermediate states $n \geqq 2$.

Thus in (32) $n = 0$ only. But we have already assumed $\langle\psi_0|\Omega(\alpha)|\psi_0\rangle = \langle\psi_0|\Omega|\psi_0\rangle$. So (32) and the last term in (31) will in our approximations be zero. Thus

$$T_{10} = (\psi_1\chi_1^-|\sum I_\alpha\Omega|\psi_0\phi_0). \tag{33}$$

We note that $\Omega\phi_0$ is the total scattered wave and thus contains also all inelastically scattered waves. In accordance with our previous neglect of contributions from higher excited states we put $\Omega\phi_0 = \chi_0$ and thus get

$$T_{10} = (\psi_1\chi_1^-|\sum I_\alpha|\psi_0\chi_0^+). \tag{34}$$

According to (7) we put in the high energy approximation for the scattered nucleon wave function in coordinate space

$$\begin{aligned}\langle\chi_1^-|\mathbf{r}'_0\rangle &= \mathrm{e}^{-ik_1r'_0-(ik/2E)\int_z^\infty U_{00}\,\mathrm{d}z'}\\ \langle\mathbf{r}_0|\chi_0^+\rangle &= \mathrm{e}^{ik_0r_0-(ik/2E)\int_{-\infty}^z U_{00}\,\mathrm{d}z}\end{aligned} \tag{35}$$

where U_{00} is defined by (25a).

Next we have to study the matrix element

$$U_{10}(\mathbf{r}_0\mathbf{r}'_0) = \langle\psi_1|\sum I_\alpha|\psi_0\rangle. \tag{36}$$

We now assume t_α (or I_α) to be a function of momentum transfer only and obtain

$$U_{10}(\mathbf{r}_0\mathbf{r}'_0) = \delta(\mathbf{r}_0-\mathbf{r}'_0)\int \mathrm{e}^{-i\mathbf{q}\cdot\mathbf{r}_0}t(\mathbf{q})\rho_{0t}(\mathbf{q})\mathrm{d}\mathbf{q} \tag{37}$$

i.e. U_{10} is a local interaction, a consequence of letting t be a function of $\mathbf{q}$ only. $\rho_{0t}(\mathbf{r})$ is the overlap function

$$\rho_{0t}(\mathbf{r}) = \sum_{i=1}^{A}\int \psi_t(\mathbf{r}_1\ldots\mathbf{r}_A)\psi_0(\mathbf{r}_1\ldots\mathbf{r}_A)\mathrm{d}\tau_1\,\mathrm{d}\tau_{i-1}\,\mathrm{d}\tau_{i+1}\ldots\mathrm{d}\tau_A\ (\mathbf{r}_i = \mathbf{r}). \tag{38}$$

We compare (37) with the similar result for the elastic optical potential

$$U_{00}(\mathbf{r}_0\mathbf{r}'_0) = \delta(\mathbf{r}_0-\mathbf{r}'_0)\int \mathrm{e}^{-i\mathbf{q}\cdot\mathbf{r}_0}t(\mathbf{q})\rho_{00}(\mathbf{q})\mathrm{d}\mathbf{q}, \tag{39}$$

which is thus eq. (25a) explicitly written down. We put (37) into (34) and obtain our result for the inelastic scattered amplitude

$$\begin{aligned}f(\mathbf{k}_t,\mathbf{k}_0) = -\frac{m}{2\pi\hbar^2}&\int \mathrm{e}^{-i\mathbf{q}\cdot\mathbf{r}_0}\mathrm{e}^{-(ik/2E)\int_{-\infty}^{+\infty}U_{00}\,\mathrm{d}z}\\ &\cdot\int \mathrm{e}^{-i\mathbf{q}'\cdot\mathbf{r}_0}t(\mathbf{q}')\rho_{0t}(\mathbf{q}')\mathrm{d}\mathbf{q}'\,\mathrm{d}\tau_0.\end{aligned} \tag{40}$$

If we neglect the wave distortion that is approximate U_{00} by zero, we get the Born approximation value

$$f(\mathbf{k}_t,\mathbf{k}_0) = -\frac{m}{2\pi\hbar^2}t(\mathbf{q})\rho_{0t}(\mathbf{q}). \tag{40a}$$

We now wish to study our result (40) further, especially its spin dependence. The nucleon-nucleon scattering matrix can be written [21])

$$t(\mathbf{q}) = a(\mathbf{q}) + i\mathbf{q}\times\mathbf{k}\cdot\boldsymbol{\sigma}_0 b(\mathbf{q}) + \text{terms containing } \sigma_K \tag{41}$$

where σ_0 refers to the incident nucleon spin and σ_K to the target nucleons. Now it is well known [5, 25]) that in the elastic scattering on spin-zero nuclei the terms containing σ_K average out and only the first two terms enter into the expressions for the optical potential. In our treatment of inelastic scattering in this paper we will also limit our discussion to this case. According to Squires [9]) this is the case in inelastic spin-zero-zero transitions in the L-S coupling limit.

The derivation of the elastic optical potential has been discussed by several authors and we just, for comparison, briefly review the usual treatment. It is customary to emphasize that $\rho_{00}(\mathbf{q})$ is strongly peaked in the forward direction ($q = 0$) while $t(\mathbf{q})$ is slowly varying. It is therefore believed to be a good approximation to take the $t(\mathbf{q})$ in the forward direction, $t(0)$, out of the integral in (39) †.

We now discuss the inelastic matrix element (37) and consider two cases of which the first is just a special case which is thought to be instructive.

Case A: $a(\mathbf{q})$ and $b(\mathbf{q})$ have the same momentum-dependence except for a multiplicative constant. Thus $b(\mathbf{q}) = -\frac{1}{2}\alpha' a(\mathbf{q})$. Putting this into (40) and keeping terms up to order α' only we obtain in agreement with (10)

$$\begin{aligned} f(\mathbf{k}_1,\mathbf{k}_0) = -\frac{m}{2\pi\hbar^2}\Big[&\int e^{i\mathbf{q}\cdot\mathbf{r}} U_{10}^c\, e^{-(ik/2E)\int_{-\infty}^{+\infty} U_{00}^c\, dz}\, d\tau \\ &+\tfrac{1}{2}\alpha'\boldsymbol{\sigma}_0\int e^{i\mathbf{q}\cdot\mathbf{r}}\boldsymbol{\nabla}U_{10}^c\times\mathbf{k}\cdot e^{-(ik/2E)\int_{-\infty}^{+\infty} U_{00}^c\, dz}\, d\tau \\ &+\tfrac{1}{2}\alpha'\boldsymbol{\sigma}_0\int e^{i\mathbf{q}\cdot\mathbf{r}} U_{10}^c\,\boldsymbol{\nabla}\times\mathbf{k}\cdot e^{-(ik/2E)\int_{-\infty}^{+\infty} U_{00}^c\, dz}\, d\tau \end{aligned} \tag{42}$$

with

$$\begin{aligned} U_{00}^c &= \int e^{i\mathbf{q}\cdot\mathbf{r}} a(\mathbf{q})\rho_{00}(\mathbf{q})d\mathbf{q} \\ U_{10}^c &= \int e^{i\mathbf{q}\cdot\mathbf{r}} a(\mathbf{q})\rho_{01}(\mathbf{q})d\mathbf{q}. \end{aligned} \tag{43}$$

We note that the last term is due to the spin-orbit coupling in the distorted wave-function and is to be included in a consistent perturbation treatment of α' (cf. the footnote p. 7).

We now rewrite (42) using (13) with $a_1 = a = \frac{1}{2}\alpha'$ and $\nu \to \infty$ and obtain

$$f(\mathbf{k}_1,\mathbf{k}_0) = (1 - \tfrac{1}{2}i\alpha'\,\mathbf{q}\times\mathbf{k}\cdot\boldsymbol{\sigma}_0)\cdot\int e^{i\mathbf{q}\cdot\mathbf{r}} U_{10}^c\, e^{-(ik/2E)\int_{-\infty}^{+\infty} U_{00}^c\, dz}\, d\tau. \tag{44}$$

† Inspection of the $t(\mathbf{q})$ as obtained by Squires' from Gammel-Thaler phase-shifts suggests that this should not be a very good approximation for the lightest nuclei. This may partly explain the disagreement between the experimental and calculated [21]) polarizations for light nuclei.

We compare this result with (18) and find the same relation between spin dependent and spin independent amplitudes. Thus we get the polarization (19) with the parameters defined by (43). It is seen by (40a) that Born-approximation would give the same polarization.

Case B: In general, however, we do not expect α to be a constant but a (slowly varying) function of $\mathbf{q}$ in the region of interest. A reasonable approximation seems to be:

$$U_{10} = \int e^{-i\mathbf{q}\cdot\mathbf{r}} a(\mathbf{q})\rho_{10}(\mathbf{q})d\mathbf{q} - \tfrac{1}{2}i\sigma_0\alpha'(\theta_1)\int e^{-i\mathbf{q}\cdot\mathbf{r}}\,\mathbf{q}\times\mathbf{k}\,a(\mathbf{q})\rho_{10}(\mathbf{q})d\mathbf{q}$$
$$= U^c_{10} + \tfrac{1}{2}\alpha'(\theta_1)\sigma_0\cdot\nabla\times\mathbf{k}U^c_{10} \quad (45)$$

in the expression for the scattering amplitude with $\theta_1 = \theta$ where θ is the scattering angle †. Into the expression for U_{00} we put $\alpha'(0)$, in view of the above-mentioned strong peaking of $\rho_{00}(\mathbf{q})$ in the forward direction ††. It is easy to see that it is just this dependence $\alpha'(\theta)$ that enters into the inelastic polarization calculated in Born approximation, as then the initial and final states are just plane waves. If one wants to take care of initial and final state interactions one has however to perform an integration over momentum transfers. As however the function $\rho_{01}(\mathbf{q})$ is flat (in comparison with $\rho_{00}(\mathbf{q})$) we expect the value of $\alpha'(\mathbf{q})$ at the angle θ to be a good average value. It would of course seem interesting really to include the q-dependence of α' in the integral (45). However one must not forget that the k-dependence of t has also been neglected. It seems at present difficult to estimate the various errors.

What we essentially wish to point out by the approximation (45) is the more general expectation that there should be in the inelastic scattering a stronger reflection of the momentum-dependence of t than in the elastic scattering.

We now put (45) into (40), expand in α' and collect first order terms and rewrite the amplitudes by (13). If, as we assumed, $\alpha'(0) \neq \alpha'(\theta)$ for $\theta \neq 0$, the last term in (13) is no longer exactly zero as it was in case A. However, we say that it is small and will neglect it. In fact this term consists of two factors. One is proportional to the wave distortion and the other to the difference $\alpha'(\theta)-\alpha'(0)$. We point out that a complete neglect of the spin-orbit-coupling in the distorted wave function would give just the term $\alpha'(\theta)$ instead of the difference $\alpha'(\theta)-\alpha'(0)$, so that if one feels that the term with $\alpha'(0)$ is small and negligible one concludes that the term with $\alpha'(\theta)-\alpha'(0)$ is certainly so with $\alpha'(\theta)-\alpha'(0) < \alpha'(0)$.

† An approximation made by Squires [9]) was to take the scattering matrix $t(\theta)$ out of the integral.

†† A better approximation would seem to be to let the elastic α' also vary with angle and take out a mean value $\alpha'(\theta_0)$. As ρ_{00} and ρ_{01} are different functions the mean angle θ_0 would be different from θ_0. We might thus simulate a deviation from the simple Thomas type spin-orbit coupling by an angle-dependent coupling constant.

We thus again obtain (44) just with α' replaced by $\alpha'(\theta)$ and similarly for the polarization.

Our result for the inelastic polarization is thus identical with that previously obtained by Squires [9]), who however used quite different (cruder) approximations.

The discussion of the importance of the real part of the optical model potential, the Coulomb interaction, and the validity of our derivations in different angular regions is similar to that in the discussion of the collective model, and the conclusions are the same.

5. Conclusion

We have thus seen that it is possible to explain the experimental findings that the elastic and inelastic polarizations are rather similar and that the inelastic polarization is largely independent of mass number. An important assumption we have made is that the transition was independent of the terms in t containing σ_K. As was first shown by Tamor [25]) it is however just this reduction of t that gives so much larger polarizations in elastic scattering by nuclei than is found in nucleon-nucleon scattering. Because for inelastic transitions this reduction is characteristic for the L-S coupling, it would seem that Squires' result that the j-j coupling gives a smaller polarization than is experimentally found is valid even in more exact calculations than considered by him.

It seems that the problem requires further investigation and that conclusions regarding nuclear structure might then be obtainable.

The author thanks Professor L. Wolfenstein for stimulating discussions during the course of this work, Dr. P. Hillman for discussions on the experimental results and Dr. K. Gottfried for some interesting discussions on the problem of multiple scattering. Dr. R. J. Eden kindly read through the manuscript.

The author thanks Professor C. J. Bakker and Professor B. Ferretti for the hospitality of CERN.

References

1) W. G. Chesnut, E. M. Hafner and A. Roberts, Phys. Rev. **104** (1956) 449
2) P. Hillman, A. Johansson and H. Tyrén, Nuclear Physics **4** (1957) 648;
R. Alphonce, A. Johansson and G. Tibell, Nuclear Physics **4** (1957) 672
2a) A. Johansson, G. Tibell and P. Hillman, Nuclear Physics
3) J. M. Dickson and D. C. Salter, Nuovo Cimento **6** (1957) 235
4) H. S. Köhler, Nuovo Cimento **2** (1955) 907; H. S. Köhler, Nuclear Physics **1** (1956) 430
5) S. Fernbach, W. Heckrotte and J. V. Lepore, Phys. Rev. **97** (1955) 1059
6) W. B. Riesenfeld and K. M. Watson, Phys. Rev. **102** (1956) 1157
7) Th. A. J. Maris, Nuclear Physics **3** (1957) 213
8) M. Ruderman, Phys. Rev. **98** (1955) 267

9) E. J. Squires, Nuclear Physics **6** (1958) 504
10) N. C. Francis and K. M. Watson, Phys. Rev. **92** (1953) 291, where further references are found
11) G. Molière, Z. Naturforschung **2a** (1947) 133
12) See B. J. Malenka, Phys. Rev. **95** (1954) 522
13) L. J. Schiff, Phys. Rev. **103** (1956) 443
14) D. S. Saxon and L. J. Schiff, Nuovo Cimento **6** (1957) 614
15) M. Gell-Mann and M. Goldberger, Phys. Rev. **91** (1953) 398
16) K. M. Watson, Phys. Rev. **88** (1952) 1163
17) F. Villars, Annual Rev. of Nuclear Science **7** (1957) 185
18) D. M. Chase, Phys. Rev. **104** (1956) 838
19) L. J. Schiff, Nuovo Cimento **5** (1957) 1223
20) K. Nishimura and M. Ruderman, Phys. Rev. **106** (1957) 558
21) H. S. Köhler, Nuclear Physics **6** (1958) 161
22) H. A. Bethe, Annals of Physics **3** (1958) 190
23) Ref. in H. Feshbach, to be published in Annual Review of Nuclear Science
24) L. Wolfenstein and J. Ashkin, Phys. Rev. **85** (1952) 947
25) S. Tamor, Phys. Rev. **97** (1955) 1077

1.C *Nuclear Physics* 9 (1958/59) 65—73; © *North-Holland Publishing Co., Amsterdam*
Not to be reproduced by photoprint or microfilm without written permission from the publisher

SERIES EXPANSIONS AND VARIATIONAL METHODS FOR THE ENERGY OF A SYSTEM OF FERMIONS

R. J. EDEN
CERN, *Geneva* †

Received 2 September 1958

Abstract: The relation between a variational method and a formally complete perturbation series for the energy of a finite system of fermions is studied. If certain assumptions about convergence are valid the variational method minimises the size of the sum of correction terms in the perturbation series at the point of self consistency determined from the leading term in this series. Away from self-consistency the sum of the correction terms becomes large. Although the first few correction terms appear to represent surface energies, their sum gives a volume energy. The usual method of defining an infinite medium corresponds to a limiting process which throws away the dominant correction terms except possibly at the point of self-consistency. The limiting process elsewhere violates the conditions under which the formal series for the energy corresponds to an eigenvalue of the Schrödinger equation.

1. Introduction

One of the outstanding problems in the theory of atomic nuclei is the convergence of series expansions for the energy of a nucleus. Using the Brueckner method to overcome the hard core difficulty individual terms in the expansions become finite. For infinite nuclear matter the leading term gives fairly good agreement [1]) with empirical estimates of the energy and density, which is marred only by the uncertainties which still persist in our knowledge of internucleon forces. Several estimates [2,3]) have shown that the leading correction terms are probably small, and another estimate [4]) has shown that a partial summation of correction terms in the series also leads to a small (negative) value. All these estimates apply only to infinite systems and are made at normal density for nuclear matter; and they do not depend on either the self-consistency condition or the fact that the leading term should be a minimum at normal density.

In this paper it is assumed that the series expansion for the energy of a system of fermions is convergent. For a finite system it can then be shown that the sum of correction terms cannot be small even though individual terms may be small, except possibly when a self-consistency condition is satisfied. The size of this sum at self-consistency will depend on details of the inter-

† Usual address: Cavendish Laboratory, Cambridge, England.

particle potential which are not considered here. Important correction terms away from self-consistency include many terms which would conventionally be called many-particle clusters either in normal perturbation theory or in Brueckner theory.

Infinite nuclear matter has in the past not been studied as the limit of a large finite system. Instead it has been defined to have certain properties, including a basic representation of particles by plane wave states and conservation of total momentum in any matrix element of the internucleon potential. This definition corresponds to a limiting process from a finite system in which the number of terms in each series expansion is held fixed whilst the number of particles in the system tends to infinity. This limiting process applied to the wave function of the system violates the Schrödinger equation by removing from the series matrix elements which do not conserve momentum and which are important in a large but finite nucleus.

The principal results of this paper apply both to Brueckner theory using hard core inter-nucleon potentials, and to conventional perturbation theory for a system of fermions with a regular potential which leads to saturation. There is an additional difficulty in the Brueckner theory since it is not known whether the sum of the correction terms is negative definite (as it will be in conventional theory). In order to avoid obscuring the results by this extra difficulty the main discussion will be concerned with the leading term and correction terms in conventional perturbation theory.

2. The Perturbation Series and the Hartree-Fock Method

2.1 FINITE SYSTEMS

In this section the perturbation series and a variational method will be discussed for a saturating system of A fermions which interact through two-body potentials $v(\mathbf{r}_i-\mathbf{r}_j)$. It will be assumed (a) that $v(\mathbf{r}_i-\mathbf{r}_j)$ is a short range potential leading to saturation, (b) that individual terms of a perturbation expansion in v are finite (the situation when this does not apply will be considered in section 3), (c) that the perturbation series for the wave function and the energy are convergent within a finite range of one-body potentials which include the self-consistent potential. In some of the discussion a somewhat stronger condition than simple convergence will be implied in order to permit a limited rearrangement of terms of the series.

Denote the Hamiltonians for an unperturbed system and for the real system by H_0 and H:

$$H_0 = \sum T + \sum V, \tag{2.1}$$

$$H = \sum T + \sum v, \tag{2.2}$$

$$H' = H - H_0, \tag{2.3}$$

$$H_0\phi = E_0\phi, \quad (\phi|\phi) = 1. \tag{2.4}$$

The formal solution to the Schrödinger equation

$$H\psi = E\psi \tag{2.5}$$

has been given by Goldstone [5]):

$$\psi = \sum_{n,L'} \left\{ \frac{1}{(E_0 - H_0)} H' \right\}^n \phi, \tag{2.6}$$

$$E = E_0 + \sum_{n,L} \left(\phi | H' \left\{ \frac{1}{(E_0 - H_0)} H' \right\}^n | \phi \right). \tag{2.7}$$

These sums are taken over linked clusters, a more detailed discussion of (2.6) and (2.7) has been given elsewhere [5,6]). The energy E is formally an exact eigenvalue, independent of the choice of the unperturbed potential V provided it is within the region of convergence. It will be written in two parts:

$$E = (\phi|H|\phi) + \sum_{n \geq 1, L} \left(\phi | H' \left\{ \frac{1}{e} H' \right\}^n | \phi \right) \tag{2.8}$$

$$= E_1(\phi) + E_2(\phi) \quad . \tag{2.9}$$

We will assume that E is the lowest eigenvalue of (2.5). Then from the variational principle,

$$E \leqq E_1(\phi). \tag{2.10}$$

The wave function ϕ_0 which minimises $E_1(\phi)$ gives the Hartree-Fock self-consistent solution. The potential corresponding to ϕ_0 will be denoted V_0. From our assumption of convergence, E is independent of ϕ, hence

$$E_1(\phi) - E_1(\phi_0) = -\{E_2(\phi) - E_2(\phi_0)\}. \tag{2.11}$$

From (2.10) $E_2(\phi)$ is negative, hence it maximises to $E_2(\phi_0)$, and $|E_2(\phi_0)|$ is a minimum. Therefore the Hartree-Fock variational procedure minimises the magnitude of the sum of the series of correction terms in (2.8). If

$$E_2(\phi_0) \ll E_1(\phi_0) \tag{2.12}$$

the method provides a good approximation for the energy, and in the following discussion it will be assumed that (2.12) holds.

When V differs substantially from V_0 the left hand side of (2.11) will not be small compared to $E_1(\phi_0)$, and therefore from (2.11) and (2.12), $E_2(\phi)$ will not be small. We will examine the kind of approximation which must be used to evaluate $E_2(\phi)$ so that the equation (2.9) remains approximately satisfied.

Let

$$\delta E_1 = E_1(\phi) - E_1(\phi_0). \tag{2.13}$$

In order to discuss δE_1 more conveniently we will consider a large but finite system. Then V_0 will be approximately constant except near the edges, in a

region whose thickness is determined by the range of v and is independent of the number A of particles. The class of potentials V can be restricted to have the same characteristics without loss of generality. Then $E_1(\phi)$, $E_1(\phi_0)$ and hence δE_1 will separate approximately into a volume term (proportional to A) and a surface term (proportional to $A^{\frac{2}{3}}$), the former coming from the regions where V and V_0 are approximately constant and the latter from the regions where they change rapidly. In this approximate separation the volume terms approximately conserve total momentum whilst the surface terms do not. Both volume and surface terms can be shown to minimise at self-consistency since they correspond to diagonal and off-diagonal parts of the self-consistent potential.

The leading term in the expansion of $E_2(\phi)$ is

$$\left(\phi|H'\frac{1}{e}H'|\phi\right). \tag{2.14}$$

This contains intermediate states in which either one or two particles are excited. The terms having one particle excited in intermediate states are negative and are surface terms giving an energy proportional to $A^{\frac{2}{3}}$. This surface energy becomes zero at self-consistency. Near self-consistency it cancels the surface term in δE_1 to this order of approximation.

The terms in (2.14) for which two particles are excited in intermediate states include both volume and surface contributions. Both are negative and for short range potentials $v(\mathbf{r}_i-\mathbf{r}_j)$, the magnitude of both terms decreases as the density ρ decreases, (ρ is defined as A divided by the volume in which ϕ is appreciably different from zero). Hence for ρ less than its self-consistent value ρ_0, the right hand side of (2.11) in this first order approximation is negative for large A, whilst its left hand side is positive and can be made large. For $\rho > \rho_0$ the sign of each side of (2.11) is positive but from (2.12) they will in general be of different magnitudes.

Proceeding beyond the first order approximation (2.14) for

$$\delta E_2 = -\{E_2(\phi)-E_2(\phi_0)\} \tag{2.15}$$

we note

(a) that (2.12) ensures that the volume terms in $|\delta E_2|$ are much smaller than $|\delta E_1|$ for low density. This result can be obtained by considering a large finite nucleus for which the volume terms in $E_2(\phi_0)$ will dominate, and using the result of De Shalit and Weisskopf [4]) that the magnitude of volume correction terms decreases with density. We deduce that these volume terms cannot be responsible for maintaining the equality (2.11).

(b) the iteration of $(\frac{1}{e}H')$ in

$$\sum_{n=0}^{\infty}\left(\frac{1}{e}H'\right)^n\phi \tag{2.16}$$

leads to a localisation from the distribution of density ρ in state ϕ to the distribution ρ_0 of ψ the wave function for the real interacting system (ϕ_0 and ψ having nearly the same density ρ_0). That is to say, the combination of many surface terms may lead to a volume term (since the volume terms in (2.16) cannot cause a net localisation). The equality (2.9) is satisfied in this way:

$$\begin{aligned}\sum_{n=0}^{\infty}\left(\phi|H'\frac{1}{e}H'\left\{\frac{1}{e}H'\right\}^n|\phi\right) &\approx \left(\phi|H'\frac{1}{e}H'|\psi\right)\\ &\approx (\phi|H'|\{\psi-\phi\})\\ &= E-(\phi|H|\phi)\end{aligned} \tag{2.17}$$

where the notation $\approx$ is used to indicate that details of linked clusters and normalisation have been omitted. The precise number of terms required for the sum $E_2(\phi)$ to approximate to the form (2.17) need not concern us here except that this number must exceed $A^{\frac{1}{3}}$ when v has a range ($\approx r_0$) of order $(3\rho/4\pi)^{\frac{1}{3}}$. This number of iterations will be required to carry the perturbation H' across the volume of the system.

For high density in a saturating system $E_1(\phi)$ will normally tend to plus infinity (though a special choice of v could make it finite but greater than E). At low density $E_1(\phi)$ will tend to zero, approaching it from above if v is short range. The qualitative variation of E, $E_1(\phi)$ and $E_2(\phi)$ with ρ^{-1} is indicated in fig. 1.

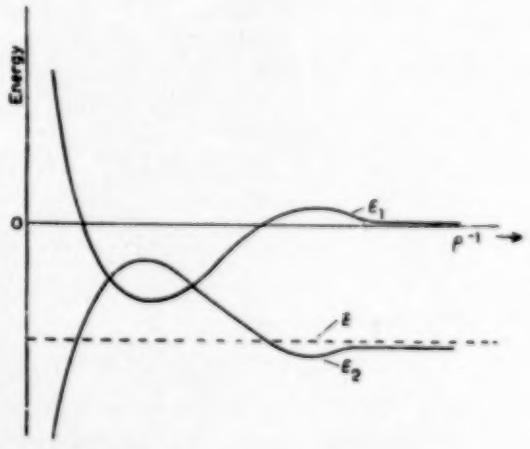

Fig. 1. Finite system.

2.2. AN INFINITE MEDIUM

The transition from a finite to an infinite medium, which corresponds to the assumptions implied in work on nuclear matter, is obtained by (i) cutting off the series expansion (2.8) at a large but finite number of terms L, (ii) allowing the number A of particles to tend to infinity whilst keeping L fixed, (iii) letting L tend to infinity.

This limiting process eliminates the effects of single particle transitions, since as A tends to infinity, the sum of a finite number of these terms will tend to zero, as each of them represents a surface energy. Since the terms responsible for the localisation of the system are omitted when $A^{\frac{1}{3}} \gg L$, the formal wave function ψ, (2.6), and the formal series (2.7) for the energy can no longer satisfy the Schrödinger equation defined by the Hamiltonian H. Therefore for nuclear matter the energy expansion E will be a function $E(\rho)$ of density. For a saturating medium $E_1(\rho)$ will have a similar behaviour to that in a finite system, but its variation will no longer be matched by $E_2(\rho)$ which contains volume terms only. $E_2(\rho)$ tends to zero for low density [4]). At high density $E_2(\rho)$ will not contain the negative contributions from single particle transitions (we have only proved these are negative to second order; it seems probable that their sum is negative but this cannot be deduced from general arguments without some knowledge of the degree of convergence of the series). This indicates the behaviour of $E(\rho)$, $E_1(\rho)$ and $E_2(\rho)$ as functions of ρ^{-1} will be as shown in fig. 2.

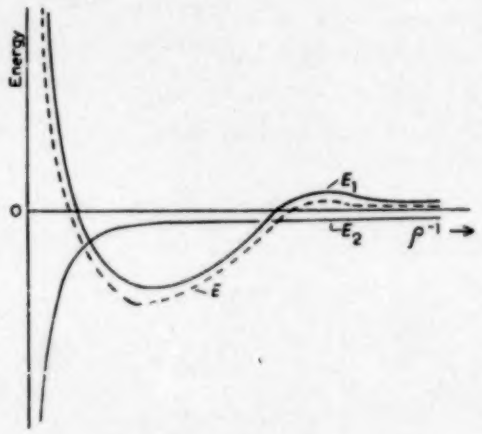

Fig. 2. Infinite medium.

2.3. HARD WALL BOUNDARY CONDITIONS

A system enclosed in a box is essentially different in behaviour from the infinite medium discussed above. The walls of the box can be represented by an additional potential W. The limiting process from finite W for a finite system to the conventional hard wall boundary conditions is obtained by setting a maximum $E_{\max}$ to the energy of any intermediate state in the series (2.8) for E, and letting $W \to \infty$ with $E_{\max}$ fixed. The condition

$$|E_{\max}| \ll |W| \tag{2.20}$$

prevents H' having any matrix elements which can appreciably alter the localisation of the wave function ψ inside the walls due to W. For density ρ higher than the normal density ρ_0 of the system, the effect of W is a com-

pression and corresponds closely to high density nuclear matter. For $\rho < \rho_0$ the system will take up its equilibrium configuration and be little affected by W. The resulting behaviour of $E(\rho)$, $E_1(\rho)$ and $E_2(\rho)$ is shown in fig. 3.

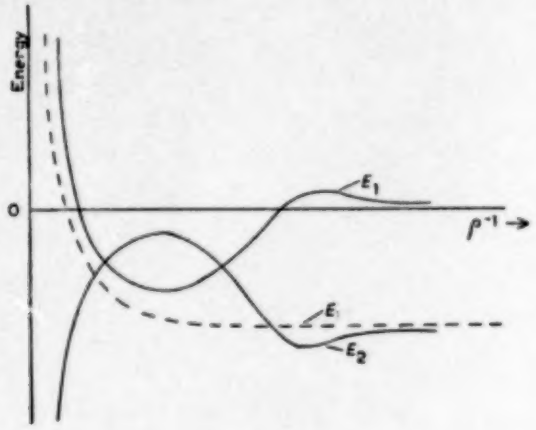

Fig. 3. Boundary walls.

3. The Brueckner Method

The Brueckner method is obtained from (2.8) by a rearrangement of the series in which the two body interaction v is replaced by an expression

$$t = v + v\frac{Q(2)}{e}t \tag{3.1}$$

where $Q(2)$ requires a change of state of two particles [6]). Then

$$E = (\phi|\sum T + \sum t|\phi) + \sum_{n \geq 1,\, \mathrm{L(i)}} \left(\phi|H_1\left\{\frac{1}{e}H_1\right\}^n|\phi\right) \tag{3.2}$$

$$= \quad E'_1(\phi) \quad + \quad E'_2(\phi). \tag{3.3}$$

The sum L(i) in (3.2) denotes linked irreducible clusters, and

$$H_1 = \sum t - \sum V.$$

Formally E is still an eigenvalue of H independent of the choice of V, so that minimising $E'_1(\phi)$ will correspond to maximising $E'_2(\phi)$. However, now $E'_1(\phi)$ does not denote an expectation value of H, so we do not know whether $E'_1(\phi)$ is always less than E. In particular we do not know a priori whether $E'_2(\phi_0)$ is positive or negative when E'_1 is a minimum. Apart from this question, if the series (3.2) is convergent, the behaviour of E, E'_1 and E'_2 is similar to that of E, E_1 and E_2 as discussed in section 2, except that owing to the hard core in v the divergences to $\pm\infty$ will occur at finite density. Their behaviour for a typical short range hard core potential is indicated in fig. 4.

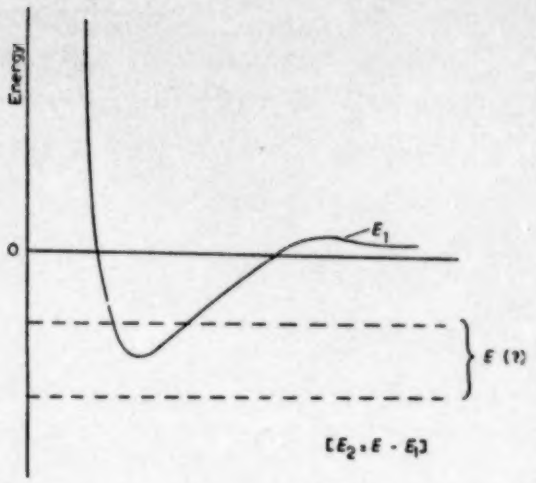

Fig. 4. Brueckner theory, finite system.

4. Conclusion

By making restrictive assumptions about convergence an ideal behaviour for a system of interacting fermions has been studied. This ideal behaviour leads to quite general results for the behaviour of the leading term and the correction terms for the energy of a finite system. These results show that

(a) certain correction terms have a large total effect even when they are small individually,

(b) the sum of the correction terms is maximised with a self- consistent potential; for normal perturbation theory this sum is negative, so its absolute value is minimised; for Brueckner theory the sign of the sum will almost certainly depend on details of the inter-particle potential.

(c) The normal definition of nuclear matter implies a limiting procedure which does not correspond to a large finite system and which leads to an energy which is no longer an eigenvalue of the Schrödinger equation, except possibly when it is minimised. Away from the minimum the formal series expansions for nuclear matter do not correspond to any meaningful physical system.

In this paper we have not considered convergence questions directly, but instead have obtained certain qualitative results which hold when the series expansions are rather well behaved. If the convergence assumptions apply only to a limited range of density, then our conclusions apply to the same range. It is hoped that further work from the viewpoint of this paper will lead to useful results with a further relaxation in the assumptions, for example if the series are only asymptotically convergent. From the other side of the problem, in considering convergence questions directly with specific interparticle forces, these general results will set a limit on what one should attempt to prove.

The author is greatly indebted to Amos De Shalit and Kurt Gottfried for many valuable discussions. He also wishes to express thanks to Professor C. J. Bakker and Professor B. Ferretti for the hospitality of CERN.

References

1) K. A. Brueckner and J. L. Gammel, Phys. Rev. **109** (1958) 102
2) K. A. Brueckner, Phys. Rev. **103** (1956) 172
3) H. A. Bethe, Phys. Rev. **103** (1956) 1353
4) A. De Shalit and V. F. Weisskopf, Annals of Physics (1959)
5) J. Goldstone, Proc. Roy. Soc. A **239** (1957) 267
6) R. J. Eden, Nuclear Reactions, Vol. 1 (North Holland Publishing Co., Amsterdam, 1959) Ch. I

2.J *Nuclear Physics* **9** (1958/59) 74—82; © *North-Holland Publishing Co., Amsterdam*
Not to be reproduced by photoprint or microfilm without written permission from the publisher

MULTIPLE PRODUCTION OF PARTICLES IN COLLISIONS BETWEEN 9 GEV PROTONS AND NUCLEONS

V. S. BARASHENKOV, V. A. BELYAKOV, E. G. BUBELEV, WANG SHOU FENG, V. M. MALTSEV, TEN GYN and K. D. TOLSTOV

Joint Institute of Nuclear Research, Laboratory of Theoretical Physics and High Energy Laboratory, Dubna, USSR

Received 25 June 1958

Abstract: Some theoretical calculations pertaining to multiple production of particles in nucleon-nucleon collisions at 7—10 GeV were presented in ref.[1]). Some preliminary experimental results obtained by irradiating photographic emulsions with the proton beam from the synchrocyclotron of the Joint Institute of Nuclear Research were given in ref.[2]). In the present paper we compare the theoretical results of ref.[1]) with the results of some new experiments. 372 stars, of which 50 were classified as proton-nucleon collisions, were recorded in NIKFI-R photographic emulsions along the tracks of ≈ 9 GeV protons accelerated in the JINR proton synchrocyclotron. The mean number of charged particles created in these collisions was 3.6 ± 0.5. The angular distribution of fast charged particles is obtained. As a whole the experimental results agree with the statistical theory of multiple particle production within the limits of the experimental errors. Some discrepancy is evident in the small angle range and may be due to the contribution of non-central impacts and to asymmetry of the angular distribution in the c.m.s.

1. Selection of Nucleon Interactions

With the help of a plunger-type target the ≈ 450 μ thick NIKFI-R photographic emulsions were introduced into the vacuum chamber of the accelerator and irradiated with protons of an energy of ≈ 9 GeV in the JINR proton synchrocyclotron.

After treatment the emulsions were examined under a magnification of 945 along the tracks of the primary protons. In this way all interaction events including scattering through angles $> 3°$ could be reliably recorded. The tracks of δ electrons produced by 9 GeV protons resembled straight relativistic tracks and hence in order to remove these impurities from the results, observations were carried out along such tracks. In three sets of measurements in which 372 stars were recorded (108 in single emulsions and 100 and 164 in emulsion stacks) 39 stars were found (9, 10 and 20 respectively in the three series) which possessed an even number of rays, no recoil nucleus or β-electron track and finally possessed not more than one grey or black track, the black tracks being observed only in the front hemisphere. Stars of this type were ascribed to interactions between the accelerated protons and free

or quasi-free protons of the emulsion nuclei, that is, to (pp) collisions.

The number of (pp) collisions is larger than one would expect from the total number of stars if the amount of hydrogen atoms in the emulsion is taken into account; however, it should be kept in mind that in a number of experiments at smaller energies approximately equal numbers of free and quasi free (pp) collisions were obtained.

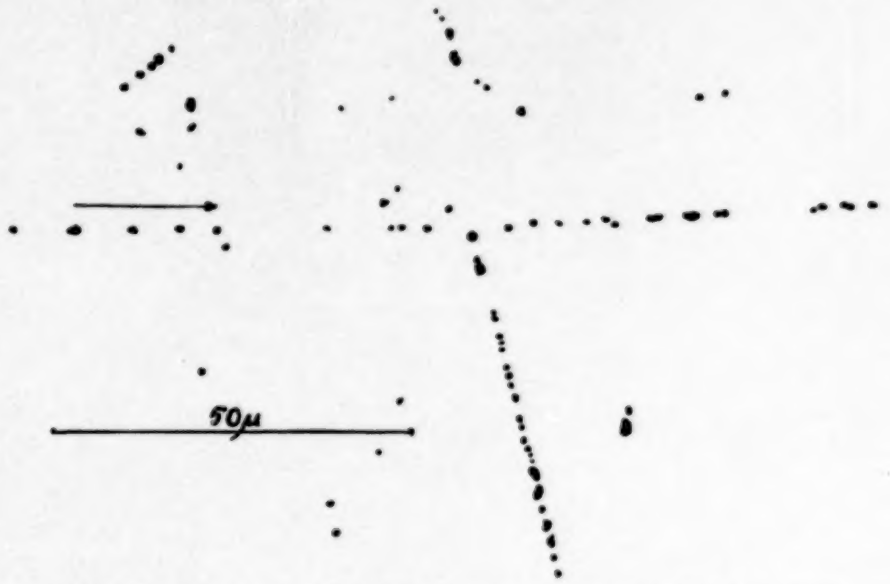

Fig. 1. Example of a star classified as an elastic (pp) collision event.

Three co-planar events satisfying the corresponding kinematic requirements were classified as elastic scattering. The photograph in fig. 1 is an example of an elastic (pp) collision selected in this way.

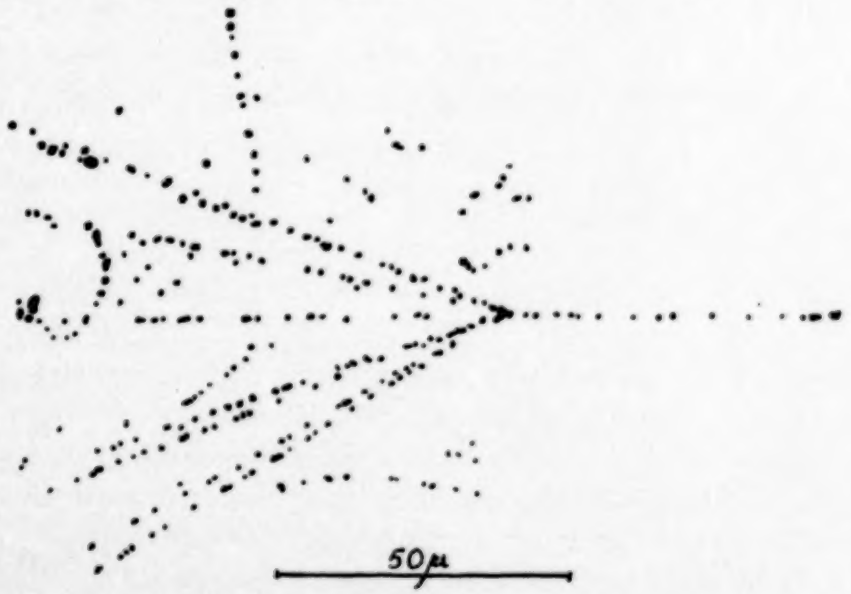

Fig. 2. (pp) collision involving the creation of 8 charged relativistic particles.

36 events were ascribed to inelastic (pp) collisions. An example of an inelastic (pp) collision chosen in this manner is shown in the photograph in fig. 2.

In an emulsion stack containing 264 stars 11 events were classified as proton-neutron, (pn), collisions. These stars had an odd number of prongs and do not exhibit recoil nuclei.

An example of a collision of this type is shown in fig. 3.

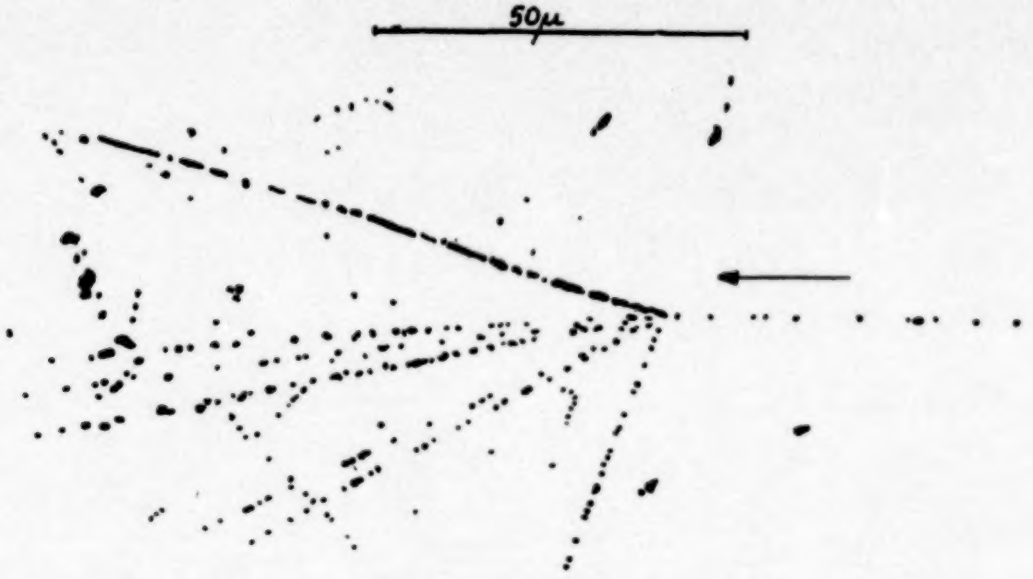

Fig. 3. (pn) collision involving the creation of 5 charged relativistic particles.

2. Prong Distribution of Stars

The prong distribution of stars referring to 37 inelastic (pp) collisions is shown in table 1. (After introduction of a geometric correction a 2-prong case was added). The average number of charged particles in (pp) collisions is

TABLE 1

Number of stars	13	17	5	2
Number of prongs	2	4	6	8

$\bar{n}_p = 3.8 \mp 0.3$. The experimental values satisfactorily agree with the value $\bar{n}_p \approx 3.5$ for (pp) collisions calculated on basis of the statistical theory of multiple production by employing the tabulated values in ref.[1]) for 10 GeV protons. If generation of strange particles is taken into account the theoretical values should be larger by a few percent.

Since the number of (pn) collisions was small, their prong distribution will not be given in this article. The average number of charged particles created

in (pn) collisions was $\bar{n}_n = 2.8 \pm 0.6$, which satisfactorily agrees with the theoretical value $\bar{n}_n \approx 3.2$ [1]).

In stars due to proton-nucleon collisions "fast particles" $n^{(s)}$ were singled out whose ionization losses $I \leqq 1.4 I_0$, where I_0 are ionization losses corresponding to the relativistic ionization plateau. Protons with an energy $E_p \geqq 0.5$ GeV as well as π mesons with $E_\pi \geqq 0.08$ GeV are considered to be $n^{(s)}$ particles. The particle frequency distribution for 37 inelastic (pp) collisions is presented in table 2. The average number of $n^{(s)}$ per star is

TABLE 2

Number of stars	9	6	7	8	2	3	1	1
Number of particles	1	2	3	4	5	6	7	8

$\bar{n}^{(s)}_{(pp)} = 3.2 \pm 0.3$. In a similar manner "fast particles" were selected from (pn) collisions. The average number of "fast particles" was $\bar{n}^{(s)}_{(pn)} = 2.5 \pm 0.6$.

In order to compare these data with the statistical theory of multiple creation we made use of the statistical weights given in ref.[1]) and under the same assumptions as employed there we calculated the momentum distributions of pions and nucleons created in the partial reactions

$$N+N \to N+N+n\pi, \quad N+N \to N'+N+n\pi,$$
$$N+N \to N'+N'+n\pi, \quad n = 0, 1, \ldots, 6$$

at $E = 10$ GeV [1]). (N' is the "isobar" symbol; see ref.[1]).)

The momentum distribution of pions and nucleons in the c.m.s. † integrated over the angles and averaged over all partial reactions is shown in fig. 4. The corresponding momentum distribution of pions and nucleons in the laboratory coordinate system is given in fig. 5. All momentum distributions are normalized to unity. (In our calculations we did not consider the small contribution of pions and nucleons created in reactions involving strange particles (see ref.[1]).) From the spectra presented above it follows that the contribution of "slow" pions ($E_\pi < 0.08$ GeV) and "slow" nucleons ($E_n < 0.5$ GeV) is small ($\approx 10\,\%$). Therefore the average numbers of "fast" charged particles $\bar{n}^{(s)}_p$ and $\bar{n}^{(s)}_n$ computed theoretically are only a few per cent smaller than the average theoretical numbers of charged particles $\bar{n}_p$ and $\bar{n}_n$: $\bar{n}^{(s)}_p \approx 3.1$, $\bar{n}^{(s)}_n \approx 2.9$. Experimentally it has been found that the fraction of "slow" particles is $15\% \pm 5\%$ of the total number of charged particles, about $\frac{2}{3}$ of them being protons. The mean energy of these protons was (120 ± 40) MeV.

† In the calculations, use was made of the nomograms made by L. G. Zastavenko (to be published).

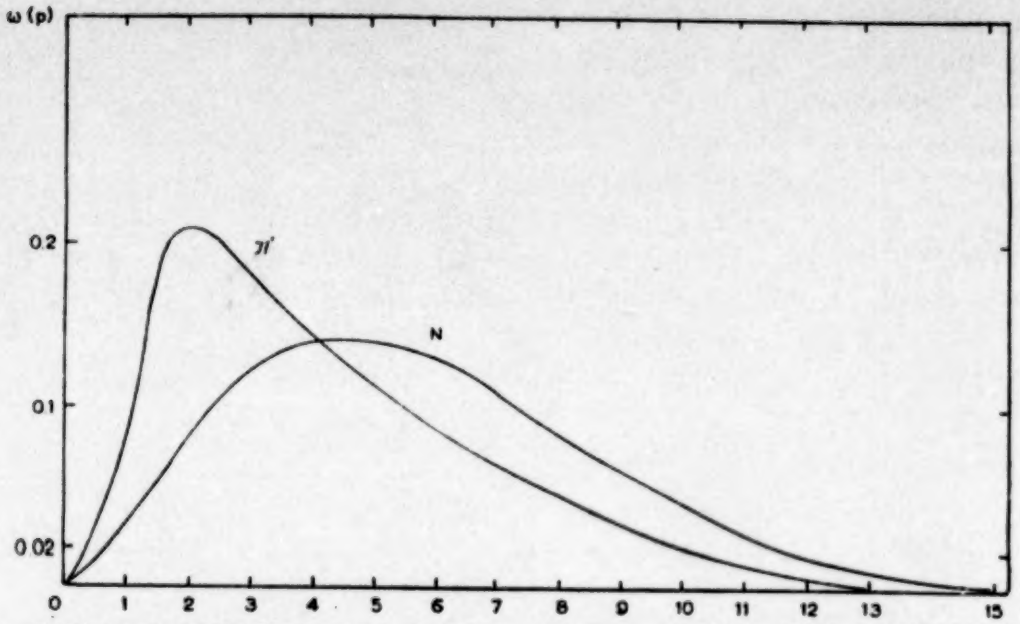

Fig. 4. Momentum distributions of pions and nucleons produced in (NN) collisions. C.m.s. Momentum values in $m_\pi c$ units are plotted along the abscissa axis.

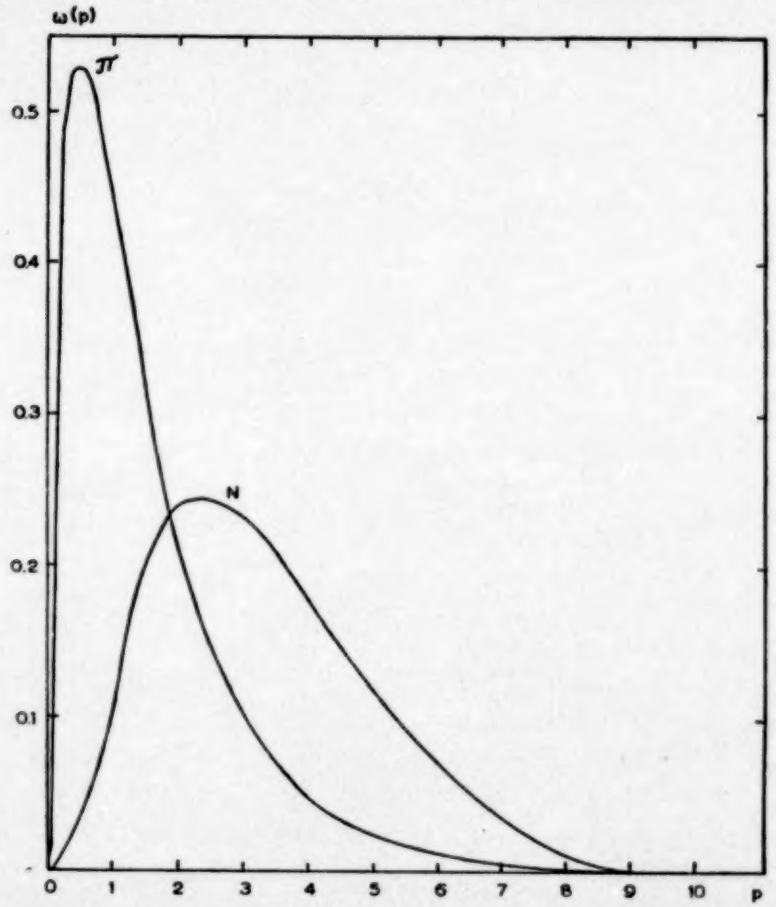

Fig. 5. Momentum distributions of pions and nucleons produced in (NN) collisions. Laboratory system. Momentum values in GeV/c units plotted along the abscissa axis.

There is good agreement between the theoretical and experimental values, $\bar{n}_p^{(s)}$ and $\bar{n}_n^{(s)}$ †. However, one notes that the fraction of "slow" protons is comparatively high.

3. Angular Distribution of Prongs in (pp) Stars

The histogram in fig. 6 represents the experimental angular distribution of particles $n_p^{(s)}$ emitted in a solid angle $\Delta\Omega = \Omega(\theta_2) - \Omega(\theta_1)$ in the laboratory system. The angle which contains half of particles $n_p^{(s)}$ is $\varphi_{\frac{1}{2}} = 16°$. The

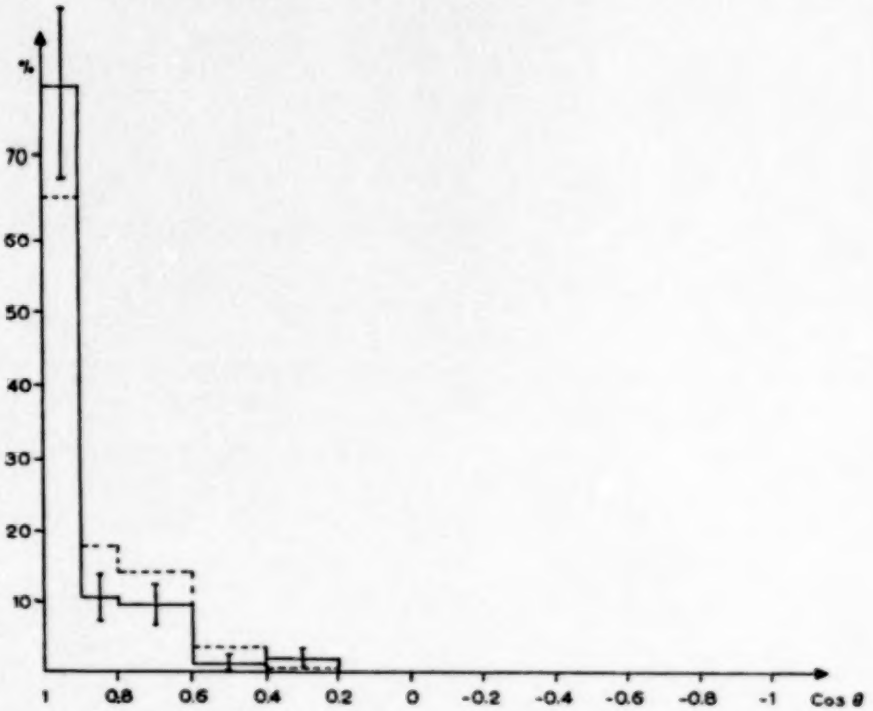

Fig. 6. Angular distribution of fast charged particles emitted in (pp) collisions in a solid angle $\Delta\Omega = \Omega(\theta_2) - \Omega(\theta)$. The continuous histogram is the experimental values. The dotted curve is the theoretical histogram. The values of angle θ are plotted along the abscissa axis. Laboratory system of coordinates.

angular distribution of pions and nucleons in the laboratory system was computed by the aid of the momentum distribution in fig. 4. under the assumption of an isotropic distribution in the c.m.s. This distribution is represented in fig. 7. The angular distributions of pions $W_\pi(\theta)$ and nucleons $W_N(\theta)$ are normalized, so that $\int_0^\pi W(\theta) \sin\theta d\theta = 1$. The angular distributions for "fast" particles $n^{(s)}$ only slightly differ from the total angular distributions. From Fig. 7 it can be seen that the nucleon angular distribution has a larger for-

† In reactions involving more than one pion ($n_\pi > 1$), the average number of charged pions is near to $\frac{2}{3}$ of the total number ($\bar{n}_p^{(t)} = 3.4$; $\bar{n}_n^{(t)} = 3.3$) and the number ot protons on the average is close to 1.2 for (pp) collisions and to unity for (pn) collisions (see ref.[2]).

ward asymmetry than pions and this corresponds to the fact that the nucleon spectrum $W_N(p)$ is harder than the pion spectrum $W_\pi(p)$ (see figs. 4 and 5). The average number of "fast" charged particles $n^{(s)}$ emerging in the solid angle was computed with the help of the angular distribution in fig. 7. The

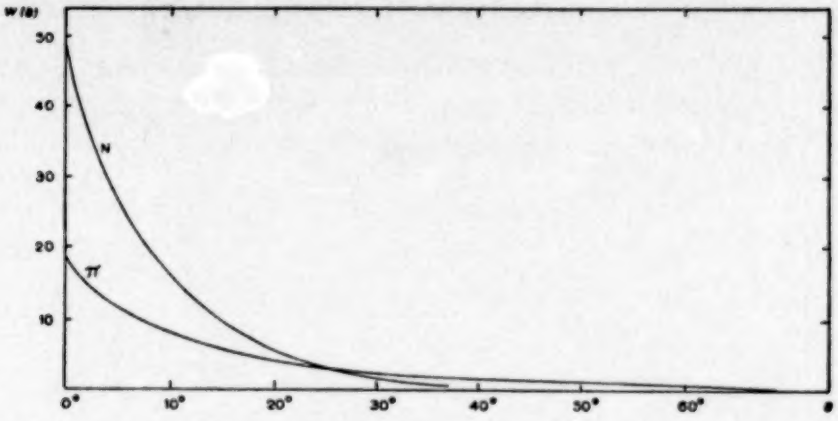

Fig. 7. Angular distribution of pions and nucleons produced in (NN) collisions. Emission angle θ plotted along abscissa axis. Laboratory system.

results of these calculations are presented in fig. 6. Within the experimental errors they satisfactorily agree with the experiments. However, in the small angle region there is an appreciable discrepancy as is evident from table 3.

TABLE 3

Angle range	Number of particles		
	Calculated	Experimental	Exp./calc.
0–3	4	9	2.2
0–5	10	19	1.9
0–10	28	39	1.4

This difference may possibly be due to an admixture of particles created by a process which cannot be described by statistical theorem I, e.g., by "peripheral collisions". A non-isotropic angular distribution corresponds to this in the c.m.s. †. It is likewise possible that the large fraction of observed "slow" protons (see above) is also related to this circumstance. These conclusions are close to those arrived at by analysis of cosmic ray experiments [5]). However, a final conclusion would require a larger amount of statistical material and a more rigorous analysis.

We now estimate the mean energy losses during pion production in (pp)

† I. I. Gurevich [4]) who investigated emulsions irradiated by cosmic rays also arrived at the conclusion that at an energy $\approx 10^{10}$ eV there is some asymmetry in the angular distribution in the c.m.s.

collisions. Taking into account the average number of charged and neutral pions created in a single (pp) collision, $\bar{n}_\pi = 3.7 \pm 0.5$, we find that for the pion momentum distribution shown in fig. 5, the mean energy expended by a primary nucleon in pion production is $\Delta E \approx 50\ \%$ of its initial energy.

In conclusion the authors are glad to thank D. I. Blokhintsev for numerous discussions of various aspects of the theory of multiple particle production and also the proton synchrocyclotron crew of the High Energy Laboratory for making these experiments possible.

Appendix

In reducing experimental results and preparing experiments it is quite frequently necessary to know the momentum distribution of pions produced in (NN) collisions for a given emission angle θ in the laboratory system.

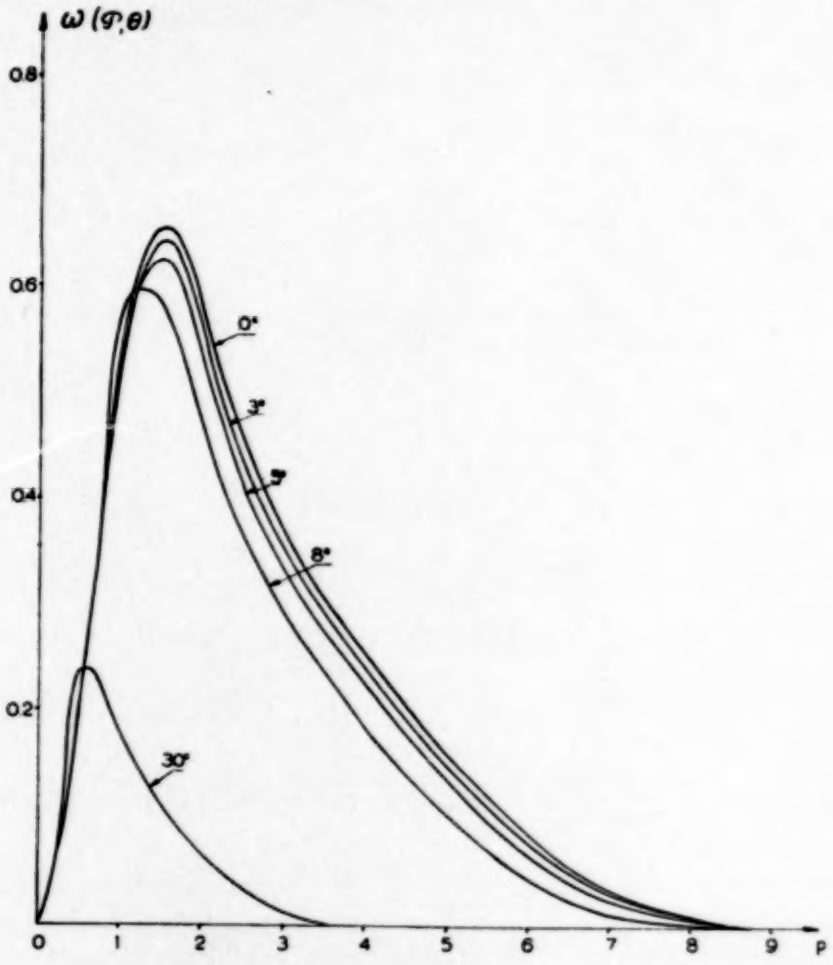

Fig. 8. Momentum spectrum of pions produced in (NN) collisions at angles of $\theta = 0°, 3°, 5°, 8°, 30°$ in the laboratory system. Momentum in GeV/c units plotted along abscissa axis.

Distributions of this type computed in accord with ref.[1]) for angles $\theta = 0°$, 3°, 5°, 8°, 30° are represented in fig. 8. Together with the angular distributions in fig. 7 these distributions were used by us for calculation of the data in table 3.

References

1) V. S. Barashenkov *et al.*, Nuovo Cimento Supplement **7** (1958) 117
2) N. P. Bogachev *et al.*, Atomnaya Energyia **4** (1958) 281
3) S. Z. Belenky *et al.*, Uspekhi Fisich. Nauk **62** (1957 no. 2
4) I. I. Gurevich, Reports at Jubilee Conference of Moscow Engineering-Technical Institute (April 1958)
5) G. T. Zatsepin, Report at Seminar of High Energy Laboratory of Joint Institute of Nuclear Research (1958)

1.E.1:
3.A

Nuclear Physics **9** (1958/59) 83—87; © *North-Holland Publishing Co., Amsterdam*
Not to be reproduced by photoprint or microfilm without written permission from the publisher

DECAY OF Eu^{152m}

INGVAR MARKLUND
Institute of Physics, Uppsala

Received 16 August 1958

Abstract: The decay of Eu^{152m} (9.2h) is investigated by means of coincidence measurements. The γ energies and intensities are measured with a crystal spectrometer and a double focusing iron yoke spectrometer. Results: 121.78, 344.3, 841.6, 963.3, 970.3, 1315.0 and 1389.3 keV.

1. Introduction

Eu^{152}($N = 89$) decays to both Sm^{152} ($N = 90$) and Gd^{152} ($N = 88$), and a sudden increase of the nuclear deformation is expected for about $N = 88$ [1]. The decay of Eu^{152} (12.2 y, measured spin 3 [2]))has been thoroughly investigated [3–8]). Gd^{152} seems to be nearly spherical, and Sm^{152} has non-spherical characteristics. In the decay of Eu^{152m} (9.2h, most probable spin 0^-) some other levels are excited [4,5]). However, a strong β^--transition (71 %) to the ground state of Gd^{152} causes difficulties in measuring the internal conversion lines. The low resolution and uncertainty of energy in earlier measurements invited this investigation, but the resulting decay scheme, fig. 1, is in substantial agreement with earlier investigations.

2. Apparatus

The low energy γ-rays were studied with a recently constructed photographic bent crystal spectrometer [9]). The quartz plane 310 was chosen to get large deflection angles. The γ-lines were measured against the well-known Ta^{182} spectrum [10]), checked in this spectrometer against eight X-ray lines [9]). Higher energies were fixed by photo-electron conversion in a double focusing iron yoke spectrometer [11]) set on 0.4 % resolution.

The coincidences were studied with a conventional fast-slow coincidence set-up ($2\tau = 5\times10^{-8}$ sec) gating a 100 channel analyser. A $2\frac{1}{2}'' \times 2''$ NaI (Tl) crystal was used as a detector in one channel and a $1'' \times 1''$ NaI(Tl) crystal or a lens spectrometer in the other channel.

3. Measurements

A γ-line of energy

$$E_\gamma = 121.78 \pm 0.05 \text{ keV}$$

was found from a 40 mg Eu_2O_3 source in the crystal spectrometer. This

result was checked by taking a new spectrum with reflection from the other side of the crystal planes, giving

$$E_\gamma = 121.77 \pm 0.05 \text{ keV}.$$

The same level is excited in the decay of Eu^{152}(12.2 y). Two crystal spectrometer measurements are published on that energy level. Boehm and Hatch [12]) and B. Andersson [13]) announce respectively

$$E_\gamma = 121.79 \pm 0.05 \text{ keV}$$

and

$$E_\gamma = 122.31 \pm 0.04 \text{ keV}.$$

We conclude that the former value is correct †. No γ-rays were observed in the region 50—200 keV with an intensity > 2 % of the 121.78 keV line.

The high energy γ-rays were accurately measured with photo-electron conversion from a 12 mg Eu_2O_3 source in a Cu capsule for total absorption of the beta rays. We used an U_2O_3 converter (3.3 mg/cm²) and measured the energies with Cs^{137} and Co^{60} as reference sources. The result is summarized in table 1. The regions 930—1000 keV and 1310—1410 keV were scanned, but

TABLE 1

Gamma energies and intensities compared with earlier measurements

Ray nr	Grodzins and Kendall [4])		Nathan and Waggoner [5])		Grodzins [14])		Wood and Nathan [15])		Present measurements		
	E_γ (keV)	Abs. trans. intens. (%)	E_γ (keV)	Abs. trans. intens. (%)	E_γ (keV)	Abs. trans. intens. (%)	E_γ (keV)	Abs. trans. intens. (%)	E_γ (keV)	Rel. intens.	Abs. trans. intens. (%)
1	120	15.2	122	14			122	14.7	121.78 ±0.05		
2	260	0.1									
3	344	2.7	344	2.6	344	2	344	2.5	344.3 ±0.3		
4	725	0.1									
5	854	14.2	837	10	837	14	838	14	841.6 ±0.3	1000	13
6	976	6.7	961	10	961	10	961	12	963.3 ±0.3	918	12
7	983	0.5	980	1.0			983	0.5	970.3 ±0.5	35	0.5
8	1327	1.2	1320	2.6			1327	0.9	1315.0 ±0.5	51	0.7
9	1380	1.0	1415	1.8			1380	0.7	1389.3 ±0.5	43	0.6
10	1390	0.04									<0.01
From Eu^{152} (12y)	1410		1415						1409.1 ±0.7		

† Since completion of this paper two new measurements have been announced each compatible with my result:

$$E_\gamma = 121.85 \pm 0.03 \text{ keV}^{20}),$$

$$E_\gamma = 121.75 \pm 0.03 \text{ keV}^{21}).$$

no other γ-ray was found of intensity > 1 % of the strongest line reported in the respective regions. The 1390 keV line, reported by Grodzins and Kendall[4]) of relative intensity 4 % of the 1380 keV line (here identified as 1389.3 keV) was not found at about 1400 keV. But a weak line of energy

$$E_\gamma = 1409.1 \pm 0.7 \text{ keV}$$

from the long lived activity was detected. No evidence of any 1511 keV γ-ray was observed of intensity > 1 % of the 1315 keV line.

The relative γ-intensities were calculated with an estimated uncertainty of about 20 %. They have then tentatively been converted to absolute transition intensities assuming a mean of the strong beta branchings reported in ref.[14]) and [15]). Internal conversion measurements gave a 344.3 keV γ-line and indications of some weak γ-lines in the region 170—260 keV.

The results from coincidence measurements are presented in table 2.

TABLE 2

Coincidence measurements

Selected energy (keV)	Coincident γ-rays collected in the 100-channel analyzer † (keV)
K 122	KX-rays, 840, 1400
KX-rays	122, 840, 960, 1400
122	KX-rays, 840, 1400
344	970
842	KX-rays, 122
963 / 970	KX-rays, 344
1315	—
1389	KX-rays, 122

† Coincidences with some more low energy γ-rays were observed but are not presented here.

4. Discussion

Coincidences with KX-rays (table 2) places four γ-lines, 121.8, 841.6, 963.3 and 1389.3 keV in cascade with the K-capture. The first excited level in Sm^{152} is found in Coulomb excitation [16]) and from half-life determination[17]) to be a 2^+ rotational level of energy 122 keV. It is fed by the 841.6 and 1389.3 keV γ-rays (table 2). The 963.3 keV ray seems to be a crossover transition from the second excited state to the ground state in agreement with the energy sum $841.6 + 121.8 = 963.4 \pm 0.4$ keV and with resonance scattering experiments [18]). The 1389 keV γ-ray is deexciting a level 1511.1 ± 0.6 keV above the ground state. That level is definitely not the same level as the $1409.1 + 121.8 = 1530.9 \pm 0.8$ keV level of spin 2^-, excited from 12 year Eu^{152} (table 1) [6,8]). The first excited state in Gd^{152} is a 2^+ level 344 keV above the ground state definitely established in the long lived activity, and

also excited here. It is fed by a 970.3 keV γ-ray (table 2), and the 1315.0 keV line is the crossover transition in agreement with the energy sum $970.3 + 344.3 = 1314.6 \pm 0.7$ keV.

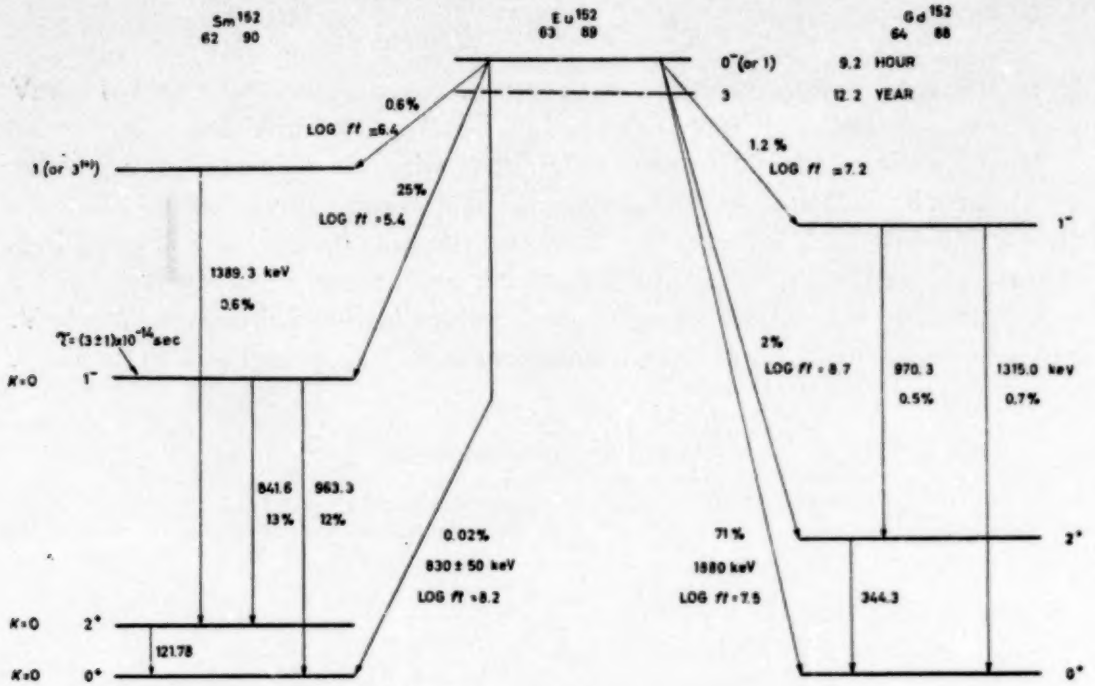

Fig. 1

The resulting decay scheme of Eu^{152m} is found in fig. 1. Log *ft* values and spin and parity assignments are collected from ref.[14]) and [15]). The assignment of 0^- to the Eu^{152m} state has been in question for a long time. However, it now seems to be fixed to 0^- by A. W. Sunyar [19]). The spin of the 1511 keV level in Sm^{152} is therefore 1, and the ground state transition is forbidden with a factor of more than a hundred according to this investigation.

The author is indebted to Professor Kai Siegbahn for his stimulating interest. I am grateful to Docent O. Beckman for valuable discussions and to the beta spectrometer group for their assistance in this work. Further my thanks are to Dr. A. W. Sunyar and Dr. O. Nathan for having their results in advance of publication, and to Mr. W. Parker for correcting the English.

References

1) B. R. Mottelson and S. G. Nilsson, Phys. Rev. **99** (1955) 1615
2) M. Abraham, R. Kedzie and C. D. Jeffries, Phys. Rev. **108** (1957) 58; Manenkov, Prokhorov, Trukhlayev and Yakovlev, Doklady Akad. Nauk, SSSR **112** (1957) 623
3) R. E. Slattery, D. C. Lu and M. L. Wiedenbeck, Phys. Rev. **96** (1954) 465
4) L. Grodzins and H. Kendall, Bull. Am. Phys. Soc. Ser. **1** (1956) 163, 164, and Nuclear Data Cards 56—5—143

5) O. Nathan and M. A. Waggoner, Nuclear Physics **2** (1957) 548
6) B. S. Dželepov and N. N. Zhukovsky, Nuclear Physics **6** (1958) 655
7) S. K. Brattacherjee, T. D. Nainan, S. Raman and B. Sahai, Nuovo Cimento **7** (1958) 501
8) B. V. Bobykin and K. M. Novik, Izv. Akad. Nauk, SSSR **21** (1957) 1556
9) O. Beckman, Nuclear Instruments **3** (1958) 27
10) Murray, Boehm, Murmier and DuMond, Phys. Rev. **97** (1955) 1007
11) G. Bäckström, Arkiv f. Fysik **10** (1956) 387
12) F. Boehm and E. N. Hatch, Nuclear Data Cards 57—1—93
13) B. Andersson, Proc. Phys. Soc. A **69** (1956) 415
14) L. Grodzins, Phys. Rev. **109** (1958) 1014
15) G. T. Wood and O. Nathan, submitted to the International Congress of Nuclear Physics, Paris (1958)
16) N. P. Heydenburg and G. M. Temmer, Phys. Rev. **100** (1955) 150
17) A. W. Sunyar, Phys. Rev. **98** (1955) 653
18) I. Marklund and L. A. Page, Nuclear Physics **9** (1958) 88
19) A. W. Sunyar, private communication
20) E. L. Chupp, J. W. M. DuMond, F. J. Gordon, R. C. Jopson and H. Narj, UCRL-1928 (2nd Rev)
21) V. A. Romanov, Izr. Akad. Nauk **22** (1958) 191

8.A *Nuclear Physics* 9 (1958/59) 88—93; © *North-Holland Publishing Co., Amsterdam*
Not to be reproduced by photoprint or microfilm without written permission from the publisher

ON THE HELICITY OF NEUTRINOS

INGVAR MARKLUND and LORNE A. PAGE †
Institute of Physics, Uppsala, Sweden

Received 16 August 1958

Abstract: In order to determine the helicity of neutrinos we have measured the sign and magnitude of polarization of γ-rays emitted in opposite direction to the neutrinos. The 963 keV γ-ray following electron-capture by Eu^{152m} is thus measured to be 80 ± 30 % circularly polarized with negative helicity. This result is in agreement with the measurement and conclusion by Goldhaber *et al.*[1]) that the emitted neutrino has negative helicity, $\boldsymbol{\sigma} \cdot \mathbf{p} = -1$ in this orbital electron capture.

1. Introduction

The famous experiment by Wu *et al.*[2]) on polarized Co^{60} nuclei was essentially a helicity experiment. When assuming a positive g-value of the Co^{60} ground state [3]), spin sequence $5 \rightarrow 4$, and conservation of angular momentum, the Wu experiment implies negative helicity †† of the negatons from Co^{60}. Page and Heinberg [4]) found that positons from Na^{22} have positive helicity. Several polarization investigations [5–9]) have been carried out since the Wu experiment. However, strictly none of these experiments says anything about neutrino helicity. Only a sense of circulation and, coincidently, a *beta* direction are measured.

In the autumn of 1957 an experiment was proposed [10]) in which the sign of helicity of the neutrino emitted in the electron capture process may be inferred from a measurement on the sign of helicity of "resonance" gamma-rays. But at that time no experiment was carried out because of source difficulties. At the same time, Goldhaber, Grodzins and Sunyar [1]) performed such an experiment. The resulting sign of helicity was opposite to that expected on the basis of the older He^6 recoil experiments [11]), but consistent with the Liverpool result [21]) for positon helicity from μ^+-decay assuming lepton conservation. The importance of this sign is such that we thought it worthwhile to carry out a neutrino helicity measurement in this laboratory. Because of the apparent scarcity of suitable decays, Eu^{152m} was chosen as the source (the same source as used in ref. [1]). Presently M. Morita and R. S. Morita [12]) suggested an experiment very similar to this one, but with Co^{60} as source, to determine if the beta interaction is an axial vector or tensor.

† Visiting Guggenheim Fellow, permanent address Physics Department, University of Pittsburgh.

†† A particle has positive helicity and is "right-handed" when its spin $\boldsymbol{\sigma}$ and momentum $\mathbf{p}$ are parallel, $\boldsymbol{\sigma} \cdot \mathbf{p} = 1$, and negative helicity when these are anti-parallel.

2. Method

If an unpolarized nucleus decays by allowed (GT) electron capture into an excited state of non-zero angular momentum, and if the emitted neutrino is polarized (according to Lee and Yang [13])), a subsequently emitted photon will be polarized with respect to the neutrino momentum $\mathbf{p}_\nu$. When the angle of emission between neutrino and photon is 180°, the photon will have its maximum momentum and maximum circular polarization. We wish to select only those γ-rays approximating this condition. That is done by nuclear resonance scattering [14]). When a photon with momentum $\mathbf{p}_\gamma$ is going out in opposite direction to the momentum $\mathbf{p}_\nu$ of the previously emitted neutrino, and $|\mathbf{p}_\gamma| = |\mathbf{p}_\nu|$, this photon obviously has the correct laboratory energy for resonance excitation of the relevant stationary nucleus. And if $|\mathbf{p}_\nu| > |\mathbf{p}_\gamma|$, then for $\mathbf{p}_\nu \cdot \mathbf{p}_\gamma + p_\gamma^2 = 0$, the momentum condition will be satisfied.

3. Source and Magnet

The nucleus Eu^{152m} is a suitable source for the described method. It has a most probable spin and parity assignment of 0^- and decays by electron capture to an excited 1^- level in Sm^{152}, 963.3 keV above the ground state (0^+) as seen in the decay scheme of Eu^{152m} in the preceding article. A neutrino energy of 890 ± 50 keV in the K-capture process can be deduced from a weak positon spectrum to the ground state of Sm^{152} [15]). Further the mean life of the 963 keV level is measured by resonance scattering to be $\tau = (3 \pm 1) \times 10^{-14}$ sec [16]). Thus a 963 keV γ-ray is generally emitted before the nucleus has lost its recoil energy from neutrino emission and the transferred momentum has about the right value. Resonance scattering is therefore a sensitive detector for the angle of emission between neutrino and photon.

We used a transmission Compton analyzer [17]) for circular polarization to measure the difference in intensity of the transmitted γ-rays when the magnetic field was reversed. The analyzer was of double toroid type and designed as in fig. 1. Each toroid has one layer of windings on the outside of a soft iron core and the ratio of the diameters is 1 : 2. When saturation is reached the magnetization in the iron is 20 kG and the stray field just outside the windings is nowhere more than two gauss. When necessary, even that may be compensated with some extra windings in the common part of the two toroids. Such a magnet will not cause any dangerous disturbances in the source or detector.

4. Experimental Arrangements and Calculations

The experimental set-up is shown in fig. 1. The Eu^{152m} source is placed in the end of a tube and inserted inside a lead housing adjacent to the double toroid. All but the magnet is circularly symmetric around the x-axis.

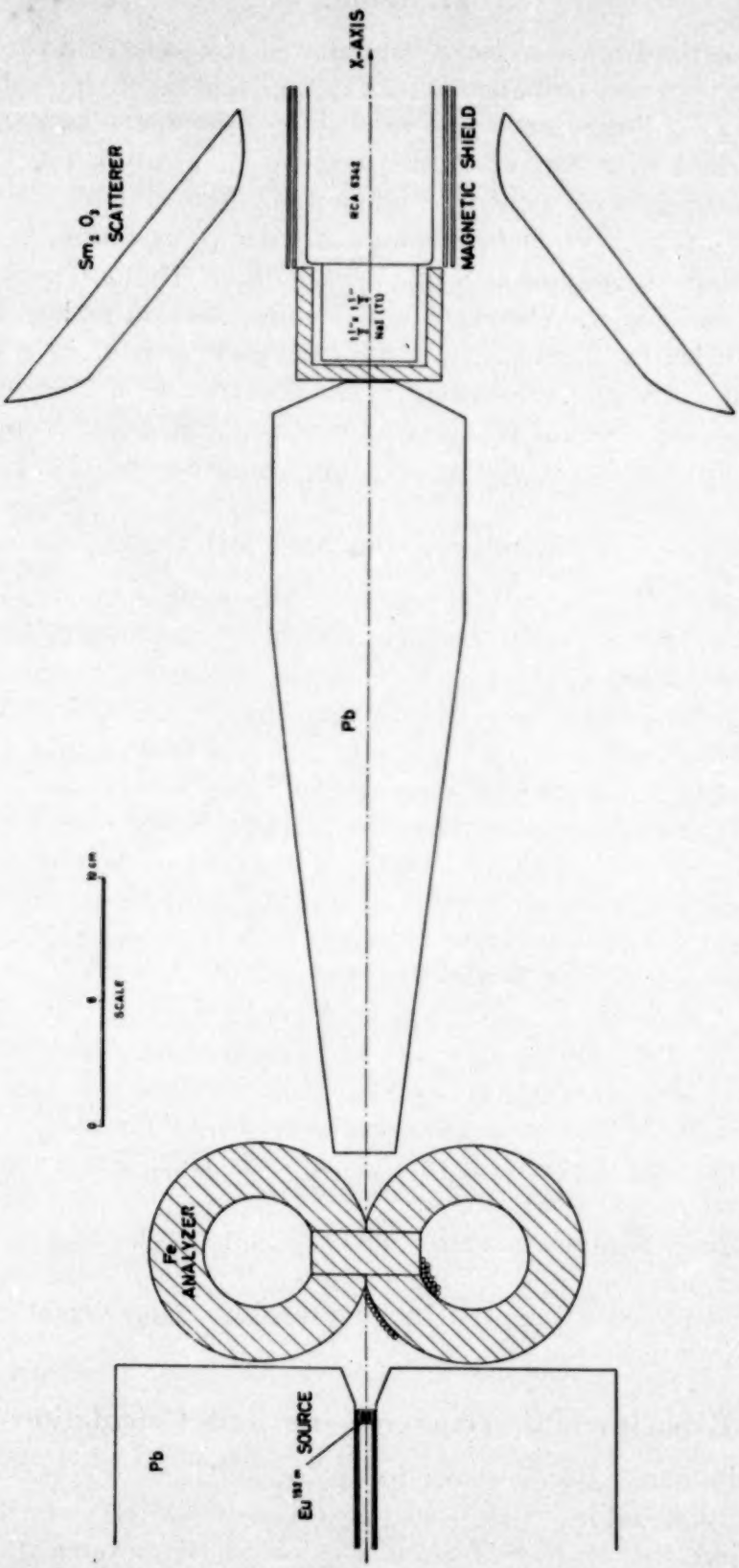

Fig. 1. Experimental set-up for analysis of circularly polarized photons to be resonance scattered.

As scatterer we used 2000 g of pure Sm_2O_3(26.8 % Sm^{152}). The $1\frac{1}{2}'' \times 1\frac{1}{2}''$ NaI(Tl) crystal is shielded from direct radiation by a lead block. Signals from the crystal are fed through an RCA 6342 photomultiplier tube, a cathode follower and a linear amplifier to three differential discriminators with scalers and mechanical registers.

The iron was fully saturated everywhere and the source dimensions were quite small (< 30 mm^3). Thus, the path length of a given 963 keV γ-ray in magnetized iron could be calculated accurately. From the diameter of the toroids (90 mm) the measured magnetization and the overall geometry of the set-up, the polarization efficiency at 963 keV is computed [18]) to be 0.017 ± 0.001. We have here simply taken one polarized electron spin per Bohr magneton as a safe upper limit, and the associated uncertainty is not included in the error quoted.

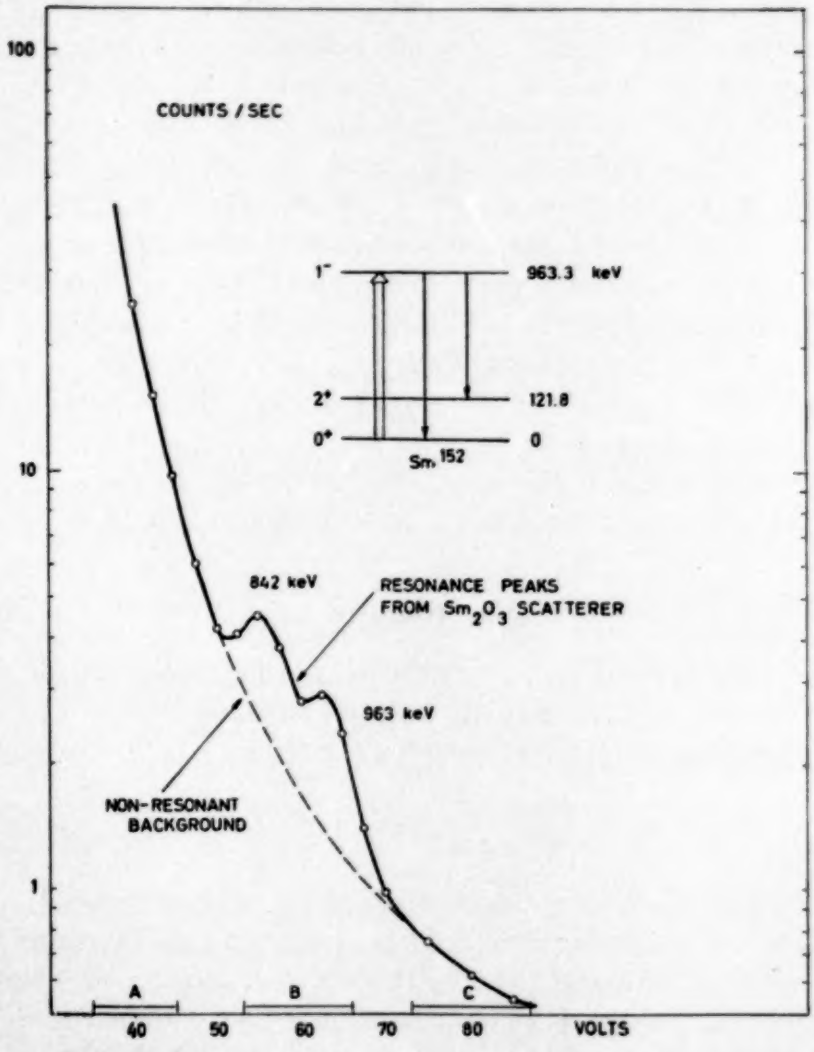

Fig. 2. Spectrum of scattered γ-rays from the decay of Eu^{152m}. The resonance peaks lie on a steeply sloping curve of non-resonant background.

5. Measurements

The electronic equipment was tested by combining a strong Cs^{137} and a Tb^{160} source so as to give a pulse-height curve similar to that from Eu^{152m}, fig. 2. With the sources in such a position as to give about ten times higher counting rate than in the later experiment, the test was carried out reversing the magnetic field every fifteen minutes. No effect was found in any channel when 6×10^6 counts were collected in the middle channel.

Eu_2O_3 was neutron irradiated in the reactor of AB Atomenergi, Stockholm. The source strength was usually about 300 mC in the beginning of a run. Most of the photons detected had been inelastically scattered, giving the steeply sloping curve in fig. 2. No peak was observed from elastic scattering[19]). The scatterer was placed in a position that was found to give a good ratio between resonant and non-resonant scattering. The mean scattering angle was then 110°. The photons were detected in three channels. Channel B accepted the resonance peaks. Channels A and C were placed on the low and high energy side as shown in fig. 2. Every five (or fifteen) minutes the channels were shut for ten seconds, during which time the magnetic field was reversed and the registers photographed and reset by an automatic unit.

The original plan was to reverse this experiment so that the source and detector would be interchanged. For suitable scattering angles one should then find an opposite sense of polarization for the two γ-rays from resonance excited Sm^{152} nuclei. The 963 keV γ-rays would keep essentially all of the original polarization, and the 842 keV γ-rays would be oppositely polarized by typically 60 % of the original polarization. The Compton analyzer should then depress one peak in fig. 2 relative to the other, and when the magnetic field is reversed the depression would act in the opposite sense. This plan, however, was not carried through due to lack of time.

6. Results

The field was reversed in a given cycle in order to correct for the decay of the source. No effect was then observed in channel A or C. Channel B registered 2.8×10^6 counts and an effect

$$\delta = \frac{N^- - N^+}{\frac{1}{2}(N^- + N^+)} = +0.014 \pm 0.004$$

was found when the non-resonant background was subtracted. N^+ is the counting rate with the magnetic field pointing towards the source and N^- the counting rate with the field in the opposite direction. This effect is therefore of the same sign as in the experiment by Goldhaber *et al.*[1]) (where the magnet was tested with bremsstrahlung from a $Sr^{90}+Y^{90}$ source with known negative helicity).

7. Conclusions

If the 963 keV γ-rays are circularly polarized to 100 % when passing the magnet, the estimated effect is $\delta = \pm 0.017$ with the + sign corresponding to negative helicity. From the figure obtained experimentally, $\delta = +0.014 \pm 0.004$, we find that the 963 keV γ-rays are circularly polarized to 80 ± 30 % and have negative helicity. Inasmuch as all the unknown effects, such as imperfect memory of initial recoil direction, can act only to degrade the final measured polarization, this result seems compatible with 100 % negative helicity of the neutrinos emitted in orbital electron capture from Eu^{152m} of spin 0^-.

An earlier experiment [4]) has shown that the helicity of the positons in a Gamow-Teller transition is positive. The combined result of these two experiments indicates that the Gamow-Teller interaction is an axial vector (A) for positon emitters [20]).

The authors are indebted to Professor Kai Siegbahn for excellent working conditions and stimulating interest. Our thanks are also to Johnson, Matthey & Company, London, for the loan of the Sm_2O_3 scatterer and to the reactor group at R1, AB Atomenergi, Stockholm, for good irradiation opportunities.

References

1) M. Goldhaber, L. Grodzins and A. W. Sunyar, Phys. Rev. **109** (1958) 1015
2) C. S. Wu, E. Ambler, R. W. Hayward, D. D. Hoppes and R. P. Hudson, Phys. Rev. **105** (1957) 1413
3) J. C. Wheatley, W. J. Huiskamp, A. N. Diddens, M. J. Steenland and H. A. Tolhoek, Physica **21** (1915) 841
4) L. A. Page and M. Heinberg, Phys. Rev. **106** (1957) 1220
5) H. Frauenfelder, R. Bobone, E. von Goeler, N. Levine, H. R. Lewis, R. N. Peacock, A. Rossi and G. De Pasquali, Phys. Rev. **106** (1957) 386
6) H. Schopper, Phil. Mag. **2** (1957) 710
7) M. Deutsch, B. Gittleman and R. W. Bauer, L. Grodzins and A. W. Sunyar, Phys. Rev. **107** (1957) 1733
8) S. Frankel, P. G. Hansen, O. Nathan and G. M. Temmer, Phys. Rev. **108** (1957) 1099
9) H. De Waard, Physica **23** (1957) 597
10) L. A. Page, Nuovo Cimento **7** (1958) 727
11) B. M. Rustad and S. L. Ruby, Phys. Rev. **97** (1955) 991;
cf. recent He^6 measurements by W. B. Herrmannsfeld, R. L. Burman, P. Stähelin, J. S. Allen and M. E. Braid, Phys. Rev. Letters **1** (1958) 61
12) M. Morita and R. S. Morita, Bull. Am. Phys. Soc. **2** (1958) 270
13) T. D. Lee and C. N. Yang, Phys. Rev. **105** (1957) 1671
14) K. G. Malmfors in Beta and Gamma-ray Spectroscopy, edited by K. Siegbahn (North-Holland Publishing Company, Amsterdam, 1955) p. 521;
F. R. Metzger, Phys. Rev. **101** (1956) 286
15) L. Grodzins and H. Kendall, Bull. Am. Phys. Soc. **1** (1956) 163
16) L. Grodzins, Phys. Rev. **109** (1958) 1014
17) S. B. Gunst and L. A. Page, Phys. Rev. **92** (1953) 970
18) L. A. Page, B. G. Pettersson and T. Lindqvist, to be published in Phys. Rev.
19) N. Cindro and K. Ilakovac, Nuclear Physics **5** (1958) 647
20) W. B. Herrmannsfeldt, D. R. Maxson, P. Stähelin and J. S. Allen, Phys. Rev. **107** (1957) 641
21) G. Culligan, S. G. Frank, J. R. Holt, J. C. Kluyver and T. Massam, Nature **180** (1957) 751

2.G *Nuclear Physics* 9 (1958/59) 94—107; © *North-Holland Publishing Co., Amsterdam*
Not to be reproduced by photoprint or microfilm without written permission from the publisher

PREDICTIONS OF THE DISTORTED WAVE THEORY OF DEUTERON STRIPPING REACTIONS

R. HUBY, M. Y. REFAI,
University of Liverpool
and
G. R. SATCHLER
Clarendon Laboratory, Oxford

Received 16 August 1958

Abstract: The distorted wave theory of stripping is presented in a rather general form, and the degree of generality is examined. The spin polarisation of (d, p) protons and the correlation function of de-excitation γ-rays are expressed on this theory as functions of statistical tensors ρ_{kq} which can in principle be calculated given the details of the process (wave functions, interaction potential etc.). The form of the polarisation and correlation are investigated, and it is shown what features of these are characteristic of the theory in general as distinct from its details. In this way experimental tests are devised to find whether observed results are compatible with stripping theory of this type. The tests consist in relations predicted between observed "experimental parameters". The cases $l = 1$ and 2 (l = orbital angular momentum of captured nucleon) are discussed fully.

1. Introduction

Much work has been done to improve on the simple, early theories of stripping [1,2]) by the use of distorted waves for the deuteron and the emergent particle [3–6]), an approach which has received support recently from the formal theory of nuclear reactions [7,8]).

This is particularly important for the spin polarisation of the emergent particle, because the simple theory predicts no polarisation. However, also the d-p (or d-n) differential cross-section and the angular distribution of decay γ-rays (d-p-γ) can be re-calculated with distorted waves. If it proves possible to get better agreement with experiment by the use of suitable distorted waves than by the simple theory, this will be very interesting as showing what distortion is in fact produced by the nucleus, and as throwing light on the nuclear mechanisms †. However, it is by no

† We certainly expect the qualitative features of the distorting potentials to be the same as those required to explain the elastic proton and deuteron scattering. However, there may be important differences. We may regard the use of distorted waves as an attempt to find better zero order functions for a perturbation series calculation and so ensure more rapid convergence. It is not clear then that the best potential for this is identical with the optical potential for elastic scattering. Levinson and Banerjee [9]) in their analysis of C^{12} (p, p′)C^{12*} required a proton potential consistently shallower than that given by the elastic scattering.

means clear yet how successful the distorted wave theory will be in these respects, and every attempt at an actual calculation requires heavy computation with a guessed distortion, which may be a bad guess. The purpose of the present paper is to study the predictions of the distorted wave theory and thus devise experimental tests of it by discovering those features which are independent of the details of the distortion. Then it is possible to examine whether the experimental results conform to such predictions, without making heavy numerical calculations. The predictions in question are features of the d-p-γ distribution, and the relation of this distribution to the spin polarisation. These effects are analysed in sections 2—5, and it is also shown how (provided the tests are satisfied) one may derive from the experiments those parameters B_{lm} which are most directly connected with the distortion to be used in the theory, together with relative values of reduced widths which are largely independent of the distortion effects.

2. The Distorted Wave Theory

We consider those varieties of stripping theory which involve distorted waves, and result in an amplitude for an A(d, p)B reaction given by a matrix element of the form

$$I = \int \psi_{\mathrm{p}}^{*}(\mathbf{k}_{\mathrm{p}}, \mathbf{r}'_{\mathrm{p}})\chi^{*}_{\mu_{\mathrm{p}}}(s_{\mathrm{p}})\chi^{*}_{I_{\mathrm{B}}, M_{\mathrm{B}}}(\xi, \mathbf{r}_{\mathrm{n}}, s_{\mathrm{n}})V_{\mathrm{np}}(|\mathbf{r}_{\mathrm{n}} - \mathbf{r}_{\mathrm{p}}|) \times \psi_{\mathrm{d}}(\mathbf{k}_{\mathrm{d}}, \mathbf{r}_{\mathrm{n}}, \mathbf{r}_{\mathrm{p}})\chi_{\mu_{\mathrm{d}}}(s_{\mathrm{n}}, s_{\mathrm{p}})\chi_{I_{\mathrm{A}}, M_{\mathrm{A}}}(\xi)\mathrm{d}\tau. \tag{2.1}$$

Here $\chi_{I_{\mathrm{A}}, M_{\mathrm{A}}}$, $\chi_{I_{\mathrm{B}}, M_{\mathrm{B}}}$ are the wave functions of the target nucleus A and final nucleus B respectively. ψ_{p} and ψ_{d} are the spatial wave functions of the proton and deuteron, as distorted by some suitable potentials (assumed spin independent but including the Coulomb field) due to the nucleus and constructed with the appropriate boundary conditions. $\chi_{\mu_{\mathrm{p}}}$ is a proton spin wave-function, and $\chi_{\mu_{\mathrm{d}}}$ is a deuteron triplet state spin wave function. V_{np} is a triplet state central potential. The coordinates are as follows: ξ are the internal coordinates of A; $\mathbf{r}_{\mathrm{n}}$, $\mathbf{r}_{\mathrm{p}}$ are the neutron and proton coordinates relative to the mass centre of A; $\mathbf{r}'_{\mathrm{p}}$ is the vector of the proton from the mass-centre of B, given by

$$\mathbf{r}'_{\mathrm{p}} = \mathbf{r}_{\mathrm{p}} - \frac{\mathbf{r}_{\mathrm{n}}}{m_{\mathrm{B}}}, \tag{2.2}$$

(m_{B} = mass number of B);

and s_{n}, s_{p} are the spin coordinates of neutron and proton. $\mathbf{k}_{\mathrm{d}}$, $\mathbf{k}_{\mathrm{p}}$ are the reduced wave numbers of the initial and final channels. Most published "distorted wave" calculations [3–6]) of stripping take the form (2.1), and the original amplitude of Butler's theory [1]) can also be expressed in this form [10]). These theories have usually required the integration to be restricted to the

region $r_n > R$, where R is an effective radius of the nucleus, and they have often made other simplifications; but the form of (2.1) need not be considered tied down to these. On the other hand, (2.1) implies certain approximations of its own:

(1) The distorting potentials are spin-independent. While spin-orbit coupling is undoubtedly present for both deuterons and nucleons, it is only a few MeV in magnitude compared to the considerably stronger main potential. Thus it cannot play a major role except perhaps at wide angles where the various amplitudes are all quite small. The calculation of Newns and Refai [4]) supports this conclusion.

(2) The correct matrix elements should include a contribution from that part of V_p (the interaction between proton and target nucleus) which remains after subtracting the distorting potential used for ψ_p.

(3) Exchange contributions resulting from anti-symmetrising the wave-functions are neglected [11–13]).

(4) We assume V_{np} is a central potential, and hence

(5) the deuteron wave function separates into space and spin factors, ψ_d and χ_{μ_d}. The tensor effects (i.e. effects arising from the small D-state part of the deuteron wave function, and the tensor component of the interaction V_{np}) are expected to be small, in both the polarisation and the γ-correlation. No polarisation arises from tensor forces when plane wave functions are used, and therefore the tensor corrections require to be combined with distortion corrections in order to produce polarisation. As regards the γ-correlation, it is found that there are no cross-terms between the S and D states of the deuteron, so any corrections are due to the square of the D-state amplitude only.

(6) The nuclei and the corresponding distorting potentials are assumed spherical. The effects due to even strongly deformed nuclei are in general quite small, though they may occasionally cause difficulty when relative reduced widths are being extracted from experimental data [14]).

We now investigate the consequences of (2.1). It is possible to carry out the integration over ξ, and (introducing Clebsch-Gordan coefficients) write the nuclear overlap integral

$$\int \chi^*_{I_B, M_B}(\xi, \mathbf{r}_n, s_n)\chi_{I_A, M_A}(\xi)\mathrm{d}\xi$$
$$= \sum_{j, \mu_j, l, m, \mu_n} (I_A M_A, j\mu_j | I_B M_B)(lm, \tfrac{1}{2}\mu_n | j\mu_j)\theta^*_{jl} u^*_l(r_n) \qquad (2.3)$$
$$\times i^{-l} Y_l^m(\theta_n, \phi_n)^* \chi_{\mu_n}(s_n)^*.$$

Here j and l are the total and orbital angular momenta with which the stripped neutron enters the nucleus. χ_{μ_n} is a neutron spin wave function, and u_l is a normalised orbital wave function. The coefficient θ_{jl} is a "reduced

width amplitude". θ_{jl} and u_l are made real by suitable phasing †. It is implied in (2.3) that $u_l(r_n)$ does not depend on j, so that the θ_{jl}'s carry the main nuclear structure information, as has been discussed elsewhere on the basis of the shell model [15]) and the collective model [16]). However, the treatment below could easily be generalised to allow for possible dependence of u on j: this would require the insertion of an extra suffix j on the quantities B_{lm}. Substitution of (2.3) in (2.1) yields

$$I = \sum_{j,\mu_j,l,m,\mu_n} (I_A M_A, j\mu_j | I_B M_B)(lm, \tfrac{1}{2}\mu_n | j\mu_j) \times (\tfrac{1}{2}\mu_p, \tfrac{1}{2}\mu_n | 1\mu_d)\sqrt{2l+1}\,\theta_{jl} B_{lm}, \tag{2.4}$$

where

$$B_{lm} = (2l+1)^{-\frac{1}{2}} \int \psi_p^*(\mathbf{k}_p, \mathbf{r}'_p) u_l^*(r_n) i^{-l} Y_l^m(\theta_n, \phi_n)^* \times V_{np}(|\mathbf{r}_p - \mathbf{r}_n|)\psi_d(\mathbf{k}_d, \mathbf{r}_n, \mathbf{r}_p)\mathrm{d}\mathbf{r}_n \mathrm{d}\mathbf{r}_p. \tag{2.5}$$

All measurable quantities in stripping are determined by the θ_{jl}'s and the matrix elements B_{lm}, which are amplitudes for the absorption of the neutron with quantum numbers (l, m), and are closely related to the A_l^m of Horowitz and Messiah [3]) and the B^{lm} of Tobocman [5]). The B_{lm}'s are practically independent of nuclear structure (which enters them only through u_l), and they may be expected not to be very sensitive to the choice of optical potential, or indeed to any of the other variables which enter. This relative insensitivity of the B_{lm}'s enables one to *compare* cross-sections for a given l value for reactions leading to different levels in the same nucleus or neighbouring nuclei, and so obtain *relative* reduced widths θ_{jl} with comparatively little error.

When plane waves are used, for example, B_{lm} reduces to the usual Butler form if the integration is limited to $r_n > R$. If we take as axis of quantisation the direction of the recoil momentum

$$\mathbf{k} = \mathbf{k}_d - (m_A/m_B)\mathbf{k}_p, \tag{2.6}$$

then (normalising the plane waves like exp $(i\mathbf{k}\cdot\mathbf{r})$),

$$B_{lm}(\text{Butler}) = -\frac{\sqrt{4\pi}\hbar^2 R^2}{2m_n^*} G(|\mathbf{k}_p - \tfrac{1}{2}\mathbf{k}_d|) \times u_l(R)\left[\frac{\mathrm{d}j_l(kR)}{\mathrm{d}R} - \frac{1}{h_l^{(1)}(i\kappa R)}\frac{\mathrm{d}h_l^{(1)}(i\kappa R)}{\mathrm{d}R} j_l(kR)\right]\delta_{m,0} \tag{2.7}$$

where G is the Fourier transform of the deuteron internal wave function, as in ref.[2]); m_n^* is the reduced mass of the system (n-A); and $\hbar^2\kappa^2/2m_n^*$ is the separation energy of the bound neutron. Since it will be convenient later to change the frame of quantisation, we note from (2.5) that B_{lm} transforms like Y_l^{m*}.

† To this end we have employed the combination $(i^l Y_l^m)^*$ in (2.3) rather than Y_l^{m*}, but the latter has more usually been used in the literature [3, 5, 16, 18]).

All measurable quantities depend quadratically on the matrix elements, and therefore we define a density matrix

$$\rho_{lm;\,l'm'} = B_{lm} B^*_{l'm'} \tag{2.8}$$

and statistical tensors † [17])

$$\rho_{kq}(l, l') = \sum_{m,\,m'} (-1)^{l'-m'} (lm, l'-m'|kq) \rho_{lm;\,l'm'}. \tag{2.9}$$

In the plane wave limit, and with **k** as quantisation axis, as in (2.7), only ρ_{k0} is non-zero.

We are concerned with the differential cross-section for stripping, the polarisation of the emitted protons, and the d-p-γ correlation. These can be calculated from the matrix elements I (2.4) by well-known methods (see for example ref.[5])) and expressed in terms of the above quantities.

3. Differential Cross-Section and Polarisation

The (d, p) differential cross-section is (taking the wave functions ψ_p, ψ_d to be normalised like exp $(i\mathbf{k}\cdot\mathbf{r})$)

$$\begin{aligned}\sigma(\mathbf{k}_p, \mathbf{k}_d) &= \frac{m_p^* m_d^* k_p (2I_B+1)}{8\pi^2 \hbar^4 k_d (2I_A+1)} \sum_{j,l} \theta^2_{jl} \Big(\sum_m |B_{lm}|^2\Big) \\ &= \frac{m_p^* m_d^* k_p (2I_B+1)}{8\pi^2 \hbar^4 k_d (2I_A+1)} \sum_{j,l} (2l+1)^{\frac{1}{2}} \theta^2_{jl} \rho_{00}(l, l),\end{aligned} \tag{3.1}$$

where m_p^*, m_d^* are the reduced masses in the initial and final channels.

The component of polarisation of the proton spin in the direction of the quantisation axis is

$$\begin{aligned}P(\mathbf{k}_p, \mathbf{k}_d) &= \frac{2\sum_{j,l} (-1)^{j-l-\frac{1}{2}} \theta^2_{jl} (2j+1)^{-1} \big(\sum_m m|B_{lm}|^2\big)}{3\sum_{j,l} \theta^2_{jl} \big(\sum_m |B_{lm}|^2\big)} \\ &= \frac{2\sum_{j,l} (-1)^{j-l-\frac{1}{2}} \theta^2_{jl} (2j+1)^{-1} [l(l+1)(2l+1)]^{\frac{1}{2}} \rho_{10}(l, l)}{3^{\frac{1}{2}} \sum_{j,l} (2l+1)^{\frac{1}{2}} \theta^2_{jl} \rho_{00}(l, l)}.\end{aligned} \tag{3.2}$$

When only one l value is important, (3.2) reduces to

$$P_l(\mathbf{k}_p, \mathbf{k}_d) = \tfrac{1}{3} \left[\frac{\theta^2_{l+\frac{1}{2}}}{l+1} - \frac{\theta^2_{l-\frac{1}{2}}}{l}\right] \frac{\langle m\rangle}{\theta^2_{l+\frac{1}{2}} + \theta^2_{l-\frac{1}{2}}}, \tag{3.3}$$

where $\langle m\rangle$ is the mean value of the component of orbital angular momentum along the quantisation axis:

$$\langle m\rangle = \frac{\sum_m m|B_{lm}|^2}{\sum_m |B_{lm}|^2}. \tag{3.4}$$

† These tensors differ from the $\rho_{kq}(l, l')$ of a previous manuscript [18]). The $\rho_{kq}(l, l')$ defined there are $i^{l+l'}(-1)^q(l0, l'0|k0)$ times the $\rho_{k,-q}(l, l')$ used here.

The polarisation vector in fact lies along the direction $\mathbf{n}$ of $\mathbf{k}_d \times \mathbf{k}_p$, and it will be convenient now to take this as the axis of quantisation †. Eq. (3.3) illustrates the mechanism whereby the polarisation is produced. The distorting potentials tend to "polarise" the orbital vector $\mathbf{l}$ of the captured neutron, by favouring captures on one side of the nucleus for a given outgoing $\mathbf{k}_p$ so that $\langle m \rangle \neq 0$. The spin coupling within the residual nucleus which then favours one of the two $j = l \pm \frac{1}{2}$ values for the neutron capture transmits this polarisation to the neutron spin. In turn, through the spin coupling in the incident deuteron which favours parallel neutron and proton spins, this polarisation is transmitted to the released protons we observe. Clearly $|\langle m \rangle| \leqq l$, so if only one j contributes (for example with zero spin target) we get the well known rule that $|P| \leqq \frac{1}{3}$ if $j = l - \frac{1}{2}$ and $|P| \leqq \frac{1}{3} l/(l+1)$ if $j = l + \frac{1}{2}$. Experimentally [19]) in the region of stripping angles the polarisation seèms to attain a large fraction of this maximum, with $\langle m \rangle$ positive along $\mathbf{n}$. Further, we can compare the polarisation P_+, from a capture with only $j = l + \frac{1}{2}$ to that P_- when $j = l - \frac{1}{2}$ only, for the corresponding proton directions. If these occur in the same, or neighbouring nuclei, with similar energies so that $\langle m \rangle$ is similar for both reactions, the distorted wave theory predicts

$$P_+/P_- = -l/(l+1).$$

The asymmetry induced in the differential cross-section for the inverse (p, d) pick-up reaction, when polarised protons are used, is obtained immediately from reciprocity [20]:

$$\sigma(\mathbf{k}_p, \mathbf{k}_d)_{\text{pol.}} = \sigma(\mathbf{k}_p, \mathbf{k}_d)_{\text{unpol.}}[1 + \mathbf{P} \cdot \mathbf{n} P(\mathbf{k}_p, \mathbf{k}_d)], \tag{3.5}$$

where $\mathbf{P}$ is the polarisation of the incident protons, while $P(\mathbf{k}_p, \mathbf{k}_d)$ is given by (3.2), and $\mathbf{n}$ is now, in the pick-up reaction, the unit vector along $\mathbf{k}_p \times \mathbf{k}_d$.

4. Proton-γ Angular Correlation

The correlation function for the emission of γ-rays in the direction (θ, ϕ) when B decays from I_B to a lower level $I_B{}'$ may first be written in a form which is generally valid, independently of the assumption that I_B is formed by the stripping mechanism:

$$W(\mathbf{k}_p, \mathbf{k}_d, \theta, \phi) \propto \sum_{L, L', k, q} F_k(LL' I_B{}' I_B)(2k+1)^{-\frac{1}{2}} \rho_{kq}(I_B, I_B) \times C_L C_{L'} Y_k{}^q(\theta, \phi), \tag{4.1}$$

where the $\rho_{kq}(I_B, I_B)$ are statistical tensors describing the polarisation of I_B after it has been formed, constructed similarly to (2.9); the F_k's are the well-known γ-emission coefficients (e.g. ref.[17]), eq. (19.7)); L (or L') is the

† In the earlier manuscript [18]), the corresponding 'primed' coordinate system has its z' axis along $-\mathbf{n}$, the direction of $\mathbf{k}_p \times \mathbf{k}_d$.

γ-multipolarity, allowing for multipole mixtures, C_L being the corresponding multipole amplitude, equivalent to the $(j_2||L_2||j)$ of ref. [21]). k takes even values not greater than $2I_B$ or $2L_{max}$. The $\rho_k{}^q$'s satisfy a hermiticity condition (ensuring the reality of W):

$$\rho^*_{kq}(I_B, I_B) = (-1)^q \rho_{k,-q}(I_B, I_B), \tag{4.2}$$

(so that ρ_{k0} is real). The γ-distribution must have symmetry of reflection through the d-p reaction plane, and if we choose the axis of quantisation in the direction $\mathbf{n}$ of $\mathbf{k}_d \times \mathbf{k}_p$ this requires that q take only even values. If we now assume the stripping mechanism (i.e. the scattering amplitude I is given by (2.4)) the $\rho_{kq}(I_B, I_B)$'s are subject to further restriction, being expressible in terms of the $\rho_{kq}(l, l')$'s by

$$\rho_{kq}(I_B, I_B) = \frac{(2I_B+1)^{\frac{1}{2}}}{2(2I_A+1)} \sum_{j,l,j',l'} \frac{\theta_{jl}\theta_{j'l'}(-1)^{l'}\eta_k(jj'I_A I_B)\rho_{kq}(l, l')}{(l0, l'0|k0)}, \tag{4.3}$$

where η_k is the coefficient tabulated by Satchler [22]). Here k cannot exceed $2l_{max}$ or $2j_{max}$. The $\rho_{kq}(l, l')$'s (2.9) satisfy a hermiticity condition similar to (4.2):

$$\rho^*_{kq}(l, l') = (-1)^{l'-l+q} \rho_{k,-q}(l', l), \tag{4.4}$$

and the reflection symmetry of the system is expressed (if the quantisation axis is $\mathbf{n}$) by the condition that B_{lm} (cf. 2.5) exist only for even $(l-m)$, from which it follows that $\rho_{kq}(l, l')$ exists only for even q.

When plane waves are used to describe the (d, p) reaction the residual nucleus behaves as though neutrons had been captured from a beam incident along $\mathbf{k}$, (2.6). So the angular distribution of de-excitation γ-rays is the same as for a resonant (n, γ) capture reaction, provided they are measured in coincidence with outgoing protons along $\mathbf{k}_p$ so that $\mathbf{k}$ is defined. $\mathbf{k}$ is then an axis of azimuthal as well as back-forward symmetry for the γ-rays. Experimental observation of this symmetry axis then lends strong evidence for the direct, stripping, nature of the reaction, and measurements of the correlation yield information on the relative reduced widths for capture with $j = l \pm \frac{1}{2}$, which cannot be obtained from the proton distribution alone.

Distortion of the proton and deuteron waves also distorts the simple p-γ correlation. The degree of anisotropy is changed, and some azimuthal and left-right asymmetry about the $\mathbf{k}$ axis is introduced. However, as already pointed out, the reaction plane containing $\mathbf{k}_d$ and $\mathbf{k}_p$ always remains a plane of symmetry for the γ-rays, that is, up-down symmetry is preserved.

Our study of the polarisation allows us to put upper limits on the effects of the distortion on the p-γ correlation. We noted that maximum polarisation occurs, for a given capture l, when only the projection along $\mathbf{n}$, $m = l$ or $-l$ occurs: that is, only B_{ll} or $B_{l,-l}$ is non-zero. It follows then from (2.9) that only $\rho_{k0}(l, l)$ (quantisation referred to $\mathbf{n}$) is non-vanishing. Since ρ_{kq} is

associated with $Y_k^q(\theta, \phi)$ in the p-γ correlation, all dependence on ϕ has been removed: the correlation is isotropic in the (d, p) reaction plane. Perpendicular to this plane the correlation is similar to that found in the plane when plane waves are used, except that the coefficient of $P_k(\cos\theta)$ is multiplied by $f_k(l)$,

$$f_k(l) = \frac{(ll, l-l|k0)}{(l0, l0|k0)}(-1)^l,$$

$$f_0 = 1; \quad f_2 = -\frac{(2l-1)}{(l+1)}; \quad f_4 = \frac{2(2l-1)(2l-3)}{(l+1)(l+2)}.$$

5. Experimental Tests of the Distorted Wave Theory

We investigate how the above formulae can be confronted with experiment. There are two questions:

(1) How to devise tests of the theory, i.e. to find predicted features which depend only on the form of the theory, not on the particular values of the unknowns B_{lm}.

(2) How to determine the unknowns B_{lm} from experiment. It would then remain the task for theory to fix the scattering potentials and other features so as to yield the observed values of the B_{lm}'s.

We shall consider that the directions of $\mathbf{k}_d$ and $\mathbf{k}_p$ are fixed, giving rise to one fixed set of numbers B_{lm}. Since we exclude comparison of different $\mathbf{k}_d$ and $\mathbf{k}_p$ directions, we must exclude consideration of the d-p angular distribution, confining our attention to the polarisation P and the p-γ correlation: the d-p angular distribution has been exhaustively discussed elsewhere. This means that we shall not be concerned with the absolute values of the amplitudes B_{lm}, which appear only in (3.1).

To remove possible ambiguities due to our lack of knowledge of the θ_{jl}'s we assume that only one value of l and one of j are involved: this can be achieved by suitable choice of the levels studied, using the selection rules of angular momentum addition

$$\mathbf{l}+\mathbf{\tfrac{1}{2}} = \mathbf{j}; \quad \mathbf{j}+\mathbf{I}_A = \mathbf{I}_B, \tag{5.1}$$

and for parity

$$\pi_A(-1)^l = \pi_B.$$

We shall assume all the spins and parities are known. We count the number of parameters in the quantities B_{lm}; these will be referred to as "theoretical parameters". Since $(l-m)$ is even, there are $(l+1)$ non-zero B_{lm}'s, and since they are complex, they contain $2(l+1)$ real parameters. However, two of these are unobservable for present purposes: (i) a common phase factor, (ii) a common normalisation factor. There remain then $2l$ real theoretical parameters which affect observation. From observation of P and W we

obtain information about the statistical tensors $\rho_{kq}(l, l)$, which we therefore denote "experimental parameters". We may allow for the indeterminateness of absolute magnitudes by normalising ρ_{00} to unity. From P, by (3.2) we then obtain $\rho_{10}(l, l)$ immediately. From W, by (4.1) we can obtain directly the $\rho_{kq}(I_B, I_B)$'s, if the γ-multipole is pure, but otherwise the mixture parameters C_L must be known. Next, by (4.3), we obtain the $\rho_{kq}(l, l)$'s. In the most favourable circumstances, $k_{max} = 2l$ (this requires $j = l+\frac{1}{2}$, which we shall generally assume), and then the number of ρ_{kq}'s measurable from P and W (not counting ρ_{00}) is $(l+1)^2$. On allowing for the hermiticity relations, (4.2) or (4.4), the ρ_{kq}'s contain just as many, $(l+1)^2$, real experimental parameters. On stripping theory these all depend on the $2l$ real theoretical parameters. Therefore stripping theory must lead to $(l+1)^2-2l = l^2+1$ relations between the real experimental parameters. These relations are obtained by eliminating the B_{lm}'s, and therefore constitute tests of stripping theory independent of the details (question 1). Further, it will be possible to solve for the relative B_{lm}'s (question 2). However, there will be ambiguities in these results, due to the quadratic dependence of the ρ's on the B's. In particular we shall be able to predict the polarisation P from the harmonic coefficients of the distribution W, but it can be shown that only the magnitude of the polarisation is predictable, not its sign. This result can be proved more generally, whatever model be used, i.e. any distribution W which is associated with a polarisation P is also compatible with the polarisation $-P$. There are additional tests of the theory in the form of inequalities, e.g. the limitations on P described in section 3.

The above considerations reduce to a special, simple case on the Butler theory. As explained in section 2, in this case the quantisation axis is most conveniently re-chosen along **k**, and then the only B's are those with $m = 0$, and the only ρ_{kq}'s are those with $q = 0$:

$$\rho_{k0} \propto (-1)^l(l0, l0|k0). \tag{5.2}$$

Thus there are no free parameters: the polarisation is zero, and the γ-correlation is completely fixed. In analysing experimental results, one will first compare them with the predictions of the Butler theory, and then see if they give better agreement with the weaker predictions of the distorted wave theory.

Section 6 contains a detailed discussion of the case $l = 1$, and 7 of $l = 2$ ($l = 0$ is trivial).

6. Case $l = 1$

This was discussed by Horowitz and Messiah [23]). For the γ-angular distribution we now have in a favourable case $k_{max} = 2$, and we shall first

discuss the form which the angular distribution (4.1) takes under this restriction: these considerations therefore apply independently of the stripping mechanism or choice of l, and only require that k be limited by some selection rule. The most convenient reference frame is that with z in the **n** direction, and x in the **k** direction. (4.1) may now be written in the form:

$$W(\mathbf{k}_p, \mathbf{k}_d, \theta, \phi) \propto |+A_2^0 P_2(\cos\theta)+A_2^2 P_2^2(\cos\theta)\cos 2(\phi-\phi_0), \quad (6.1)$$

(A_2^0, A_2^2 and ϕ_0 are real) or alternatively

$$W(\mathbf{k}_p, \mathbf{k}_d, \theta, \phi) \propto a l_\gamma^2+b m_\gamma^2+c n_\gamma^2, \quad (6.2)$$

where l_γ, m_γ, n_γ are the direction cosines of the photon with respect to three orthogonal axes x', y', z, of which z is as before along **n**, but x' makes the angle ϕ_0 with x. The relation between the coefficients in (6.1) and (6.2) is

$$A_2^0 = \frac{2c-a-b}{a+b+c}, \qquad A_2^2 = \frac{a-b}{2(a+b+c)}. \quad (6.3)$$

We may compare the surface W† given by (6.2) with the special limit of it given by the Butler theory. In the latter case the x axis (**k**) is an axis of azimuthal isotropy and back-forward symmetry, so that the W surface resembles a spheroid. The surface (6.2) is of lower symmetry, resembling an ellipsoid, its principal semi-axes being a, b and c, of which c is still along **n**, but a and b are displaced though ϕ_0 from x and y. If we wish to explain the distribution (6.2) by distorted wave stripping theory, we say that the distortion has displaced the stripping axis through ϕ_0, and has introduced azimuthal anisotropy about the new axis. However, the a and b axes are in fact of identical symmetry, and in analysing a given experimental correlation there is no unique means of specifying one of the symmetry axes in the reaction plane as the "displaced stripping axis" in preference to the other. We therefore introduce a convention: the correlation should first be calculated on the Butler theory††, and then, according as this predicts the **k** direction to be the direction of greatest W or least W, we identify, in the observed correlation, the "displaced stripping axis" a to be either the major or minor observed axis in the d-p plane, respectively. This fixes ϕ_0 uniquely, and ensures that $\phi_0 = 0$ in the Butler limit, for which also $b = c$. The freedom in choice of axes corresponds to allowing A_2^2 in (6.1) and (6.3) to be either positive or negative: the sign of A_2^2 is fixed once the axes a and b have been identified. The distribution (6.1) or (6.2) can be determined completely by γ measurements in the d-p plane and in the single direction **n**.

The γ distribution (6.1) together with the polarisation contains four "real experimental parameters" A_2^0, A_2^2, ϕ_0 and P, which we may use in-

† i.e. the surface whose polar coordinates are (W, θ, ϕ).

†† If insufficient data are available to permit the Butler calculation, then the specification of the a axis may in fact be made quite arbitrarily after all.

stead of the ρ_{kq}'s. We proceed to confront these results with the distorted wave stripping theory for $l = 1$ and $j = \frac{3}{2}$, as in section 5. This treatment leads to $(l+1)^2 = 4$ real experimental parameters, and to $2l = 2$ real theoretical parameters. Consequently, while in the general case our observed A_2^0, A_2^2, ϕ_0 and P are all independent, in distorted stripping theory they must be subject to two relations.

The theoretical parameters are contained in $B_{1\pm1}$, and in terms of these A_2^0, A_2^2 and ϕ_0 (using (4.1), (4.3), (2.9) and (2.8)) are

$$A_2^0 = -\frac{\eta_2(jjI_AI_B)\sum_{LL'} F_2(LL'I_B{}^1I_B)C_LC'_L}{2\sum_L C_L{}^2}, \tag{6.4}$$

$$-\frac{2A_2^2}{A_2^0} = \frac{2}{\left|\frac{B_{1,-1}}{B_{1,1}}\right| + \left|\frac{B_{1,1}}{B_{1,-1}}\right|} = \lambda(\text{say}), \tag{6.5}$$

$$2\phi_0 = \arg(-B_{1,-1}/B_{1,1}). \tag{6.6}$$

We shall regard λ and ϕ_0, here defined as functions of the B's, as our two real theoretical parameters. Since (6.4) does not in fact contain the B's, this formula for A_2^0 constitutes one of the desired experimental tests of the theory. A subsidiary test is given by the inequality $0 \leqq \lambda \leqq 1$ in (6.5). This has interesting consequences, given also that in the Butler theory $B_{1,-1} = -B_{11}$, which assigns to λ its upper limit of 1, so that distortion must cause a diminution of λ. To bring this out, we write the distribution in the stripping plane as $[1+\alpha\cos^2(\phi-\phi_0)]$, where

$$\alpha = \frac{a-b}{b} = \frac{-6A_2^0\lambda}{2-A_2^0(1-3\lambda)}, \tag{6.7}$$

and we write the distribution in the plane $\phi = \phi_0$ as $[1+\beta\cos^2\theta]$, where

$$\beta = \frac{c-b}{b} = \frac{3A_2^0(1-\lambda)}{2-A_2^0(1-3\lambda)}. \tag{6.8}$$

Since A_2^0 is independent of distortion, and $0 \leqq \lambda \leqq 1$, it follows from (6.7) that the magnitude of the anisotropy in the d-p plane is always less than (or equal to) that predicted by the Butler theory†; while from (6.8), the anisotropy in the $\phi = \phi_0$ plane is of opposite sign to that in the d-p plane. If λ is progressively reduced due to increasing distortion, the anisotropy (6.7) steadily diminishes and the anisotropy (6.8) steadily grows. This is illustrated in fig. 1.

† The sign of the anisotropy has been fixed by convention above.

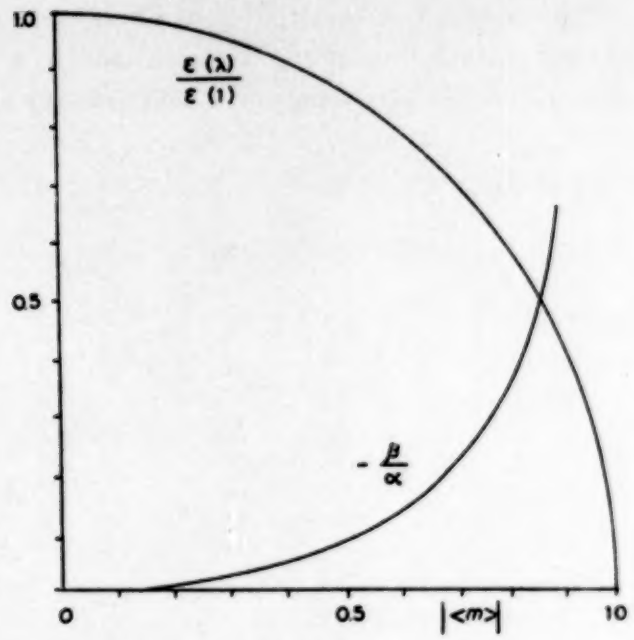

Fig. 1. Relation between the nucleon polarisation produced by distorted waves and the effect on the gamma-ray angular distribution for $l = 1$ captures. The nucleon polarisation is $P = -\frac{1}{2}\langle m\rangle$ for $j = \frac{1}{2}$ captures, or $P = +\frac{1}{6}\langle m\rangle$ for $j = \frac{3}{2}$ captures. The anisotropy in the reaction plane is given by $\varepsilon = [W(0)-W(\frac{1}{2}\pi)]/[W(0)+W(\frac{1}{2}\pi)]$. α and β are defined by eqs. (6.7) and (6.8); λ is given by (6.5) and $|\langle m\rangle| = (1-\lambda^2)^{\frac{1}{2}}$. Then $\varepsilon(\lambda)/\varepsilon(1) = \lambda$.

The last experimental parameter P is found from (3.2) and (6.5) to be a function of λ:

$$P = \frac{2}{3}\frac{(-1)^{j-l-\frac{1}{2}}(|B_{11}|^2-|B_{1,-1}|^2)}{(2j+1)(|B_{11}|^2+|B_{1,-1}|^2)} = \pm\frac{2}{3}\frac{(1-\lambda^2)^{\frac{1}{2}}}{(2j+1)}. \qquad (6.9)$$

This equation, together with (6.5), constitutes the second relation to test the theory, illustrated in fig. 1. If from the observed γ-correlation we calculate λ by (6.5), then (6.9) predicts the magnitude of P, but not the sign.

Putting the experimental parameters in (6.5), (6.6) and (6.9) we can solve uniquely for the ratio $B_{1,-1}/B_{11}$. The polarisation is more sensitive to distortion than is the γ-correlation function. This can be seen by comparing the dependence of λ (6.5) and P(6.9) on B_{1-1}/B_{11} in the region of $B_{1,-1}/B_{11} = -1$. For example, when λ has fallen only to 0.9, P has already risen to 44 % of its maximum (fig. 1).

7. Case $l = 2$

This case does not lend itself to any such special treatment as does $l = 1$. For the γ-angular distribution we have $k_{\max} = 4$ in a favourable case. By harmonic analysis of the measured W (4.1) and use of (4.3), we may determine the $\rho_{kq}(l, l)$'s for even k and q. The harmonic analysis is possible if γ measurements are made in three planes, e.g. the d-p scattering plane, and

the planes $\phi = 0$ and $\phi = \frac{1}{2}\pi$. These ρ_{kq}'s contain $(l+1)^2-1 = 8$ real experimental parameters, which we may regard as the real and imaginary parts of the ρ_{kq}'s for $q \geqq 0 (k \neq 0)$. These ρ_{kq}'s are given in terms of the B's by

$$\begin{aligned}
\rho_{00}(2,2) &= \frac{1}{\sqrt{5}}(|B_{22}|^2+|B_{2,-2}|^2+|B_{20}|^2), \\
&\quad \text{(normalised to unity)} \\
\rho_{20} &= \sqrt{\tfrac{2}{7}}(|B_{22}|^2+|B_{2,-2}|^2-|B_{20}|^2), \\
\rho_{22} &= \sqrt{\tfrac{2}{7}}(B_{22}B_{20}^*+B_{20}B_{2,-2}^*), \qquad (7.1) \\
\rho_{40} &= \frac{1}{\sqrt{70}}(|B_{22}|^2+|B_{2,-2}|^2+6|B_{20}|^2), \\
\rho_{42} &= \sqrt{\tfrac{3}{14}}(B_{22}B_{20}^*+B_{20}B_{2,-2}^*), \\
\rho_{44} &= B_{22}B_{2,-2}^*.
\end{aligned}$$

Since the B's contain $2l = 4$ real parameters, there are four real relations between these ρ's, which may be found from (7.1):

$$\rho_{42} = \tfrac{1}{2}\sqrt{3}\rho_{22}, \qquad (7.2)$$

(this contains two real relations),

$$\rho_{40} = \tfrac{1}{2}\sqrt{\tfrac{7}{2}}\rho_{00}-\tfrac{1}{4}\sqrt{5}\rho_{20}. \qquad (7.3)$$

The fourth relation is too complicated to be of any use, and is therefore omitted.

The polarisation P is

$$P = \frac{4(-1)^{j-l-\frac{1}{2}}(|B_{22}|^2-|B_{2,-2}|^2)}{3(2j+1)(|B_{22}|^2+|B_{2,-2}|^2+|B_{20}|^2}, \qquad (7.4)$$

which can be expressed in terms of the ρ's obtained from the γ-distribution:

$$P = \pm\frac{4}{3\sqrt{5}(2j+1)}\left[\left(\frac{\sqrt{5}}{2}+\frac{\sqrt{7}}{2\sqrt{2}}\frac{\rho_{20}}{\rho_{00}}\right)^2-4\left|\frac{\rho_{44}}{\rho_{00}}\right|^2\right]^{\frac{1}{2}}, \qquad (7.5)$$

and this provides the remaining test of the theory. We can solve (7.1) and (7.4) for the B's.

References

1) S. T. Butler, Proc. Roy. Soc. A **208** (1951) 559
2) A. B. Bhatia, K. Huang, R. Huby and H. C. Newns, Phil. Mag. **43** (1952) 485
3) J. Horowitz and A. M. L. Messiah, J. Physique Rad. **14** (1953) 695
4) H. C. Newns and M. Y. Refai, Proc. Phys. Soc. **71** (1958) 627
5) W. Tobocman, Report no. 29, Nuclear Physics Lab., Case Institute of Technology (1956)
6) W. Tobocman and M. H. Kalos, Phys. Rev. **97** (1955) 132
7) C. Bloch, Nuclear Physics **4** (1957) 503
8) G. E. Brown and C. T. de Dominicis, Proc. Phys. Soc. A **70** (1957) 686
9) C. A. Levinson and M. K. Banerjee, Annals of Physics **3** (1958) 67

10) P. B. Daitch and J. B. French, Phys. Rev. **85** (1952) 695
11) A. P. French, Phys. Rev. **107** (1957) 1655
12) N. T. S. Evans and A. P. French, Phys. Rev. **109** (1958) 1272
13) G. E. Owen and L. Madansky, Phys. Rev. **105** (1957) 1766
14) J. Sawicki and G. R. Satchler, Nuclear Physics **7** (1958) 289
15) J. B. French and B. J. Raz, Phys. Rev. **104** (1956) 1411
16) G. R. Satchler, Annals of Physics **3** (1958) 275
17) S. Devons and L. J. B. Goldfarb, Handbuch der Physik, Ed. S. Flügge **42** (Springer, Berlin, 1957) p. 362
18) G. R. Satchler, Analysis of Deuteron Stripping Reactions (unpublished)
19) J. C. Hensel and W. C. Parkinson, Phys. Rev. **110** (1958) 128
20) R. J. Blin-Stoyle, Proc. Phys. Soc. A **65** (1952) 452
21) L. C. Biedenharn and M. E. Rose, Revs. Mod. Phys. **25** (1953) 729
22) G. R. Satchler, Proc. Phys. Soc. A **66** (1953) 1081
23) J. Horowitz and A. M. L. Messiah, J. Physique Rad. **15** (1954) 142

4.E *Nuclear Physics* 9 (1958/59) 108—115; © *North-Holland Publishing Co., Amsterdam*
Not to be reproduced by photoprint or microfilm without written permission from the publisher

THE DECAY OF ^{73}Ga

C. YTHIER

Université de Strasbourg

R. K. GIRGIS †, R. A. RICCI †† and R. VAN LIESHOUT

Instituut voor kernphysisch Onderzoek, Amsterdam

Received 3 September 1958

Abstract: The isotope ^{73}Ga was produced by fast neutron and deuteron bombardments of natural and enriched germanium; the decay was studied with scintillation and absorption techniques. The half-life is 4.85 ± 0.10 hours; there are two beta branches of 1.19 (94 %) and 0.4 (≈ 6 %) MeV. Three gamma rays of 0.295, 0.745 and 1.04 MeV have been found, the first one of which is in coincidence with the higher energy beta group. A decay scheme is proposed (see fig. 1).

1. Introduction

Siegel and Glendenin [1,2]) first reported the nucleide ^{73}Ga as a fission product. It was found to decay with a half-life of 5.0±0.5 hours; the maximum beta energy was determined by absorption to be 1.35 MeV, the absence of gamma radiation was noted. It has also been produced by these same authors from natural germanium, with pile neutrons. Irradiation of natural germanium with 100 MeV X radiation from a betatron [3]) also yielded a 5 hour gallium activity, emitting a beta spectrum with 1.4 MeV maximum energy. The same 5 hour activity was found in the gallium fraction from arsenic irradiated with 50 MeV X rays [4]) and in 190 MeV deuteron fission of bismuth [5]). The decay of ^{73}Ga seems to have been investigated by Johansson and Orring [6]), who only mention the fact that the conversion lines due to its 0.53 sec ^{73}Ge daughter are observed with both 5 hour Ga and with 76 day ^{73}As with the same relative intensity. This last fact constitutes the best basis for the assignment of the 5 hour activity to mass number 73, especially since the work of Campbell [7]) has definitely established the assignment of the 0.53 sec ^{73}Ge isomer.

In our work [8]) on ^{74}Ga we found a strong gamma ray at ≈300 keV which persisted after the decay of the 8 min ^{74}Ga activity and which could not be assigned to the 14 hour ^{72}Ga decay. Since its half-life turned out to be ≈5 hours, we undertook a further study of the ^{73}Ga activity.

† On leave of absence from the Faculty of Science, University of Cairo, Giza, Egypt, U.A.R
†† On leave of absence from the Politecnico di Torino, Torino, Italia.

2. Production and Chemical Procedures; Measurements

The activity was produced a number of times by fast neutron bombardment of natural germanium of high purity in the form of germanium dioxide. The 24-MeV internal deuteron beam of the synchrocyclotron bombarded a Be probe behind which the germanium target was placed. In a few runs of this type the activity was obtained as a byproduct in our study of the 8 min ^{74}Ga activity; in those cases the irradiation lasted from 8 to 10 minutes. Additional irradiations with fast neutrons on natural germanium of up to one hour duration were performed to obtain stronger sources. In one case a target of germanium enriched in mass 76 was used. (Composition of this source: Mass 70 : 3.71 %; 72 : 5.00 %; 73 : 1.69 %; 74 : 8.95 %; 76 : 80.65 %; impurities : < 0.5 %.) When bombarded with 26-MeV deuterons (3 μAh) this target produced a strong source of ^{73}Ga by (d, αn) in addition to the 8 min activity from the (d, α) reaction.

When ^{74}Ga was the main activity desired, the following chemical procedure † was used. The germanium dioxide was dissolved and the germanium extracted with carbon tetrachloride, after which the gallium fraction was extracted with isopropyl ether and finally precipitated with cupferron; duration of this procedure approximately 15 minutes.

When the ^{73}Ga was the main product desired, the irradiated target was left to decay for a few hours. Since the 3 hour ^{71}Zn, if present, could falsify our results, special care was taken to verify that the decontamination from zinc was complete.

From the chemical procedures employed we feel quite sure that both the 5 hour activity and the 8.0 ± 0.1 min activity, as produced by deuteron and neutron bombardment of natural and enriched germanium, are gallium isotopes. From the formation of the 8 min activity by the reactions : 87 % ^{76}Ge (d, α)Ga chem and 87 % ^{74}Ge(n, p)Ga chem and from energy considerations we can conclude that this 8 min activity should be assigned †† to mass 74. The formation of the 5 hour activity by the reactions 87 % ^{76}Ge (d, αn)Ga chem and 87 % ^{74}Ge (n, pn)Ga chem can be considered as additional proof that this is mass 73.

The gamma ray spectrum was measured with a 2.5 cm $\times$ 2.5 cm NaI(Tl) crystal, the beta spectrum with a 4 cm $\times$ 1 cm stilbene crystal. This stilbene crystal was covered with a 200 μg/cm^2 aluminium reflector, while the window consisted of an $\approx$2.5 mg/cm^2 aluminium foil. Beta-gamma coincidences were measured by the same method. The various spectra were displayed on a 100 channel RIDL kicksorter. The experimental set-up and the method of

† All chemical separations were carried out by C. Ythier; they are only briefly mentioned here and will be described in detail in a forthcoming thesis by this author (Université de Strasbourg, 1958).

†† The results of the study of the 8 min activity will be published elsewhere [8]).

calibration and analysis were the same as those used in the study [8–11]) of ^{74}Ga, ^{76}Br and ^{78}As. The beta spectrum was also measured by absorption techniques; an end window Geiger-Müller counter with a 2.5 mg/cm^2 mica window was used.

3. Results

The results of the various measurements are collected in table 1. The

TABLE 1

^{73}Ga was produced by ^{76}Ge(24−MeV d, αn) chem and by Ge(fast n) chem
$T_{\frac{1}{2}} = 4.85 \pm 0.10$ hours

	Energy (MeV)	Rel. intens.	Method
β^-	0.40 ±0.15	4½ ±2	abs
	1.19 ±0.04	95 ±7	scin; abs
γ(^{73}Ge)	0.054±0.001	9 ±1	scin
	0.295±0.003	97	,,
	0.745±0.010	6 ±1	,,
	1.040±0.015	≈1	,,
$\gamma\beta$	(0.295 γ)(1.19 β^-)		scin
0.295 γ/1.19 β^- = 1.02±0.07 (^{198}Au comparison)			scin
0.013 γ not observed as photon			
No 0.068 γ(< 0.5); no 0.815 γ(< 2)			
No 1.5 β^-(< 5)			

half-life of ^{73}Ga was determined to be 4.85±0.10 hours. The best value was obtained by following the decay of the beta radiation of the gallium fraction produced by deuteron bombardment of enriched ^{76}Ge, since disturbing activities were relatively weak in this case. This value is in good agreement with that deduced from the decay of the various gamma rays. Owing to the interference of 14 hour ^{72}Ga, only a less accurate (though certainly compatible) value was derived from the decay of the gallium fractions produced by fast neutron bombardment of natural germanium and of enriched ^{74}Ge (87 %).

The decay scheme proposed from the measurements is shown in fig. 1. The outstanding feature is the occurrence of a strong beta branch with a maximum energy of 1.19±0.04 MeV, followed by a 295±3 keV gamma ray. It was shown by beta-gamma coincidence measurements with the scintillation crystals that these two radiations were in coincidence and that the maximum energy of the coincident beta group was the same as that of the highest energy beta branch (see fig. 2). Additional evidence for this was

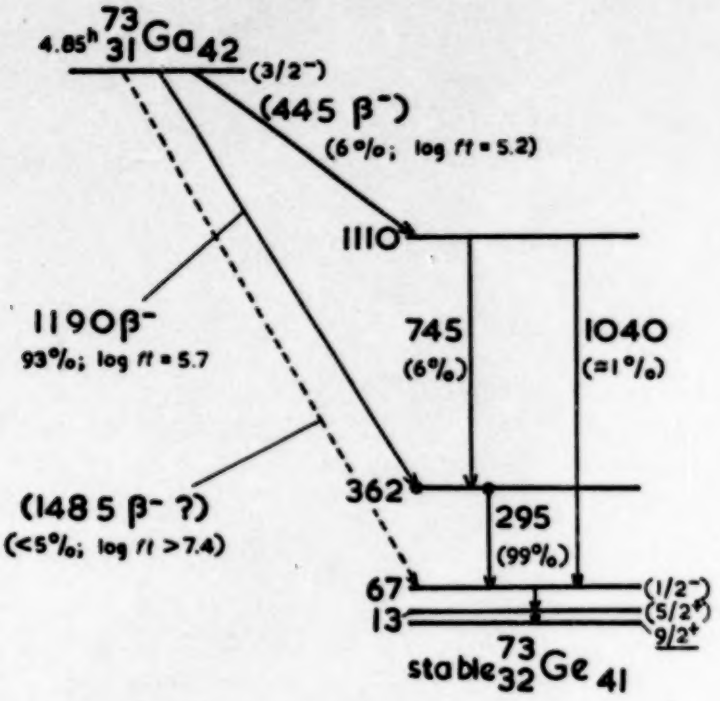

Fig. 1. Proposed decay scheme for ^{73}Ga.

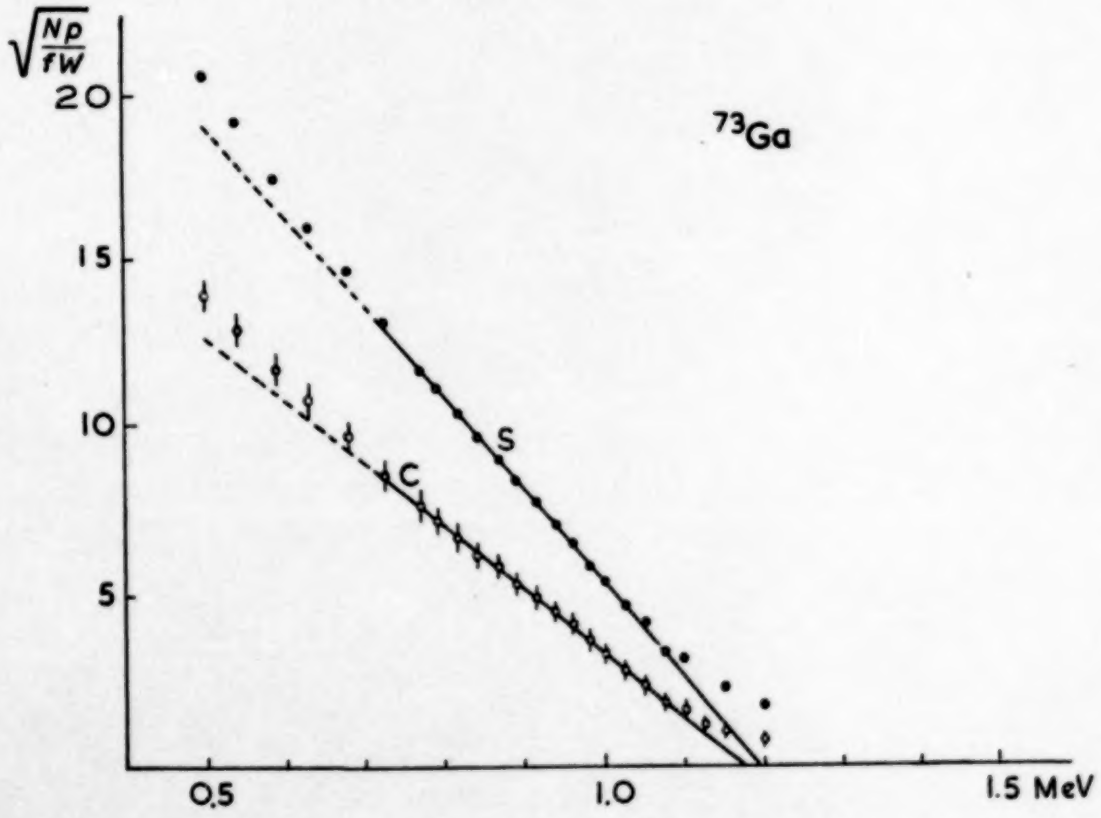

Fig. 2. Kurie diagrams of the ^{73}Ga beta spectrum measured directly (curve labelled S) and in coincidence with the 295 keV gamma ray (curve labelled C). The contribution due to 14 hour ^{72}Ga was subtracted.

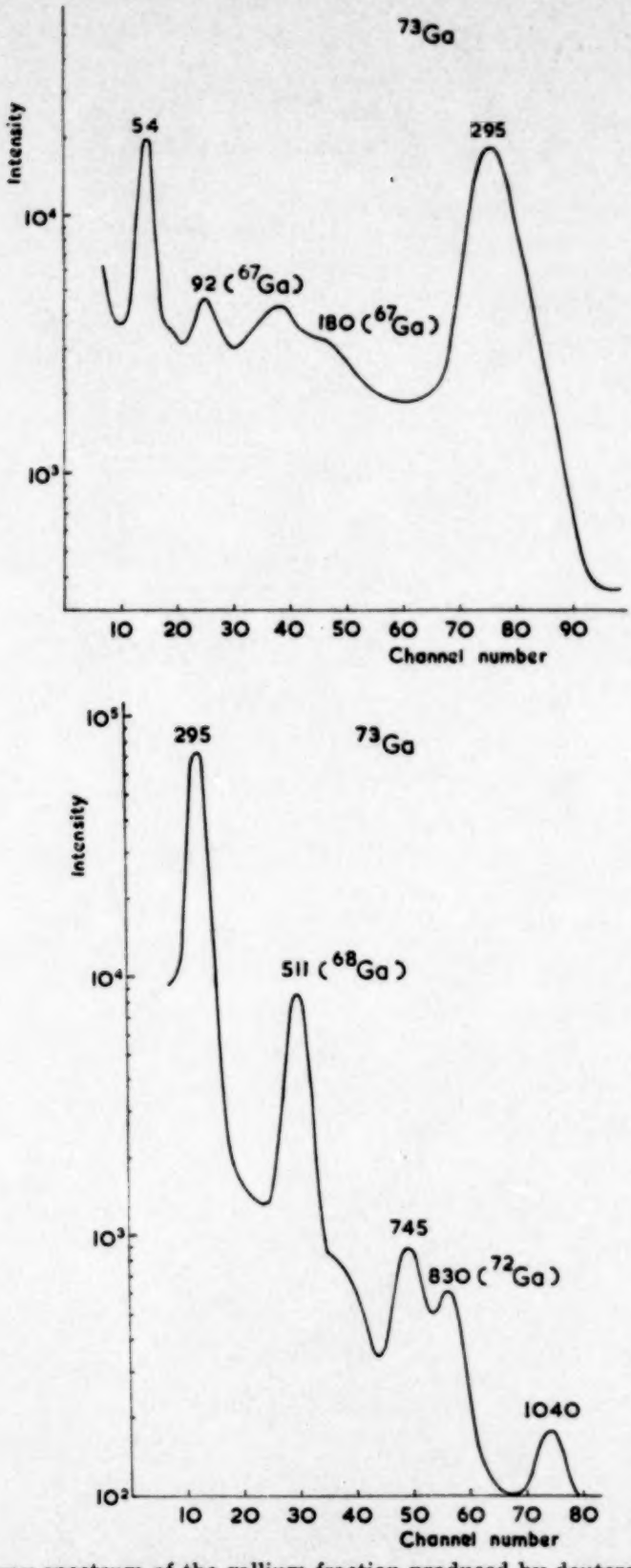

Fig. 3. Gamma ray spectrum of the gallium fraction produced by deuteron bombardment of enrichted (81 %) ^{76}Ge: a) low energy region; b) high energy region.

found from the intensity of the 295 keV gamma ray relative to that of the 1.19 MeV beta group. This determination was based upon comparison with a ^{198}Au source: the two sources were measured under identical conditions with the stilbene and the sodium iodide crystal.

If the 54 keV gamma ray, emitted by the ^{73}Ge isomer, is mainly magnetic quadrupole radiation (for a discussion of this assignment, see ref.[1])), its theoretical total conversion coefficient is 8.1 (E2 would give 7.5; all other multipolarities yield conversion coefficients which are at least a factor 15 larger or smaller). Therefore, the relative total transition probabilities of the 295 keV transition and of the 54 keV transition are 97 : (81$\pm$9) if the first one is M1 and 97 : (73$\pm$9) if it is E2. This means that the 295 keV transition populates the isomeric level at 67.4 keV in ^{73}Ge. A careful check was made to ascertain that the relative intensities of these two gamma rays were the same in the various gallium fractions produced by the different methods outlined above.

The total decay energy of ^{73}Ga is therefore determined to be 1.55$\pm$0.04 MeV. The two remaining gamma rays listed in table 1 could arise from a single excited state at 1.11$\pm$0.01 MeV as indicated by the energy match. This interpretation receives additional support from the absorption measurements of the beta spectrum. In addition to the main branch at 1.18$\pm$0.10 MeV, a second beta branch is clearly present. Its energy and relative intensity, although not very accurately known, fit very well. In the scintillation spectrum the scattering effects at energies below 0.5 MeV obscured any weak lower energy branch.

The two gamma rays at 745$\pm$10 keV and 1040$\pm$15 keV could only be assigned unambiguously to ^{73}Ga from the study of the gallium fraction produced from enriched ^{76}Ge (see fig. 4). The relative intensity and half-life of the higher energy ray showed conclusively that it was only for a small fraction due to the 14 hour ^{72}Ga and the 68 min ^{68}Ga contaminations present in this source. In the gallium fractions produced by other means, the 745 keV gamma ray was always present but only as a small bump in the valley of the much stronger 830 keV peak due to ^{72}Ga; the 1040 keV line from ^{73}Ga was completely obscured by the ^{72}Ga spectrum (see fig. 4).

No beta branch with an energy of 1.4 to 1.6 MeV could be found, neither in the absorption measurements, nor in the coincident or direct scintillation measurements.

We did not detect the gamma rays of 68 and 815 keV, known [12,13]) from Coulomb excitation experiments with enriched ^{73}Ge. This is hardly surprising since they should originate from transitions between even parity levels, which can only be populated from ^{73}Ga by first forbidden beta transitions. The 13 keV gamma ray (see decay scheme) is not evident in the gamma ray spectrum, because it is very highly converted.

If ^{73}Ga has a ground state spin of $\frac{3}{2}$ like ^{67}Ga, ^{69}Ga and ^{71}Ga, the spins of which have been measured, the absence of a beta transition to the isomeric level in ^{73}Ge is somewhat surprising. This absence could be understood if the

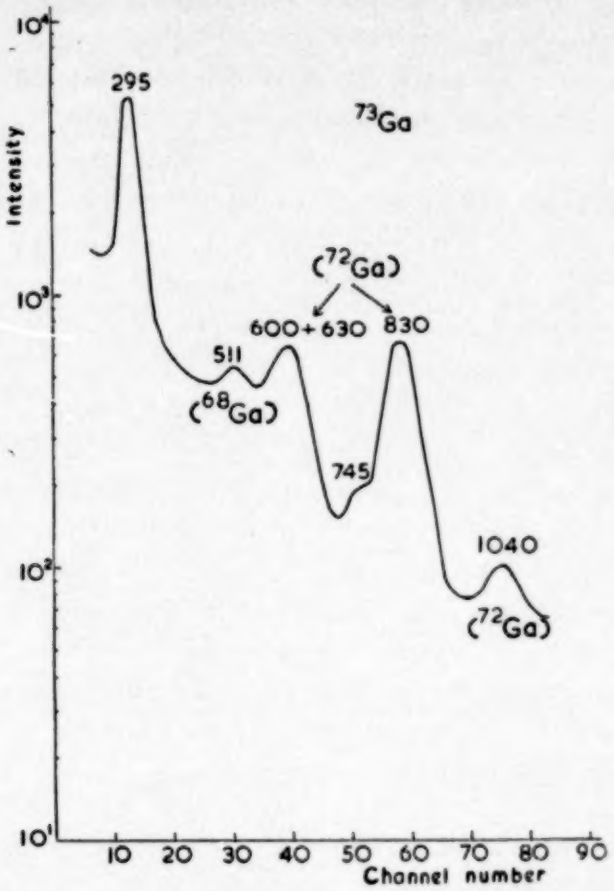

Fig. 4. High energy gamma ray spectrum of the gallium fraction produced by fast neutron bombardment of natural germanium.

spin of ^{73}Ga were $f_{\frac{3}{2}}$; ^{65}Zn is the only other case where a ground state spin of $f_{\frac{3}{2}}$ has to be assumed for N or $Z < 37$. The electron capture transition from the groundstate of ^{73}As to the ^{73}Ge isomeric level is rather fast ($\log ft = 4.4$), thereby showing that the ^{73}As spin is very probably $\frac{3}{2}^-$. There is not enough decay energy available [1]) to populate the level in ^{73}Ge at 362 keV.

The authors wish to thank Prof. Dr. P. C. Gugelot and Prof. Dr. A. H. W. Aten Jr. for their interest in this work and the personnel of the synchro-cyclotron for the various irradiations. We also thank Miss E. A. van der Eijk for her help. One of the authors (R.K.G.) is indebted to the Egyptian Atomic Energy Commission for a grant. A second author (C.Y.) wishes to thank the Centre National de la Recherche Scientifique, Paris and the Nederlandse Organisatie voor Zuiver Wetenschappelijk Onderzoek (Z.W.O.) for a grant.

We are indebted to the Société „La Vieille Montagne", Angleur, Belgium for having put at our disposal samples of germanium and germanium dioxide of high purity. The sources of enriched germanium were supplied from the Atomic Energy Research Establishment, Harwell, England.

This work was performed as part of the research program of the Stichting voor Fundamenteel Onderzoek der Materie (F.O.M.), which is financially supported by the Nederlandse Organisatie voor Zuiver Wetenschappelijk Onderzoek (Z.W.O.).

References

1) K. Way, R. W. King, C. L. McGinnis and R. van Lieshout, Nuclear Level Schemes, $A = 40$ to $A = 92$, U.S. Atomic Energy Commission Report TID-5300 (U.S. Government Printing Office, Washington D.C., 1955)
2) J. M. Siegel and L. E. Glendenin, NNES—PPR **9** (1950) 549; Journal Am. Chem. Soc. **68** (1946) 2411
3) M. L. Perlman, Phys. Rev. **75** (1949) 988
4) R. B. Holtzman and N. Sugarman, Phys. Rev. **87** (1952) 633
5) R. H. Goeckermann and I. Perlman, Phys. Rev. **76** (1949) 628
6) S. Johansson and J. Orring, mentioned in S. Johansson, Arkiv för Fysik **4** (1952) 723; ref.[12])
7) E. C. Campbell and F. Nelson, Phys. Rev. **107** (1957) 502;
E. C. Campbell, R. W. Peelle and F. C. Maienschein, ORNL—1798 (1954)
8) W. Schoo, B. L. Schram, H. L. Polak, R. K. Girgis, R. A. Ricci, R. van Lieshout and C. Ythier, Physica **24** (1958) to be published
9) R. A. Ricci, Physica **23** (1957) 693
10) B. L. Schram, H. L. Polak, W. Schoo, R. K. Girgis, R. A. Ricci, R. van Lieshout and C. Ythier, Physica **24** (1958) to be published
11) R. K. Girgis, R. A. Ricci and R. van Lieshout, to be published
12) G. M. Temmer and N. P. Heydenburg, Phys. Rev. **104** (1956) 967; **96** (1954) 426
13) D. G. Alkhazov, D. S. Andreyev, A. P. Greenberg and I. H. Lemberg, Nuclear Physics **2** (1956) 65; Physica **22** (1956) 1129A

1.C *Nuclear Physics* 9 (1958/59) 116—123: © *North-Holland Publishing Co., Amsterdam*

Not to be reproduced by photoprint or microfilm without written permission from the publisher

ON THE REARRANGEMENT ENERGY OF NUCLEAR MATTER

P. MITTELSTAEDT
CERN, *Geneva*

Received 2 August 1958

Abstract: The extent to which the rearrangement energy of nuclear matter can be explained by the Brueckner two-body cluster approximation is investigated. Using the formalism of Gomes, Walecka and Weisskopf, it is shown that the exclusion principle and the requirement of self-consistency lead to a rearrangement energy. The contributions to the rearrangement energy due to higher cluster corrections are discussed by comparing the results so obtained with the phenomenological data. These higher order corrections are found to be relatively unimportant, in disagreement with the critique of the Brueckner theory recently put forward by Hugenholtz and van Hove.

1. Introduction

In the description of the properties of nuclear matter by an independent particle model it becomes apparent that this model must be extended by the inclusion of an important correction term, the so-called rearrangement energy [1,2,3]). If one removes a nucleon from the nucleus in the independent particle model the separation energy is given by the interaction of this chosen particle with the nucleons of the residual nucleus. Furthermore, the separation of a particle results in a change of the effective interaction between the nucleons of the residual nucleus. This means that in a sudden (non-adiabatic) separation of a nucleon, the residual nucleus is left in an excited state. This excitation energy Δ, the so-called rearrangement energy, must therefore be taken into account in the calculation of the separation energy.

That such a rearrangement energy cannot be neglected can be shown by a phenomenological theory of nuclear matter. If one uses the effective mass approximation for the single particle potential $U(k) = U_0+U_1k^2/k_F^2$ (k_F is the Fermi momentum), and remembers that the separation energy S of a nucleon in the equilibrium state equals the mean binding energy, one obtains the following two equations [1,3]):

$$-S = \tfrac{3}{5}T+\tfrac{1}{2}U_0+\tfrac{3}{10}U, \tag{1}$$

$$-S = T+U_0+U_1+\Delta, \tag{2}$$

where T is the Fermi energy and Δ the rearrangement energy mentioned

above. If, for S and T, one uses the empirical values, and also takes into consideration the experimental values of the optical potential for nuclear reactions, one obtains for Δ the result $\Delta = 18.6$ MeV.

As was first pointed out by Brueckner [2]), a rearrangement energy can be obtained within the framework of his theory if one assumes that the effective interaction depends on the density †. Basing our arguments on the formulation of the Brueckner theory given by Gomes, Walecka and Weisskopf [6]) ††, we will show that such a density dependence really exists and is due to the exclusion principle and the self-consistency of this perturbation treatment.

G.W.W. have shown that in addition to the potential energy due to the attractive forces, an important correction to the kinetic energy of a Fermi gas arises from the repulsive hard core forces. This latter correction comes from the greater curvature of the wave function near the hard core [8, 9, 10]). In sect. 3 it will be shown that this hard core correction is very closely connected to the rearrangement energy mentioned above.

The extent to which the rearrangement energy as calculated in the G.W.W. formalism agrees with the experimental value of Δ is discussed in sect. 4, using the numerical results of G.W.W. and of Brueckner and Gammel. It will be shown that the contributions to the rearrangement energy coming from higher cluster corrections (and not included in the Brueckner theory) are not very important, which is in good agreement with recent results of de Shalit and Weisskopf [7]).

2. The G.W.W. Formalism

For the calculation of the binding energy of a nucleon in the G.W.W. formalism we write the energy of a system of A particles in the following form:

$$E = E_0 + \tfrac{1}{2} \sum_{\alpha,\beta} U_{\alpha\beta} \tag{3}$$

where E_0 is the energy of a free Fermi gas and $U_{\alpha\beta}$ means the energy shift which comes from the interaction of a pair of particles in the states α and β. If we describe these states by the momenta $\mathbf{k}$ and $\mathbf{k}'$ of the particles in question, write $U(\mathbf{k}, \mathbf{k}')$ instead of $U_{\alpha\beta}$, and replace the sum by an integral, we obtain for the energy correction

$$U = \tfrac{1}{2} \frac{4\Omega}{(2\pi)^3} \int \mathrm{d}\mathbf{k} \int \mathrm{d}\mathbf{k}' U(\mathbf{k}, \mathbf{k}') \tag{4}$$

where Ω is the volume of nuclear matter. With

† For this question see also Skyrme [4]) and Squires [5]). The author is indebted to Dr. Skyrme for valuable information on his unpublished results.

†† To be quoted as G.W.W.

$$U(k, k') = \frac{1}{(4\pi)^2}\int d\omega \int d\omega' U(\mathbf{k}, \mathbf{k}') \tag{5}$$

where $d\omega$ is the element of angle belonging to $d\mathbf{k}$, it follows that

$$U = \tfrac{1}{2}\left(\frac{2}{\pi^2}\right)^2 \Omega^2 \int_0^{k_F}\int_0^{k_F} dk\, dk'\, k^2 k'^2 U(k, k'). \tag{6}$$

Furthermore, we define the single particle potential

$$U(k) = \left(\frac{2}{\pi^2}\right) \Omega \int_0^{k_F} dk'\, k'^2 U(k, k'). \tag{7}$$

To estimate $U(\mathbf{k}, \mathbf{k}')$ we start from the following ansatz for the forces between the nucleons:

$$v(r) = v^A(r) + v^c(r)$$

where

$$v^A(r) = \begin{cases} 0 & 0 \leqq r \leqq c \\ -\frac{1}{2}V_0(1+P) & c \leqq r \leqq b \\ 0 & b \leqq r < \infty \end{cases} \tag{8a}$$

is the attractive force (P is the space exchange operator) and

$$v^c(r) = \begin{cases} +\infty & r \leqq c \\ 0 & r > c \end{cases} \tag{8b}$$

is the repulsive hard core force. According to G.W.W. this leads to

$$U(\mathbf{k}, \mathbf{k}') = \left\langle \psi_{\mathbf{k}\mathbf{k}'} \middle| -\frac{\hbar^2}{2m^*}(\nabla_1^2 + \nabla_2^2 + k^2 + k'^2) + v \middle| \psi_{\mathbf{k}\mathbf{k}'} \right\rangle \tag{9}$$

where the two body wave function $\psi_{\mathbf{k}\mathbf{k}'}(\mathbf{r}_1, \mathbf{r}_2)$ is a solution of the Bethe-Goldstone equation

$$\left[-\frac{\hbar^2}{2m^*}(\nabla_1^2 + \nabla_2^2) + 2U_0 - \varepsilon_{\mathbf{k}\mathbf{k}'}\right] \psi_{\mathbf{k}\mathbf{k}'} = -Q^F_{\mathbf{k}\mathbf{k}'}(v\psi_{\mathbf{k}\mathbf{k}'}); \tag{10}$$

$\varepsilon_{\mathbf{k}\mathbf{k}'}$ is the eigenvalue and $Q^F_{\mathbf{k}\mathbf{k}'}$ is the projection operator which excludes all the Fourier components of the Fermi gas except $\mathbf{k}$ and $\mathbf{k}'$; m^* is the self-consistent value of the effective mass, and the single particle potential $U(k)$ is given by

$$U(k) = U_0 + U_1 k^2/k_F^2$$

in the effective mass approximation, where $m^*/m = T/(T+U_1)$. For the following investigations we will write $U(\mathbf{k}, \mathbf{k}')$ as a sum with

$$U(\mathbf{k}, \mathbf{k}') = U^A(\mathbf{k}, \mathbf{k}') + U^c(\mathbf{k}, \mathbf{k}') \tag{11}$$

with

$$U^{A}(\mathbf{k},\mathbf{k}') = \langle \psi_{\mathbf{k}\mathbf{k}'} | v^{A} | \psi_{\mathbf{k}\mathbf{k}'} \rangle,$$
$$U^{c}(\mathbf{k},\mathbf{k}') = \left\langle \psi_{\mathbf{k}\mathbf{k}'} \left| -\frac{\hbar^2}{2m^*}(\nabla_1^2+\nabla_2^2+k^2+k'^2) \right| \psi_{\mathbf{k}\mathbf{k}'} \right\rangle, \tag{12}$$

taking account of (8), (9), (10).
From this one obtains the corresponding separation

$$U(k) = U^{A}(k)+U^{c}(k), \tag{13}$$

$$U = U^{A}+U^{c}. \tag{14}$$

Since $\psi_{\mathbf{k}\mathbf{k}'}$ does not depend very much on v^{A}, as was shown by G.W.W., U^{c} is essentially the correction to the kinetic energy of a Fermi gas of particles with mass m^* due to a hard core repulsion.

3. The Rearrangement Energy

To estimate the rearrangement energy in the formalism of G.W.W. we start from the separation energy S of a nucleon. Because of (2)

$$-S = \frac{\mathrm{d}\varepsilon}{\mathrm{d}\rho} = T+U(k_F)+\Delta \tag{15}$$

where ρ is the particle density and $\varepsilon = E/\Omega$ the corresponding energy density. If, according to (3), we divide the energy into $E = E_0+U$, recall (15) and $\mathrm{d}(E_0/\Omega)/\mathrm{d}\rho = T$ we find that

$$\frac{\mathrm{d}(U/\Omega)}{\mathrm{d}\rho} = U(k_F)+\Delta. \tag{16}$$

Putting

$$\eta(k,k') = U(k,k')\Omega, \tag{17}$$

it follows from (5) that

$$\frac{U}{\Omega} = \tfrac{1}{2}\left(\frac{2}{\pi^2}\right)^2 \int_0^{k_F}\int_0^{k_F} \mathrm{d}k\,\mathrm{d}k'\,k^2k'^2\eta(k,k'). \tag{18}$$

Furthermore

$$\mathrm{d}\,\frac{(U/\Omega)}{\mathrm{d}\rho} = \frac{\pi^2}{2k_F^2}\frac{\mathrm{d}}{\mathrm{d}k_F}\left(\frac{U}{\Omega}\right),$$

and therefore from (18)

$$\mathrm{d}\,\frac{(U/\Omega)}{\mathrm{d}\rho} = \left(\frac{2}{\pi^2}\right)\int_0^{k_F}\mathrm{d}k\,k^2\eta(k,k_F)+\frac{1}{\pi^2k_F^2}\int_0^{k_F}\int_0^{k_F}\frac{\mathrm{d}}{\mathrm{d}k_F}\eta(k,k')k^2k'^2\mathrm{d}k\mathrm{d}k'.$$

Comparison with (7) shows that the first term is

$$\frac{2}{\pi^2}\int_0^{k_F}\mathrm{d}k\,k^2\eta(k,k_F) = U(k_F), \tag{19}$$

which, together with (16), implies that the rearrangement energy is

$$\Delta = \frac{1}{\pi^2 k_F^2}\int_0^{k_F}\int_0^{k_F} \mathrm{d}k\,\mathrm{d}k'\,k^2 k'^2 \frac{\mathrm{d}}{\mathrm{d}k_F}\eta(k, k'). \tag{20}$$

For the following investigations it is more useful to express the rearrangement energy directly in terms of the matrix elements (9). On account of (17) it follows that

$$\Delta = \frac{1}{2A}\left[\frac{4\Omega}{(2\pi)^3}\right]^2 \int \mathrm{d}\mathbf{k}' \int \mathrm{d}\mathbf{k}'' \left\{\rho \frac{\mathrm{d}}{\mathrm{d}\rho} U(\mathbf{k}', \mathbf{k}'') - U(\mathbf{k}', \mathbf{k}'')\right\}. \tag{21}$$

If, moreover, we use the separation (11) there results a separation of Δ into

$$\Delta = \Delta^{\mathrm{A}} + \Delta^{\mathrm{c}}: \tag{22}$$

Δ^{A} is that part of the rearrangement energy which is induced by the attractive forces, and Δ^{c} is the part which comes from the hard core forces †.

For the calculation of

$$\Delta^{\mathrm{A}} = \frac{1}{2A}\left[\frac{4\Omega}{(2\pi)^3}\right]^2 \int \mathrm{d}\mathbf{k}' \int \mathrm{d}\mathbf{k}'' \left\{\rho \frac{\mathrm{d}}{\mathrm{d}\rho} U^{\mathrm{A}}(\mathbf{k}', \mathbf{k}'') - U^{\mathrm{A}}(\mathbf{k}', \mathbf{k}'')\right\}, \tag{23}$$

it is sufficient to evaluate the matrix elements $U^{\mathrm{A}}(\mathbf{k}', \mathbf{k}'')$ in the Born approximation. As was shown by G.W.W., the Bethe-Goldstone wave function $\psi_{\mathbf{k}\mathbf{k}'}(\mathbf{r}_1, \mathbf{r}_2)$ is almost equal to the free particle wave function, so that for the evaluation of (12a) the use of the Born approximation is justified. The wave function of a free particle normalized in the volume Ω is

$$\phi_{\mathbf{k}}(\mathbf{r}) = \Omega^{-\frac{1}{2}} \mathrm{e}^{i\mathbf{k}\cdot\mathbf{r}}. \tag{24}$$

From this we obtain the free two particle wave function for unequal particles

$$\varphi^{\mathrm{u}}_{\mathbf{k}'\mathbf{k}''}(\mathbf{r}_1, \mathbf{r}_2) = \phi_{\mathbf{k}'}(\mathbf{r}_1)\phi_{\mathbf{k}''}(\mathbf{r}_2) \tag{25}$$

and for equal particles

$$\varphi^{\mathrm{e}}_{\mathbf{k}'\mathbf{k}''}(\mathbf{r}_1, \mathbf{r}_2) = \frac{1}{\sqrt{2}}\left(\phi_{\mathbf{k}'}(\mathbf{r}_1)\phi_{\mathbf{k}''}(\mathbf{r}_1) - \phi_{\mathbf{k}'}(\mathbf{r}_2)\phi_{\mathbf{k}''}(\mathbf{r}_1)\right).$$

If one calculates the matrix element

$$U^{\mathrm{A}}(\mathbf{k}', \mathbf{k}'') = \langle \psi_{\mathbf{k}'\mathbf{k}''} | v^{\mathrm{A}} | \psi_{\mathbf{k}',\mathbf{k}''} \rangle \tag{26}$$

in the Born approximation using the ansatz (8) for the forces, it follows that

$$U^{\mathrm{A}}_{\mathrm{u,e}}(\mathbf{k}', \mathbf{k}'') = \langle \varphi^{\mathrm{u,e}}_{\mathbf{k}',\mathbf{k}''} | V(r)(1+P) | \varphi^{\mathrm{u,e}}_{\mathbf{k}'\mathbf{k}''} \rangle \tag{27}$$

where

$$V(r) = \begin{cases} -\frac{1}{2}V_0 & c \leqq r \leqq b \\ 0 & r < c, \qquad r > b. \end{cases}$$

For equal particles, the matrix element vanishes on account of the Serber operator $(1+P)$. For unequal particles one obtains

† Strictly speaking, Δ^{c} depends also on the attractive forces through the effective mass m^*.

$$U_u^A(\mathbf{k}', \mathbf{k}'') = -\frac{4\pi V_0}{\Omega}\int_c^b r^2 dr \left(1+\frac{\sin 2kr}{2kr}\right) \tag{28}$$

where k is the relative momentum and r is the relative distance. Since $\Omega = A/\rho$ and b and c are independent of ρ, $U_u^A(\mathbf{k}', \mathbf{k}'')$ depends linearly on ρ. Therefore, the integrand of (23) vanishes, and

$$\Delta^A = 0. \tag{29}$$

From the assumption that the Born approximation can be applied to the calculation of (26) it follows that the rearrangement energy

$$\Delta = \Delta^c = -\frac{U^c}{A} + \frac{\rho}{A}\,\tfrac{1}{2}\left[\frac{4\Omega}{(2\pi)^3}\right]^2 \int d\mathbf{k}' \int d\mathbf{k}''\, \frac{d}{d\rho} U^c(\mathbf{k}', \mathbf{k}'') \tag{30}$$

depends only on the matrix elements $U^c(\mathbf{k}', \mathbf{k}'')$, but not on $U^A(\mathbf{k}', \mathbf{k}'')$. From this result, however, it cannot be concluded that Δ^c is independent of the attractive forces, because $U^c(\mathbf{k}', \mathbf{k}'')$ depends on the effective mass. On account of the self-consistency, however, the value of m^* is mainly dependent on the attractive forces † so that $U^c(\mathbf{k}', \mathbf{k}'')$, and therefore also Δ^c, are dependent on v^A.

4. Discussion

The investigations of the last section have a physical meaning only if Δ^c is essentially different from zero, and approximately equal to the phenomenological value $\Delta = 18.6$ MeV. Above all, it is by no means clear whether Δ^c, as defined by (30), gives the main contribution to the rearrangement energy, or whether higher cluster corrections, which are not taken into account in this formalism, have to be made responsible for the value of 18.6 MeV. The opinion that the rearrangement energy is only due to the higher cluster corrections was recently asserted in a paper by Hugenholtz and van Hove [11]). However, we will show that in the Brueckner two-body cluster approximation a rearrangement energy of the right order of magnitude is obtained by taking account of the exclusion principle and the self-consistency of this perturbation treatment. The disagreement with the opinion just quoted comes from the fact that in the investigation of Hugenholtz and van Hove the self-consistency was not taken into account. Instead, these authors used a cluster expansion in which a rearrangement energy — apart from the contributions due to the exclusion principle †† — can only be obtained by taking into account the higher order correction terms.

† Private communication from Prof. Weisskopf.

†† In the paper of Hugenholtz and van Hove quoted above the expression $E_F = T + V(k_F)$ was given for the so-called "Fermi energy" E_F in the two-body cluster approximation. However, this relation is not quite correct, for even in the two-body cluster approximation a further correction term due to the exclusion principle must be added. (See also the following discussion.)

First of all, it is important to note that for $U^c(\mathbf{k}', \mathbf{k}'')$ and Δ^c an argument analogous to that which led to $\Delta^A = 0$ cannot be carried out. The vanishing of Δ^A is based on the fact that U depends linearly on ρ, which is due to the applicability of the Born approximation to the calculation of $U^A(\mathbf{k}', \mathbf{k}'')$. However, for the calculation of

$$U^c(\mathbf{k}', \mathbf{k}'') = \left\langle \psi_{\mathbf{k}'\mathbf{k}''} \middle| -\frac{\hbar^2}{2m^*}(\nabla_1^2+\nabla_2^2+k'^2+k''^2) \middle| \psi_{\mathbf{k}'\mathbf{k}''} \right\rangle$$

the Born approximation cannot be applied, since $U^c(\mathbf{k}', \mathbf{k}'')$ would vanish identically in that approximation. Hence, for this calculation the Bethe-Goldstone wave function must be used. Apart from the density dependence of the wave function, which comes from the normalization volume Ω, and which was already taken into account in the calculation of $U^A(\mathbf{k}', \mathbf{k}'')$ (eq. (17)), the solution $\psi_{\mathbf{k}'\mathbf{k}''}(\mathbf{r}_1, \mathbf{r}_2)$ of the Bethe-Goldstone equation has additional density dependences due to

1) the projection operator $Q^F_{\mathbf{k}'\mathbf{k}''}$ in (10), which depends on k_F and therefore on ρ: the contribution to the rearrangement energy which comes from this projection operator, i.e. from the exclusion principle, is the correction term which was mentioned in the footnote †† on p. 121;

2) the density dependence of the effective mass in (10), as required by the self-consistency.

From the calculation of the matrix elements $U^c(\mathbf{k}', \mathbf{k}'')$ there result additional density dependences:

3) The integration over the relative coordinate leads to a density dependence. For the sake of simplicity we shall discuss this point in the special case $\mathbf{k}'+\mathbf{k}'' = 0$, in which case the integration over the centre of mass coordinate can be carried out immediately. We then see that, whereas in (28) the limits of the integration c and b are independent of ρ, the domain of integration in the calculation of $U^c(\mathbf{k}', \mathbf{k}'')$ extends over the whole volume Ω (apart from the small region $0 \leqq r \leqq c$) † (cf. footnote †† on p. 121).

4) The operator

$$-\frac{\hbar^2}{2m^*}(\nabla_1^2+\nabla_2^2+k'^2+k''^2)$$

depends on the self-consistent value m^* and therefore on the density ρ.

After these qualitative considerations, from which we concluded that $U^c(\mathbf{k}', \mathbf{k}'')$ must depend strongly on ρ, and therefore Δ^c is essentially different from zero, we will discuss the question of how well Δ^c agrees quantitatively with the phenomenological value.

A quantitative statement for $\Delta = \Delta^c$ can be made most easily if we use the

† This integration can be restricted to the region below the point $r = \lambda_F$, above which $\psi_{\mathbf{k}'\mathbf{k}''}$ is practically equal to the free two body wave function. However, this healing distance λ_F again depends on ρ.

numerical results for the binding energy and the effective mass given by G.W.W. Using the constants $c = 0.4 \times 10^{-13}$ cm, $b = 2.3 \times 10^{-13}$ cm $V_0 = 28.4$ MeV for the ansatz (8a) and (8b), the energy E can be calculated as a function of ρ. This function has a minimum at $k_F = 1.35 \times 10^{13}$ cm^{-1}. The minimum values of the binding energy and of the effective mass are $E/A = -6.9$ MeV and $m^*/m = 0.68$. Since at equilibrium eqs. (1) and (2) are valid, the rearrangement energy can be obtained from the given values of E/A, m^* and k_F by means of (1) and (2). The result is that $\Delta = 7.2$ MeV. The deviation of this value from the phenomenological one comes from the fact that the calculated values k_F and E/A are very different from the experimental ones. The reason for this deviation is the oversimplified ansatz (8), as can be seen from the calculations of Brueckner and Gammel [12]). Instead of (8) these authors used the much more realistic forces of Gammel and Thaler. From the values of E/A, m^* and k_F at equilibrium calculated by them, and again using (1) and (2) one obtains the value $\Delta = 17.7$ MeV, which is in a very good agreement with the phenomenological one.

These quantitative results show that the main part of the rearrangement energy can be deduced from the self-consistent Brueckner theory and is not affected by higher cluster correction terms. These results are in good agreement with the investigations of de Shalit and Weisskopf, which show that these higher order corrections can change the results of the Brueckner theory by about 10 %.

The author is greatly indebted to Profs. C. Bloch, N. M. Hugenholtz, V. F. Weisskopf and Dr. E. J. Squires for many stimulating discussions.

References

1) V. F. Weisskopf, Nuclear Physics **3** (1957) 423
2) K. A. Brueckner, Phys. Rev. **110** (1958) 597
3) P. Mittelstaedt, Preprint (1958)
4) T. H. R. Skyrme, Proc. Rehovoth Conf. 1957 (North-Holland Publishing Co., Amsterdam, 1958) p. 20
5) E. J. Squires, Paris Conf. on Nucl. Phys. (1958)
6) L. J. Gomes, J. D. Walecka and V. F. Weisskopf, Annals of Phys. **3** (1958) 241
7) A. de Shalit and V. F. Weisskopf, Preprint (1958)
8) H. A. Bethe and J. Goldstone Proc. Roy. Soc. A **238** (1957) 551
9) K. Huang and C. N. Yang, Phys. Rev. **105** (1957) 767
10) C. N. Yang and T. D. Lee, Phys. Rev. **105** (1957) 1119
11) N. M. Hugenholtz and L. van Hove, Physica **24** (1958) 363
12) K. A. Brueckner and J. L. Gammel, Phys. Rev. **109** (1958) 1023

7.A *Nuclear Physics* **9** (1958/59) 124—139; © *North-Holland Publishing Co., Amsterdam*

Not to be reproduced by photoprint or microfilm without written permission from the publisher

ON THE ONE-DIMENSIONAL SPINOR MODEL OF THIRRING

T. PRADHAN

Institute for Theoretical Physics, University of Copenhagen †

Received 30 June 1958

Abstract: Thirring's method of solution, in so far as it pertains to the construction of the S-matrix, is discussed and an expression for the S-operator in terms of certain constants of motion of the model is obtained. It is also shown that some modifications in the method employed by Glaser to obtain an explicit and complete solution of the model are necessary in view of the fact that the number-density operators in the model are not c-numbers. Certain other features of the model, such as the vanishing of the rest-mass of physical particles and the possible existence of "ghost" difficulty, are also discussed.

1. Introduction

Recently, W. Thirring [1]) proposed a soluble model of a self-coupled relativistic spinor field in one space and one time dimension for the study of the structure of interacting fields. He was able to show that the theory is renormalizable, and worked out certain renormalized matrix elements of Heisenberg field operators. Subsequently, V. Glaser [2]), by solving the coupled field equations, was able to obtain the most general matrix element for field operators and an explicit expression for the S-operator. In obtaining these solutions, Glaser treats the number-density operators as c-numbers. But a closer examination of the commutators of these operators shows that, even if they vanish for most points of space-time, there are nevertheless certain regions where they behave in a very singular way and where one cannot, without further investigation, put them equal to zero.

In the present paper, we wish firstly to discuss certain features of Thirring's solution and show how to construct the S-matrix from these solutions. Secondly, we wish to show that the results of Glaser, with certain exceptions, are valid even when the number-density operators are treated as operators. The non-commutativity of these operators affects the results in the calculations of vacuum expectation values such as the field renormalization constant and Green's functions, etc. We shall also discuss other features like the vanishing of the exact rest-mass of particles and the possibility of having "ghost" trouble in the model.

† On leave of absence from (and present address) Ravenshaw College, University of Utkal, Cuttack, India.

2. General Features of the Model

The model has the Lagrangian

$$\mathscr{L} = \frac{1}{2i}\int_{-\infty}^{+\infty} \mathrm{d}x\{\bar{\psi}\gamma_\mu(\partial_\mu\psi) - (\partial_\mu\bar{\psi})\gamma_\mu\psi\} + 2g\int_{-\infty}^{+\infty} \mathrm{d}x\bar{\psi}\psi\bar{\psi}\psi, \tag{1}$$

from which the following field equation is obtained:

$$-i\gamma_\mu\partial_\mu\psi + 2g(\bar{\psi}\psi)\psi = 0. \tag{2}$$

The γ-matrices have the two-dimensional representation

$$\gamma_1 = i\sigma_1, \quad \gamma_2 = \beta = \sigma_2, \quad \text{and} \quad \gamma_5 = \gamma_1\gamma_2 = \sigma_3, \tag{3}$$

with the anti-commutation properties

$$\{\gamma_\mu, \gamma_\nu\} = -2\delta_{\mu\nu}, \quad \delta_{11} = -\delta_{22} = 1, \quad \delta_{12} = \delta_{21} = 0.$$

The Heisenberg field operators, ψ_τ, obey the equal-time anticommutation relations

$$\begin{aligned} &\{\psi_\tau(x, t), \psi_{\tau'}^*(x', t)\} = \delta_{\tau\tau'}\delta(x-x'), \\ &\{\psi_\tau(x, t), \psi_{\tau'}(x', t)\} = \{\psi_\tau^*(x, t), \psi_{\tau'}^*(x', t)\} = 0. \end{aligned} \tag{4}$$

The model has the following constants of mation:

$$P_\mu = -i\int_{-\infty}^{+\infty} \mathrm{d}x\bar{\psi}\{\gamma_2\partial_\mu + \tfrac{1}{2}\delta_{\mu 2}\gamma_\nu\partial_\nu\}\psi, \tag{5}$$

and

$$Q_\tau = \int_{-\infty}^{+\infty} \mathrm{d}x\psi_\tau^*\psi_\tau. \tag{6}$$

On introducing the variables $u = x + t$ and $v = x-t$, and making use of the fact that $\psi_\tau(x, t)\psi_\tau(x, t) = 0$, the field equation (2) can be written as

$$\frac{\partial\psi_1}{\partial u} - ig\psi_2^*\psi_2\psi_1 = 0, \tag{7a}$$

$$\frac{\partial\psi_2}{\partial v} + ig\psi_1^*\psi_1^*\psi_2 = 0. \tag{7b}$$

In the limit $g = 0$, $\psi_\tau \to \varphi_\tau$, eqs. (7a) and (7b) take the simple form

$$\frac{\partial\varphi_1}{\partial u} = 0, \quad \frac{\partial\varphi_2}{\partial v} = 0, \tag{8}$$

and hence $\varphi_1 \equiv \varphi_1(v)$, $\varphi_2 \equiv \varphi_2(u)$. These free-field operators φ_τ, have the following anti-commutation relations for all space-time points:

$$\{\varphi_1(v), \varphi_1^*(v')\} = \delta(v-v'), \quad \{\varphi_2(u), \varphi_2^*(u')\} = \delta(u-u'), \tag{9}$$

all the other anticommutators being identically zero. And they have the momentum representation

$$\varphi_1(v) = \frac{1}{\sqrt{2\pi}} \int_{-\infty}^{+\infty} \mathrm{d}p C_1(p) \mathrm{e}^{ipv}, \tag{10a}$$

$$\varphi_2(u) = \frac{1}{\sqrt{2\pi}} \int_{-\infty}^{+\infty} \mathrm{d}p C_2(p) \mathrm{e}^{ipu}. \tag{10b}$$

The corresponding anti-commutation relation for the C_τ's are

$$\begin{aligned} \{C_\tau(p), C_{\tau'}^*(p')\} &= \delta_{\tau\tau'}\delta(p-p'), \\ \{C_\tau(p), C_{\tau'}(p')\} &= \{C_\tau^*(p), C_{\tau'}(p')\} = 0. \end{aligned} \tag{11}$$

These C_τ's are related to the creation and annihilation operators by the relation

$$C_\tau(p) = U_\tau(p)a(p) + V_\tau(p)b^*(-p), \tag{12}$$

with

$$U(p) = \begin{pmatrix} \theta(p) \\ \theta(-p) \end{pmatrix} \quad \text{and} \quad V(p) = \begin{pmatrix} \theta(-p) \\ \theta(p) \end{pmatrix}.$$

3. Thirring's Solution

Thirring [1]) solves the model by explicitly constructing the exact eigenstates of P_μ. He constructs these states by letting ψ_1^* and ψ_2^* operate on a reference state $|0)$, which is also an eigenstate of P_μ with zero eigenvalue, i.e., $P_\mu|0) = 0$, and which has the property: $\psi_\tau(x, t)|0) = 0$. This state, in other words, has no particles, but is full of anti-particles. An arbitrary eigenstate $\Psi_\mathfrak{a}$ can be written as

$$\begin{aligned} \Psi_\mathfrak{a} &= \prod_{\alpha\beta}^{NN'} \iint \mathrm{d}x_\alpha \mathrm{d}y_\beta \Phi_\mathfrak{a}(x_1, \ldots x_N; y_1, \ldots y_{N'}) \mathrm{e}^{+iq_\alpha^{(\mathfrak{a})}x_\alpha + ip_\beta^{(\mathfrak{a})}y_\beta} \psi_1^*(x_\alpha)\psi_2^*(y_\beta)|0) \\ &= \prod_{\alpha\beta}^{NN'} \iint \mathrm{d}x_\alpha \mathrm{d}y_\beta \chi_{q_1^{(\mathfrak{a})}, \ldots q_N^{(\mathfrak{a})}; p_1^{(\mathfrak{a})} \ldots p_{N'}^{(\mathfrak{a})}}(x_1, \ldots x_N; y_1, \ldots y_{N'}) \psi_1^*(x_\alpha)\psi_2^*(y_\beta)|0). \end{aligned} \tag{13}$$

The time variable t is same for all ψ_τ^*'s and has been put equal to zero. In order to get the connection of $\Psi_\mathfrak{a}$ with the physical states, it is convenient to go to the limit of vanishing interaction ($g \to 0$), i.e., we have to visualize them in terms of free fields. In this limit, $\Phi_\mathfrak{a} \to 1$, $\psi_\tau^* \to \varphi_\tau^*$ and so

$$\Psi_\mathfrak{a} \to \prod_{\alpha\beta}^{NN'} (\sqrt{2\pi})^{-N-N'} C_1^*(q_\alpha^{(\mathfrak{a})}) C_2^*(p_\beta^{(\mathfrak{a})})|0). \tag{14}$$

Here, we have made use of the Fourier representation (10) of the φ_τ's. Since, according to eq. (12),

$$C_1^*(q) = \begin{cases} a^*(q) & \text{for} \quad q > 0, \\ b(-q) & \text{for} \quad q < 0, \end{cases}$$

and

$$C_2^*(p) = \begin{cases} b(-p) & \text{for} \quad p > 0, \\ a^*(p) & \text{for} \quad p < 0, \end{cases}$$

it is clear that, in the limit $N \to \infty, N' \to \infty$ and for all q_α's < 0, all p_β's > 0, Ψ_a will be the vacuum state. Other states are constructed from (13) by suitably choosing the p's and q's as explained elaborately by Thirring. The states are, so-to-speak, constructed by first putting bare particles together and then letting them interact. The interaction between the bare particles is completely represented by χ_a. In other words, the states Ψ_a are complicated superpositions of bare particle states, The Schrödinger equation for Ψ_a is

$$H\Psi_a = E_a\Psi_a. \tag{15}$$

From eqs. (2) and (5) we have

$$H = P_1 = i\int_{-\infty}^{+\infty} dx \left\{\psi_1^*(x)\frac{\partial\psi_1(x)}{\partial x} - \psi_2^*(x)\frac{\partial\psi_2(x)}{\partial x}\right\} - 2g\int_{-\infty}^{+\infty} dx\psi_1^*\psi_2^*\psi_1\psi_2. \tag{16}$$

Operating H on Ψ_a given by (13) and commuting, with the aid of equal-time anti-commutation rules (4), the ψ_1 and ψ_2 contained in H all the way to the right until they annihilate the reference state $|0)$, one gets from eq. (14) the following differential equation for χ_a:

$$\left[i\sum_{\alpha=1}^{N}\frac{\partial}{\partial x_\alpha} - i\sum_{\beta=1}^{N'}\frac{\partial}{\partial y_\beta} + 2g\sum_{\alpha\beta}^{NN'}\delta(x_\alpha - y_\beta) + E_a\right]\chi_a = 0. \tag{17}$$

By correctly imposing boundary conditions, we shall obtain the "incoming wave", "out-going wave", and "standing wave" solutions of this differential equation. For this end, we write

$$\chi_a(x_1, \ldots x_N; y_1, \ldots y_{N'}) = \prod_{\alpha\beta}^{NN'} F_{\alpha\beta}^{(a)}(x_\alpha, y_\beta), \tag{18a}$$

and

$$E_a = \sum_{\alpha=1}^{N} q_\alpha^{(a)} - \sum_{\beta=1}^{N'} p_\beta^{(a)} = \sum_{\alpha\beta}^{NN'} E_{\alpha\beta}^{(a)}. \tag{18b}$$

It then follows from eq. (17) that

$$\left[-i\frac{\partial}{\partial x_\alpha} + i\frac{\partial}{\partial y_\beta} - 2g\delta(x_\alpha - y_\beta) - E_{\alpha\beta}^{(a)}\right]F_{\alpha\beta}^{(a)}(x_\alpha, y_\beta) = 0. \tag{19}$$

In integral form, the above equation can be written as follows:

$$F_{\alpha\beta}^{(a)s}(x_\alpha, y_\beta) = f_{\alpha\beta}^{(a)}(x_\alpha, y_\beta) + \mathscr{P}\frac{2g}{E_{\alpha\beta}^{(a)} + i\dfrac{\partial}{\partial x_\alpha} - i\dfrac{\partial}{\partial y_\beta}}\delta(x_\alpha - y_\beta)F_{\alpha\beta}^{(a)s}(x_\alpha, y_\beta), \tag{20a}$$

$$F_{\alpha\beta}^{(a)\pm}(x_\alpha, y_\beta) = f_{\alpha\beta}^{(a)}(x_\alpha, y_\beta) + \frac{2g}{E_{\alpha\beta}^{(a)} + i\dfrac{\partial}{\partial x_\alpha} - i\dfrac{\partial}{\partial y_\beta} \pm i\varepsilon}\delta(x_\alpha - y_\beta)F_{\alpha\beta}^{(a)\pm}(x_\alpha, y_\beta). \tag{20b}$$

In eq. (20a) $\mathscr{P}$ stands for principal value, indicating that the principal

value is to be taken at the singularity of the second term. The $F^{(a)s}_{\alpha\beta}(x_\alpha, y_\beta)$ are the "standing wave" solutions †, whereas the $F^{(a)\pm}_{\alpha\beta}(x_\alpha, y_\beta)$ are scattering solutions. The small imaginary term in the denominator of eq. (20b) specifies uniquely as to how the singularity is to be treated. These two equations (20a) and (20b) are written in the Lippmann-Schwinger [4]) fashion. $F^{a(+)}_{\alpha\beta}(x_\alpha, y_\beta)$ is the "incoming wave" solution and $F^{a(-)}_{\alpha\beta}(x_\alpha, y_\beta)$ is the "outgoing wave" solution. $f^{(a)}_{\alpha\beta}(x_\alpha, y_\beta)$ obeys the equation

$$\left(-i\frac{\partial}{\partial x_\alpha}+i\frac{\partial}{\partial y_\beta}-E^{(a)}_{\alpha\beta}\right) f^{(a)}_{\alpha\beta}(x_\alpha, y_\beta)=0, \tag{21a}$$

whose normalized solution is immediately seen to be

$$f^{(a)}_{\alpha\beta}(x_\alpha, y_\beta)=\frac{1}{2\pi}\,\mathrm{e}^{+iq^{(a)}_\alpha x_\alpha+ip^{(a)}_\beta y_\beta}. \tag{21b}$$

Dropping, for the moment, the boundary conditions as well as the α's and β's in eqs. (20), we can write quite generally

$$F^{(a)}(x, y)=f^{(a)}(x, y)+\frac{2g}{E^{(a)}+i\dfrac{\partial}{\partial x}-i\dfrac{\partial}{\partial y}}\,\delta(x-y)F^{(a)}(x, y), \tag{22}$$

and, since the $f^{pq}(x, y)=(\frac{1}{2}\pi)\exp(iqx+ipy)$ form a complete set of solutions of eq. (21a), we can re-write eq. (22) in the form

$$\begin{aligned}F^{(a)}(x, y)&=f^{p^{(a)}, q^{(a)}}(x, y)\\&+2g\int_{-\infty}^{+\infty}\int_{-\infty}^{+\infty}\mathrm{d}x_0\mathrm{d}y_0\int_{-\infty}^{+\infty}\int_{-\infty}^{+\infty}\mathrm{d}p\mathrm{d}q\,\frac{|f^{p,q}(x, y)\rangle\langle f^{p,q}(x_0, y_0)|}{q^{(a)}-p^{(a)}+i\dfrac{\partial}{\partial x}-i\dfrac{\partial}{\partial y}}\,\delta(x_0-y_0)F^{(a)}(x_0, y_0)\\&=f^{p^{(a)}, q^{(a)}}(x, y)+2g\int_{-\infty}^{+\infty}\mathrm{d}x_0\int_{-\infty}^{+\infty}\mathrm{d}y_0\,F^{(a)}(x_0, y_0)G_0(x, y|x_0, y_0)\,\delta(x_0-y_0),\end{aligned} \tag{23}$$

where

$$\begin{aligned}G_0(x, y|x_0, y_0)&=\int_{-\infty}^{+\infty}\mathrm{d}p\int_{-\infty}^{+\infty}\mathrm{d}q\,\frac{|f^{p,q}(x, y)\rangle\langle f^{p,q}(x_0, y_0)|}{q^{(a)}-p^{(a)}+i\dfrac{\partial}{\partial x}-i\dfrac{\partial}{\partial y}}\\&=\frac{1}{(2\pi)^2}\int_{-\infty}^{+\infty}\mathrm{d}p\int_{-\infty}^{+\infty}\mathrm{d}q\,\frac{\mathrm{e}^{+iq(x-x_0)+ip(y-y_0)}}{(q^{(a)}-p^{(a)})-(q-p)},\end{aligned} \tag{24}$$

is the Green's function for the differential eq. (19). On performing the integrations in eq. (24) with the proper handling of the singularity we obtain

$$G_0{}^s(x, y|x_0, y_0)=\frac{1}{2i}\,\varepsilon(x-x_0)\,\delta(x-x_0+y-y_0)\mathrm{e}^{+i(y-y_0)(q^{(a)}-p^{(a)})}, \tag{25a}$$

† "Standing wave" solutions have been, in recent times, used by M. L. Goldberger in problems of scattering theory [3]).

$$G_0^{(\pm)}(x, y|x_0, y_0) = \pm i\theta(\pm x \mp x_0)\,\delta(x-x_0+y-y_0)\,e^{+i(y-y_0)(q^{(a)}-p^{(a)})}. \quad (25b)$$

Substitution of G_0 in eq. (23) and subsequent solution by iteration, give two different sets of results for $F(x, y)$:

$$F^{a(\pm)}(x, y) = \frac{1+\frac{1}{2}ig\varepsilon(x-y)}{1\mp\frac{1}{2}ig} f^{p^{(a)},q^{(a)}}(x, y), \quad F^{a(s)}(x, y) = \frac{1+\frac{1}{2}ig\varepsilon(x-y)}{1+\frac{1}{4}g^2} f^{p^{(a)},q^{(a)}}(x, y); \quad (26a)$$

and

$$F^{a(\pm)}(x, y) = e^{\pm ig\theta(\pm x\mp y)} f^{p^{(a)},q^{(a)}}(x, y), \quad F^{a(s)}(x, y) = \tfrac{1}{2}(F^{(+)}+F^{(-)}); \quad (26b)$$

depending on whether the δ-function in the integrals occurring in the iterated solution are used as they stand or as the limit of smooth functions. The former treatment gives (26a) and the latter gives (26b). This ambiguity is responsible for the discrepancy between the results of Thirring and Glaser [2, 5]) for the matrix elements of ψ_τ. Since δ-functions give meaningful and unambiguous results when treated as limits of smooth functions, we shall adopt the result (26b) as the correct one. It is worth while pointing out at this point that Thirring, in his work [1]), uses the "standing wave" solutions of the form occurring in (26a). We are, however, interested in the scattering solutions (26b). Combining the results of eqs. (13), (18) and (26) we obtain, for the scattering eigenstates, the following expression:

$$\Psi_a^{(\pm)}(q_1^{(a)}, \ldots q_N^{(a)}; p_1^{(a)}, \ldots p_{N'}^{(a)}) = \prod_{\alpha\beta}^{NN'} \iint dx_\alpha\, dy_\beta\, B_{\alpha\beta}^{(\pm)}(x_\alpha, y_\beta) e^{+iq_\alpha^{(a)}x_\alpha + ip_\beta^{(a)}y_\beta} \psi_1^*(x_\alpha)\psi_2^*(y_\beta)|0), \quad (27)$$

with

$$B_{\alpha\beta}^{(\pm)} = e^{\pm ig\theta(\pm x_\alpha \mp y_\beta)}.$$

We can now construct the S-matrix quite readily by making use of the relation

$$\langle b|S|a\rangle = \langle \Psi_b^{(-)}|\Psi_a^{(+)}\rangle, \quad (28)$$

where

$$|a\rangle = \lim_{g\to 0} \Psi_a^{(+)}, \quad \text{and} \quad |b\rangle = \lim_{g\to 0} \Psi_b^{(+)}.$$

Substitution of $\Psi^{(\pm)}$ from eq. (27) in the above relation (28) gives

$$\langle b|S|a\rangle = \prod_{\alpha\beta}^{NN'} \prod_{\eta\sigma}^{NN'} \iint dx_\alpha\, dy_\beta \iint dx'_\eta\, dy'_\sigma (0|\psi_2(y'_\sigma)\psi_1(x'_\eta)\psi_1^*(x_\alpha)\psi_2^*(y_\beta)|0) \times B_{\alpha\beta}^{(+)}(x_\alpha, y_\beta) B_{\eta\sigma}^{(-)}(x'_\eta, y'_\sigma) e^{+iq_\alpha^{(a)}x_\alpha + ip_\beta^{(a)}y_\beta - iq_\eta^{(b)}x'_\eta - ip_\sigma^{(b)}y'_\sigma},$$

which, after some algebraic manipulations, reduces to the simple result

$$\langle b|S|a\rangle = (\det A_1)(\det A_2), \quad (29)$$

with

$$A_1^{\alpha\beta} = \delta(q_\alpha^{(a)} - q_\beta^{(b)})e^{ig} \quad \text{and} \quad A_2^{\alpha\beta} = \delta(p_\alpha^{(a)} - p_\beta^{(b)})e^{ig}.$$

One can work out in the same way and show that

$$\langle b|Q_1 Q_2|a\rangle = (\det D_1)(\det D_2), \tag{30}$$

with

$$D_1^{\alpha\beta} = \delta(q_\alpha^{(a)} - q_\beta^{(b)}) \quad \text{and} \quad D_2^{\alpha\beta} = \delta(p_\alpha^{(a)} - p_\beta^{(b)}).$$

It is quite clear from eqs. (29) and (30) that

$$S = e^{igQ_1Q_2}. \tag{31}$$

This is identical to the result of Glaser [2]). It is easily seen from this expression that there is just a change of phase after two colliding particles penetrate or get reflected from each other, and this change of phase is independent of the momenta of the particles. There is no production of particles as a result of collision, since the S-matrix is diagonal in the physical particle representation — a fact which is obvious from eq. (31).

One would expect, from very simple considerations of energy and momentum, that, when two mass-less particles collide, and are constrained to move in a straight line, the result of such a collision is either penetration or reflection, the penetration or reflection coefficient being unity (due to the identity of the particles, reflection and penetration are indistinguishable). The only additional information we get from our detailed considerations leading to eq. (31) is that a change of phase takes place on penetration. This phase change obviously is a result of self-interaction. It can produce observable effects, i.e., give penetration coefficients less than unity, only through interference phenomena. In fact, Thirring [5]) has shown how one can get interference effects by constructing beams of particles whose charge is not well-defined. In such a case it is possible to get exchange reactions with finite probability.

4. Glaser's Solution

As mentioned in the introduction, Glaser [2]) solves the model by directly integrating the coupled field eqs. (7a) and (7b) in terms of "incoming" field operators [6]). He treats these equations as c-number system of differential equations, and gets the solution

$$\psi_1(u, v) = \varphi_1(v)e^{ig\int_{-\infty}^{u} du'\varphi_2^*(u')\varphi_2(u')} = \varphi_1(v)e^{ig\int_{-\infty}^{u} du'\rho_2(u')}, \tag{32a}$$

$$\psi_2(u, v) = \varphi_2(u)e^{ig\int_{v}^{+\infty} dv'\varphi_1^*(v')\varphi_1(v')} = \varphi_2(u)e^{ig\int_{v}^{+\infty} dv'\rho_1(v')}, \tag{32b}$$

where the φ_τ's are the "incoming" field operators which satisfy the free-field eqs. (8), fulfill the anticommutation relations (9), and have Fourier representation (10). The Fourier components obey the relations (11) and (12).

The justification for the above c-number solutions is provided by the assertion that all the ρ_τ's commute with themselves for all space-time points, i.e.,

$$[\rho_1(v), \rho_1(v')] = [\rho_2(u), \rho_2(u')] = 0, \tag{33}$$

and hence can be treated as c-numbers in the process of solving the entire problem. But the fact that eq. (33) is not correct, is seen by explicitly evaluating the commutators appearing there. One obtains, for example,

$$[\rho_2(u), \rho_2(u')] = \delta(u-u')(\varphi_2^*(u)\varphi_2(u')-\varphi_2^*(u')\varphi_2(u)) \equiv \begin{cases} \infty \times 0 \to u = u', \\ 0 \to u \neq u', \end{cases}$$

in the limit of L, the periodicity length, going to infinity. This commutator is thus indeterminate at $u = u'$. Calculation of matrix elements of the above commutator between physical states shows that they are highly singular and oscillate, near $u = u'$, with infinite amplitudes. For instance, the vacuum expectation value of this commutator works out to be

$$\langle 0|[\rho_2(u), \rho_2(u')]|0\rangle = -\frac{i}{\pi}\delta(u-u')\frac{\mathscr{P}}{u-u'} = \frac{i}{2\pi}\delta'(u-u') \neq 0. \tag{34}$$

In view of this, one is not entitled to treat the ρ_τ's as c-numbers, and it is clear that Glaser's work, where ample use of the c-number character of the ρ_τ's has been made, requires re-examination and scrutiny.

If we take the c-number solutions (32a) and use them to make a perturbation-theoretic calculation of the Green's function $G_{12}^{(+)} = \langle 0|\psi_1(u_1, v_1)\psi_1^*(u_2, v_2)|0\rangle$, we get

$$\begin{aligned} G_{12}^{(+)}(u_1, v_1|u_2, v_2) &= \langle 0|\psi_1(u_1, v_1)\psi_1^*(u_2, v_2)|0\rangle \\ &= \langle 0|\varphi_1(v_1)\varphi_1^*(v_2)|0\rangle\langle 0|e^{ig\int_{u_2}^{u_1} du\,\rho_2(u)}|0\rangle \\ &= S_{12}^{(+)}(v_1|v_2)\left[1-\frac{1}{2!}g^2\left\langle 0\left|\left(\int_{u_2}^{u_1} du\rho_2(u)\right)^2\right|0\right\rangle + \ldots\right]. \end{aligned} \tag{35}$$

Here we have taken $\langle 0|\rho_2(u)|0\rangle = \langle 0| : \rho_2(u) : |0\rangle = 0$. Straightforward calculation shows that the second term in the above perturbation expansion, and in fact each term, is independent of (u_1-u_2), except that for $u_1 = u_2$ all but the first term vanishes. This implies that

$$G_{12}^{(+)}(u_1, v_1|u_2, v_2) = B(g)S_{12}^{(+)}(v_1|v_2), \tag{36}$$

where $B(g)$ is a multiplicative constant which is a function of g alone and which is unity for the special case $u_1 = u_2$. This is in complete disagreement with the covariant perturbation theory calculation of $G_{12}^{(+)}$ (up to order g^2) by Thirring [1]). This example shows how one can run into trouble by using the c-number solutions (32a) and (32b).

In the following, we shall demonstrate how most of the work of Glaser can be retained in solving the theory with the ρ_τ's treated as operators and

not c-numbers. For this, we return to the coupled field equations (7). These equations tell us that

$$\frac{\partial}{\partial u}\left(\psi_2^*(u, v)\psi_2(u, v)\right) = 0, \quad \text{and} \quad \frac{\partial}{\partial v}\left(\psi_1^*(u, v)\psi_1(u, v)\right) = 0,$$

which implies $\psi_1^*(u, v)\psi_1(u, v) = \varphi_1^*(v)\varphi_1(v)$ and $\psi_2^*(u, v)\psi_2(u, v) = \varphi_2^*(u)\varphi_2(u)$. This enables us to write the coupled field equations in the form

$$\frac{\partial\psi_1}{\partial u} - ig(\varphi_2^*\varphi_2)\psi_1 = 0, \tag{37a}$$

$$\frac{\partial\psi_2}{\partial v} + ig(\varphi_1^*\varphi_1)\psi_2 = 0. \tag{37b}$$

These differential equations can be written in the integral form

$$\psi_1(u, v) = \varphi_1(v) + ig\int_{-\infty}^{u} du'\,\varphi_2^*(u')\varphi_2(u')\psi_1(u', v), \tag{38a}$$

$$\psi_2(u, v) = \varphi_2(u) + ig\int_{v}^{+\infty} dv'\,\varphi_1^*(v')\varphi_1(v')\psi_2(u, v'), \tag{38b}$$

which can be immediately recognized to correspond to the standard covariant form

$$\psi_\alpha(\hat{x}) = \varphi_\alpha(\hat{x}) + \int d^2x'\, S_R^{\alpha\beta}(\hat{x}-\hat{x}')j_\beta(\hat{x}'), \quad \hat{x} = (x, t),$$

with S_R taking the simple form $S_R(\hat{x}) = i\beta(t)\delta(x+\alpha t)$ for the model. Since $\rho_1(v) = \varphi_1^*(v)\varphi_1(v)$, and $\rho_2(u) = \varphi_2^*(u)\varphi_2(u)$ are not c-numbers, solutions of these equations cannot, in general, be written in the form of eqs. (32a) and (32b). The solutions can, however, be written in the following iterated form:

$$\begin{aligned}\psi_1(u, v) &= \varphi_1(v)\left(1 + \sum_{n=1}^{\infty}(ig)^n\int_{-\infty}^{u}du_1\int_{-\infty}^{u_1}du_2\ldots\int_{-\infty}^{u_{n-1}}du_n\rho_2(u_1)\ldots\rho_2(u_n)\right)\\ &= \varphi_1(v)\left(e^{ig\int_{-\infty}^{u}du'\rho_2(u')}\right)_+ = \varphi_1(v)U_1(u, -\infty),\end{aligned} \tag{39a}$$

$$\begin{aligned}\psi_2(u, v) &= \varphi_2(u)\left(1 + \sum_{n=1}^{\infty}(ig)^n\int_{v}^{+\infty}dv_1\int_{v_1}^{+\infty}dv_2\ldots\int_{v_{n-1}}^{+\infty}dv_n\rho_1(v_1)\ldots\rho_1(v_n)\right)\\ &= \varphi_2(u)\left(e^{ig\int_{v}^{+\infty}dv'\rho_1(v')}\right)_+ = \varphi_2(u)U_2(+\infty, v),\end{aligned} \tag{39b}$$

where $(\,)_+$ stands for an ordering quite similar to time-ordering. Since $\psi_\tau^*\psi_\tau = \varphi_\tau^*\varphi_\tau$, $\tau = 1, 2$, we have the unitarity relation for the operators U_τ

$$U_\tau^* U_\tau = 1. \tag{40}$$

One can also check that $U_\tau^* = U_\tau^{-1}$, which follows from the solutions (39). In order to be able to compute matrix elements of ψ_τ between physical

states, we have to express U_τ in a form where all the creation operators stand to the left of all the annihilation operators. For this, we have first of all to deduce the commutation properties of U_τ. Now it follows from eq. (39a) that

$$U_1^{-1}(u, -\infty)\varphi_2(u_0)U_1(u, -\infty)$$
$$= \varphi_2(u_0) + \sum_{n=1}^{\infty} (ig)^n \int_{-\infty}^{u} du_1 \int_{-\infty}^{u_1} du_2 \ldots \int_{-\infty}^{u_{n-1}} du_n [\rho_2(u_n), [\ldots, [\rho_2(u_1), \varphi_2(u_0)] \ldots]],$$

and since $[\rho_2(u_1), \varphi_2(u_0)] = -\delta(u_1-u_0)\varphi_2(u_0)$,
we can evaluate the continued commutators and obtain

$$U_1^{-1}(u, -\infty)\varphi_2(u_0)U_1(u, -\infty)$$
$$= \varphi_2(u_0)\left(1+\sum_{n=1}^{\infty} (ig)^n \int_{-\infty}^{u} du_1 \int_{-\infty}^{u_1} du_2 \ldots \int_{-\infty}^{u_{n-1}} du_n\, \delta(u_n-u_0) \ldots \delta(u_1-u_0)\right).$$

If we do straightforward integrations in each term in the right-hand side of this identity and then perform the summation, we get

$$U_1^{-1}(u, -\infty)\varphi_2(u_0)U_1(u, -\infty) = \frac{1+\frac{1}{2}ig(u-u_0)}{1-\frac{1}{2}ig}, \tag{41a}$$

whereas if we treat the δ-functions as limits of smooth c-number functions, do the summation first and integration afterwards, we get, in the limit

$$U^{-1}(u, -\infty)\varphi_2(u_0)U_1(u, -\infty) = \{1+(e^{ig}-1)\theta(u-u_0)\}\varphi_2(u_0). \tag{41b}$$

This latter result is identical to Glaser's equation (13). This identity is the key to the solution of the whole problem, as we shall see below. The ambiguity between the results (41a) and (41b) is the exact counterpart of the ambiguity between the results (26a) and (26b) encountered in the previous section in the discussion of the solutions of Thirring. We shall use the results (41b) just as we used (26b) on the previous occasion. From this result we obtain, for the commutator of U_1 with the field operator φ_2, the following result:

$$[\varphi_2(u_0), U_1(u, -\infty)] = (e^{ig}-1)\theta(u-u_0)U_1(u, -\infty)\varphi_2(u_0),$$

which in the momentum representation of $\varphi_2(u_0)$ reads:

$$[C(p), U_1(u, -\infty)] = \sum_{p'} K_{pp'}U_1(u, -\infty)C(p'), \tag{42}$$

where

$$C(p) = C_2(p)e^{ipu}, \quad \text{and} \quad K_{pp'} = \frac{1-e^{ig}}{2\pi i}\,\frac{1}{p-p'+i\varepsilon}.$$

Having obtained the commutator of U_1 with $C(p)$, our next task is to bring the annihilation operators C_- to the right, and the creation operators C_+ to the left of U_1 in the R.H.S. of eq. (42). For this, we follow Glaser and decompose eq. (42) into its creation and annihilation part:

$$[C_+(p), U_1] = \sum_{p'} \theta(p)K_{pp'}U_1C_+(p') + \sum_{p'} \theta(p)K_{pp'}U_1C_-(p'), \tag{43a}$$

$$[C_-(p), U_1] = \sum_{p'} \theta(-p) K_{pp'} U_1 C_+(p') + \sum_{p'} \theta(-p) K_{pp'} U_1 C_-(p'). \quad (43b)$$

The first of these two equations can be written in the form of an integral equation

$$f_1(p) + \sum_{p'} \theta(p)\theta(p') K_{pp'} f_1(p') = g_1(p) \quad (44)$$

with

$$f_1(p) = U_1 C_+(p) \text{ and } g_1(p) = C_+(p) U_1 - \sum_{p'} \theta(p) K_{pp'} U_1 C_-(p').$$

One can see that $f_1(p)$ contains the creation operator to the right of U_1; $g_1(p)$ contains the creation operator to the left of U_1 and annihilation operator to the right of U_1. The solution of integral equation (44),

$$f_1(p) = g_1(p) + \sum_{p'} \theta(p) G_{pp'} \theta(p') g_1(p'), \quad (45)$$

where

$$G_{pp'} = \frac{1-e^{-ig}}{2\pi i} \left(\frac{p_+}{p'_-}\right)^{g'/2\pi} \frac{1}{p-p'+i\varepsilon}, \quad g' = g + 2n\pi,$$
$$n = 0, \pm 1, \pm 2, \ldots$$

gives us $f_1(p)$ in terms of $g_1(p)$, i.e., tells us how to do the desired switching of appropriate operators from the "wrong" side to the "correct" side of U_1. Using (45) and the identity

$$\sum_{p'} (\delta_{pp'} + \theta(p') G_{pp'}) K_{p'p''} = -G_{pp''},$$

in the R.H.S. of eq. (42), we obtain

$$[U_1, C_2(p)] = \sum_{p'} G_{p'p} e^{-i(p-p')u} (U_1 C_{2(-)}(p') + C_{2(+)}(p') U_1), \quad (46)$$

from which it is possible to obtain all the matrix elements of U_1 and hence the matrix elements of ψ_1, in terms of $\langle 0|U_1|0\rangle$. The manipulations following eq. (41b) are mere repetitions of Glaser's work. We have sketched them for the sake of completeness. The treatment that follows is however different.

Since $C_2(p)$ and $C_2^*(p)$ are a complete set of anti-commuting operators obeying anticommutation relations (11), and since U_1 is a function of $\sum_{pp'} T_{pp'} C_2^*(p) C_2(p')$, $T_{pp'}$ being some unknown kernel, it can be shown that

$$[U_1, C_2(p)] = \frac{\partial U_1}{\partial C_2^*(p)}, \quad (47)$$

and hence eq. (46) takes the form of a differential equation

$$\frac{\partial U_1}{\partial C_2^*(p)} = \sum_{p'} G_{pp'} e^{-i(p-p')u} \mathrm{SN}(U_1 C_2(p')), \quad (48)$$

where SN stands for semi-normal product — a product where creation

operators stand to the left of U_1 and annihilation operators to the right of U_1, as they do in eq. (46). Integration of eq. (48) gives our final result

$$U_1(u, -\infty) = Z^{\frac{1}{2}}\mathrm{N}\big(\exp \sum_{pp'} G_{pp'} e^{-i(p-p')u} C_2^*(p) C_2(p')\big), \tag{49}$$

where $Z^{\frac{1}{2}} = \langle 0|U_1|0\rangle$ and where N stands for Wick's [7]) normal product. From eqs. (39a) and (49) we obtain for the renormalized ψ_{1r}:

$$\psi_{1r}(u, v) = \varphi_1(v)\mathrm{N}\big(\exp \sum_{pp'} G_{pp'} e^{-i(p-p')u} C_2^*(p) C_2(p')\big), \tag{50}$$

from which the matrix elements of ψ_{1r} between physical states can be readily computed. This is exactly the same expression as obtained by Glaser treating the ρ_τ's as c-numbers. We, on the other hand, have treated the ρ_τ's as operators.

However, it does not seem possible to determine $Z^{\frac{1}{2}} = \langle 0|U_1|0\rangle$ explicitly from either the semi-ordered or the ordered expressions worked out above. In order to be able to do this, we have to obtain an "anti-ordered" expression for U_1, i.e. an expression where the creation operators, instead of being on the left of the annihilation operators, are to the right of them. Such anti-ordered expressions can be obtained from the "ordered" ones by knowing the required commutation rules †. But we would prefer to obtain an "anti-ordered" expression for U_1, starting from the eq. (43b) just the same way as we obtained the ordered expression starting from eq. (43a). We get an integral equation quite similar to eq. (44):

$$f_2(p) + \sum_{p'} \theta(-p) K_{pp'} \theta(-p') f_2(p') = g_2(p'), \tag{51}$$

where $f_2(p) = U_1 C_-(p)$ and $g_2(p) = C_-(p) U_1 - \sum_{p'} \theta(-p) K_{pp'} U_1 C_+(p')$, and whose solution is given by

$$f_2(p) = g_2(p) + \sum_{p'} \theta(-p)\theta(-p') R_{pp'} g_2(p'), \tag{52}$$

with

$$R_{pp'} = \frac{1-e^{-i\sigma}}{2\pi i}\left(\frac{p'_+}{p_-}\right)^{-\sigma'/2\pi} \frac{1}{p-p'-i\varepsilon}.$$

We now use this solution in the R.H.S. of (42) for switching of the creation and annihilation operators to the appropriate sides of U_1 and obtain

$$[U_1, C_2(p)] = \sum_{p'} R_{pp'} e^{-i(p-p')u}\big(C_{2(-)}(p') U_1 + U_1 C_{2(+)}(p')\big). \tag{53}$$

With the use of eq. (47) in the above identity followed by integration, the final anti-ordered expression is easily found to be

$$U_1(u, -\infty) = \overline{\mathrm{N}}\big(\exp \sum_{pp'} R_{pp'} e^{-i(p-p')u} C_2^*(p) C_2(p')\big), \tag{54}$$

† Schwinger has shown, in a case simpler than the present one, how one can obtain an ordered exponential from an anti-ordered one. See appendix B of reference [8]).

where $\overline{\mathrm{N}}$ stands anti-ordering. In order to obtain $\langle 0|U_1|0\rangle$, we first differentiate both sides of eq. (54) with respect to g and then take the vacuum expectation values of the resulting expressions. This gives us

$$\frac{\partial}{\partial g}\langle 0|U_1|0\rangle = \sum_{pp'} \frac{\partial R_{pp'}}{\partial g}\langle 0|\mathrm{S}\overline{\mathrm{N}}(U_1 C^*(p)C(p'))|0\rangle, \tag{55}$$

$\mathrm{S}\overline{\mathrm{N}}$ standing for "semi-anti-ordered" product, i.e., a product where all creation operators are commuted to the right of U_1 and all annihilation operators to the left of U_1, as though they were anticommuting among themselves and commuting with U_1. Explicit calculation gives

$$\frac{\partial}{\partial g}\langle 0|U_1|0\rangle = \sum_{pp'} \frac{\partial}{\partial g}\left\{\frac{1-\mathrm{e}^{-ig}}{2\pi i}\left(\frac{p'_+}{p_-}\right)^{-g'/2\pi}\right\}\frac{\langle 0|U_1|0\rangle}{p-p'-i\varepsilon}Q_{pp'}, \tag{56}$$

with

$$Q_{pp'} = \delta(p-p')\{\theta(p)\theta(p')+\theta(-p)\theta(-p')\}+\varepsilon(p)\varepsilon(p')G_{p'p},$$

from which $\langle 0|U_1|0\rangle$ can be obtained by integration. This result is to be compared with the corresponding result obtained by Glaser which we give below:

$$\frac{\partial}{\partial g}\langle 0|U_1|0\rangle = -\sum_{pp'}\frac{1}{2\pi i}\frac{\langle 0|U_1|0\rangle}{p-p'+i\varepsilon}\left(\theta(p)\delta(p-p')-\theta(p)\theta(-p')G_{p'p}\right). \tag{57}$$

The two results (56) and (57) do not agree. This means that the c-number treatment of the problem does not give the right answer as far as calculation of $Z^{\frac{1}{2}}$ is concerned, but this error does not affect the renormalized matrix elements. On the other hand, errors of this very type are almost bound to occur in an exact calculation of quantities such as the Green's function:

$$\begin{aligned} G^{(+)}_{12}(u_1, v_1|u_2, v_2) &= S^{(+)}_{12}(v_1|v_2)\langle 0|U_1(u_1, -\infty)U_1{}^*(u_2, -\infty)|0\rangle \\ &= S^{(+)}_{12}(v_1|v_2)\langle 0|U_1(u_1, u_2)|0\rangle, \end{aligned}$$

where one has to evaluate $\langle 0|U_1(u_1, u_2)|0\rangle$ instead of the $\langle 0|U_1(u, -\infty)|0\rangle$ evaluated on eq. (56). We have already seen how perturbation-theoretic considerations indicate that the c-number solutions give the wrong answer in this particular case of $G^{(+)}_{12}$.

The non-commutativity of the ρ_τ's does not alter Glaser's result for the S-operator, since

$$\begin{aligned} S = S(+\infty, -\infty) &= \left(\mathrm{e}^{2ig\int_{-\infty}^{+\infty}\int_{-\infty}^{+\infty}\mathrm{d}x\mathrm{d}t\,\rho_1(x-t)\rho_2(x+t)}\right)_+ \\ &= (\mathrm{e}^{igQ_1Q_2})_+ = \mathrm{e}^{igQ_1Q_2}. \end{aligned}$$

The time-ordering in the last step can be omitted, since Q_1 and Q_2 are constants of motion. This cannot be done for finite times, because neither the ρ_τ's, nor integrals of them over finite time intervals do commute with themselves or are constants of motion.

5. Vanishing of Rest Mass

For the sake of completeness of a discussion of the model, we shall show in this section that the well-known γ_5 invariance [9]) exists for this model. This leads to the vanishing of the exact rest mass of physical particles. The Dirac equation for a physical particle with momentum p can be written as

$$-i\gamma_\mu\partial_\mu\langle p|\psi|0\rangle+2g\langle p|\psi(\bar{\psi}\psi)|0\rangle = 0. \tag{58}$$

Here, $|p\rangle$ is a non-degenerate physical one-particle state vector with momentum p and $|0\rangle$ is the physical vacuum state. Since $\psi|0\rangle$ is a single bare particle state, $\langle p|\psi|0\rangle$ is the probability amplitude for finding a physical particle in a bare particle state. In other words, it is the wave function of a physical particle. The question is whether the second term in eq. (58) is equivalent to a mass term, i.e., whether

$$2g\langle p|\bar{\psi}(\bar{\psi}\psi)|0\rangle = m\beta\langle p|\psi|0\rangle.$$

If this is the case, then eq. (56) can be written as

$$-i\gamma_\mu\partial_\mu\langle p|\psi|0\rangle+m\beta\langle p|\psi|0\rangle = 0, \tag{58}$$

implying thereby that the mass-less bare particles acquire a mass as a result of self-interaction. We shall now see that this possibility is ruled out on account of γ_5 invariance. Substitution of $\psi = \gamma_5\psi' = \sigma_3\psi'$ in eq. (58) gives the following equation for ψ':

$$-i\gamma_\mu\partial_\mu\langle p|\psi'|0\rangle+2g\langle p|\psi'(\bar{\psi}'\psi')|0\rangle = 0.$$

This has a form identical with the equation for ψ. The same substitution in eq. (59) gives

$$-i\gamma_\mu\partial_\mu\langle p|\psi'|0\rangle-m\beta\langle p|\psi'|0\rangle = 0,$$

but this does not have the same form as eq. (58). It differs from eq. (58) in the sign of the mass term. Consequently, equations of the type (59) cannot be equivalent to eq. (58) unless the mass m is identically zero. This concludes the proof of the fact that the exact rest mass of physical particles is identically zero. The same conclusion has been reached by Thirring [1]) from perturbation theory calculation of Green's function $G_{12}^{(+)}$ for the model.

6. Possible Existence of Ghost States

As discussed by Thirring [1]), the physical contents of the model is best visualized by the introduction of external sources. To this purpose, he introduces an arbitrarily weak source whose interaction with the field is represented by the Lagrangian

$$\mathscr{L}' = \int dx(\bar{\psi}(x)\eta(x)+\bar{\eta}(x)\psi(x)), \tag{60}$$

$\eta(x)$ being the source-function which goes to zero for $t = \pm\infty$, and which

anticommutes with ψ and ψ^*. Such a source can create particles or anti-particles with an arbitrary number of pairs. The ratio, R, of the probability amplitudes of creating a particle plus a pair to that of creating a single particle, is given (in the lowest order of approximation in η) by

$$R = \frac{\int d^2x(\langle 3|\bar{\psi}(x)|0\rangle\eta(x) + \bar{\eta}(x)\langle 3|\psi(x)|0\rangle)}{\int d^2x(\langle 1|\bar{\psi}(x)|0\rangle\eta(x) + \bar{\eta}(x)\langle 1|\psi(x)|0\rangle)} . \tag{61}$$

This ratio is finite even though both the numerator and the denominator are zero. Because of this finiteness of R, there seems to be no urgent necessity for coupling-constant renormalization in this theory. On the other hand, if one has to speak in terms of observable quantities, one must define, in some arbitrary way, an observable coupling constant g_0. This is needed irrespective of whether the unrenormalized coupling constant g is finite or not. In an infinite theory (i.e. with an infinite unrenormalized coupling constant), renormalization is needed to remove the infinity and to express cross-sections etc. in terms of a finite (renormalized) coupling constant, whereas, in a finite theory, renormalization amounts to a redefinition of the coupling constant. There exist several ways of doing this in any given theory. In quantum electrodynamics, all the different definitions are equivalent due to Gauge invariance; in meson theory, they are not so [10]). In the present model, one way of defining the observable coupling constant g_0 is to require that the ratio R in eq. (59), in the limit of zero momenta of the created particles (and antiparticles), is equal to its Born approximation (in g) value, the coupling constant appearing in the B.A. being the observable coupling constant g_0. In going to this limit one encounters an infra-red divergence, which is avoided by having a small mass for the particles. From (61) and (49) we find, in this limit,

$$\lim \frac{R(\text{exact})}{R(\text{B.A.})} = \frac{\sin \frac{1}{2}g}{\frac{1}{2}g}, \tag{62}$$

and hence the definition of g_0 is given by

$$g_0 = 2 \sin \tfrac{1}{2}g, \quad |g| \leqq \pi. \tag{63}$$

This relation sets an upper limit to the observable coupling constant g_0, this limit being $g_0^{\max} = 2$. This means, the Källén-Pauli [11]) ghost difficulty is most likely to occur in this model if one has to have observable coupling constants greater than $g_0^{\max} = 2$. This difficulty is not so serious in this model — in fact it is purely academic — as it is in the Lee-Model where $g_0^{\max} = 0$ [11]), and possibly in quantum electrodynamics, where $g_0^{\max}$ may be zero [12]). In order to investigate the consequences of having $g_0 > 2$ in the present model, one has to work out the exact single-particle propagator and look for its poles in momentum space for all values of g_0. The ghost states, if they are present, will show up as poles with negative residues.

The author wishes to thank Prof. G. Källén for suggesting the present investigations, for his constant help and encouragement throughout the work, and for making available the preprints of the works by W. Thirring and V. Glaser. He also wishes to express his gratefulness to Prof. Niels Bohr for the hospitality granted at the Institute for Theoretical Physics, Copenhagen, and for providing a Fellowship from grants to the Institute by the Ford Foundation. Thanks are also due to Prof. Aage Bohr for his kind interest and to the members and guests at the Institute for many fruitful discussions.

References

1) W. Thirring, Annals of Physics **3** (1958) 91
2) V. Glaser, An explicit solution of the Thirring Model (CERN, Geneva) (blue-print)
3) M. L. Goldberger, Phys. Rev. **84** (1951) 929
4) B. Lippmann and J. Schwinger, Phys. Rev. **79** (1950) 469
5) W. Thirring, On Interacting Spinor Fields in One Dimension (University of Washington, Seattle, Washington, March 1958) (blue-print)
6) G. Källén, Ark. för Phys. **2** (1950) 187; C. N. Yang and D. Feldman, Phys. Rev. **79** (1950) 972
7) G. C. Wick, Phys. Rev. **80** (1950) 268
8) J. Schwinger, Phys. Rev. **93** (1954) 615
9) A. Salam, Nuovo Cimento **5** (1957) 299
10) A. Thellung, Helv. Phys. Acta **25** (1952) 307; G. Källén, Nuovo Cimento **12** (1954) 217; S. Deser, M. L. Goldberger and W. Thirring, Phys. Rev. **94** (1954) 711
11) G. Källén and W. Pauli, Mat. Fys. Medd. Dan. Vid. Selsk. **30** (1955) no. 7
12) L. D. Landau and I. Pomeranchuk, Dokl. Akad. Nauk., USSR **102** (1955) 489; see also S. Kamefuchi, Mat. Fys. Medd. Dan. Vid. Selsk. **31** (1957) no. 6

2.E *Nuclear Physics* **9** (1958/59) 140—162; © *North-Holland Publishing Co., Amsterdam*
Not to be reproduced by photoprint or microfilm without written permission from the publisher

EINTEILCHEN-STRAHLUNGSÜBERGÄNGE IM OPTISCHEN MODELL DES ATOMKERNS

F. BECK

Institut für theoretische Physik der Universität München †

Eingegangen am 29. Juli 1958

Abstract: Using the "distorted wave approximation" and employing for the nuclear interaction a complex square well potential, the single particle contribution to the radiative capture of neutrons incident on a medium weight nucleus is calculated. Numerical results are obtained for the upper end of the γ-spectrum, $d\sigma(n, \gamma)/dE_\gamma$, for an incident energy of 20 MeV, and for the integrated cross section, $\sigma(n, \gamma)(E_n)$, in the energy region 10 MeV $\leqq E_n \leqq$ 20 MeV. These results agree fairly well with experimental data on (p, γ)-reactions, available in this energy region (figs. 1, 5 and 6), and a closer agreement of the integrated cross section is obtained by adding to the single particle part the compound nucleus contribution for the process in question. The radiation from compound nucleus states contributes a non negligible amount up to about 15 MeV incident energy. The presence of an absorbing part in the potential does not change the order of magnitude of the cross section compared to the value obtained in a real potential, up to an absorption strength of $V_1 = 10.5$ MeV.

1. Einleitung

Einige neuere Experimente [2,3]) über den Strahlungseinfang von Protonen mittlerer Energie (10—20 MeV im Laborsystem) geben Aufschluß über den Wirkungsquerschnitt $\sigma(p, \gamma)$ in diesem Energiebereich. Dabei wurde von Cohen [2]) der Wirkungsquerschnitt in Abhängigkeit von der Beschußenergie E_p und der Massenzahl A des beschossenen Kerns gemessen, während Gugelot [3]) die Energieverteilung der ausgesandten γ-Strahlung für die Reaktion Cu(p, γ) Zn mit $E_p = 18$ MeV bestimmte. Die qualitativen Ergebnisse dieser Untersuchungen sind:

1. Der Wirkungsquerschnitt $\sigma(p, \gamma)$ ist in dem betrachteten Energieintervall größenordnungsmäßig konstant. Dasselbe gilt für die Abhängigkeit von der Massenzahl A des beschossenen Kerns.

2. Die spektrale Verteilung der ausgesandten γ-Strahlung nimmt mit abnehmender γ-Energie steil zu. Das energiereiche Ende der Kurve zeigt den für ein Bremsstrahlungsspektrum zu erwartenden Verlauf.

Eine quantitative Zusammenstellung der Ergebnisse findet sich in Tab. 1 bzw. Fig. 1.

† Vorgetragen auf der International Conference on Nuclear Reactions, Amsterdam, Juli 1956 [1]).

Zur theoretischen Beschreibung dieser Ergebnisse wird man zunächst das statistische Modell heranziehen, das sich im allgemeinen bei der Berechnung von Reaktionsquerschnitten in dem hier interessierenden Energiebereich gut bewährt. Cohen [3]) wies jedoch darauf hin, daß dieses Modell im vorliegenden Fall zu erheblichen Diskrepanzen mit dem unter 1. aufgeführten experimentellen Verhalten des Wirkungsquerschnitts führt. Dieses Verhalten läßt sich qualitativ viel eher durch die Annahme von Einteilchen-Übergängen verstehen.

Im Rahmen der Vorstellungen, die man sich nach dem Erfolg des optischen Modells vom Ablauf einer Kernreaktion zu machen hat, kann man diesen zeitlich in drei Stadien unterteilen (Weisskopf [4])), wir führen die Numerierung etwas anders durch als dort):

1. Der *Anfangs-Zustand.* Hier hat das einlaufende Nukleon den Wechselwirkungsbereich noch nicht erreicht, und der Zustand wird streng durch ein (antisymmetrisiertes) Produkt aus den Zuständen des einlaufenden Nukleons und dem Grundzustand des Target-Kerns beschrieben.

2a. Der *Einteilchen-Zustand.* Dies ist der Zeitabschnitt, in dem das einlaufende Nukleon zwar schon mit den Nukleonen des Target-Kerns in Wechselwirkung steht, aber im wesentlichen noch die gesamte Anregungsenergie des Compoundsystems trägt. Im Eingangskanal kann man die Wechselwirkung des einlaufenden Nukleons mit den Target-Nukleonen durch einen Mittelungsprozeß vereinfachen, wobei die Gesamtheit der aus dem Eingangskanal herausstreuenden Prozesse durch ein imaginäres Potential vertreten wird, das zu einer Absorption im Eingangskanal führt. Die Mittelung bezieht sich auf die Orte der Target-Nukleonen und ein kleines Energieintervall der Anregungsenergie (Optisches Modell [5])).

2b. Das *Compoundsystem.* Simultan mit dem „Einteilchenzustand" werden in zunehmendem Maß Zustände angeregt, bei denen das einlaufende Nukleon aus dem Eingangskanal entfernt ist. Im Eingangskanal drückt sich dies durch den Imaginärteil im Potential aus. Die entstehenden neuen Zustände geben zu „Reaktionen mit Gedächtnis" Anlaß ("direct interactions").

2c. Der *Compound-Kern.* Er bildet das Ende der zeitlichen Entwicklung des Compoundsystems und stellt den Zustand dar, bei dem die Anregungsenergie statistisch auf sämtliche Nukleonen verteilt ist. Der Compound-Kern führt zu Reaktionen „ohne Gedächtnis", gemäß der Bohrschen Unabhängigkeitshypothese.

3. Der *Endzustand.* In ihm befinden sich sämtliche Reaktionsprodukte außerhalb der gegenseitigen Wechselwirkung als auslaufende Zustände in den Reaktionskanälen. Die Beiträge aus den Stadien 2a, 2b einerseits und 2c andererseits zu ein und demselben Reaktionskanal addieren sich wegen der auftretenden Zeitdifferenzen ohne merkliche Interferenz, falls man im Ein-

gangskanal Wellenpakete verwendet, deren Energiebreite groß ist gegen den mittleren Abstand der Breit-Wigner-Resonanzen [9]).

Die eingangs geschilderte Diskrepanz zwischen den Aussagen des statistischen Modells und den experimentellen Ergebnissen führt zu der Vermutung, daß ein wesentlicher Anteil der Strahlungsreaktionen vom Einteilchen- und Compound-Zustand (Stadien 2a und 2b) herrührt. Dieser Anteil stellt also Einteilchen-Übergänge des einlaufenden Nukleons bzw. der wenigen, durch direkte Wechselwirkung angeregten Nukleonen dar, die *vor* dem Erreichen der chaotischen Verhältnisse des Compound-Kerns (Stadium 2c) erfolgen. Dies paßt zu anderweitig beobachteten Abweichungen von den Vorhersagen des statistischen Modells [6]), erscheint jedoch zunächst zweifelhaft wegen der „Langsamkeit" elektromagnetischer Übergänge. Auf der anderen Seite ist die freie Weglänge eines einlaufenden Nukleons in Kernmaterie relativ groß (einige Kernradien im vorliegenden Fall) [7]), sodaß die Verteilung der Energie auf das Gesamtsystem langsam genug erfolgen mag, um Bremsstrahlungsübergänge wahrscheinlich zu machen.

In Verfolgung dieses Bildes berechnen wir im Hauptteil dieser Untersuchung (Abschnitt 3) den Einteilchenbeitrag zum Wirkungsquerschnitt für Strahlungsreaktionen unter Verwendung der "distorted wave approximarion" [8]). Hierzu bestimmen wir in 1. störungstheoretischer Näherung die Übergangswahrscheinlichkeit zwischen Eigenzuständen des komplexen Kernpotentials, das die Wechselwirkung zwischen den Nukleonen im Einteilchenzustand beschreibt. Als Störung betrachten wir die Ankoppelung der Nukleonen an das Strahlungsfeld.

Diese Behandlung trägt der Bildung des Compoundsystems durch die Absorption im Eingangskanal Rechnung. Es ist somit möglich, den Beitrag zur Reaktion, der von Zuständen des Compound-Kerns herrührt, und den wir in Abschnitt 2 im statistischen Modell abschätzen, dem Einteilchenbeitrag additiv zuzufügen †. Da die Verwendung eines komplexen Potentials einer Energie-Mittelung im Eingangskanal entspricht, was physikalisch der Verwendung lokalisierter Zustände äquivalent ist, findet eine merkliche Interferenz aus den bei Besprechung des „Endzustands" angegebenen Gründen nicht statt. Die Addition beider Anteile führt zu einer wesentlichen Verbesserung der Übereinstimmung mit dem Experiment im unteren Teil des hier behandelten Energiebereichs (Abschnitt 4, insbes. Fig. 6).

Die hier verwendete Methode, Strahlungsreaktionen mittels der distorted wave approximation im optischen Modell zu behandeln, ist unabhängig von unserer Untersuchung von Kurşunoğlu [10]) entwickelt worden, jedoch ohne numerische Ergebnisse anzugeben. Verschiedene Autoren [11–13]) verwendeten

† Vernachlässigt werden bei dieser Behandlung Übergänge im „Anfangsstadium" des Compoundsystems (Stadium 2b).

die distorted wave approximation zur Beschreibung von Oberflächen-Reaktionen.

2. Der Wirkungsquerschnitt im statistischen Modell

Um die Größenordnung von $\sigma(\mathrm{p}, \gamma)$ im statistischen Modell kennenzulernen, wollen wir eine einfache Abschätzung durchführen †. In diesem Modell ist der Wirkungsquerschnitt für die in Rede stehende Reaktion gegeben durch

$$\sigma(\mathrm{p}, \gamma)(E_\mathrm{c}) = \sigma_\mathrm{c}(\mathrm{p}) G_\gamma(E_\mathrm{c}). \tag{1}$$

Dabei ist $\sigma_\mathrm{c}(\mathrm{p})$ der Wirkungsquerschnitt für die Bildung des Compound-Kerns durch das einfallende Proton, $G_\gamma(E_\mathrm{c})$ die Wahrscheinlichkeit dafür, daß das Compound-System durch γ-Emission zerfällt:

$$G_\gamma(E_\mathrm{c}) = \frac{\Gamma_\gamma(E_\mathrm{c})}{\sum\limits_\beta \Gamma_\beta(E_\mathrm{c})}; \tag{2}$$

Γ_γ ist die Breite für den Strahlungszerfall des Compound-Kerns, im Nenner steht die Summe der partiellen Breiten erstreckt über sämtliche offenen Kanäle β.

Wir führen die Abschätzung von $\sigma(\mathrm{p}, \gamma)$ gemäß (1) für eine Massenzahl aus Tab. 1 durch, die auch den folgenden Rechnungen zugrunde liegt, nämlich für die Reaktion $\mathrm{Ni}^{60}(\mathrm{p}, \gamma)\mathrm{Cu}^{61}$, mit $5\ \mathrm{MeV} \leqq E_\mathrm{p} \leqq 20\ \mathrm{MeV}$. Dabei berücksichtigen wir bei der Berechnung von Γ_γ nur elektrische Dipolstrahlung, da die Breiten für M1- und E2-Übergänge für die hier interessierenden Energien jeweils um eine Größenordnung kleiner sind als für den E1-Übergang (s. hierzu Abschn. II auf Seite 148). Weiterhin berücksichtigen wir bei der im Nenner von $G_\gamma(E_\mathrm{c})$ (Gl. (2)) auftretenden Summe nur den wahrscheinlichsten Zerfallsmodus, der im vorliegenden Fall die Emission eines Neutrons ist ††. Schließlich verzichten wir bei der Berechnung der Breiten Γ_γ und Γ_n auf eine Berücksichtigung der Auswahlregeln. Soweit sich diese Vernachlässigung, da sie in Zähler und Nenner von G_γ auftritt, nicht kompensiert, bedingt sie einen Faktor in $\sigma(\mathrm{p}, \gamma)$, der sicher nicht wesentlich von der Anregungsenergie abhängt, sodaß die Abhängigkeit von E_p, auf die es uns hier im Wesentlichen ankommt, nicht schwerwiegend verfälscht werden dürfte.

† Die Formeln, von denen hier ausgegangen wird, finden sich z.B. bei J. M. Blatt und V. F. Weisskopf, Theoretical Nuclear Physics (John Wiley, New York, 1952) (im folgenden mit „BW" zitiert), insbesondere die Abschnitte XII, 7 und VIII, 6. Eine ähnliche Abschätzung führte Cohen [2]) durch.

†† Konsequenterweise müssen wir den vom statistischen Modell als am wahrscheinlichsten vorausgesagten Zerfallsmodus wählen. Experimentell ergibt sich für Protonen-induzierte Reaktionen ein Überwiegen der (p, p′) — über die (p, n) — Reaktionen. Dies widerspricht jedoch der dieser Abschätzung zugrunde gelegten Bohrschen Unabhängigkeitshypothese.

Unter diesen Voraussetzungen ergibt sich für $\Gamma_\gamma(E_c)(E_c = E_p+B$; mit B = Bindungsenergie des Protons †)

$$\Gamma_\gamma(E_c) = \frac{D(E_p+B)}{2\pi} F_\gamma, \tag{3a}$$

$$F_\gamma \approx \frac{3\pi}{2}\frac{e^2}{\hbar c}\left(\frac{R}{\hbar c}\right)^2 D_0^{-1}\int_{E_p}^{E_p+B} (\hbar\omega)^3 \frac{\mathrm{d}(\hbar\omega)}{D(E_p+B-\hbar\omega)}. \tag{3b}$$

Hierin bedeuten R den Kernradius, $D(E_p+B)$ den Termabstand in der Umgebung der Anregungsenergie, D_0 dieselbe Größe in der Nähe des Grundzustands und $\hbar\omega$ die Energie der ausgesandten Strahlung ††.

Wir haben in (3b) bei der Integration nur solche Übergänge berücksichtigt, für die eine nachfolgende Teilchen-Emission des Restkerns ausgeschlossen ist ($0 \leqq E_f \leqq B$). Dies entspricht der Annahme, daß die (p, γ)-Reaktion mit der Aussendung *eines* hochenergetischen γ-Quants verbunden ist, Kaskadenemission also keine Rolle spielt. Da Integration des von Gugelot bestimmten spektralen Wirkungsquerschnitts über das hochenergetische Ende des Spektrums (s. Fig. 1) größenordnungsmäßig mit dem von Cohen für dieselbe Einfallsenergie gemessenen Wert (s. Tab. 1) übereinstimmt, scheint die hier zugrunde gelegte Annahme den experimentellen Ergebnissen nicht zu widersprechen.

Für $\Gamma_n(E_c)$ erhalten wir

$$\Gamma_n(E_c) = \frac{D(E_p+B)}{2\pi} F_n, \tag{4a}$$

$$F_n \approx \frac{2M}{\hbar^2}\int_0^{\varepsilon_n^{\max}} \varepsilon_\nu \sigma_c(\varepsilon_\nu) \frac{\mathrm{d}\varepsilon_\nu}{D(\varepsilon_n^{\max}-\varepsilon_\nu)}, \tag{4b}$$

wobei ε_ν die kinetische Energie des emittierten Neutrons in Kanal ν, $\sigma_c(\varepsilon_\nu)$ den Wirkungsquerschnitt für die Bildung des Compoundkerns durch ein in Kanal ν einlaufendes Neutron und $\varepsilon_n^{\max}$ die für Neutronenemission maximal zur Verfügung stehende kinetische Energie ($\varepsilon_n^{\max} = E_p+B_p-B_n \approx E_p$) bedeuten. Die hier angegebene Form für Γ_n folgt aus dem $\Gamma \propto D$ — Gesetz und aus der Reziprozitätsbeziehung für Kernreaktionen.

Für $G_\gamma(E_c)$ erhalten wir schließlich mit (3a, b) und (4a, b)

$$G_\gamma(E_c) = \frac{F_\gamma}{F_n} \approx \tfrac{3}{4}\frac{e^2}{\hbar c}\frac{w_0}{Me^2}\pi R^2 \frac{\int_0^{B_p}(E_p+B_p-\varepsilon)^3 w(\varepsilon)\mathrm{d}\varepsilon}{\int_0^{E_p}\varepsilon_\nu\sigma_c(\varepsilon_\nu)w(E_p-\varepsilon_\nu)\mathrm{d}\varepsilon_\nu}, \tag{5}$$

† Die Anregungsenergie des Compound-Kerns ist vom Grundzustand aus gerechnet. Der Unterschied zwischen Labor- und Schwerpunktsystem ist bei dem hier vorliegenden Massenverhältnis zu vernachlässigen.

†† Gl. (3a, b) ist die für Dipolstrahlung spezialisierte Formel (7.23) in BW.

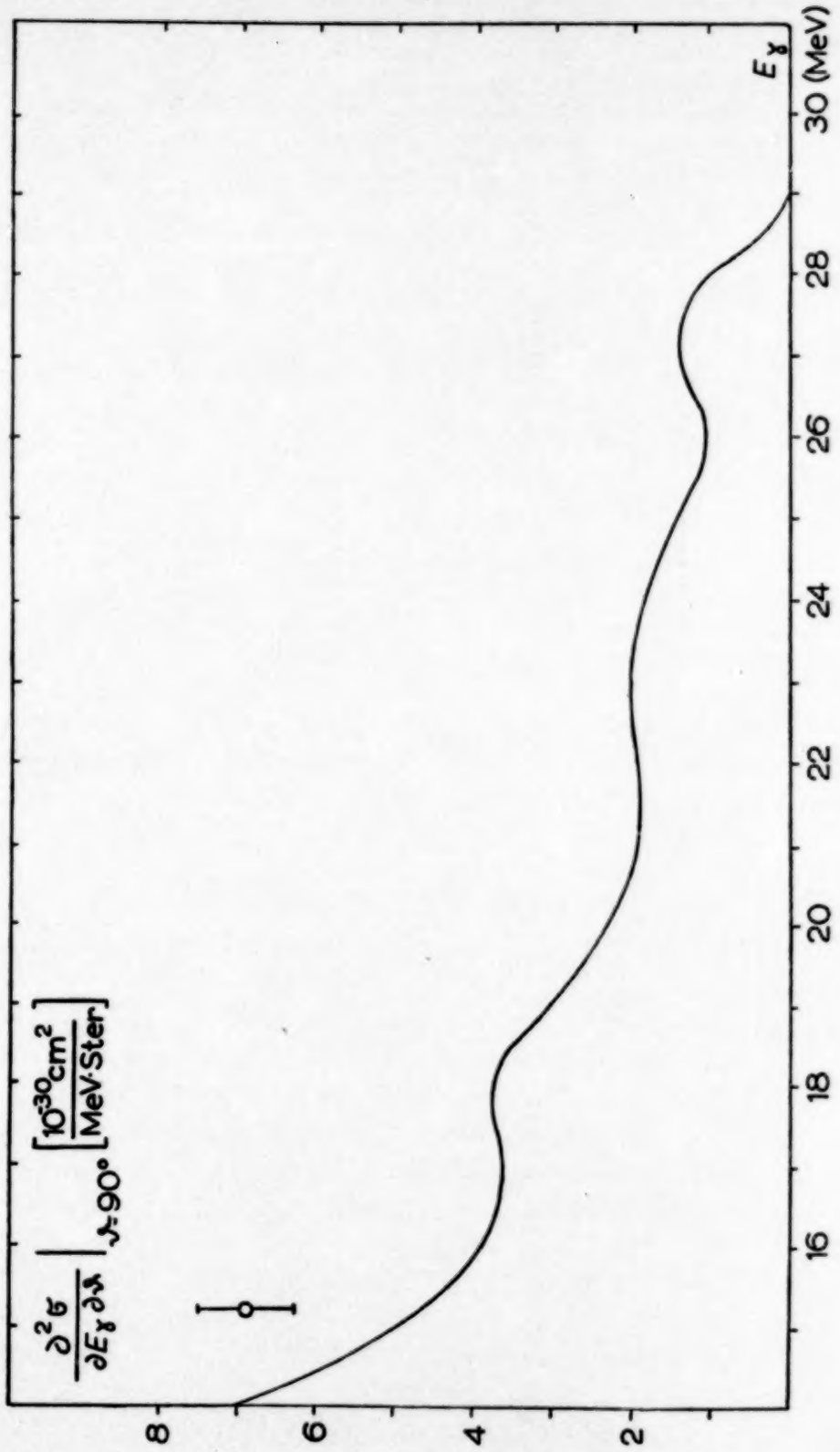

Fig. 1. Experimentelles γ-Spektrum der Reaktion $Cu^{63,65}(p, \gamma)Zn^{64,66}$ mit $E_p = 18$ MeV (nach P. C. Gugelot [3]).

TABELLE 1

Reaktion	Energie des einfallenden Protons E_p (MeV)	Wirkungsquerschnitt (mb)
$C^{12}(p, \gamma)N^{13}$	5	2.5
	11	1.8
$Fe^{54}(p, \gamma)Co^{55}$	11	0.33
$Ni^{60}(p, \gamma)Cu^{61}$	10	0.9
	16	0.7
	21	0.9
	22.5	0.9
$Zn^{64}(p, \gamma)Ga^{65}$	8	1.3
	11	1.2
$Bi^{209}(p, \gamma)Po^{210}$	10	0.17
	15	0.63
	20	0.43
	22.5	0.26

Wirkungsquerschnitte für (p, γ)-Reaktionen nach B. L. Cohen [3]). Die Werte für $Bi^{209}(p, \gamma)Po^{210}$ stammen von E. Kelly, UCRL-1044.

wobei $w(\varepsilon) \equiv D^{-1}(\varepsilon)$ die Termdichte darstellt. Mit der aus dem statistischen Modell unter speziellen Voraussetzungen folgenden Beziehung zwischen Termdichte und Anregungsenergie

$$w(\varepsilon) = Ce^{2\sqrt{a\varepsilon}}$$

und den Zahlwerten $C = 0.3$ MeV^{-1}, $a = 2$ MeV^{-1}(die für Anregungsenergien ≈ 1 MeV für die hier betrachtete Massenzahl $A = 61$ die richtige Termdichte und Kerntemperatur liefern), sowie dem aus BW, Fig. 6.3 entnommenen F_n ergibt sich für das Verzweigungsverhältnis $G_\gamma(E_c)$ der in Fig. 2 dargestellte Verlauf. Ebenfalls eingetragen ist der Wirkungsquerschnitt (Gl. (1)) mit dem aus BW, Fig. 4.3 entnommenen $\sigma_c(p)$.

Vergleich mit den entsprechenden Werten aus Tab. 1 (die für die hier näher betrachtete Reaktion ebenfalls in Fig. 2 dargestellt sind) zeigt eine erhebliche Diskrepanz bezüglich der Abhängigkeit des Wirkungsquerschnitts von der Beschußenergie E_p. Unabhängig von der groben Natur der hier gegebenen Abschätzung dürfte das statistische Modell kaum in der Lage sein, der experimentell beobachteten größenordnungsmäßigen Konstanz von $\sigma(p, \gamma) = f(E_p)$ Rechnung zu tragen. Dies liegt daran, daß F_γ im wesentlichen einer Potenz von E_p proportional ist, während in F_n die Abhängigkeit $w(E_p)$ eingeht. Die Termdichte wächst aber ganz allgemein bei einem stark entarteten Vielteilchensystem von Fermionen (aus kombinatorischen Gründen) exponentiell, also stärker als jedes Potenzgesetz, mit

der Anregungsenergie. Der qualitative Verlauf von $G_\gamma(E_c)$ dürfte somit in Fig. 2 richtig wiedergegeben sein.

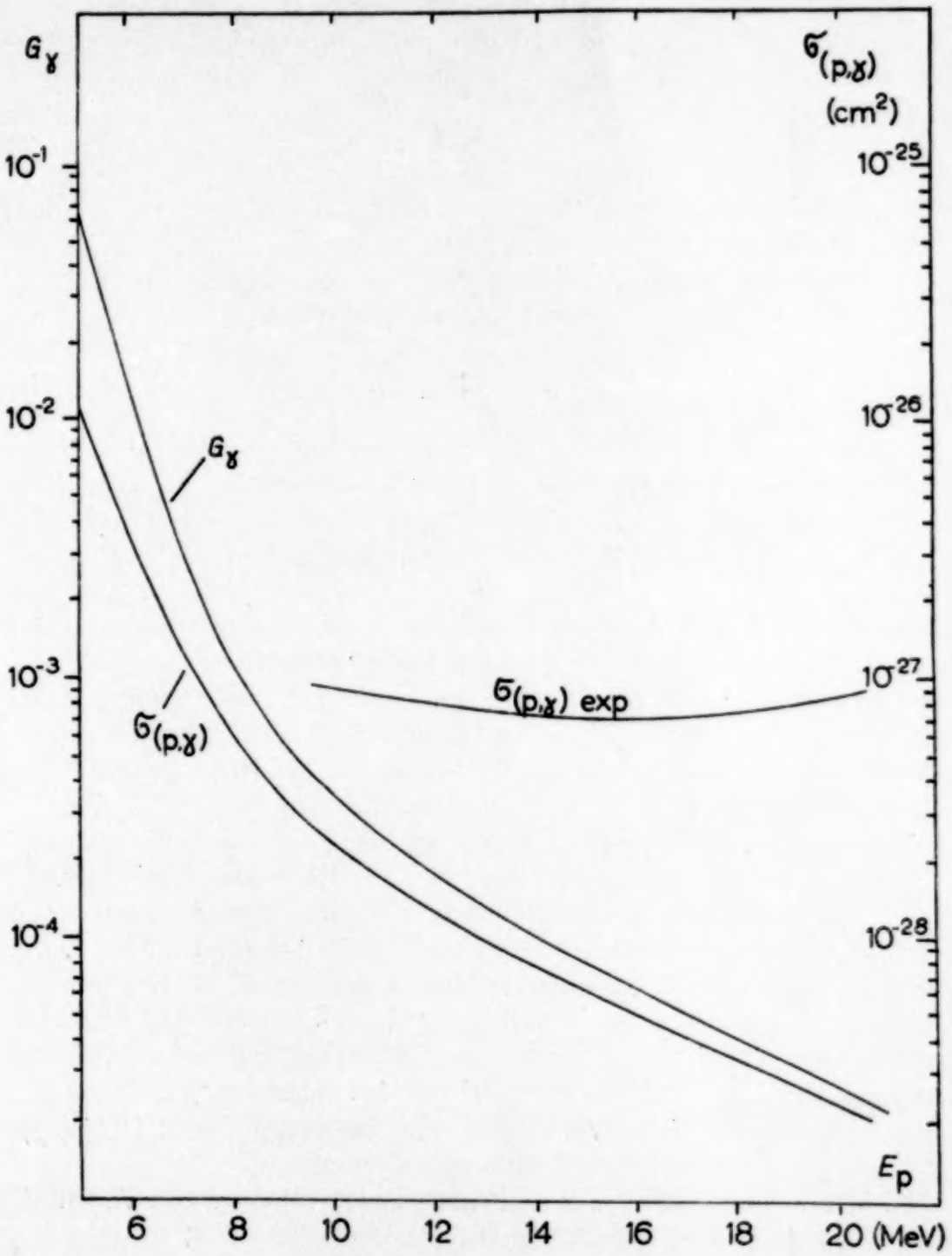

Fig. 2. Verzweigungsverhältnis G_γ und Wirkungsquerschnitt $\sigma(p, \gamma)$ als Funktion der Beschußenergie E_p nach der im Text gegebenen Abschätzung im statistischen Modell. Ebenfalls eingetragen ist der experimentelle Wirkungsquerschnitt für die Reaktion $Ni^{60}(p, \gamma)Cu^{61}$ (nach Tab. 1).

3. Berechnung der Übergangswahrscheinlichkeit und des Wirkungsquerschnitts

Der Wirkungsquerschnitt für eine Kernreaktion, die vom Eingangskanal i zum Ausgangskanal f verläuft, hängt mit der sekundlichen Übergangswahrscheinlichkeit T_{fi} zusammen durch

$$\sigma_{fi} = \frac{T_{fi}}{(\rho v^r)_i}; \tag{6}$$

$(\rho v^r)_i$ ist der Teilchenstrom der einfallenden (ebenen) Welle, die wir im folgenden auf $\rho = 1$ normieren werden. Der Strom ist dann gleich der Relativgeschwindigkeit v_i^r zwischen Projektil und Target.

In erster störungstheoretischer Näherung wird bekanntlich

$$T_{fi} = \frac{2\pi}{\hbar} |H_{fi}|^2 \rho_f. \tag{7}$$

Das Matrixelement der Störung ist mit H_{fi} bezeichnet und ρ_f ist die Zahl der Endzustände pro Energieeinheitsintervall. Wir werten nun (6) und (7) für Strahlungsübergänge aus, wobei wir folgendes Modell zugrunde legen:

I. Als eine wesentliche Vereinfachung der Rechnung vernachlässigen wir in der Wechselwirkung zwischen einlaufendem Teilchen und Kern den Coulomb-Anteil. Die Vermeidung von Coulomb-Eigenfunktionen erschien notwendig, um mit normalem Aufwand für die numerische Rechnung zum Ziel zu kommen †. Streng genommen liefern die Ergebnisse somit nur den Wirkungsquerschnitt für (n, γ)-Reaktionen. Da jedoch die hier diskutierten Einfallsenergien etwa doppelt so groß sind wie die Höhe der Coulomb-Barriere ($\approx$ 7 MeV für $Z = 29$), sollten die Wirkungsquerschnitte für (n, γ)- und (p, γ)-Prozesse der Größenordnung nach und die spektrale Verteilung der γ-Strahlung im energiereichen Ende übereinstimmen. In beiden Fällen rührt nämlich der Hauptanteil der Strahlung wegen des steilen Abfalls des Kernpotentials vom Rückstoß der Protonen im Kern her. Die für Dipolstrahlung maßgeblichen „effektiven Ladungen" für Neutron und Proton sind dem Betrage nach annähernd gleich. Die für Protonen zusätzlich auftretende Bremsstrahlung im Coulomb-Feld liefert hauptsächlich Beiträge im „weichen" Teil des Spektrums. Wir werden daher die Ergebnisse der Rechnung unter gewissen Vorbehalten mit den experimentell für (p, γ)-Prozesse vorliegenden Ergebnissen vergleichen dürfen.

II. Wir berücksichtigen nur elektrische Dipolstrahlung. Das Verhältnis von magnetischem zu elektrischem Dipolmoment hat die Größenordnung v/c, dies ist in unserem Fall etwa 10^{-1}. Das Verhältnis des elektrischen Quadrupol- zum elektrischen Dipolmoment ist von der Größenordnung

† Rechnungen mit der WKB-Methode sind zur Zeit im Gange, jedoch ist dieses Näherungsverfahren im hier interessierenden Energie- und Massenzahlbereich nicht sehr zuverlässig.

κR(κ = Wellenzahl des emittierten Lichtquants, R = Kernradius), was wiederum etwa 10^{-1} ist. Da die Multipolmomente in die Übergangswahrscheinlichkeit quadratisch eingehen, würde die Berücksichtigung von magnetischer und höherer elektrischer Multipolstrahlung Korrekturen der Ordnung 1 % liefern.

III. Einlaufendes Nukleon und Kern-Nukleonen werden als spinlose Teilchen behandelt. Auf die Matrixelemente hat diese Vereinfachung keinen merklichen Einfluß, denn die magnetische Spin-Strahlung ist im allgemeinen von der Größenordnung der magnetischen Bahn-Strahlung, also nach der Abschätzung unter II. vernachlässigbar. Die Auswahlregeln, die sich für den Übergang in (diskrete) Schalenmodellzustände mit definiertem Drehimpuls ergeben, berücksichtigen wir durch die entsprechenden statistischen Gewichte.

IV. Innerhalb des Kerns bewegt sich das an der Reaktion beteiligte Nukleon in einem komplexen Kastenpotential $V = -V_0(1+i\zeta)$ (optisches Modell). Der Parameter ζ ist energieabhängig; für Zustände mit negativen Einteilchenenergien, die also im Kern gebunden sind, setzen wir $\zeta = 0$, da man für kleine Anregungsenergien des Kerns das Schalenmodell als gute Näherung betrachten darf. Die Zustandsabhängigkeit des Potentials zerstört nicht die Orthogonalität der zur Berechnung des Matrixelements benötigten Wellenfunktionen. Da diese sich im Drehimpuls notwendig unterscheiden, ist die Orthogonalität bereits durch die Winkelanteile gesichert. Diese Feststellung ist für die Anwendbarkeit der Störungstheorie wichtig.

Unter den Voraussetzungen I—IV berechnen wir das in Gl. (7) auftretende Matrixelement. Unter Benutzung der Tatsache, daß der Schwerpunkt des Gesamtsystems eine Konstante der Bewegung ist, läßt sich der Dipol-Operator als Funktion der Koordinate des einfallenden Neutrons allein schreiben. Diesem ist dann eine effektive Ladung $e_{eff} = -eZ/A$ zuzuschreiben †. Für das Matrixelement des Dipol-Operators ergibt sich (r, ϑ, φ

† Die Ableitung in BW, Kap. XII, 7B für die effektive Nukleonenladung läßt sich auf unser Problem nicht unmittelbar übertragen, da r, ϑ, φ hier die Abstandskoordinaten zwischen einfallendem Neutron und Schwerpunkt des Beschußkernes sind. Jedoch führt folgende Überlegung zum Ziel (die wir der Einfachheit halber nur für $Q_{1,0}$ wiedergeben): Bezeichne die Folge $\mathbf{r}_i$ die Koordinaten der $A-1$ Nukleonen des Beschußkernes von einem festen Zentrum aus; $\mathbf{r}_n$ das entsprechende für das einfallende Neutron. Dann definieren die Beziehungen

$$\sum_{i=1}^{A-1} \mathbf{r}_i + \mathbf{r}_n = A\,\mathbf{R}$$

$$-\frac{1}{A-1}\sum_{i=1}^{A-1} \mathbf{r}_i + \mathbf{r}_n = \mathbf{r}$$

Gesamt-Schwerpunkt $\mathbf{R}$, und Abstand des Neutrons vom Schwerpunkt des Beschußkernes $\mathbf{r}$. Dem Schwerpunkt des Beschußkernes geben wir die Koordinate $\mathbf{G}$:

$$\mathbf{G} = \frac{1}{A-1}\sum_{i=1}^{A-1} \mathbf{r}_i.$$

Der Dipoloperator $Q_{1,0}$ ist proportional der Summe der z-Koordinaten sämtlicher Z Protonen:

bezeichnen die Relativkoordinaten von einfallendem Neutron und Kern, wobei wir die Polarachse parallel der Einfallsrichtung wählen)

$$Q_{1m} = e_{\text{eff}} \int \psi_f^*(r, \vartheta, \varphi) r Y_{1m}^*(\vartheta, \varphi) \psi_1(r, \vartheta, \varphi) \mathrm{d}\tau. \tag{8}$$

Mit diesem Übergangs-Moment erhalten wir aus der klassischen Strahlungstheorie †

$$T_{fi} = \frac{16\pi}{9} \frac{\kappa^3}{\hbar} \sum_{m=-1}^{+1} |Q_{1m}|^2 \cdot z_f(\mathrm{n}) \tag{9}$$

wobei κ die Wellenzahl des emittierten Photons bezeichnet ($\kappa = \omega/c$); $z_f(\mathrm{n})$ gibt die Zahl der Neutronen-Endzustände an. (Das Phasenraumvolumen der Photonenzustände ist in (9) bereits implizit berücksichtigt.)

Die in Gl. (8) auftretenden stationären Zustände des Neutrons sind Lösungen der Einteilchen-Schrödingergleichung mit dem Potential

$$V(r) = \begin{cases} -V_0(1+i\zeta) & (r < R) \\ 0 & (r > R) \end{cases} \tag{10}$$

und den für das Streuproblem geltenden Randbedingungen. Wir beginnen mit dem Anfangszustand $\psi_1(r, \vartheta, \varphi)$. Außerhalb des Kerns ($r > R$) muß die Lösung eine ebene Welle (der Dichte Eins) plus eine auslaufende Kugelwelle (von der elastischen Streuung herrührend) beschreiben. Da wir die Polarachse in die Richtung des Ausbreitungsvektors der ebenen Welle gelegt haben, und da unser Streupotential kugelsymmetrisch ist, hängt der Gesamtzustand nicht vom Azimut φ ab. Entwickeln wir, wie üblich, auch die ebene Welle nach Kugelwellen, so nimmt die Wellenfunktion folgende Gestalt an:

$$\psi_1(r, \vartheta) = \sum_{l=0}^{\infty} \frac{\varphi_l(k_1 r)}{k_1 r} Y_{l,0}(\vartheta) \quad (r \geqq R) \qquad k_1^2 = \frac{2M}{\hbar^2} E_1 \tag{11a}$$

$$Q_{1,0} = e \sum_{i=1}^{Z} r_i \cos\vartheta_i = e[ZG\cos\theta_G + \sum_{i=1}^{Z} d_i \cos\vartheta_{d_i}]$$

wobei $\mathbf{d}_i = \mathbf{r}_i - \mathbf{G}$ den Abstand des i-ten Protons vom Kern-Schwerpunkt angibt. Wegen

$$\mathbf{G} = \mathbf{R} - (\mathbf{r}/A)$$

wird

$$e \sum_{i=1}^{Z} r_i \cos\vartheta_i = eZR\cos\theta_R - \frac{eZ}{A} r\cos\vartheta + e \sum_{i=1}^{Z} d_i \cos\vartheta_{d_i}$$

und

$$e\langle \mathrm{f}| \sum_{1}^{Z} r_i \cos\vartheta_i |\mathrm{i}\rangle = -\frac{eZ}{A} \langle \mathrm{f}| r\cos\vartheta |\mathrm{i}\rangle \quad (\mathrm{i} \neq \mathrm{f})$$

da beim Übergang aus dem Anfangs- in den Endzustand der Schwerpunkt des Gesamtsystems, sowie, bei der hier angenommenen Wechselwirkung, die Verteilung der Protonen im Beschußkern erhalten bleiben, ihre Nichtdiagonal-Elemente also verschwinden.

† Zur Ableitung von (8) und (9) s.z.B. BW, Kap. XII.

mit

$$\begin{aligned}\varphi_l(z) &= i^{l+1}\sqrt{\pi(2l+1)}[\varphi_l^{(-)}(z)-\eta_l\varphi_l^{(+)}(z)]\\ \varphi_l^{(-)}(z) &= -z[n_l(z)+ij_l(z)] \quad \text{(einlaufend)}\\ \varphi_l^{(+)}(z) &= -z[n_l(z)-ij_l(z)] \quad \text{(auslaufend)};\end{aligned} \tag{11b}$$

$j_l(z)$ und $n_l(z)$ sind die bzw. sphärischen Bessel- und Neumann-Funktionen der Ordnung l †.

Im Kerninnern machen wir die gleiche Entwicklung

$$\begin{aligned}\psi_1(r,\vartheta) &= \sum_{l=0}^{\infty}\frac{\chi_l(K_1 r)}{K_1 r}\,Y_{l,0}(\vartheta) \quad (r \leqq R)\\ K_1^2 &= \frac{2M}{\hbar^2}\{E_1+V_0[1+i\zeta(E_1)]\}.\end{aligned} \tag{12a}$$

Jedoch sind hier in der Entwicklung nur sphärische Besselfunktionen zugelassen, da nur für ein bei $r = 0$ verschwindendes $\chi(Kr)$ das entsprechende $\psi(r,\vartheta)$ Lösung der ursprünglichen Schrödingergleichung wird. Wir schreiben

$$\chi_l(z) = \alpha_l z j_l(z). \tag{12b}$$

Gl. (11a, b) und (12a, b) geben die vollständige Wellenfunktion des Anfangszustandes. Die Konstanten η_l und α_l (für $l = 0, 1, 2, \ldots$) bestimmen sich aus den Grenzbedingungen an der Kernoberfläche $r = R$.

Bei der Berechnung der Wellenfunktion des Endzustandes haben wir zwei Fälle zu unterscheiden:

a.) Übergänge ins Kontinuum ($E_f > 0$). Hierbei ist das Neutron in der Lage, den Kern wider zu verlassen ((n, γn')-Prozeß), oder aber durch weitere Strahlungsaussendung in den Grundzustand überzugehen. Für Protonen kommt bei Endenergien $E_f \lesssim \frac{1}{2}E_1$ (nach dem ersten Übergang) wegen der Coulomb-Barriere praktisch nur noch die letztere Möglichkeit in Betracht. Wir lassen jedoch diese Folgeprozesse, die sich an den ersten Übergang anschließen, außer Betracht.

b.) Übergänge in gebundene Zustände ($-B \leqq E_1 < 0$ mit B = Bindungsenergie). Hier schließt sich, falls nicht sofort der Grundzustand erreicht wird, ebenfalls ein Folgeprozeß (überwiegend γ-Aussendung) an, den wir wiederum außer Betracht lassen ††.

† Bezüglich der Definition dieser Funktionen und ihres Zusammenhangs mit den gewöhnlichen, halbzahligen Besselfunktionen s.z.B. Morse-Feshbach, Methods of Theoretical Physics (McGraw-Hill, New York, 1953) Kap. 11.3.

†† Zum oberen Ende des Spektrums, $\frac{1}{2}(E_1+B) < E_\gamma \leqq E_1+B = E_{\gamma\max}$, kann die sekundäre Strahlung, falls die Energie des ersten Quants in diesem Intervall liegt, nichts beitragen. Ist die Energie des ersten Quants kleiner als es diesen Grenzen entspricht, so wird, wegen der dann stark begünstigten Teilchenaussendung ((n, n')-Prozeß), die Übergangswahrscheinlichkeit gegen die der Einfachprozesse sicher vernachlässigbar.

Für den unter a.) genannten Endzustand ist die Wellenfunktion durch den Gl. (11) und (12) ähnliche Entwicklungen gegeben, wobei jedoch der Ausbreitungsvektor der ebenen Welle gegenüber dem Anfangszustand in eine andere Richtung weisen kann. Ferner haben wir als Randbedingung jetzt eine *auslaufende* ebene Welle und eine *einlaufende* Kugelwelle anzusetzen [14]). Mit ϑ', φ' als Polarkoordinaten in Bezug auf die neue Ausbreitungsrichtung wird

$$\psi_f(r, \vartheta') = \sum_{l=0}^{\infty} \frac{\varphi_l^*(k_f r)}{k_f r} Y_{l,0}(\vartheta') \quad (r \geqq R) \tag{13}$$

$$\psi_f(r, \vartheta') = \sum_{l=0}^{\infty} \frac{\chi_l^*(K_f r)}{K_f^* r} Y_{l,0}(\vartheta') \quad (r \leqq R) \tag{14}$$

mit $\varphi_l(z)$, $\chi_l(z)$ aus (11b) bzw. (12b). Mit Hilfe des Additionstheorems der sphärischen Kugelfunktionen drücken wir dies in den Koordinaten des Anfangszustandes aus:

$$\psi_f(r, \vartheta, \varphi, \theta, \phi) = \sum_{l=0}^{\infty} \sum_{m=-l}^{+l} \begin{Bmatrix} \dfrac{\varphi_l^*(k_f r)}{k_f r} \\ \dfrac{\chi_l^*(K_f r)}{K_f^* r} \end{Bmatrix} \left(\frac{4\pi}{2l+1}\right)^{\frac{1}{2}} Y_{lm}^*(\theta, \phi) Y_{lm}(\vartheta, \varphi); \tag{13a, 14a}$$

θ, ϕ ist der Raumwinkel, in den das Neutron bei der Strahlungsaussendung gestreut wird †.

Die in (9) auftretende Dichte der Neutronen-Endzustände ist in Fall a.) gegeben durch

$$z_f(n) = \frac{M \cdot p_f}{(2\pi\hbar)^3} \mathrm{d}E_n \, \mathrm{d}\Omega_n; \tag{15}$$

p_f bezeichnet den Impulsbetrag des Neutrons im Endzustand und $\mathrm{d}\Omega_n$ das Raumwinkel-Element, in das der Ausbreitungsvektor der ebenen Welle im Endzustand weist. Da wir uns für das γ-Spektrum, nicht für das Neutronenspektrum, interessieren, schreiben wir unter Verwendung von $|\mathrm{d}E_n|_{E_\gamma = \mathrm{const}} = |\mathrm{d}E_\gamma|_{E_n = \mathrm{const}}$ (Energiesatz)

$$z_f(\mathrm{n}) = \frac{M \cdot p_f}{(2\pi\hbar)^3} \mathrm{d}E_\gamma \, \mathrm{d}\Omega_n. \tag{15a}$$

In Fall b.) gehören die Endzustände des Neutrons zum diskreten Energiespektrum. Um hier eine explizite Darstellung für die Wellenfunktionen zu gewinnen, bestimmen wir die Eigenzustände in dem der Rechnung zugrunde gelegten Potentialkasten, Gl. (10), (mit $\zeta = 0$). Dies liefert selbstverständlich nicht die richtigen Schalenmodell-Eigenwerte. Da jedoch die Dipol-

† Sowohl im Anfangs- wie auch im Endzustand erfährt das Neutron elastische Streuung (entsprechend einem von 1 verschiedenen η_l in (11b)). Genau genommen ist somit θ, ϕ der räumliche Ablenkungswinkel eines Neutrons, das keine elastische Streuung erfahren hat.

matrixelemente, wie zu erwarten und wie die Rechnung bestätigt, nicht sehr stark energieabhängig sind, genügt es, die Korrektur für die richtigen Schalenmodellenenergien in den energieabhängigen Faktoren, die in Gl. (9) neben dem Matrixelement auftreten, allein vorzunehmen.

Wir erhalten somit die Lösungen

$$\psi_f^{n,l,m}(r,\vartheta,\varphi) = \begin{cases} \dfrac{\varphi_l(k_{f,n,l}\cdot r)}{k_{f,n,l}\cdot r} & (r \geqq R) \\ \dfrac{\chi_l(K_{f,n,l}\cdot r)}{K_{f,n,l}\cdot r} & (r \leqq R) \end{cases} \cdot Y_{l,m}(\vartheta,\varphi) \tag{16}$$

mit

$$\begin{aligned} \varphi_l(z) &= B_l z h_l^{(1)}(iz) \\ \chi_l(z) &= A_l z j_l(z); \end{aligned} \tag{16a}$$

$h_l^{(1)}$ sind die sphärischen Hankelfunktionen 1. Art.

Die Eigenwerte $K_{f,n,l}$ und $k_{f,n,l}$ bestimmen sich aus den Randbedingungen. Bezüglich der z-Komponente des Drehimpulses (Quantenzahl m) liegt Entartung vor. Bei der Bestimmung der Normierungskonstanten können wir den exponentiell abfallenden Teil der Lösung (im Bereich $r > R$) vernachlässigen:

$$|A_l|^2 = [R^3 \int_0^1 [j_l(K_f R\cdot x)]^2 x^2 \mathrm{d}x]^{-1} \approx \frac{(K_f\cdot R)^2}{R_3}. \tag{17}$$

Schließlich ist hier, da es sich um Übergänge in diskrete Endzustände handelt, $z_f(\mathrm{n}) = 1$ zu setzen.

Wir sind nun in der Lage, den Wirkungsquerschnitt entsprechend Gl. (6) explizit anzugeben. Wir unterscheiden wieder die beiden verschieden zu behandelnden Fälle $E_f > 0$ und $E_f < 0$.

a.) $E_f > 0$, *Übergänge ins Kontinuum.*

Entsprechend (6), (8), (9) und (15a) erhalten wir

$$\frac{\mathrm{d}\sigma(\mathrm{n},\gamma)(E_1,E_\gamma)}{\mathrm{d}E_\gamma} = \frac{16\pi}{9}\frac{\kappa^3}{\hbar v_1^r}\frac{Mp_f}{(2\pi\hbar)^3}\left(\frac{eZ}{A}\right)^2$$
$$\times \left|\int_0^\infty \mathrm{d}r \int_{-1}^{+1} \mathrm{d}\cos\vartheta \int_0^{2\pi} \mathrm{d}\varphi r^2 \psi_f^*(r,\vartheta,\varphi,\theta,\phi) r y_{1m}^*(\vartheta,\varphi)\psi_1(r,\vartheta)\right|^2 \mathrm{d}\Omega_\mathrm{n}. \tag{18}$$

Setzen wir hier die Wellenfunktionen (12) und (14a) ein, so kommt nach Ausführung der Integrationen über ϑ und φ, sowie über Ω_n, da wir uns nicht für die Richtung des Neutrons interessieren,

$$\frac{\mathrm{d}\sigma(\mathrm{n},\gamma)(E_1,E_\gamma)}{\mathrm{d}E_\gamma} = \frac{1}{6}\frac{M}{\hbar^2}\frac{Mc}{\hbar}\frac{e^2}{\hbar c} R^5 \left(\frac{Z}{A}\right)^2 (KR)^3 \frac{v_f}{v_1^r} \sum_{l=0}^{\infty}\sum_{m=-1}^{+1} |Q'_{lm}|^2 \tag{19a}$$

mit

$$|Q'_{l,m}|^2 = (2l+1)|\bar{\alpha}_l^f|^2 \cdot |(2l-1)\bar{\alpha}_{l-1}^i V(l-1, 1, l; 0, 0, 0)V(l-1, 1, l; 0, m, -m) \times \int_0^1 j_l(X_f^* x) j_{l-1}(X_1 x) x^3 \mathrm{d}x - (2l+3)\bar{\alpha}_{l+1}^i V(l+1, 1, l; 0, 0, 0)V(l+1, 1, l; 0, m, -m) \times \int_0^1 j_l(X_f^* x) j_{l+1}(X_1 x) x^3 \mathrm{d}x. \quad (20a)$$

Die Konstanten $\bar{\alpha}_l$ stehen mit den in (12b) eingeführten Amplituden α_l in der Beziehung

$$\alpha_l = -i^{l+1}\sqrt{\pi(2l+1)}\bar{\alpha}_l.$$

Ferner bedeuten $X = KR$ und $V(a, b, c; \alpha, \beta, \gamma)$ die von der Winkelintegration herrührenden Racah-Koeffizienten †. Gl. (20a) enthält die Auswahlregeln für elektrische Dipolstrahlung als Folge der Winkelintegrationen.

b.) $E_f < 0$, *Übergänge in gebundene Zustände.*

Mit (6), (8), (9) und (16) erhalten wir, wieder nach Ausführung der Winkelintegrationen,

$$\sigma(\mathrm{n}, \gamma)(E_1, E_{\mathrm{n},l}) = \frac{\pi}{3} R^5 \left(\frac{Z}{A}\right)^2 (\kappa R)^3 \frac{e^2}{\hbar v_1^r} \sum_{m=-1}^{+1} |Q'_{lm}|^2 \quad (19b)$$

mit $|Q'_{lm}|^2$ wie in Gl. (20a), wobei jedoch hier $|\bar{\alpha}_l^f|^2$ durch $|A_l|^2$ zu ersetzen ist. Bei der Integration ist der Bereich negativer kinetischer Energie ($r > R$), in dem die Wellenfunktion rasch exponentiell abfällt, vernachlässigt.

4. Numerische Ergebnisse und Vergleich mit dem Experiment

Wegen des erheblichen Aufwands an numerischer Rechnung, der zur Bestimmung der Amplituden α_l der Wellenfunktionen im Kerninnern notwendig ist, beschränken wir uns bei der Auswertung der obigen Formeln für den Wirkungsquerschnitt auf einen Kern. Um sowohl mit Gugelots Ergebnissen an $Cu^{63,65}(p, \gamma)Zn^{64,66}$ (Fig. 1) als auch mit denen von Cohen an $Ni^{60}(p, \gamma)Cu^{61}$ (Tab. 1) vergleichen zu können, sind die Rechnungen mit $A = 61$, $Z = 29$ (Cu^{61}) durchgeführt. Die Korrektur für Gugelots höhere Massenzahl berücksichtigen wir lediglich in der expliziten R-Abhängigkeit der Gl. (19a, b). Um zunächst das energiereiche Ende des γ-Spektrums zu bestimmen, wurden die in Fig. 3 schematisch angedeuteten Übergänge berechnet. Dort sind auch die der Rechnung zugrunde liegenden Konstanten angegeben, für die wir die üblichen, die Streudaten am besten wiedergebenden Werte genommen haben. Der Gang der Rechnung ist folgender. Zunächst müssen die in Gl. (20a, b) auftretenden Amplituden $\bar{\alpha}_l$ bestimmt werden. Sie stehen mit den Streuamplituden η_l in der Beziehung

† Zur Definition der Racahschen V-Koeffizienten s.z.B. E. V. Condon und G. H. Shortley, Theory of Atomic Spectra (Cambridge University Press, 1951) S. 76–77.

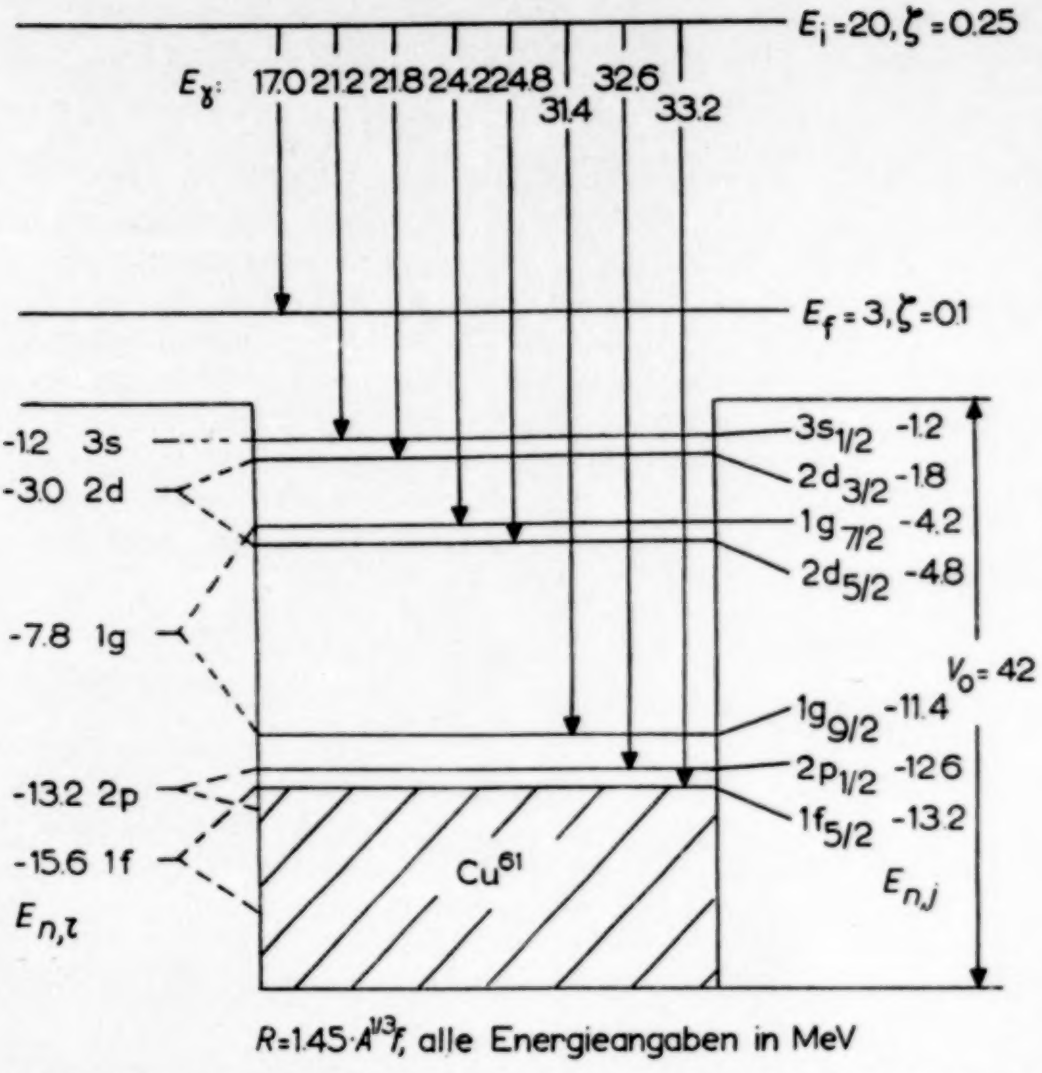

Fig. 3. Zur Berechnung des γ-Spektrums für die Reaktion $Cu^{61}(n, \gamma)Cu^{62}$. Es sind die Schalenmodellniveaus des Grundzustands und der angeregten Zustände für Neutronen eingetragen, ferner die Eigenwerte unseres vereinfachten Modells (ohne Spin-Bahn-Kopplung) das der Bestimmung der Wellenfunktion dient.

$$\bar{\alpha}_l = \frac{(1-\eta_l) n_l(kR) + i(1+\eta_l) j_l(kR)}{j_l(K_r R) + i\Lambda R j'_l(K_r R)} \tag{21}$$

wobei wir, wegen der Kleinheit des Imaginärteils im Potential, die Näherungen

$$K = \left\{\frac{2M}{\hbar^2}[E + V_0(1+i\zeta)]\right\}^{\frac{1}{2}} = K_r + i\Lambda$$

$$K_r \approx \left[\frac{2M}{\hbar^2}(E+V_0)\right]^{\frac{1}{2}}; \quad \Lambda \approx K_r \frac{\zeta}{2(1+E/V_0)}$$

und

$$j_l[(K_r + i\Lambda)R] \approx j_l(K_r R) + i\Lambda R j'_l(K_r R)$$

verwandt haben. Ein für die numerische Rechnung bequemes Verfahren zur Bestimmung der η_l mit Hilfe von Rekursionsformeln wurde von Feshbach, Porter und Weisskopf [5]) angegeben.

Für den Übergang ins Kontinuum ($E_t = 3$ MeV) können eine ganze Reihe von l-Werten miteinander kombinieren s. Gl. (20a). Die Begrenzung der Summe wird durch die Zentrifugalbarriere für den tieferen Zustand bestimmt. Die Rechnung zeigt, daß für diesen Zustand $|\tilde{\alpha}_5|/|\tilde{\alpha}_4| \approx 4\times 10^{-2}$ wird. Es genügt also die l-Summe in (19a) bis zu $l = 4$ auszuwerten, da sie dort mit guter Näherung konvergiert. Wir verzichten darauf, weitere Werte im Kontinuum zu bestimmen. Wie in der Einleitung bemerkt, verliert die Rechnung für wesentlich kleinere γ-Energien $E_\gamma \lesssim \frac{1}{2}(E_1+B)$ wegen der Vernachlässigung von Mehrfachprozessen ihren Sinn. In der Umgebung des berechneten Punktes $E_t = 3$ MeV können wir aber die Energieveränderlichkeit in (19a) unter Konstanthaltung der (schwach energieabhängigen) $\Sigma|Q'_{lm}|^2$ bestimmen. Wir erhalten dann

$$\mathrm{d}\sigma(\mathrm{n},\gamma)/\mathrm{d}E_\gamma \propto E_\gamma^3(E_1-E_\gamma)^{\frac{1}{2}} \quad \text{(bei festem } E_1\text{)}. \tag{22}$$

Diese Funktion hat ein Maximum für $E_\gamma = \frac{5}{6}E_1$.

Für die Übergänge in diskrete Zustände werten wir, wie schon angedeutet, die Matrixelemente mit den Eigenfunktionen des vereinfachten Potentials (ohne Spin-Bahn-Kopplung) aus und korrigieren für die Schalenmodell-eigenwerte (mit Spin-Bahn-Kopplung) in den energieabhängigen Faktoren. Ferner berücksichtigen wir die statistischen Gewichte bei der Niveau-Aufspaltung.

Das so erhaltene Energiespektrum ist in Fig. 4 dargestellt. Es ist hier der differentielle Wirkungsquerschnitt
$\partial^2\sigma(\mathrm{n},\gamma)/\partial E\gamma\,\partial\vartheta$ bzw. $\mathrm{d}\sigma(\mathrm{n},\gamma)/\mathrm{d}\vartheta$ für $\vartheta = 90°$ aufgetragen, der sich aus dem im Text berechneten durch Multiplikation mit der Winkelverteilung für Dipolstrahlung ergibt. Dies entspricht der in Fig. 1 aufgetragenen experimentellen Kurve, die für $\vartheta = 90°$ gewonnen wurde. Das experimentelle Spektrum ist mit einem γ-Spektrometer relativ schlechten Auflösungsvermögens † erhalten. Um einen besseren Vergleich mit diesem Ergebnis zu ermöglichen, haben wir in Fig. 5 die Übergänge in die diskreten Zustände „verschmiert". Dazu bilden wir

$$\frac{1}{E_K-E_{K-1}}\frac{\mathrm{d}\sigma(\mathrm{n},\gamma)}{\mathrm{d}\vartheta}\bigg|_{\vartheta=90°} \approx \frac{\partial^2\sigma(\mathrm{n},\gamma)}{\partial E_\gamma\,\partial\vartheta}\bigg|_{\vartheta=90°} \quad \text{für} \quad E_{K-1} < E_t < E_K$$

wobei k die diskreten Zustände der Reihe nach numeriert. Die so entstehende Rechteck-Kurve interpolieren wir durch einen stetigen Kurvenzug.

Vergleich mit der experimentellen Kurve (Fig. 1) zeigt im oberen Ende

† Das Auflösungsvermögen ist durch die erreichbare Größe des Spektrometer-Einkristalls begrenzt. Man benötigt für die hier auftretenden γ-Energien bereits sehr große Kristalle.

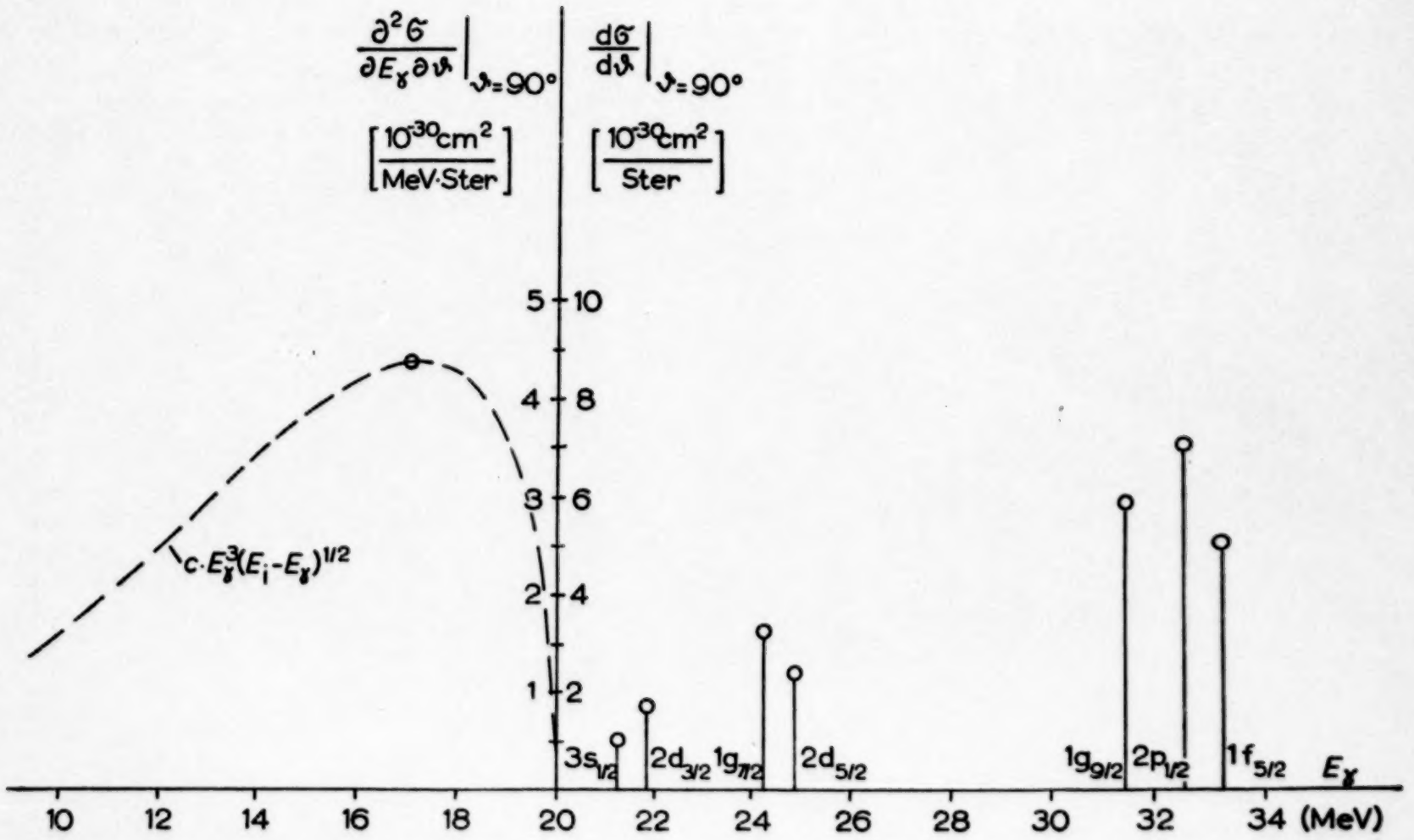

Fig. 4. Berechnete (n, γ)-Wirkungsquerschnitte für Übergänge ins Kontinuum ($E_\gamma < 20$ MeV) und in gebundene Zustände ($E_\gamma > 20$ MeV) für eine Neutronen-Energie $E_i = 20$ MeV. Gerechnet ist im Kontinuum nur der Wert für $E_\gamma = 17$ MeV. Die gestrichelte Kurve gibt die Variation des außerhalb des Matrixelements stehenden Faktoren wieder.

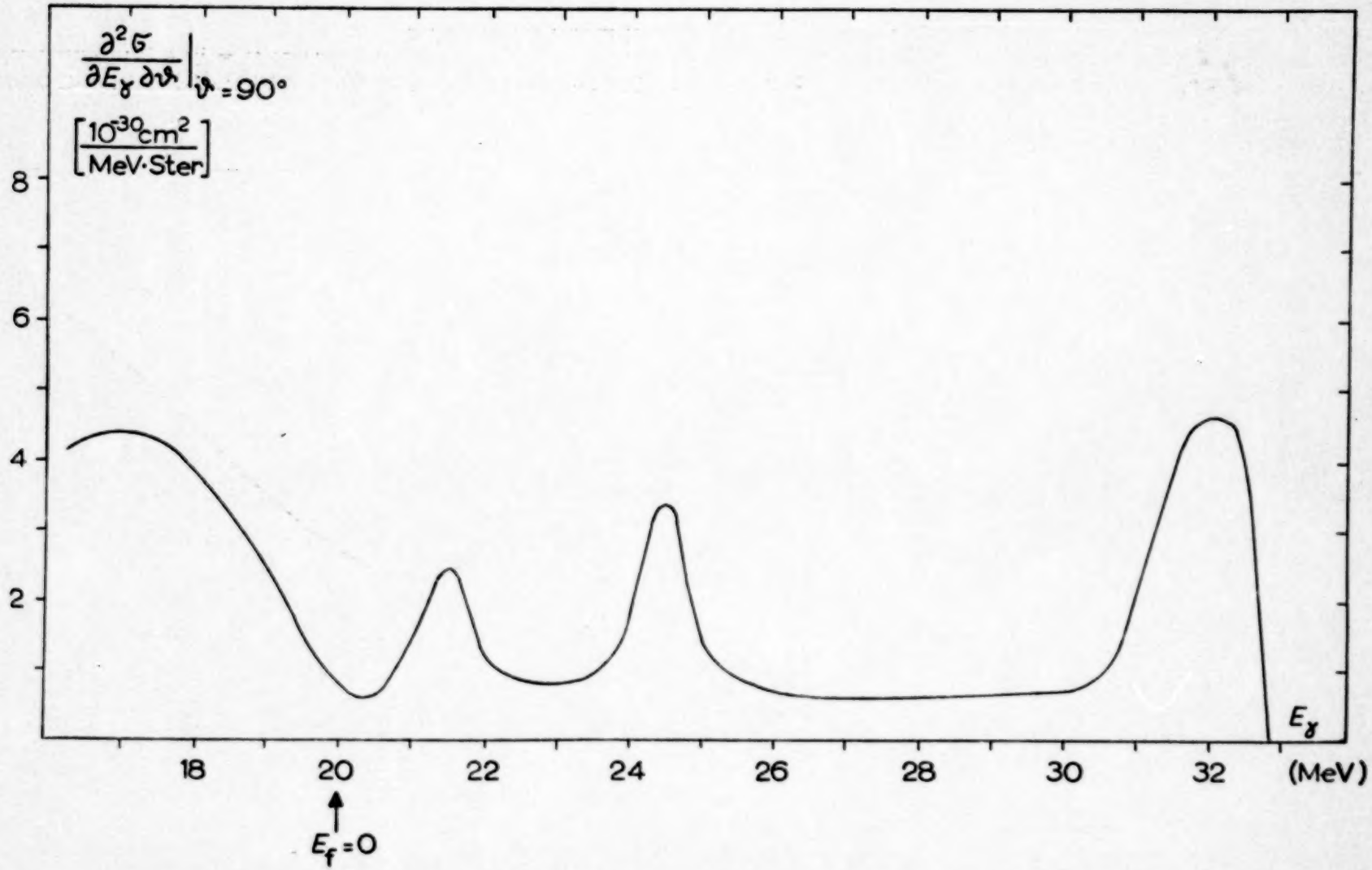

Fig. 5. Theoretisches γ-Spektrum der Fig. 4, nach der im Text angegebenen Weise aufgelöst. Zum Vergleich mit dem experimentellen Spektrum der Fig. 1 sind die gleichen Maßstäbe wie dort gewählt.

des Spektrums eine relativ gute Übereinstimmung. Die beiden Maxima, die den Häufungen der Niveaus in der 50-er bzw. 82-er Schale entsprechen, finden sich im experimentellen Spektrum andeutungsweise wieder. Der sich aus dem Experiment für den Einfang des Protons ergebende Q-Wert ($Q_{\text{exp}} \approx 10$ MeV; im Verlauf der Rechnung wurde diese Größe mit B bezeichnet) ist geringer als der aus der Rechnung für das Neutron folgende ($Q_{\text{th}} = 13.2$ MeV). Dies spiegelt das wohlbekannte Ergebnis wider, daß ein den Streudaten angepaßter Potentialtopf (der der Wahl unserer Konstanten entspricht) eine zu große Bindungsenergie liefert.

Eine erhebliche Diskrepanz ergibt sich im mittleren Teil des Spektrums ($E_\gamma \approx E_1$). Hier zeigt die theoretische Kurve das für Bremsstrahlung charakteristische Maximum Gl. (22), während experimentell der Wirkungsquerschnitt mit kleiner werdenden γ-Energien monoton und stark zunimmt. Der Grund für diese Diskrepanz ist wahrscheinlich in den hier nicht mehr vernachlässigbaren Mehrquanten-Übergängen zu suchen (s. hierzu Anmerkung auf S. 151). Die Bedeutung dieser Kaskadenprozesse ist jedenfalls für Protonen weitaus größer als für Neutronen, da das Proton nach einmal erfolgtem Übergang in einen tieferen Energiezustand durch die Coulomb-Barriere sehr stark daran gehindert wird den Kern wieder zu verlassen. Es wäre daher interessant, unser Ergebnis mit einem experimentellen (n, γ)-Spektrum zu vergleichen. Leider liegen unseres Wissens nach solche im hier betrachteten Energiebereich noch nicht vor. Es besteht auch die Möglichkeit, daß das experimentelle (p, γ)-Spektrum den weichen Teil der Strahlung ($E_\gamma \lesssim 15$ MeV) nicht richtig wiedergibt, da sich dort der Beitrag von sekundären „γ-Verunreinigungen" nicht gut übersehen läßt.

Um den gesamten Einfangquerschnitt als Funktion der Beschußenergie zu erhalten und mit den Messungen von Cohen (Tab. 1) zu vergleichen, wurde die eben geschilderte Rechnung auch noch für die Energien $E_1 = 10$ MeV und $E_1 = 15$ MeV durchgeführt, jedoch ohne den Übergang ins Kontinuum zu berücksichtigen. Aufsummation der Übergänge in die einzelnen diskreten Niveaus ergibt dann den Einfangquerschnitt. Es wurden hier für den Ausgangszustand zwei Werte des Parameters ζ gerechnet, nämlich $\zeta = 0.1$, entsprechend einem Imaginärteil des Potentials von $V_1 = 4.2$ MeV und $\zeta = 0.25$, entsprechend $V_1 = 10.5$ MeV. Nach der Rechnung von Lane und Wandel [7]) sollte der erste der beiden Werte in der Gegend von $E_1 = 10$ MeV, der zweite bei $E_1 = 20$ MeV zutreffend sein.

Das Ergebnis ist in Fig. 6 dargestellt. Die obere gestrichelte Kurve ergibt sich für $\zeta = 0.1$, die untere für $\zeta = 0.25$. Die dazwischenliegende Kurve stellt eine Interpolation, entsprechend der Energieveränderlichkeit von ζ [7]) dar. Ebenfalls eingetragen ist der Beitrag der Compound-Strahlung nach der Abschätzung in Abschnitt 2. Wie schon erwähnt, ergibt sich der gesamte Wirkungquerschnitt für Strahlungseinfang durch einfache Summation von

Einteilchen- und Compound-Anteil. Dies ergibt die ausgezogen gezeichnete Kurve. Die Summe ist im gezeigten Energiebereich nahezu konstant. Anzeichen für eine Resonanzstruktur sind nur in der Einteilchenkurve für $\zeta = 0.1$ im oberen Ende zu erkennen. Es ist verständlich, daß diese Andeutung einer Resonanz für $\zeta = 0.25$ nicht auftritt, da mit zunehmenden

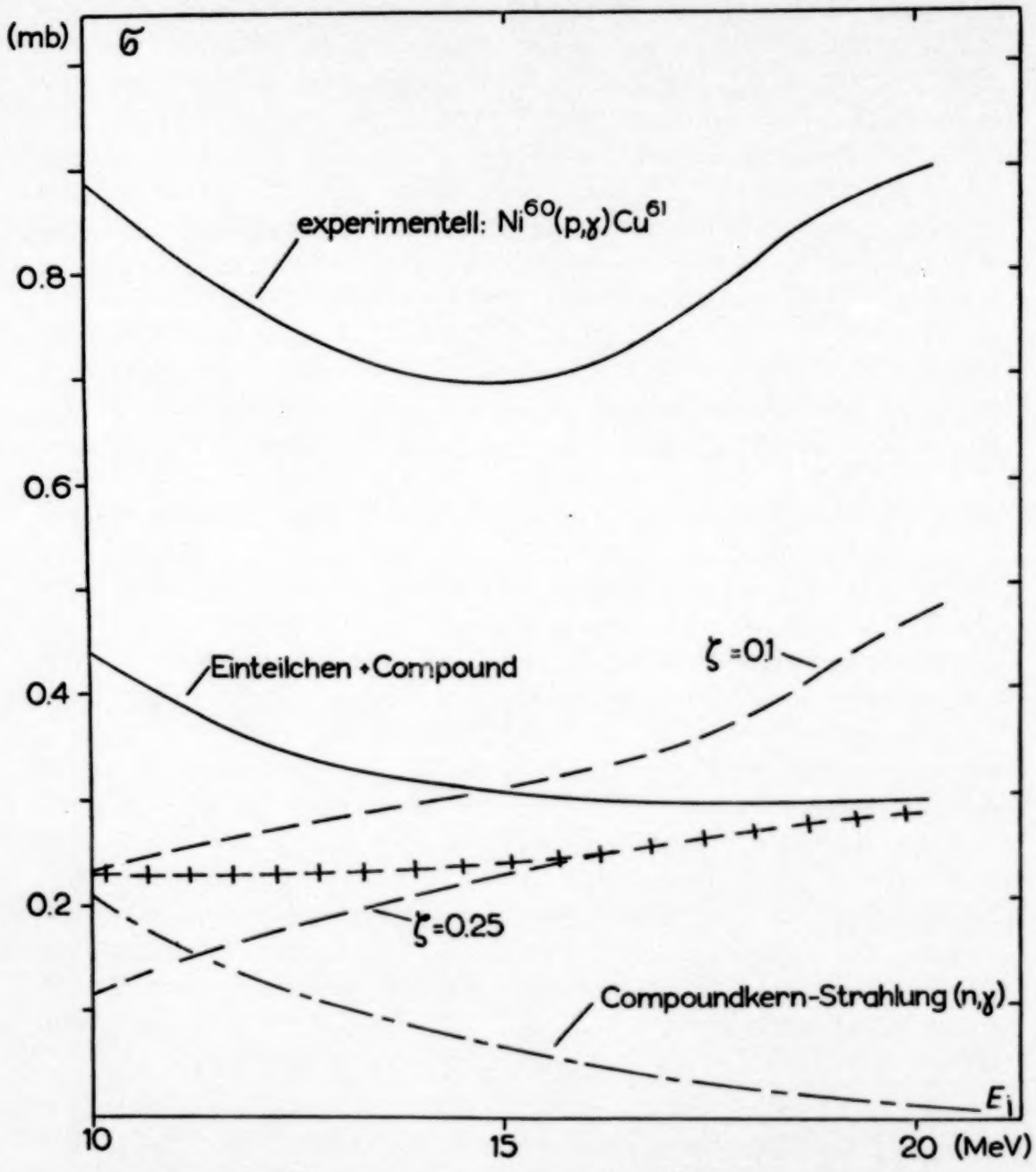

Fig. 6. Theoretische Werte des Neutronen-Einfangquerschnitts als Funktion der Beschuß-Energie. Die mittlere gestrichelte Kurve stellt eine Interpolation zwischen $\zeta = 0.1$ ($V_1 = 4.2$ MeV) und $\zeta = 0.25$ ($V_1 = 10.5$ MeV) dar, entsprechend der Energieabhängigkeit des Imaginärteils im Potential. Die experimentelle Kurve ist dieselbe wie in Fig. 2, der Beitrag der Compoundkern-Strahlung ist wieder im statistischen Modell abgeschätzt.

Imaginärteil des Potentials die Einteilchenresonanzen mehr und mehr verschwinden. Jedoch ist der dargestellte Energiebereich nicht groß genug, um Aussagen über das Auftreten von Großraum-Resonanzen zu gewinnen.

Von $E_1 \approx 15$ MeV an speilt der Compound-Anteil keine wesentliche Rolle mehre. Der rasche Abfall der Compound-Strahlung mit zunehmender Beschußenergie wird von der Einteilchenstrahlung kompensiert. Gegenüber der experimentellen (p, γ)-Kurve liegen die theoretischen Werte allerdings um etwa einen Faktor 2 zu tief. Jedoch sind Cohens Ergebnisse wahrscheinlich durch einen nicht berücksichtigten systematischen Fehler um einen ähnlichen Faktor zu groß †.

Auf Grund von Näherungen im Verlauf der numerischen Rechnung mögen sämtliche hier angegebenen numerischen Ergebnisse um einen Faktor der Größenordnung 1 verfälscht sein. Es kam uns aber in dieser Arbeit insbesondere auf die Klärung der Frage an, ob die Strahlung von Einteilchenzuständen aus in dem hier behandelten Energiebereich eine merkliche Rolle speilt und etwa in der Lage ist, die eingangs erwähnte, zwischen statistischem Modell und den experimentellen Ergebnissen auftretende Diskrepanz zu beseitigen. Hierfür ist die erreichte Genauigkeit der Rechnung ausreichend.

5. Zusammenfassung

Für die Reaktion Cu^{61}(n, γ)Cu^{62} wurde der Wirkungsquerschnitt der Strahlung von Einteilchenbahnen aus in 1. störungstheoretischer Näherung im Energiebereich 10 MeV $\lesssim E_1 \lesssim$ 20 MeV bestimmt. Dabei haben wir im Kerninnern die Wellenfunktionen des optischen Modells verwendet, um der Bildung von Compound-Zuständen Rechnung zu tragen. Anlaß der Rechnung war das aus sehr allgemeinen Überlegungen folgende Versagen des statistischen Modells, die annähernde Konstanz des Wirkungsquerschnitts mit der Beschußenergie zu erklären. Das Ergebnis der Rechnung wird mit experimentellen Ergebnissen für (p, γ)-Reaktionen in demselben Massenzahl- und Energiegebiet verglichen, da entsprechende (n, γ)-Experimente noch nicht vorliegen. Der Unterschied sollte gemäß qualitativer Überlegungen für den Einfangquerschnitt und das energiereiche Ende des Spektrums nicht erheblich sein. Diesen Teil des Spektrums gibt die Rechnung, verglichen mit dem Experiment, auch befriedigend wieder. Ebenso folgt für den integrierten Wirkungsquerschnitt die Konstanz mit der Beschußenergie. Der Strahlungsanteil von Compound-Zuständen fügt sich dem im optischen Modell berechneten σ(n, γ) additiv zu. Um eine bessere Vergleichsbasis mit dem Experiment zu haben, sind Rechnungen in demselben Modell für geladene Teilchen im Gange.

† P. C. Gugelot, private Mitteilung.

Herrn Professor V. F. Weisskopf möchte ich für den Hinweis auf das dieser Arbeit zugrunde liegende Problem und für viele anregende Diskussionen sehr herzlich danken. Ebenso gebührt mein herzlicher Dank Herrn Professor P. C. Gugelot für Mitteilung seiner experimentellen Ergebnisse vor der Veröffentlichung und für eine Einführung in den experimentellen Sachverhalt. Dr. G. Lanza vom Massachusetts Institute of Technology danke ich für seine Hilfe bei einigen numerischen Rechnungen. Dem Massachusetts Institute of Technology, Cambridge, Mass., USA und den Mitarbeitern der theoretischen Gruppe im Dept. of Physics bin ich für die Gastfreundschaft während der Jahre 1954 und 1955, der Deutschen Forschungsgemeinschaft und dem Institute for Nuclear Science am MIT für die finanzielle Ermöglichung dieses Aufenthalts zu großem Dank verpflichtet.

Literatur

1) F. Beck, Physica **22** (1956) 1164
2) B. L. Cohen, Phys. Rev. **100** (1955) 206
3) P. C. Gugelot, Report on the Brookhaven Conference on Statistical Aspects of the Nucleus; und private Mitteilung
4) V. F. Weisskopf, Revs. Mod. Phys. **29** (1957) 174
5) H. Feshbach, C. E. Porter und V. F. Weisskopf, Phys. Rev. 96 (1954) 448; W. B. Riesenfeld, und K. M. Watson, Phys. Rev. **104** (1956) 492
6) A. M. Lane, Revs. Mod. Phys. **29** (1957) 191
7) A. M. Lane, und C. F. Wandel, Phys. Rev. **98** (1955) 1524
8) N. F. Mott und H. S. Massey, The Theory of Atomic Collisions, 2nd edition (Oxford University Press, London, 1950) p. 144f
9) F. L. Friedman und V. F. Weisskopf, in Niels Bohr and the Development of Physics (Pergamon Press, London, 1955)
10) B. Kursunoglu, Phys. Rev. **105** (1957) 1846
11) J. Horowitz und A. M. L. Messiah, J. phys. radium **14** (1953) 695
12) W. Tobocman und M. M. Kalos, Phys. Rev. **97** (1955) 132
13) J. A. Lamarsh und H. Feshbach, Phys. Rev. **104** (1956) 1633
14) G. Breit und H. A. Bethe, Phys. Rev. **93** (1954) 888

1. D. 2 *Nuclear Physics* 9 (1958/59) 163—177; © *North-Holland Publishing Co., Amsterdam*
Not to be reproduced by photoprint or microfilm without written permission from the publisher

ON THE CALCULATION OF THE Y_{40} DEFORMATION IN STRONGLY DEFORMED HEAVY NUCLEI

KERSTIN KJÄLLQUIST
Institute for Theoretical Physics, University of Lund

Received 15 April 1958

Abstract: The equilibrium Y_{40} deformation in strongly deformed heavy nuclei is calculated, treating the Y_{40} term as a small perturbation of a spheroidal potential, characterized by a comparatively great Y_{20} deformation. The equilibrium deformation is determined from the condition that the deformation of the potential and of the nuclear density calculated from the wave equation with this potential shall be equal. Numerical values are given for even isotopes of Th, U, Pu, Cm, Cf, Fm.

1. Introduction

In the shell model one assumes a spherically symmetric potential. However, nuclei with proton and neutron numbers very different from those corresponding to closed shells have large deformations, as is shown e.g. by their large quadrupole moments. Calculations with a spheroidal potential have been done by S. G. Nilsson and others [1]) and show a remarkable agreement with important experimental data. This is especially true of the spins and parities of the low excited levels, which can be determined from the single-particle level order given by these authors. In his paper, S. G. Nilsson also gives a theoretical determination of the equilibrium Y_{20}-deformation. The total energy of the nucleus is calculated as a function of the deformation ε, which is then determined by the condition

$$\frac{\partial E_{\text{tot}}}{\partial \varepsilon} = 0.$$

It will be of interest to determine also deformations of higher multipole order. Y_{30}-deformations, where the first non-vanishing contribution is of second order, have been treated by Lee and Inglis [2]), who have discussed the stability of the deformation by a perturbation theory, starting from the wave functions of a spheroidal harmonic-oscillator potential. We shall try to calculate the equilibrium Y_{40}-deformation, adding to the spheroidal potential a term proportional to Y_{40}. In particular, we shall make numerical calculations for the heavy nuclei Th, U, Pu, Cm, Cf, Fm. For these nuclei, P. O. Fröman [3]) has deduced values of the Y_{40}-deformation from experimental evidence on α-decay.

2. The Y_{20} Deformation

In the following we shall regard the Y_{40}-term as a small perturbation of a potential with a comparatively great Y_{20}-deformation, which is the case treated by S. G. Nilsson. The following calculations will use his asymptotic eigenfunctions and so we shall first give a brief survey of his methods.

The following single-particle Hamiltonian of a spheroidal nucleus has been chosen:

$$\begin{aligned} H &= H_0+C\mathbf{l}\cdot\mathbf{s}+D\mathbf{l}^2, \\ H_0 &= T+V_0, \qquad V_0 = \tfrac{1}{2}m\left[\omega_x^2(x^2+y^2)+\omega_z^2 z^2\right], \\ \omega_x &= \omega(\varepsilon)(1+\tfrac{1}{3}\varepsilon), \qquad \omega_z = \omega(\varepsilon)(1-\tfrac{2}{3}\varepsilon). \end{aligned} \tag{1}$$

The condition of constant volume gives $\omega_x^2\,\omega_z = \omega_0^3 = \text{const}$. In the equation $H_0\varphi_n^0 = E_n^0\varphi_n^0$ it is convenient to introduce the substitution

$$\xi = x\sqrt{\frac{m\omega_x}{\hbar}}, \qquad \eta = y\sqrt{\frac{m\omega_x}{\hbar}}, \qquad \zeta = z\sqrt{\frac{m\omega_z}{\hbar}},$$

$$\xi^2+\eta^2 = \rho^2,$$

$$H_0 = H_\xi+H_\eta+H_\zeta,$$

where

$$H_\xi = \tfrac{1}{2}\hbar\omega_x\left(-\frac{\partial^2}{\partial\xi^2}+\xi^2\right).$$

H_0 is diagonal in the representation $|n_\xi\rangle|n_\eta\rangle|n_\zeta\rangle$ where $|n_\xi\rangle$ is defined by

$$H_\xi|n_\xi\rangle = \hbar\omega_x\,(n_\xi+\tfrac{1}{2})|n_\xi\rangle.$$

The eigenvalues of H_0 are given by

$$E_0 = \hbar\omega_z\,(n_\zeta+\tfrac{1}{2})+\hbar\omega_x\,(n_\xi+n_\eta+1)$$

or, expressed in ε,

$$E_0 = \hbar\omega(\varepsilon)\left[(N+\tfrac{3}{2})+\varepsilon\,\frac{n_\perp-2n_\zeta}{3}\right], \tag{2}$$

where

$$N = n_\zeta+n_\perp, \qquad n_\perp = n_\xi+n_\eta.$$

An energy level characterized by n_ζ and $n_\perp$ is degenerate to the order of $n_\perp+1$. To this is added the spin degeneracy. We now choose linear combinations $|n_\perp\Lambda\rangle$ of the base vectors $|n_\xi\rangle|n_\eta\rangle$ so that

$$(l_\zeta-\Lambda)|n_\perp\Lambda\rangle = 0. \tag{3}$$

The vectors $|n_\zeta\rangle|n_\perp\Lambda\rangle|\Sigma\rangle$ (where $|\Sigma\rangle$ = the spin vector) form a complete set and H_0 is diagonal in this representation. Here $\Lambda = \pm1, \pm3, \ldots \pm n_\perp$ for odd $n_\perp$ and $= 0, \pm2, \ldots \pm n_\perp$ for even $n_\perp$.

In the limit of very strong deformation, these eigenfunctions are approximate solutions to a Hamiltonian in which $\mathbf{l}\cdot\mathbf{s}$ and $\mathbf{l}^2$ terms are included. For the deformations we shall consider, this approximation is a good one, the main contributions to the energy by $\mathbf{l}\cdot\mathbf{s}$ and $\mathbf{l}^2$ coming from the diagonal terms. To simplify the calculations, we shall drop the $\mathbf{l}\cdot\mathbf{s}$ and $\mathbf{l}^2$ terms, but as we use the eigenfunctions given above and the level order given by the exact calculations, their main influence on the deformation is thus taken into account.

The total wave function φ, which describes the nucleons in the deformed potential, is a Slater-determinant of single particle wave functions of the occupied states.

If we imagine the overall potential to represent the effect of two-body forces we can identify the total energy of the nucleus with

$$E_{\text{tot}} = \langle\varphi|\sum_i H_i|\varphi\rangle - \tfrac{1}{2}\langle\varphi|\sum_i V_i|\varphi\rangle \tag{4}$$

which is the energy expression one gets in the theory of self-consistent field, when exchange forces are neglected.

The equilibrium deformation ε is now given by the condition

$$\frac{\partial E_{\text{tot}}}{\partial\varepsilon} = 0.$$

3. The Y_{40} Deformation

As was mentioned above the Y_{40}-deformation will be regarded as a small perturbation superimposed on the Y_{20}-deformation. Now, an important feature in the expression of E_{tot} is that the operator

$$\sum_i H_i - \tfrac{1}{2}\sum_i V_i,$$

contrary to the usual case in calculating energies, is not the Hamiltonian of the wave function. Therefore, as will be shown in a forthcoming paper, perturbation expansions will show special new properties. Calculation of the second order contribution to the energy will in general require second order wave functions. This is in contrast to the usual situation, where only first order wave functions are needed.

In this paper we shall calculate the equilibrium deformation from the condition that the deformation of the potential and of the nuclear density calculated from the wave equation with this potential shall be equal.

We now start from a Hamiltonian with the potential

$$V = \alpha^2 V^0 + \delta_4 V', \tag{5}$$

where

$$V^0 = \tfrac{1}{2}m\,(\omega_x^2(x^2+y^2)+\omega_z^2 z^2), \tag{6}$$

and

$$V' = \frac{m\omega_0^2}{2} \frac{r^4 Y_{40}}{R_0^2} \qquad (R_0 = r_0 \sqrt[3]{A}). \tag{7}$$

By introducing the factor α we can in a simple manner take into account the condition of constant volume.

We have the solutions of the unperturbed problem

$$(T+V^0)\varphi_n^0 = E_n^0 \varphi_n^0 \tag{8}$$

and by substituting $\omega_x \to \alpha\omega_x$, $\omega_z \to \alpha\omega_z$ and $E_n^0 \to \alpha E_n^0$ we get the solutions to

$$(T+\alpha^2 V^0)\psi_n^0 = \alpha E_n^0 \psi_n^0. \tag{9}$$

In our calculations we can therefore use only $\delta_4 V'$ as perturbation potential. From these ψ_n we get a new total wave function ψ.

The potential, whose equipotential surfaces are functions of δ_4, is created by the nuclear matter. Because of the small range of nuclear forces, the surfaces of equal potential and of equal density must approximately coincide.

Starting from the deformed potential we can get the density in two ways. The first is given by the statistical theory of Thomas-Fermi, which gives the nuclear density at any point consistent with the potential at that point.

$$\rho_{T-F} = n(\mathbf{r}) = \frac{(2m(E-V(r))^{\frac{3}{2}}}{3\pi^2\hbar^3}.$$

The other way is to get an expression for the density by calculating $\psi^* \psi$ from the Schrödinger-equation with our deformed potential. This density depends on our choice of representation and on the assumed level order.

Consistency demands that the Y_{40}-deformations of these two densities are the same. We express this by an integral condition:

$$\frac{\iiint r^4 Y_{40} \rho \mathrm{d}V}{\iiint r^4 \rho \mathrm{d}V} = \frac{\langle\psi| \sum_\kappa r_\kappa^4 Y_{40}(\theta_\kappa)|\psi\rangle}{\langle\psi| \sum_\kappa r_\kappa^4 |\psi\rangle}. \tag{10}$$

We first give an illustration for a nucleus of constant density ρ. If we write the nuclear radius in the form

$$R = R_0(1+\sum_n \beta_n Y_{n0})$$

and form the expression

$$\frac{\iiint r^n \rho Y_{n0} \mathrm{d}V}{\iiint r^n \rho \mathrm{d}V},$$

this gives a measure of the Y_{n0}-deformation. Assuming all β_n small, we get the simple expression

$$\frac{\iiint r^n \rho Y_{n0}\,\mathrm{d}V}{\iiint r^n \rho \mathrm{d}V} = \frac{\iint \frac{R^{n+3}}{n+3}\rho Y_{n0}\,\mathrm{d}\Omega}{\iint \frac{R^{n+3}}{n+3}\rho \mathrm{d}\Omega} = \frac{n+3}{4\pi}\cdot\beta_n.$$

In our calculations where the Y_{20}-deformation is not small we shall treat it as constant when varying δ_4. We determine it from the equation

$$\frac{\iint r^2 Y_{20}\rho \mathrm{d}V}{\iint r^2 \rho \mathrm{d}V} = \frac{\langle\varphi|\sum_\kappa r_\kappa^2 Y_{20}(\theta_\kappa)|\varphi\rangle}{\langle\varphi|\sum_\kappa r_\kappa^2|\varphi\rangle}. \tag{11}$$

This deformation is the same as the one we get by minimizing the energy, using the same total wave function and neglecting the $\mathbf{l}\cdot\mathbf{s}$ and $\mathbf{l}^2$ terms.

4. Calculation of the Integral Condition for δ_4

4.1. LEFT-HAND SIDE OF EQ. (10)

We shall not use a constant density here but instead a density $\rho = C(E-V)^{\frac{3}{2}}$ that is consistent with our choice of

$$V = \alpha^2\frac{m}{2}\left(\omega_x^2(x^2+y^2)+\omega_z^2 z^2\right)+\delta_4\frac{m\omega_0^2}{2}\cdot\frac{r^4 Y_{40}}{R_0^2}. \tag{12}$$

We now perform the transformation

$$\omega_x x \to \omega_0 x' \text{ etc.}, \qquad z' = r'\cos\theta';$$
$$\mathrm{d}V = \mathrm{d}V' \qquad (\text{since } \omega_x^2\omega_z = \omega_0^3);$$
$$r^4 Y_{40}(\theta) = r'^4 Q_1(\theta'), \qquad Q_1(\theta') = a_1 Y_{40}(\theta')+b_1 Y_{20}(\theta')+c_1 Y_{00}(\theta');$$
$$r^4 = r'^4 Q_2(\theta'), \qquad Q_2(\theta') = \sqrt{4\pi}\left(a_2 Y_{40}(\theta')+b_2 Y_{20}(\theta')+c_2 Y_{00}(\theta')\right).$$

Here

$$a_1 = \tfrac{1}{35}(8\gamma^2+24\gamma\beta+3\beta^2),$$
$$b_1 = \tfrac{6}{7\sqrt{5}}(2\gamma^2-\gamma\beta-\beta^2),$$
$$c_1 = \tfrac{3}{5}(\gamma-\beta)^2,$$
$$c_2 = \tfrac{1}{15}(3\gamma^2+4\gamma\beta+8\beta^2),$$

with

$$\left(\frac{\omega_0}{\omega_x}\right)^2 = \gamma, \qquad \left(\frac{\omega_0}{\omega_z}\right)^2 = \beta;$$

a_2 and b_2 will not be needed.

After this transformation the left-hand side of eq. (10) becomes

$$\frac{\iiint r^4 Y_{40}\rho \mathrm{d}V}{\iiint r^4 \rho \mathrm{d}V} = \frac{\iiint (E-V)^{\frac{3}{2}}\cdot r'^4 Q_1(\theta')\mathrm{d}V'}{\iiint (E-V)^{\frac{3}{2}}\cdot r'^4 Q_2(\theta')\mathrm{d}V'}$$

where

$$V = \frac{m\omega_0^2\alpha^2}{2}\left(r'^2+\delta_4\frac{r'^4 Q_1(\theta')}{\alpha^2 R_0^2}\right).$$

If we neglect terms of higher order in δ_4, we get

$$\frac{\iiint r^4 Y_{40}\rho dV}{\iiint r^4\rho dV} = \frac{c_1\sqrt{4\pi}-\frac{21}{4}\frac{E}{m\omega_0^2}\frac{1}{R_0^2}(a_1^2+b_1^2+c_1^2)\delta_4}{c_2 4\pi-\frac{21}{4}\frac{E}{m\omega_0^2}\frac{1}{R_0^2}\sqrt{4\pi}(a_1a_2+b_1b_2+c_1c_2)\delta_4} \quad (13)$$

An estimate of the δ_4 term in the denominator shows that it can be neglected.

4.2. RIGHT-HAND SIDE OF EQ. (10)

$$\frac{\langle\psi|\sum_\kappa r_\kappa^4 Y_{40}(\theta_\kappa)|\psi\rangle}{\langle\psi|\sum_\kappa r_\kappa^4|\psi\rangle} = \frac{\sum_\kappa\langle\psi_\kappa|r^4 Y_{40}|\psi_\kappa\rangle}{\sum_\kappa\langle\psi_\kappa|r^4|\psi_\kappa\rangle}. \quad (14)$$

We use the notations κ, λ, μ for occupied states, k, l, m for unoccupied states, K, L, M for all states. Using the expressions for ψ_κ, we get to the first order of δ_4

$$\langle\psi_\kappa|r^4 Y_{40}|\psi_\kappa\rangle = \langle\psi_\kappa^0|r^4 Y_{40}|\psi_\kappa^0\rangle+2\delta_4\sum_L a_L^{(1)}\langle\psi_\kappa^0|r^4 Y_{40}|\psi_L^0\rangle$$

and

$$\langle\psi_\kappa|r^4|\psi_\kappa\rangle = \langle\psi_\kappa^0|r^4|\psi_\kappa^0\rangle+2\delta_4\sum_L a_L^{(1)}\langle\psi_\kappa^0|r^4|\psi_L^0\rangle$$

where

$$r^4 Y_{40} = \frac{9}{16\sqrt{\pi}}[\tfrac{8}{3}z^4-8z^2(x^2+y^2)+(x^2+y^2)^2]$$

and

$$a_L^{(1)} = \frac{\langle\psi_L^0|V'|\psi_\kappa^0\rangle}{[E_\kappa^0-E_L^0]} \quad (L\neq\kappa),$$

$$a_\kappa^{(1)} = 0.$$

If we make the transformations

$$\xi = x\sqrt{\frac{m\omega_x}{\hbar}}, \qquad \eta = y\sqrt{\frac{m\omega_x}{\hbar}}, \qquad \zeta = z\sqrt{\frac{m\omega_z}{\hbar}}$$

and use the previous expressions for ω_x, ω_z we get

$$\frac{\langle\psi|\sum_\kappa r_\kappa^4 Y_{40}(\theta_\kappa)|\psi\rangle}{\langle\psi|\sum_\kappa r_\kappa^4|\psi\rangle} = \frac{9}{16\sqrt{\pi}}\cdot\frac{\sum_\kappa A_{\kappa\kappa}+\delta_4 f\frac{\hbar\omega(\varepsilon)}{(1-\frac{2}{3}\varepsilon)}\sum_\kappa\sum_l\frac{A_{\kappa l}A_{l\kappa}}{(E_\kappa^0-E_l^0)}}{\sum_\kappa B_{\kappa\kappa}+\delta_4 f\frac{\hbar\omega(\varepsilon)}{(1-\frac{2}{3}\varepsilon)}\sum_\kappa\sum_l\frac{B_{\kappa l}A_{l\kappa}}{(E_\kappa^0-E_l^0)}} \quad (15)$$

where

$$A_{KL} = \langle \psi_K^0 | \tfrac{8}{3}\zeta^4(1+\tfrac{1}{3}\varepsilon)^2 - 8\zeta^2\rho^2(1+\tfrac{1}{3}\varepsilon)(1-\tfrac{2}{3}\varepsilon) + \rho^4(1-\tfrac{2}{3}\varepsilon)^2 | \psi_L^0 \rangle,$$
$$B_{KL} = \langle \psi_K^0 | \zeta^4(1+\tfrac{1}{3}\varepsilon)^2 + 2\zeta^2\rho^2(1+\tfrac{1}{3}\varepsilon)(1-\tfrac{2}{3}\varepsilon) + \rho^4(1-\tfrac{2}{3}\varepsilon)^2 | \psi_L^0 \rangle, \quad (16)$$
$$f = \frac{9}{16\sqrt{\pi}} \frac{\hbar}{m\omega_0} \frac{1}{R_0^2}.$$

The base vectors $|\psi_K^0\rangle$ are the eigenvectors for the harmonic oscillator in cylindrical coordinates and we shall write them $|n_\zeta n_\perp \Lambda\Sigma\rangle$:

$$|n_\zeta n_\perp \Lambda\Sigma\rangle = |n_\zeta\rangle |n_\perp \Lambda\rangle |\Sigma\rangle.$$

$\langle\zeta|n_\zeta\rangle$ are the usual Hermite functions and[4])

$$\langle \rho, \varphi | n_\perp \Lambda\rangle = N\, e^{i\Lambda\varphi} e^{-\frac{1}{2}\rho^2} F_{|\Lambda|, n_\perp}(\rho).$$

It follows that matrix elements $\langle n_\perp \Lambda | \rho^n | n'_\perp \Lambda' \rangle$ are equal to zero if $\Lambda \neq \Lambda'$. We need in our calculations the matrix elements

$$\langle n_\zeta n_\perp \Lambda\Sigma | \zeta^4 | n'_\zeta n'_\perp \Lambda' \Sigma' \rangle = \delta_{n_\perp n'_\perp} \delta_{\Lambda\Lambda'} \delta_{\Sigma\Sigma'} \langle n_\zeta | \zeta^4 | n'_\zeta \rangle,$$
$$\langle n_\zeta n_\perp \Lambda\Sigma | \zeta^2\rho^2 | n'_\zeta n'_\perp \Lambda' \Sigma' \rangle = \delta_{\Lambda\Lambda'} \delta_{\Sigma\Sigma'} \langle n_\zeta | \zeta^2 | n'_\zeta \rangle \langle n_\perp \Lambda | \rho^2 | n'_\perp \Lambda \rangle, \quad (17)$$
$$\langle n_\zeta n_\perp \Lambda\Sigma | \rho^4 | n'_\zeta n'_\perp \Lambda' \Sigma' \rangle = \delta_{n_\zeta n'_\zeta} \delta_{\Lambda\Lambda'} \delta_{\Sigma\Sigma'} \langle n_\perp \Lambda | \rho^4 | n'_\perp \Lambda \rangle.$$

The elements $\langle n_\zeta | \zeta^4 | n'_\zeta \rangle$ and $\langle n_\zeta | \zeta^2 | n'_\zeta \rangle$ can easily be calculated from the generating function for the Hermite polynomials. The matrix elements

$$\langle n_\perp \Lambda | \rho^2 | n'_\perp \Lambda \rangle \text{ and } \langle n_\perp \Lambda | \rho^4 | n'_\perp \Lambda \rangle$$

are calculated in the appendix.

We get the following selection rules:

for ζ^4:

$$n_\zeta = \begin{cases} n'_\zeta \\ n'_\zeta \pm 2, \\ n'_\zeta \pm 4 \end{cases} \quad n_\perp = n'_\perp, \quad \Lambda = \Lambda', \quad \Sigma = \Sigma';$$

for $\zeta^2\rho^2$:

$$n_\zeta = \begin{cases} n'_\zeta \\ n'_\zeta \pm 2, \end{cases} \quad n_\perp = \begin{cases} n'_\perp \\ n'_\perp \pm 2, \end{cases} \quad \Lambda = \Lambda', \quad \Sigma = \Sigma';$$

and for ρ^4:

$$n_\zeta = n'_\zeta, \quad n_\perp = \begin{cases} n'_\perp \\ n'_\perp \pm 2, \\ n'_\perp \pm 4 \end{cases} \quad \Lambda = \Lambda', \quad \Sigma = \Sigma',$$

where

$$\begin{aligned}
&\langle n_\zeta|\zeta^2|n_\zeta\rangle = n_\zeta+\tfrac{1}{2}\\
&\langle n_\zeta|\zeta^2|n_\zeta+2\rangle = \tfrac{1}{2}\sqrt{(n_\zeta+1)(n_\zeta+2)}\\
&\langle n_\zeta|\zeta^4|n_\zeta\rangle = \tfrac{3}{2}(n_\zeta{}^2+n_\zeta+\tfrac{1}{2})\\
&\langle n_\zeta|\zeta^4|n_\zeta+2\rangle = (n_\zeta+\tfrac{3}{2})\sqrt{(n_\zeta+1)(n_\zeta+2)}\\
&\langle n_\zeta|\zeta^4|n_\zeta+4\rangle = \tfrac{1}{4}\sqrt{(n_\zeta+1)(n_\zeta+2)(n_\zeta+3)(n_\zeta+4)}
\end{aligned} \tag{18}$$

and

$$\begin{aligned}
&\langle n_\perp \Lambda|\rho^2|n_\perp \Lambda\rangle = n_\perp+1\\
&\langle n_\perp \Lambda|\rho^2|n_\perp+2, \Lambda\rangle = \tfrac{1}{2}\sqrt{(n_\perp+2)^2-\Lambda^2}\\
&\langle n_\perp \Lambda|\rho^4|n_\perp \Lambda\rangle = \tfrac{3}{2}n_\perp{}^2+3n_\perp+2-\tfrac{1}{2}\Lambda^2\\
&\langle n_\perp \Lambda|\rho^4|n_\perp+2, \Lambda\rangle = (n_\perp+2)\sqrt{(n_\perp+2)^2-\Lambda^2}\\
&\langle n_\perp \Lambda|\rho^4|n_\perp+4, \Lambda\rangle = \tfrac{1}{4}\sqrt{[(n_\perp+2)^2-\Lambda^2][(n_\perp+4)^2-\Lambda^2]}.
\end{aligned} \tag{19}$$

If the occupied state κ belongs to the shell N, it follows from the selection rules for ζ^4, $\zeta^2\rho^2$ and ρ^4 that $A_{\kappa l}$ is zero unless the non-occupied state l belongs to one of the shells N, $N+2$ and $N+4$.

If the state κ is characterized by the quantum numbers N, n_ζ, $n_\perp$ and the state l by $N' n'_\zeta n'_\perp$, we get the following scheme for the energy-denominators:

N'	$n'\zeta$	$n'_\perp$	$-(E_\kappa{}^0-E_l{}^0)/\hbar\omega(\varepsilon)$
N	$n_\zeta-2$	$n_\perp+2$	2ε
$N+2$	$n_\zeta+2$	$n_\perp$	$2(1-\frac{2}{3}\varepsilon)$
$N+2$	n_ζ	$n_\perp+2$	$2(1+\frac{1}{3}\varepsilon)$
$N+4$	$n_\zeta+4$	$n_\perp$	$4(1-\frac{2}{3}\varepsilon)$
$N+4$	$n_\zeta+2$	$n_\perp+2$	$4(1-\frac{1}{6}\varepsilon)$
$N+4$	n_ζ	$n_\perp+4$	$4(1+\frac{1}{3}\varepsilon)$

An estimate of $\delta_4 \int [\hbar\omega(\varepsilon)/(1-\frac{2}{3}\varepsilon)]\, B_{\kappa l}\, A_{l\kappa}/(E_\kappa{}^0-E_l{}^0)$ shows that it can be neglected. Our calculations are made for even nuclei with proton number between 90—100 and neutron number between 138—154. We take a level order essentially in agreement with the exact calculations by S. G. Nilsson.

We begin with the proton number 90. The shells $N = 0, 1, 2, 3, 4$ are completely filled, and in the shells $N = 5$ and 6 the following states are occupied: $|500+\rangle|411+\rangle|411-\rangle|322+\rangle|322-\rangle|320+\rangle|233+\rangle|144+\rangle$ $|600+\rangle|511+\rangle$. For the even proton numbers 92 to 100, the states are occupied in the order $|231+\rangle|422+\rangle|233-\rangle|055+\rangle|333+\rangle$. (The states are denoted $|n_z n_\perp \Lambda\Sigma\rangle$, with $\Sigma = \pm\frac{1}{2}$ written as $\pm$).

For neutron number 138 the shells $N = 0, 1, 2, 3, 4, 5$ are completely filled and in $N = 6$ and 7 the following states are occupied: $|600+\rangle|511+\rangle$ $|511-\rangle$ $|422+\rangle$ $|422-\rangle$ $|420+\rangle$ $|333+\rangle$ $|331+\rangle$ $|244+\rangle$ $|155+\rangle$

$|066+\rangle$ $|700+\rangle$ $|611+\rangle$. For the even numbers 140 to 154, the order is: $|522+\rangle$ $|333-\rangle$ $|433+\rangle$ $|331-\rangle$ $|242+\rangle$ $|244-\rangle$ $|344+\rangle$ $|153+\rangle$.

4.3. THE INTEGRAL CONDITION

The integral condition for the equilibrium deformation of δ_4 can now be written in the following simplified form:

$$\frac{8}{9}\frac{c_1}{c_2}\sum_\kappa B_{\kappa\kappa}-\delta_4 f\frac{112}{27}\frac{E}{\hbar\omega_0}\frac{a_1^2+b_1^2+c_1^2}{c_2}\sum_\kappa B_{\kappa\kappa}$$
$$=\sum_\kappa A_{\kappa\kappa}+\delta_4 f\frac{\hbar\omega(\varepsilon)}{1-\frac{2}{3}\varepsilon}\sum_\kappa\sum_1\frac{A_{\kappa 1}^2}{E_\kappa^0-E_1^0}\,. \tag{20}$$

The maximum energy E fluctuates comparatively much from one nucleus to another, as we have taken the level order from the exact calculation. We shall instead take the maximum energy E from the smoothed curve of the maximum energy as a function of the number of particles, filled in a consistent way. The protons for our nuclei have energy values around 6.5 $\hbar\omega(\varepsilon)$ and the neutrons around 7.5 $\hbar\omega(\varepsilon)$. For every nucleus we use the weighted value, having regard to the number of protons and neutrons.

An approximate value for

$$f=\frac{9}{16\sqrt{\pi}}\frac{\hbar}{m\omega_0}\frac{1}{R_0^2} \tag{21}$$

may be obtained by calculating the mean energy for the particles assuming a Thomas-Fermi distribution. We get

$$\frac{\hbar}{m\omega_0}\frac{1}{R_0^2}=\frac{0.8}{\sqrt[3]{1.5A}}. \tag{22}$$

5. Numerical Results and Discussion

Table 1 gives for the different nuclei the values of

$$A=\tfrac{1}{2}\sum_\kappa A_{\kappa\kappa},\quad B=\tfrac{1}{2}\frac{8}{9}\frac{c_1}{c_2}\sum_\kappa B_{\kappa\kappa},\quad A-B,$$
$$C=\tfrac{1}{2}\frac{112}{27}\frac{E}{\hbar\omega_0}\frac{a_1^2+b_1^2+c_1^2}{c_2}\sum_\kappa B_{\kappa\kappa},$$
$$D=-\tfrac{1}{2}\frac{\hbar\omega(\varepsilon)}{1-\frac{2}{3}\varepsilon}\sum_\kappa\sum_1\frac{A_{\kappa 1}^2}{E_\kappa^0-E_1^0},\quad C-D$$

and

$$\delta_4=-\frac{1}{f}\frac{A-B}{C-D}. \tag{23}$$

From the deformed potential we can now calculate the deformation of the nuclear surface

$$R=R_0(1+\beta_2 Y_{20}+\beta_4 Y_{40}+\ldots), \tag{24}$$

and compare with the values given by P. O. Fröman [3]).

We find that

$$\beta_4 = -\frac{\delta_4}{2} + \frac{8\sqrt{\pi}}{35}\varepsilon^2 + \frac{24\sqrt{\pi}}{385}\varepsilon^3 \ldots \tag{25}$$

The values of β_4 are given in table 1 and in fig. 1.

Our calculations have been made with eigenfunctions which are good approximations also when the terms $\mathbf{l}^2$ and $\mathbf{l}\cdot\mathbf{s}$ are included in the Hamiltonian, the main contributions of these terms coming from the diagonal terms. As also the level order is taken from the exact calculations including these terms, their main influence on the deformation is taken into account.

Now the energy denominators in D contain the diagonal terms of $\mathbf{l}^2$ and $\mathbf{l}\cdot\mathbf{s}$ (those of $\mathbf{l}\cdot\mathbf{s}$ cancelling). We have calculated their influence for the two nuclei Th^{228} and Fm^{254}. D is in both cases found to increase with about 14 %. Generally, D can be expected to increase in this manner for all the nuclei. Thus $C-D$ decreases and the absolute values of δ_4 increase. For the nuclei with δ_4 equal to zero β_4 is not changed. The solid line in fig. 1 gives estimated values of β_4 with the effect of the $\mathbf{l}^2$-term in the energy differences included.

Our calculations are also sensitive to the assumptions about the density ρ. We have used the statistical expression corresponding to a harmonic oscillator potential. The $\mathbf{l}^2$-term serves to depress the high angular momentum states, which gives a nuclear density intermediate between that of a square well potential and a harmonic oscillator. If we assume constant density in the nucleus, C decreases by about 17%. That makes the β_4 curve still steeper. The dotted curve represents an average between these two densities.

Fröman has analyzed the experimental data on the transition probabilities for the α-decay of even nuclei to rotational bands of daughter nuclei with spins $0+$, $2+$, $4+$. As it is not possible to separate the effect of the nuclear shape from that of the α-wave-function for the nuclear surface, this function is assumed constant and thus the actual deformation parameters β_2, β_4 are replaced by effective values. The transitions to $2+$ and $4+$ are especially sensitive to the nuclear deformation parameters β_2 and β_4 respectively. Fröman calculates β_4 under two alternative assumptions:

1) β_2 is fixed to 0.24; β_4 is determined so that the calculated transition probabilities for $0+ \rightarrow 4+$ agree with the corresponding empirical values.

2) Both β_2 and β_4 are determined so that the transition probabilities agree for $0+ \rightarrow 2+$ and for $0+ \rightarrow 4+$.

The calculations are made for different elements by averaging over the isotopes for which empirical data are available.

As mentioned above, calculations of β_4 according to another method are in progress, which may facilitate a more detailed comparison with the results of the analysis of the α-decay.

TABLE 1

		ε	A	B	$A-B$	C	D	$C-D$	δ_4	β_4
	138	0.278	1042	835	207	310 000	209 000	101 000	−0.056	0.062
Th	140	0.290	1133	935	198	336 000	221 000	115 000	−0.047	0.061
90	142	0.293	1097	964	133	346 000	225 000	121 000	−0.030	0.053
	144	0.299	1094	1022	72	363 000	231 000	132 000	−0.015	0.047
	138	0.277	1009	837	172	312 000	208 000	104 000	−0.045	0.056
U	140	0.289	1081	933	148	338 000	221 000	117 000	−0.035	0.054
92	142	0.292	1064	966	98	348 000	224 000	124 000	−0.022	0.048
	144	0.298	1068	1026	42	366 000	231 000	135 000	−0.009	0.043
	146	0.300	1052	1056	−4	376 000	233 000	143 000	0.001	0.039
	138	0.286	1045	908	137	331 000	215 000	116 000	−0.033	0.052
	140	0.297	1116	1002	114	357 000	238 000	129 000	−0.025	0.051
Pu	142	0.300	1101	1037	64	368 000	231 000	137 000	−0.013	0.046
94	144	0.306	1106	1100	6	386 000	237 000	149 000	−0.001	0.042
	146	0.308	1091	1131	−40	397 000	240 000	157 000	0.007	0.038
	148	0.305	1047	1123	−76	397 000	238 000	159 000	0.013	0.034
	142	0.299	1071	1140	31	371 000	231 000	140 000	−0.006	0.042
Cm	144	0.305	1077	1103	−26	390 000	238 000	152 000	0.005	0.038
96	146	0.307	1061	1134	−73	400 000	240 000	160 000	0.013	0.035
	148	0.304	1018	1123	−105	401 000	239 000	162 000	0.018	0.031
	146	0.296	1032	1061	−29	384 000	235 000	149 000	0.006	0.036
	148	0.293	988	1053	−65	385 000	234 000	151 000	0.012	0.032
Cf	150	0.290	940	1043	−103	385 000	234 000	151 000	0.019	0.027
98	152	0.290	896	1059	−163	392 000	235 000	157 000	0.030	0.022
	154	0.282	849	1012	−163	384 000	233 000	151 000	0.031	0.019
Fm 100	154	0.285	833	1047	−214	395 000	237 000	158 000	0.039	0.016

I wish to thank Prof. T. Gustafson for his kind interest in this work, for help and stimulating discussions. My thanks are further due to Prof. A. Bohr and Dr. B. Mottelson for suggesting this problem and for all the time they have given for discussions. I also want to thank Drs. S. G. Nilsson and S. B. Nilsson for help and valuable suggestions.

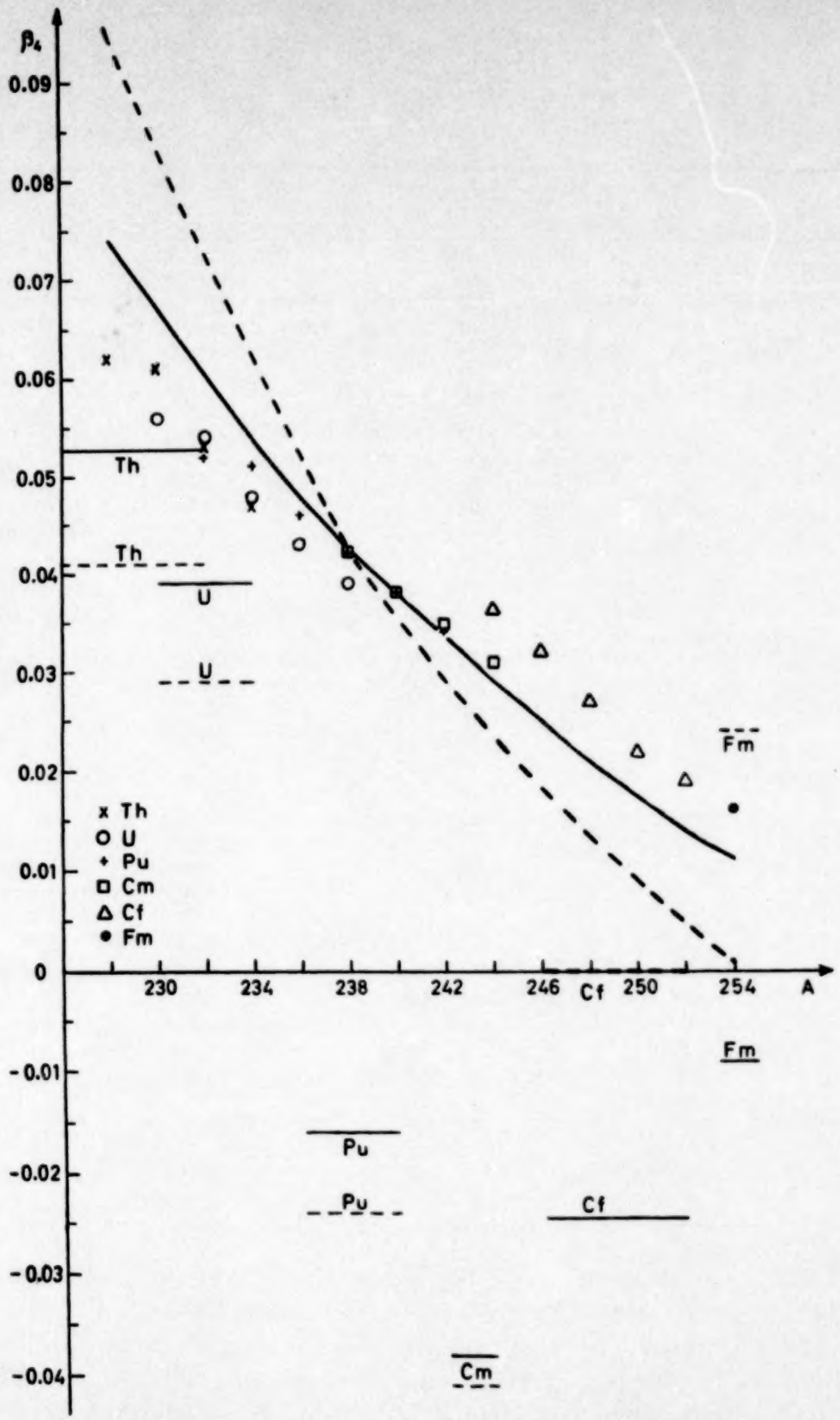

Fig. 1. The calculated values of β_4 for the different isotopes are plotted according to table 1. The solid curve gives the estimated values of β_4 with the effect of the I^2-term in the energy differences included. The dotted curve gives the average of β_4 for the cases of ρ = constant and $\rho = \rho_{\text{Thomas-Fermi}}$, account being taken of the corrected energy denominators. The solid and dotted horizontal lines for the different elements give Fröman's semi-empirical values according to assumption 1 and 2, respectively.

Appendix

We expand $|n_\perp \Lambda\rangle = \sum_{n_\xi} a_{n_\xi n_\eta} |n_\xi\rangle |n_\eta\rangle$,

where

$$n_\xi + n_\eta = n_\perp .$$

Using this condition we get

$$\begin{aligned}\langle n_\perp \Lambda|\rho^2|n_\perp \Lambda\rangle &= \sum_{n'_\xi} \sum_{n_\xi} a^*_{n'_\xi n'_\eta} a_{n_\xi n_\eta} \langle n'_\xi|\langle n'_\eta|(\xi^2+\eta^2)|n_\xi\rangle|n_\eta\rangle \\ &= \sum_{n_\xi} |a_{n_\xi n_\eta}|^2 (n_\xi + \tfrac{1}{2} + n_\eta + \tfrac{1}{2}) = n_\perp + 1. \qquad \text{(A.1)}\end{aligned}$$

It also follows that the only non-diagonal elements of ρ^2 that are non-zero are $\langle n_\perp \Lambda|\rho^2|n_\perp \pm 2, \Lambda\rangle$.

In the same way we can write

$$\langle n_\perp \Lambda|\rho^4|n_\perp \Lambda\rangle = \sum_{n'_\xi} \sum_{n_\xi} a^*_{n'_\xi n'_\eta} a_{n_\xi n_\eta} \langle n'_\xi|\langle n'_\eta|(\xi^4 + 2\xi^2\eta^2 + \eta^4)|n_\xi\rangle|n_\eta\rangle$$

but here the $\xi^2\eta^2$ will give non-diagonal terms. We get after simplifications

$$\begin{aligned}&\langle n_\perp \Lambda|\rho^4|n_\perp \Lambda\rangle \\ &= \tfrac{3}{2} n_\perp{}^2 + \tfrac{5}{2} n_\perp + 2 + \tfrac{1}{2} \sum_{n_\xi} [a_{n_\xi n_\eta} a^*_{n_\xi+2, n_\eta-2} \sqrt{(n_\eta - 1) n_\eta (n_\xi + 1)(n_\xi + 2)} \\ &+ a_{n_\xi n_\eta} a^*_{n_\xi-2, n_\eta+2} \sqrt{(n_\xi - 1) n_\xi (n_\eta + 1)(n_\eta + 2)} - 2 n_\xi n_\eta |a_{n_\xi n_\eta}|^2].\end{aligned}$$

We can get an expression for this sum over n_ξ using the condition that $l_\zeta |n_\perp \Lambda\rangle = \Lambda |n_\perp \Lambda\rangle$:

$$-i \left(\xi \frac{\partial}{\partial \eta} - \eta \frac{\partial}{\partial \xi}\right) \sum_{n_\xi} a_{n_\xi n_\eta} |n_\xi\rangle |n_\eta\rangle = \Lambda \sum_{n_\xi} a_{n_\xi n_\eta} |n_\xi\rangle |n_\eta\rangle .$$

$\langle \xi | n_\xi \rangle$ are the Hermite orthogonal functions

$$N_{n_\xi} e^{-\xi^2/2} H_{n_\xi}(\xi)$$

with

$$N_{n_\xi} = \left(\frac{1}{\sqrt{\pi}} \cdot \frac{1}{2^{n_\xi} n_\xi !}\right)^{\frac{1}{2}}.$$

If we use the relations for the Hermite polynomials

$$\begin{aligned}H_{n_\xi+1}(\xi) - 2\xi H_{n_\xi}(\xi) + 2 n_\xi H_{n_\xi-1}(\xi) &= 0 \\ H'_{n_\xi}(\xi) &= 2 n_\xi H_{n_\xi-1}(\xi)\end{aligned}$$

we get

$$\begin{aligned}&-i \left(\xi \frac{\partial}{\partial \eta} - \eta \frac{\partial}{\partial \xi}\right) N_{n_\xi} N_{n_\eta} e^{-\xi^2/2} e^{-\eta^2/2} H_{n_\xi}(\xi) H_{n_\eta}(\eta) \\ &= -i N_{n_\xi} N_{n} \; e^{-\xi^2/2} e^{-\eta^2/2} [n_\eta H_{n_\eta-1}(\eta) H_{n_\xi+1}(\xi) - n_\xi H_{n_\xi-1}(\xi) H_{n_\eta+1}(\eta)].\end{aligned}$$

It follows that

$$l_\zeta|n_\xi\rangle|n_\eta\rangle = -i(\sqrt{n_\eta(n_\xi+1)}|n_\xi+1\rangle|n_\eta-1\rangle-\sqrt{n_\xi(n_\eta+1)}|n_\xi-1\rangle|n_\eta+1\rangle)$$

and

$$\begin{aligned} l_\zeta^2|n_\xi\rangle|n_\eta\rangle = +[&(2n_\xi n_\eta+n_\xi+n_\eta)|n_\xi\rangle|n_\eta\rangle \\ &-\sqrt{(n_\eta-1)n_\eta(n_\xi+1)(n_\xi+2)}|n_\xi+2\rangle|n_\eta-2\rangle \\ &-\sqrt{(n_\xi-1)n_\xi(n_\eta+1)(n_\eta+2)}|n_\xi-2\rangle|n_\eta+2\rangle]. \end{aligned}$$

$$\sum_{n_\xi} a_{n_\xi n_\eta} l_\zeta^2|n_\xi\rangle|n_\eta\rangle = \Lambda^2 \sum_{n_\xi} a_{n_\xi n_\eta}|n_\xi\rangle|n_\eta\rangle.$$

Multiplication on both sides with $\sum_{n'_\xi} a^*_{n'_\xi n'_\eta}\langle n'_\xi|\langle n'_\eta|$ gives

$$\begin{aligned} \Lambda^2 = n_\perp - \sum_{n_\xi}[&a_{n_\xi n_\eta} a^*_{n_\xi+2,n_\eta-2}\sqrt{(n_\eta-1)n_\eta(n_\xi+1)(n_\xi+2)} \\ &+a_{n_\xi n_\eta} a^*_{n_\xi-2,n_\eta+2}\sqrt{(n_\xi-1)n_\xi(n_\eta+1)(n_\eta+2)}-2n_\xi n_\eta|a_{n_\xi n_\eta}|^2]. \end{aligned}$$

Thus we have a simple expression for the sum in the right hand side of $\langle n_\perp \Lambda|\rho^4|n_\perp \Lambda\rangle$. We get

$$\langle n_\perp \Lambda|\rho^4|n_\perp \Lambda\rangle = \tfrac{3}{2}n_\perp{}^2+3n_\perp+2-\tfrac{1}{2}\Lambda^2. \qquad \text{(A.2)}$$

We can use this formula to obtain the matrix elements

$$\langle n_\perp \Lambda|\rho^2|n_\perp+2, \Lambda\rangle.$$

In fact,

$$\langle n_\perp \Lambda|\rho^4|n_\perp \Lambda\rangle = \sum_{n'_\perp \geqq \Lambda}\langle n_\perp \Lambda|\rho^2|n'_\perp \Lambda\rangle\langle n'_\perp \Lambda|\rho^2|n_\perp \Lambda\rangle.$$

As we have shown we get non-zero elements only for

$$n'_\perp = \begin{cases} n_\perp \\ n_\perp \pm 2 \end{cases}.$$

We get

$$\begin{aligned} &|\langle n_\perp \Lambda|\rho^2|n_\perp-2, \Lambda\rangle|^2+|\langle n_\perp \Lambda|\rho^2|n_\perp+2, \Lambda\rangle|^2+|\langle n_\perp \Lambda|\rho^2|n_\perp \Lambda\rangle|^2 \\ &\qquad = \tfrac{3}{2}n_\perp{}^2+3n_\perp+2-\tfrac{1}{2}\Lambda^2. \end{aligned}$$

Putting

$$|\langle n_\perp \Lambda|\rho^2|n_\perp+2, \Lambda\rangle|^2 = a_2 n_\perp{}^2+a_1 n_\perp+a_0+b\Lambda^2$$

and

$$|\langle n_\perp \Lambda|\rho^2|n_\perp-2, \Lambda\rangle|^2 = a_2(n_\perp-2)^2+a_1(n_\perp-2)+a_0+b\Lambda^2$$

we get one solution:

$$|\langle n_\perp \Lambda|\rho^2|n_\perp+2, \Lambda\rangle|^2 = \tfrac{1}{4}[(n_\perp+2)^2-\Lambda^2].$$

The general solution will be $\frac{1}{4}[(n_\perp+2)^2-\Lambda^2]+F(n_\perp \Lambda)$, where $F(n_\perp \Lambda) = -F(n_\perp+2, \Lambda)$. For $\Lambda = n_\perp$ we only get contributions for $n'_\perp = \Lambda$ and $\Lambda+2$ and we get

$$|\langle \Lambda, \Lambda|\rho^2|\Lambda+2, \Lambda\rangle|^2 = \Lambda+1$$

which gives

$$F(\Lambda, \Lambda) = 0 \quad \text{and} \quad F(\Lambda+2k, \Lambda) = 0.$$

Therefore

$$\langle n_\perp \Lambda|\rho^2|n_\perp+2,\ \Lambda\rangle = \tfrac{1}{2}\sqrt{(n_\perp+2)^2-\Lambda^2} \tag{A.3}$$

is the general solution, apart from an unimportant phase factor.

In the same way we get

$$\begin{aligned}\langle n_\perp \Lambda|\rho^4|n_\perp+2, \Lambda\rangle &= \langle n_\perp \Lambda|\rho^2|n_\perp \Lambda\rangle\langle n_\perp \Lambda|\rho^2|n_\perp+2, \Lambda\rangle \\ &\quad +\langle n_\perp \Lambda|\rho^2|n_\perp+2, \Lambda\rangle\langle n_\perp+2, \Lambda|\rho^2|n_\perp+2, \Lambda\rangle \\ &= (n_\perp+2)\sqrt{(n_\perp+2)^2-\Lambda^2}\end{aligned} \tag{A.4}$$

and

$$\begin{aligned}\langle n_\perp \Lambda|\rho^4|n_\perp+4, \Lambda\rangle &= \langle n_\perp \Lambda|\rho^2|n_\perp+2, \Lambda\rangle\langle n_\perp+2, \Lambda|\rho^2|n_\perp+4, \Lambda\rangle \\ &= \tfrac{1}{4}\sqrt{[(n_\perp+2)^2-\Lambda^2][(n_\perp+4)^4-\Lambda^2]}.\end{aligned} \tag{A.5}$$

References

1) S. G. Nilsson, Mat. Fys. Medd. Dan. Vid. Selsk. **29** (1957) no. 16;
K. Gottfried, Phys. Rev. **103** (1956) 1017;
S. Moszkowski, Phys. Rev. **99** (1955a) 303
2) Kiuck Lee and D. R. Inglis, Phys. Rev. **108** (1957) 774
3) P. O. Fröman, Mat. Fys. Medd. Dan. Vid. Selsk. **1** (1957) no. 3
4) L. Pauling and E. B. Wilson, Introduction to Quantum Mechanics (McGraw-Hill, New York, 1935) p. 111

10.D *Nuclear Physics* 9 (1958/59) 178: © *North-Holland Publishing Co., Amsterdam*

BOOK REVIEWS

J. G. WILSON & S. A. WOUTHUYSEN (Editors), *Progress in elementary particle and cosmic ray physics* (volume IV) (North-Holland Publishing Co., Amsterdam, 1958. xii—470 pages. 45 fl.)

The last volume of this well-established series contains five chapters, written by eminent experts, on problems of great topical interest: the strangeness of the new particles and its possible theoretical interpretations (d'Espagnat and Prentki), the K-mesons (Walker), the interaction of μ-mesons with matter (Fowler and Wolfendale), the primary cosmic radiation (a long treatise by S. F. Singer), the origin of cosmic radiation (Ginzburg). These surveys deal with many problems whose understanding is still very imperfect, and which accordingly call for further research. Not only are they invaluable as a guide in such investigations, but their quality is such that they will retain their usefulness even if a few sections are rendered antiquated by the rapid progress in some of the fields covered.

L. R.

M. SCHWARZSCHILD, *Structure and evolution of the stars* (Princeton University Press, 1958. xvii—296 pages. $ 6.00)

The present book is too much on the fringe of nuclear physics to be reviewed at great length; it deserves, however, to be brought to the attention of those nuclear physicists who for some practical reason or from sheer curiosity wish to acquaint themselves with the present state of our views on stellar evolution: it is indeed conceived as a general introduction into the subject, and it is tersely written, with great competence and clarity. It is symbolic of the fluidity of our astrophysical conceptions that the book is produced in offset from a typescript. The work is carefully done, and the appearance of the text and the diagrams is remarkably neat.

L. R.

J. S. ALLEN, *The neutrino* (Princeton University Press, 1958. viii—168 pages. $ 4.50)

The ambition of this monograph is to collect all that is known (or was known till March 1958) about the neutrino. The survey of the experimental material is indeed very complete and critical. The experiments are described in great detail. The theory, however, is not presented systematically; in fact, there are signs that the author is not *au fait* of the finer points. Although the theoretical implications of each experiment are given, this is not done critically, and no clear picture of the situation emerges; this considerably detracts from the value of the book. It was also bad luck that the progress of the printing did not leave the author any chance of doing justice to the recent developments which have rounded off the subject so nicely. Still, statements in need of modification on this count are corrected in foot-notes, and longer sections added in proof to several chapters deal, albeit summarily, with the latest work.

L. R.

L. EISENBUD and E. P. WIGNER, *Nuclear structure* (Princeton University Press, 1958. viii—128 pages. $ 4.00)

Here is an introduction to nuclear physics which rivals in excellence the similar one by Landau and Smorodinsky. The present treatment lacks the brilliance of the Russian text, but it is more thorough and goes somewhat more into details. It is quite natural that the ideas introduced by the senior author, partly in collaboration with the junior one, should occupy a prominent place in the exposition: they are indeed so fundamental that they have become common good and are often mentioned without explicit reference to their initiator. That we have now from his own hand a connected account of the whole subject, is highly gratifying: beginners and experts alike are sure to derive from its perusal instruction and inspiration.

L. R.

10.A *Nuclear Physics* **9** (1958/59) 179; © *North-Holland Publishing Co., Amsterdam*

NEWS ITEM

EUROPEAN NUCLEAR ENERGY AGENCY

Background Information

1. Structure and Objectives of E.N.E.A.

The European Nuclear Energy Agency of the Organisation for European Economic Co-operation operates under the general direction of a Steering Committee comprising representatives of the seventeen Member countries of O.E.E.C., the Associated countries Canada and the U.S.A., and Spain. The main objective of the Agency is to promote co-operation between Member countries in developing nuclear energy for all peaceful purposes. Its executive power derives from, and is exercised through, the Council of O.E.E.C., to which the E.N.E.A. Steering Committee submits its recommendations for approval.

The work of the Agency is mainly carried out through technical committees and working parties, which may be concerned with any (or all) of the stages of a project from initial "problem study" to the operation of specialised plant or (in the case of health or safety studies) to the preparation of draft regulations for subsequent legal ratification. One of the most important of these committees is that formed in February of this year, under the presidency of Professor Perrin of France and Sir John Cockcroft of the United Kingdom, to examine possible methods of collaboration among Member countries in the development of experimental and prototype reactors, so as to determine as soon as possible the best type, both technically and economically, for the production of power.

2. Major Technical Projects Under Way

The first major project organised by E.N.E.A. was the internationally owned and operated Chemical Processing Company (Eurochemic) which is constructing a plant for refining and processing Europe's irradiated nuclear fuels. This plant, to be built near the Belgian Nuclear Research Centre at Mol, is being financed from the Company's $ 20 million capital, subscribed partly by the Governments and partly by Private Industry in the Member countries. It is expected to begin operation in 1961.

Two other main projects are an experimental "boiling water" reactor (in which heavy water is used both as moderator and for heat removal from the core), and a high-temperature gas-cooled reactor (with ceramic fuel elements operating at some 1000° C) using helium for heat extraction. The boiling water reactor has already been built at Halden (Norway) by the Norwegian Institute of Atomic Energy, and is expected to begin operation before the end of the year. It will be the only "boiling water" reactor in Europe and the first of its type in the world to use heavy water.

The high-temperature gas-cooled reactor, the final arrangements for which are currently under discussion within O.E.E.C., is to be built by the United Kingdom Atomic Energy Authority at their new experimental site at Winfrith Heath: this, too, will be the first of its type in the world.

A further project is an investigation of the possibility of producing heavy water in Iceland using the geothermic steam available there.

3. Other Projects

Besides projects mainly concerned with technical developments, E.N.E.A. has set up a number of committees which are dealing with some of the ancillary problems essential to the development of nuclear power in Europe. These problems concern such matters as health

standards, third party liability and insurance in the event of accidents involving nuclear hazards, the supply and training of technical and scientific personnel (generally agreed to be of vital importance) and, finally, the development of a system of inspection and control which, both technically and legally, can be relied upon to prevent the use of the joint facilities for military purposes.

4. Relations with other Nuclear Organisations

E.N.E.A. is expressly bound by its Statute to take account, in the performance of its duties, of the work done by the other international organisations in the nuclear field, and to co-operate with them in all possible ways.

The two Organisations with the most closely linked interests are the European Atomic Energy Community (Euratom) and the International Atomic Energy Agency.

The former, although covering largely the same technical field as E.N.E.A., has very different objectives. It seeks to bring about a close association in nuclear matters between the six countries which are already linked in the European Coal and Steel Community and in the Common Market, and which are thus moving towards progressively closer integration. This, however, should not prejudice technical co-operation between the Six and the other countries of Western Europe which are in a position to make a valuable contribution to the development of the nuclear industry. E.N.E.A. provides the machinery for ensuring this co-operation between all European Countries.

With the International Atomic Energy Agency, which includes many countries outside Europe, E.N.E.A. is in close contact in the fields of health, safety, and security control. These are indeed matters of world-wide importance, and present many difficult international problems.

Report no. 1

The E.N.E.A. was founded on 1st February 1958, and its first Report was presented to the Council of Europe at Strasbourg on the 15th October 1958. It covers its activities during the first six months of operation, and gives details about the projects enumerated above. It is published as an 80-page typewritten pamphlet, with some illustrations. The Agency's address is 38 Boulevard Suchet, Paris 16e.

NORTH-HOLLAND BOOKS

Just out

INTERNAL CONVERSION COEFFICIENTS

by

M. E. ROSE

Chief Physicist,
Oak Ridge National Laboratory

9 x 12½" XXII + 176 pages 40s.

THE CONTENTS

I INTRODUCTION

1. Definition of the Internal Conversion Process
2. The Selection Rules, Mixtures of Multipoles
3. Theoretical Considerations
4. Method of Calculation and Explanation of the "Tables"

II NUMERICAL RESULTS

K shell Internal Conversion Coefficients; L_I, L_{II}, L_{III}, subshell Internal Conversion Coefficients; Total M shell Internal Conversion Coefficients, $Z \geqq 65$; M_I, M_{II}, M_{III}, M_{IV}, M_V, subshell Internal Conversion Coefficients, $Z \geqq 65$; Radial Integrals for K Conversion

To those who have been concerned with the general and specific questions of nuclear structure, the importance of accurate calculations of internal conversion coefficients has been very apparent for a long time. It was about ten years ago that the first extensive and sufficiently accurate calculations of these coefficients were published and since then they have played a central role in the attempt to understand nuclear decay processes. These initial results of a decade ago constituted the first step in a program, which has since been pursued by the author and his co-workers, aimed at providing a comprehensive and thorough compilation of these conversion coefficients. At the same time the physical basis of the calculations has been progressively modified so as to improve the results. At the present time, as this program has culminated, the conversion coefficients have been obtained for the K shell, the L shell with all its subshells, and the M shell with all its subshells.

For the K and L shells, where these effects are important, the influence of finite nuclear size (due to the modification of the electron wave functions) and the influence of screening by the atomic electrons have both been included in a complete manner. The results for the coefficients are now available for a wide range of transition energies and for all atomic numbers from very light nuclei to extremely heavy ones.

Previous to the publication of this book a portion of these results had been circulated through private correspondence. In addition to collecting in one place all these results, which have hitherto appeared in this informal way, the present tables provide a tenfold extension of tables. These tables, therefore, represent a very complete compendium of all the numerical information about internal conversion coefficients.

In addition to the tabulation of conversion coefficients there appears a short table of transition *amplitudes* for K conversion. These are important for a number of applications: (1) The dynamic nuclear structure effects on internal conversion, which exists for some very heavy nuclei. (2) All phenomena involving conversion electrons wherein the direction of motion is observed. In the latter category, angular correlation and polarization of electrons following beta decay may be mentioned.

Sole Agency for U.S.A.: Interscience Publishers Inc. - New York

NORTH-HOLLAND PUBLISHING COMPANY - AMSTERDAM

NORTH-HOLLAND BOOKS

out in December *out in December*

NUCLEAR REACTIONS Vol. I

Edited by: P. M. ENDT, University, Utrecht - M. DEMEUR, Free University, Brussels

6 x 9″ xii + 502 pages 115 illus. Guilders 43,— 86s.

CONTENTS

Ch. I: R. J. Eden, Cambridge
Theory of the Nucleus as a Many-Body System

Ch. II: J. P. Elliott, Harwell
The Shell Model

Ch. III: J. H. Fremlin, Birmingham
Heavy Ion Reactions

Ch. IV: L. J. B. Goldfarb, Manchester
Angular Correlations and Polarization

Ch. V: Erich Vogt, Chalk River
Resonance Reactions, Theoretical

Ch. VI: H. E. Gove, Chalk River
Resonance Reactions, Experimental

Ch. VII: K. J. le Couteur, Canberra
The Statistical Model

Ch. VIII: D. J. Hughes and R. L. Zimmerman, Brookhaven
Neutron Resonances in Heavy Nuclei

Ch. IX: P. C. Gugelot, Amsterdam
A Survey of Scattering and Reaction Experiments with Medium Energy Nucleons and Alpha Particles

Ch. X: A. K. Kerman, Cambridge
Nuclear Rotational Motion

NUCLEAR SPECTROSCOPY TABLES

By A. H. WAPSTRA, G. J. NIJGH and R. VAN LIESHOUT

7½ x 10½″ viii + 136 pages Guilders 30,— 60s.

CONTENTS

Ch. I: Mathematical Tables
Ch. II: Atomic Constants
Ch. III: Elements and Isotopes
Ch. IV: Heavy Particles
Ch. V: Electrons
Ch. VI: Gamma Rays
Ch. VII: X-rays and Auger Electrons
Ch. VIII: Angular Distributions and Correlations
Ch. IX: Nuclear Models
Ch. X: Calibration Standards

QUANTUM PARTICLE DYNAMICS

By JAMES McCONNELL, Professor of Mathematical Physics, Maynooth, Ireland

6 x 9″ xii + 252 pages Guilders 20,— 40s.

CONTENTS

Ch. I: Special Theory of Relativity
Ch. II: Introduction to Quantum Theory
Ch. III: Schrödinger's Wave Mechanics
Ch. IV: Heisenberg's Matrix Mechanics
Ch. V: Angular Momentum
Ch. VI: Systems of Particles
Ch. VII: The Dirac Equation
Ch. VIII: Quantisation of the Electromagnetic Field
Ch. IX: Photoelectric and Compton Effects
Ch. X: Bremsstrahlung and Electron Pair Production
Ch. XI: Nuclear Forces
Ch. XII: Mesons and Nucleons

Sole Agency for U.S.A.: Interscience Publishers Inc. - New York

NORTH-HOLLAND PUBLISHING COMPANY - AMSTERDAM